DOCTORAL RESEARCH IN
"EVOLUTIONARY BIOLOGY AND ECOLOGY"

CICLE XXXIII

Coordinator Prof. Barbujani Guido

THE ROLE OF COMMON MACROFAUNA HOLOBIONTS

IN BENTHIC NITROGEN CYCLING

Ph.D. candidate   Supervisor

Dott. Mindaugas Žilius   Prof. Giuseppe Castaldelli

2018/2020

CONTENT

ABSTRACT

In estuarine systems, interactions between microbes and macrofauna are likely widespread and may establish through multiple mechanisms. Macrofauna, besides grazing, bioturbating sediments and ventilating burrows, can host or inoculate microbes from ambient environment. Macrofauna hosts and their associated microbes form holobionts, which are biological and functional units capable of performing multiple processes. However, they are largely understudied due to methodological limitations or oversimplification of experimental approaches. Therefore, the cumulative effects of holobionts are rarely accounted for in biogeochemical studies and their actual magnitude may be underestimated when assessing ecosystem-wide processes.

In this thesis, we investigated the contribution of common macrofauna in shallow estuarine benthic sediments with emphasis on the role of ecological interactions between microbes and their invertebrate hosts on regulation of nitrogen (N) cycling processes. We used a combination of ecological, biogeochemical, and molecular approaches to partitioning the direct and indirect role of macrofauna including bioturbation, physiological and holobionts activities in benthic habitats.

The results show that all macrofauna holobionts hosted active and complex microbiomes, capable of different N transformations, such as denitrification, dissimulative nitrate reduction to ammonium, and dinitrogen fixation. The detection of N transformations in common macrofauna holobionts highlights hidden and interactive effects among microbes and animals. In tropical estuarine system, abundant fiddler crab holobionts are a net dinitrogen (N_2) sink, with N_2 fixation exceeding N losses, and as a significant source of ammonium and dissolved organic N to the surrounding environment. On the contrary, the role of the holobionts in the temperate and boreal estuarine systems were of minor importance as compared to the activity of sediment-associated microbial communities. There, distinct macrofauna taxa in community altered benthic metabolism and N cycling directly by impacting respiration and excretion rates and indirectly by reworking sediment.

The findings in this thesis further support that main biogeochemical processes in sediment are predominantly the result of the collective effects of different functional groups and their mutual interactions with associated microbes. Although the role of holobionts in colder systems was relatively low to this found in tropics, however this might be different along seasons or habitats. In the future, more studies should address environmental or biological factors that regulate holobionts activity across different taxa of macrofauna and habitats.

LIST OF ORIGINAL PUBLICATIONS

This thesis is based on assemblage of the following publications:

I. Samuiloviene, A., M. Bartoli, S. Bonaglia, U. Cardini, I. Vybernaite-Lubiene, U. Marzocchi, J. Petkuviene, T. Politi, A. Zaiko, **M. Zilius**, 2019. The effect of chironomid larvae on nitrogen cycling and microbial communities in soft sediments. *Water* 11: 1931.

    Highlights:
    *   Chironomid larvae harboured a unique array of bacteria compared to those found in ambient sediments.
    *   Active microbial communities in host were capable of multiple nitrogen (N) transformations, with considerably higher metabolic potential than those in surrounding sediments.
    *   The chironomid larvae by creating microniches enhanced rates of N recycling and removal.

II. **Zilius, M.**, S. Bonaglia, E. Broman, V. G. Chiozzini, A. Samuiloviene, F.J.A. Nascimento, U. Cardini, M. Bartoli, 2020. N_2 fixation dominates nitrogen cycling in a mangrove fiddler crab holobiont. *Scientific Report* 10, 13966.

    Highlights:
    *   Microbiome associated with fiddler crab carapace was capable of both aerobic and anaerobic pathways of the N cycle.
    * N_2 fixation was the dominant pathways compared to other N cycling processes associated with fiddler crab microbiota.
    *   Nitrogen stable isotope natural abundances of fiddler crab carapace-associated biofilms indicating active microbial N_2 fixation.

III. Politi, T., R. Barisevičiūtė, M. Bartoli, S. Bonaglia, U. Cardini, G. Castaldelli, A. Kančauskaitė, U. Marzocchi, J. Petkuviene, A. Samuiloviene, I. Vybernaite-Lubiene, A. Zaiko, **M. Zilius**. 2021. A bioturbator, a holobiont, and a vector: The multifaceted role of *Chironomus plumosus* in shaping N-cycling. *Freshwater Biology* 66(6), 1036–1048.

    Highlights:
    *   Chironomid larvae pumping nitrate (NO_3^-)–rich bottom water within burrows stimulated sedimentary denitrification.
    *   Besides direct effect (bioturbation) on microbial processes, chironomid larvae host versatile microbiota capable of contrasting N cycling pathways.
    *   During chirdomid metamorphosis microbes involved in different N-related microbial processes are exported to surrounding ecosystems.
    *   This study provides evidence that chironomids have a multifaceted role in shaping N-cycling in aquatic ecosystems.

IV.   Marzocchi, U., S. Bonaglia, A. Zaiko, G. Marina Quero, I. Vybernaite-Lubiene, T. Politi, A. Samuiloviene, **M. Zilius**, M. Bartoli, U. Cardini. 2021. Zebra mussel holobionts fix and recycle nitrogen in lagoon sediments. *Frontiers in Microbiology* 11, 610269.

Highlights:
- Zebra mussel primarily enhanced recycling of N to water column via release and mineralization.
- NO_3^- reduction and N_2 fixation was associated with zebra mussel holobionts.
- Active diazotrophic community of holobionts diverged substantially from those in water column.
- Mussel-associated N_2 fixation may account for substantial source of bioavailable N.

V.   **Zilius, M**., M. Bartoli, U. Marzocchi, U. Cardini, S. Bonaglia, D. Daunys, G. Castaldelli. Partitioning benthic nitrogen cycle processes among three common macrofauna holobionts. *Biogeochemistry* (resubmitted after revisions).

Highlights:
- In a macrofaunal community, distinct functional groups produced contrasting effects on the benthic N cycling.
- A community-associated versatile microbiome contributed to the benthic N-cycling.
- The present study highlight hidden and interactive effects among microbes and macrofauna.

Authors contributions:

Contribution	Manuscripts				
	I	II	III	IV	V
Conceived the idea and designed methodology	MZ, MB, IV-L	MZ, MB	MZ, UC, SB	MZ, UC, SB	MZ, MB
Sampling and experiments	AS, MB, IV-L, JP, SB	MZ,VGC	MZ, TP, JP, IV-L	MZ, IVL, MB, TP, UC	MZ, MB, UM, UC, DD
Analysis and data handling	AZ, TP	AS, EB, SB, VGC,	IV-L, JP, RB, SB, UM, AS, AK, UC, AZ	UM, UM, AZ, AS, SB, GMQ, IV-L	MZ, UM, SB
First draft	MZ, AS	MZ, MB	MZ, TP, MB	UM, UC, GMQ	MZ, MB
Writing-review, editing	MB, SB, UC, UM, JP, TP, AZ	MZ, UC, FJAN, MB, EB, SB	All authors	MZ, AZ, MB, SB, UM, UC,	All authors

Side publications not included in this thesis:

1   Politi, T., **M. Zilius**, G. Castaldelli, M. Bartoli, D. Daunys. 2019. Macrofauna affects benthic cycling pathways in a hypertrophic lagoon. *Water* 11(6), 1186.

2   Magri, M., S. Benelli, S. Bonaglia, **M. Zilius**, G. Castaldelli, M. Bartoli. 2020. The effects of hydrological extremes on denitrification, dissimilatory nitrate reduction to ammonium (DNRA) and mineralization in a coastal lagoon. Science of The Total Environment 740, 140169.

INTRODUCTION

Microbes drive much of the Earth's nitrogen (N) cycle. In estuarine ecosystems, sediments host a large diversity of microbes capable of multiple N transformations (Hunter et al., 2006; Damashek and Francis, 2018; Rasigraf et al., 2019), which produce a number of intermediate and end-compounds (Herbert, 1999). Microbially mediated benthic N transformations there are largely supported and stimulated by a range of macrofauna-related processes, collectively defined as bioturbation (Bianchi, 2007; Kristensen et al., 2012; Stief, 2013).
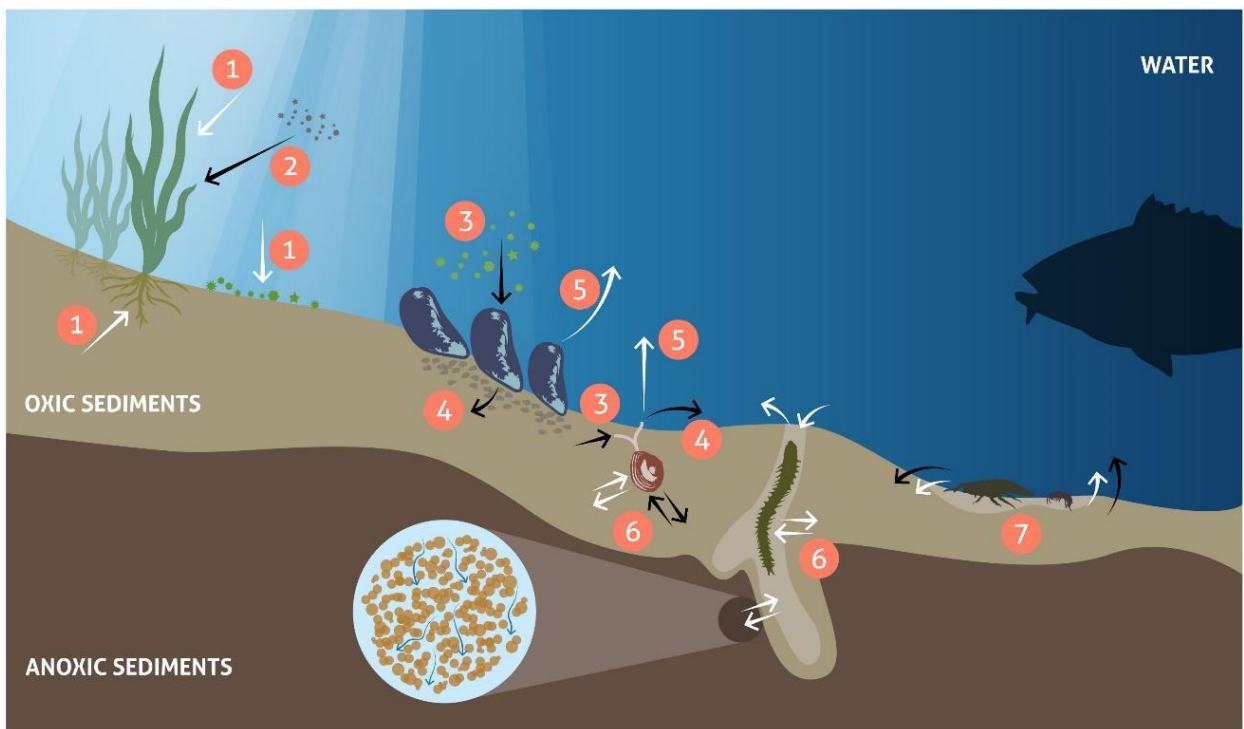

Fig. 1. Scheme summarizing benthic organism's contribution to the biogeochemical processes in estuarine systems (Ehrnsten et al., 2020): (1), sedimentation and sediment stabilization by vegetation (2), assimilation (3), biodeposition of faeces (4), nutrient excretion and respiration (5), and sediment bioturbation, including bioirrigation (6) and mixing (7).

The multiple paths by which macrofauna affect the physical and biological environment and N cycling (Fig. 1) have been scrutinized in many experimental studies (e.g. Kristensen, 2001; Quintana et al., 2013; van Nugteren et al., 2013; Bonaglia et al., 2019). For example, dense bivalve populations sustain large ammonium (NH_4^+) fluxes to the bottom water either via direct excretion or via the production of labile biodeposits stimulating microbial ammonification and alleviating N limitation (Welsh et al., 2015; Smyth et al., 2018; Cardini et al., 2019). Deep burrowing macrofauna, during ventilation, pump N- and oxygen (O_2)-rich bottom water downward (Nielsen et al., 2004; Mermillod-Blondin and Rosenberg, 2006; Renz and Foster, 2013; Murphy and Reidenbach, 2016). This stimulates microbial N cycling pathways, including ammonification,

nitrification and denitrification (Tuominen et al., 1999; Bonaglia et al., 2013; Stief, 2013; Bosch et al., 2015; Moraes et al., 2018). Therefore, in macrofauna bioturbated sediments, the abundance and the activity of microbial communities often exceed those of surrounding, non-bioturbated sediments (Gilbertson et al., 2012; Laverock et al., 2014; Yazdani Foshtomi et al., 2018; Paper I). Macrofauna may also select and host unique microbiomes, which can contribute to biogeochemical cycling (König et al., 2016; Cardini et al., 2019; Papers II, IV).

Macrofauna hosts and their associated microbes form holobionts, which are biological and functional units capable of performing multiple processes (Dittami et al., 2021). Our recent biogeochemical studies revealed for example how macrofauna-microbe holobionts might contribute to various processes of benthic N cycle, increasing its import, recycling and bioavailability to primary producers (Papers II, IV). Increasing synergy between molecular tools and the use of stable isotope probing have allowed large improvements in our understanding of elements cycling in holobionts and benthic macrofauna bioturbated sediments (Poulsen et al., 2014; Vasquez-Cardenas et al., 2016; Cardini et al., 2019; Papers II–IV).

Macrofauna holobionts in estuarine systems

Macrofauna associations with N_2 fixing bacteria are frequently observed in tropical oligotrophic habitats (e.g., coral reefs, seagrass beds; Cardini et al., 2014; Petersen et al., 2016). These microbial associations play an important role by facilitating niche adaptation and allowing their host to occupy otherwise inaccessible habitats (Shapira, 2016). One of fascinating example is the common association between seagrass, lucinid bivalves and sulphide-oxidizing bacteria, which results both in enhanced plant production due to sulphide detoxification and increased N availability, and in increased invertebrates and microbes fitness due to roots radial O_2 loss and sulphide accumulation (van der Heide et al., 2012; Cardini et al., 2019).

In estuarine areas, which often receive high loads of N discharged from rivers and, therefore, N is here in excess (Galloway et al., 2004), and thus interaction between macrofauna and microbes is rather constrained by other factors. Recent studies have shown that the collection of microbes in benthic invertebrates in both N rich and depleted environments includes a highly diverse N cycling community (Kessel et al., 2016; Stief et al., 2017, 2018; Petersen et al., 2016). The exterior body of macrofauna or its digestive system offer additional habitats for microbial communities, which are actively involved in nitrification, denitrification and dissimilatory nitrate (NO_3^-) reduction to NH_4^+ (DNRA) or dinitrogen (N_2) fixation (Caffrey et al., 2016; Arfken et al., 2017; Ray et al., 2019; Papers II–IV). Colonization may be host advantageous for specific bacteria, because of host activities, such as respiration, excretion, feeding and horizontal and vertical migrations (Wahl et al., 2012). Macrofauna, in particular burrowing, continuously migrate

vertically and horizontally across sediments, exposing their associated microbiome to different chemical gradients (e.g. from O_2 and NO_3^--rich to anoxic, NH_4^+-rich), acting as microbial community elevators or transporters. Moreover, benthic invertebrates can selectively supress specific microbial communities via grazing (Altmann et al. 2004), which may stimulate the propagation of others.

Recent studies have revealed active transcription of functional genes encoding multiple NO_3^- reduction pathways in animal bodies (Poulsen et al., 2014; Stief et al., 2018), indicating a possible hotspot for NO_3^- reduction. Even though interactions between microbes and macrofauna are likely widespread, however, they are largely understudied due to methodological limitations or oversimplification of experimental approaches. Therefore, so far it remains poorly explored, and thus understood what is a typical macrofauna-associated microbiome. Furthermore, the cumulative effects of macrofauna and their associated microbiomes are rarely accounted for in biogeochemical studies and their actual magnitude may be underestimated when assessing ecosystem-wide processes. Some studies (e.g. van der Heide et al., 2012) reveal interesting and potentially important effects produced by macrofauna holobionts on element cycling (e.g. high rates of sulphide and methane oxidation or of N_2 fixation), which may have consequences for the functioning of entire ecosystems. The interdisciplinary approaches, combining functional genomics and biogeochemical methods, are therefore needed to bridge the existing gaps of knowledge and to understand N cycling that can be attributed to invertebrate animals and their microbial partners (e.g. Petersen and Osviatic, 2018).

Why is it important to study common macrofauna holobionts?

Estuarine environments process large amounts of carbon and N during transport to the ocean; thus, they play an invaluable ecosystem services. They thus play an important yet poorly constrained role in global biogeochemical cycling and climate regulation (Regnier et al., 2013; Carstensen et al., 2020), therefore there is a lack of data for managers planning or evaluating the effects of management actions on the marine environment. The further progress in understanding benthic ecosystem functioning and biogeochemical services performed by macrofauna would help constrain data on biogeochemical cycling in estuarine environments that essential to preserving habitats as requested under the European Union (EU) Habitats Directive and to achieve a good environmental status as required under the EU Marine Strategy Framework Directive. Given the wide range of economic benefits provided by estuarine zones to many sectors, this study will result in essential knowledge that will contribute to improving quality of life along European coasts.

Today, the stability of estuarine benthic habitats is in danger, as animals are harvested by humans and key habitats are lost or degraded due to many stressors. In turn, these changes can

cause key functions (e.g. environment detoxification, nutrient recycling) of macrofauna holobionts to be lost or to become redundant for ecosystem functioning. For this reason, the study is timely and helps to better understanding the distribution, diversity and functional role of common macrofauna-associated microbes in estuarine ecosystems across a geographical gradient (subtropical, north temperate, and boreal).

In addition, simultaneous analysis of whole benthic community functioning and of the metabolic activity of single macrofauna taxa or their associated microbes may help addressing the species role in the community, and may identify interspecific interactions. The detection of N transformations in common macrofauna holobionts may highlight hidden and interactive effects among microbes and animals, which should be considered analysing benthic functioning. We expected the main biogeochemical processes in sediment to be predominantly the result of the collective effects of different functional groups and their mutual interactions with associated microbes.

AIMS OF THESIS

In this thesis, we investigated the contribution of common macrofauna in shallow estuarine benthic sediments with emphasis on the role of ecological interactions between microbes and their invertebrate hosts on regulation of N cycling processes. We used a combination of ecological, biogeochemical, and molecular approaches to partitioning the direct and indirect role of macrofauna including bioturbation, physiological and holobionts activities in benthic habitats. The main aims were:

1. To identify the role abundant fiddler crab holobionts in N cycling processes in a pristine mangrove ecosystem (SW Atlantic Ocean), Paper II.

2. Applying integrated approach, which includes benthic community (whole core) as well as holobiont (single individual) incubations, to disentangle and reconstruct N cycling in chironomid larvae reworked sediments in eutrophic freshwater lagoon (SE Baltic Sea), Papers I and III.

3. To determine the effect of simplified macrofaunal community and their associated microbes on benthic N cycling, and partition functionally distinct macrofauna holobionts contribution to the specific pathways (northern Baltic Sea), Paper V.

4. To asses a composition of macrofauna-associated microbial communities and quantify their genetic potential in N cycling processes, Papers I–IV.

The above objectives were designed to validate the following hypotheses:

Hypothesis 1: Common macrofauna holobionts are hotspots for N cycling processes in the coastal benthic compartment.

Hypothesis 2: N removal processes dominate over N_2 fixation in macrofauna holobionts.

MATERIAL AND METHODS

Study sites

Samples for experimental activities with macrofauna and their associated microbes were collected in three different estuarine environments (Fig. 2): the Cananéia (II study), the Curonian Lagoon (I, III and IV studies), and the Öre Estuary (V study). These systems cover a large geographical gradient (tropical, northern temperate and borial latitudes) allowing to desitangle holobionts role in wider context with different macrofauna taxa.

Fig. 2. Map showing geographical location of studies estuarine systems.

The estuarine system of Cananéia (tropical latitudes) is located on the south coast of Brazil. This tropical estuarine system, extending over an area of 110 km^2, is part of the Cananéia-Iguape complex and is characterized by the presence of mangroves, restingas, inland seas and islands (Cananéia, Cardoso, Comprida, and Iguape). The system receives seasonally variable nutrient inputs depending on rainfalls, however, dissolved inorganic nitrogen (DIN) concentration in this oligotrophic system rarely exceeds >4 µM of DIN (Barrera-Alba et al., 2008). Specimens of the fiddler crab were collected in their burrows during low tide from a muddy bank nearby a small channel (25º2'55.50'', 47º58'31.24'').

The Curonian Lagoon is a north temperate system (area = 1584 km^2) located along the southeast coast of the Baltic Sea. The lagoon is a shallow waterbody (mean depth = 3.8 m) that discharges to the Baltic Sea through the narrow Klaipeda strait and occasionally receives inputs

from the Baltic during periods of wind-driven tidal forcing (Zemlys et al., 2013). These events are typically of short duration and result in small increases in salinity (typically by 1–2) in the northern portion of the lagoon. Due to external and internal nutrient inputs, the lagoon is subjected to hypereutrophic conditions with peak chlorophyll a reaching 400 µg Chl-a L^{-1} (Zilius et al., 2018). Samples for I and III studies were collected at a deeper (3.5 m depth) muddy site in the central part of the lagoon (55°17'51.7"N, 21°00'36.0"E), whereas samples for IV study were taken from a shallow sandy site (1.2 m depth) of lagoon (55°20′25.9″N, 21°11′24.4″E).

The Öre Estuary is a boreal estuarine system (~71 km^2) located on the Swedish coast of the Quark Strait, between the Bothnian Bay and Bothnian Sea (northern Baltic Sea). The estuary is brackish (< 6), and oligotrophic due to limited nutrient inputs from watershed (Hellemann et al., 2017; Voss et al., 2020), which mainly consists of coniferous forests and mires. This estuary is stratified depending on spatiotemporal gradient of salinity, changing upon seasonal river discharge, and summer temperature (Brydsten and Jansson, 1989; Bartl et al., 2019). The estuarine sedimentary environment varies from silt to fine sandy deposits (Hellemann et al., 2017). Sediments and animals for experimental activities were collected along a grid of 9 sites within the dashed area comprised between monitoring stations NB3, N8 and NB7, where water depths average 17 ± 3 m (see Paper V for details).

Design of experimental activities

In each studied estuarine systems, the experimental activities with macrofauna and its associated microbes followed the similar methodological steps (Fig. 3): 1) *ecological*, 2) *functional genomics*, and 3) *biogeochemical approaches*.

The *ecological approach* was based on the identification of dominant macrofauna taxa and their putative role in benthic functioning. In this step, we used existing monitoring data about animal densities and biomass. In the result, the list of targeted macrofauna taxa and habitat characteristics was determined, which are provided in Table 1. The main studied taxa are attributed to deposit feeders and filter–feeders guilds. However, these two groups have variable bioturbation modes, implying from surface sediment reworking to deep "gallery" burrow construction. Therefore, they may create steep redox gradients across sediment-water interface, regulate electron acceptor and N availability resulting in variable stimulation of N cycling processes.

The *functional genomics approach* was employed 1) to quantify genetic potential of microbial community involved N cycling processes in the host (abundance and transcription of maker genes), 2) to identify diversity of host-associated microbial community (16S r-RNA), and 3) to screen its genetic capacity to mediate N cycling pathways (metagenome). However, different combinations of molecular techniques were frequently used to study each macrofauna holobiont.

METHODOLOGICAL APPROACH

Fig. 3. Schematic representation of experimental activities in studying invertebrate–bacteria associations.

The *biogeochemical approach* implied intact sediment cores or microcosms with reconstructed sediments, and single invertebrate incubations. Such integrated approach, which included benthic community (whole core = sediment + macrofauna holobiont) as well as holobiont (single individual) incubations, allowed us to disentangle and reconstruct N cycling in benthic community, highlighting interactive effects among the sediment, microbes and macrofauna (Papers I, III–V). Intact cores with natural benthic macrofauna communities were collected in the Öre Estuary (Paper V) and the Curonian Lagoon (Paper IV). Whereas microcosms, containing reconstructed sediments, were employed only in experiments with *C. plumosus* (Papers I and III). This approach was required due to disperse larvae distribution in soft-bottom sediments in the Curonian Lagoon, which would obscure density effect in the intact cores (Zettler and Daunys, 2007). The microcosms were pre-incubated for 15 days to allow for the establishment of stable vertical and horizontal chemical gradients and the growth of microbial communities in subsurface oxic and suboxic niches (Stocum and Plante, 2006). In contrast to the other benthic macrofauna, fiddler crabs with associated microbes periodically migrated and interact with multiple environments, including sediment, water and atmosphere; therefore we have simplified approach and studied only individuals.

All intact cores and microcosms with reconstructed sediments were maintained submerged into tanks, containing *in situ* water at ambient temperature as previously described by Benelli et al. (2018) and Zilius et al. (2018). Briefly, each core/microcosm was provided with a Teflon-coated

magnetic bar suspended 9 cm above the sediment-water interface and driven by an external magnet rotating at 40 rpm. The magnetic bars ensured water mixing within each core, avoiding sediment resuspension. The water in each tank was also stirred by aquarium pumps in order to maintain O_2 saturated conditions.

Table 1. Summary of studied macrofauna taxa in different estuarine systems. CE – the estuarine system of Cananéia, CL – the Curonian Lagoon, OE – Öre estuary; FF – filter feeder, DF – deposit feeder.

System	Macrofauna taxa	Feeding guild	Bioturbation	Habitat type
CE	*Leptuca thayeri (fiddler crab)*	DF	Burrow building	Muddy bank
CL	*Chironomus plumosus (chironomid larvae)*	DF/FF	U-shaped burrow building	Soft-bottom
CL	*Dreisena polymorpha (zebra mussel)*	FF	Reef building	Fine sand bottom
OE	*Limecola balthica (clam)*	FF/DF	Fine sediment reworking	Soft-bottom
OE	*Monoporeia affinis (amphipod)*	DF	U-shaped burrow building	Soft-bottom
OE	*Marenzelleria* spp. *(polychaete)*	DF	Gallery building	Soft-bottom

Single animals with associated bacteria (holobionts) were incubated in small Pexiglass and glass microcosms filled with filtered and/or isotope treated *in situ* water to measure holobionts-associated N transformations (i.e. NO_3^- reduction, N_2 fixation) and host physiological processes (excretion, respiration). This allowed us to tease apart direct and indirect effects of individuals in benthic metabolism and N cycling pathways. More details about single individual incubations is provided in text below and Papers III–V.

Whole core measurements

Intact cores and microcosms with sediments, containing macrofauna, were incubated following standard procedure as previously described by Dalsgaard et al. (2000). The incubation lasted from 3 to 9 h in order to keep final O_2 concentration within 20–30% of the initial value. The incubation time was specific for each experiment, and depended on 1) microbial activity, 2) macrofauna biomass, and 3) incubation temperature. At the beginning and the end of the incubation, water aliquots were collected from each core/microcosm for further dissolved gas (O_2, N_2) and nutrient (NH_4^+, NO_x^-, DON, DIP, and DSi) measurements. Samples for gas measurements were immediately fixed with 200 µL of 7M $ZnCl_2$, and for nutrient analysis were frozen at –20 ºC (see details below).

After the flux measurements, intact cores and microcosms were opened, and always left submerged in the incubation tank for 13 h. Afterwards, nitrate (NO_3^-) reduction processes were measured following the revised isotope pairing technique (r-IPT, Risgaard-Petersen et al., 2003). Briefly, all cores and microcosms were spiked with $^{15}NO_3^-$ tracer (20 mM $Na^{15}NO_3$, 98 atom % ^{15}N, Sigma Aldrich) to a final concentration of 10–40 μM depending on the *in situ* $^{14}NO_3^-$ concentration. To calculate the isotopic enrichment, water samples for NO_3^- analysis were collected prior to and after the tracer addition. At the end of incubations, the water and the sediment phases were gently mixed to a slurry. Thereafter, 20 mL aliquots of the slurry were transferred into 12 mL exetainers (Labco Ltd) allowing twice overflow, and fixed with 200 μL of 7 M $ZnCl_2$ for later $^{29}N_2$ and $^{30}N_2$ analyses (NO_3^- reduction through denitrification). An additional 40 mL subsample was collected, transferred to 50 mL falcon vials and treated with 2 g of KCl for the determination of the exchangeable NH_4^+ pool and the $^{15}NH_4^+$ fraction (NO_3^- reduction through DNRA). After the incubations the sediments from all cores were carefully sieved (0.5 mm mesh size) to retrieve macrofauna for further taxonomic identification and determination of abundance and biomass. In Paper V, total denitrification and DNRA rates were divided into rates of denitrification and ammonification of NO_3^- diffusing to anoxic sediments from the overlaying water column (D_w and $DNRA_w$, respectively) and rates of denitrification and ammonification of NO_3^- produced within sediments via nitrification (D_n and $DNRA_n$, respectively) (Bonaglia et al., 2014).

Holobiont incubations

Individual incubations were used to quantify N cycling (denitrification, DNRA, anammox and N_2 fixation) associated with the macrofauna holobionts (III–V studies). Briefly, individuals of each macrofauna taxa were incubated in small bottom-capped Plexiglas cylindrical microcosms (total volume 227 ± 3 mL) partly filled with sterilized glass beads (Ø 1–1.3 mm) and the rest with 0.22 μm bi-filtered, aerated estuary water, amended with different isotopes (see text below). Glass beads were added to create an artificial, 1–4 cm thick sterilized substrate for the invertebrates. We noticed that burrowing organisms, when incubated in water alone, tend to be stressed trying to dig and hide. Glass beads partially overcome this problem, offer the possibility to invertebrates to burrow and feel more comfortable during the incubations and to avoid overestimation of metabolic activities. The water was filtered (MCE filters, 142 mm diameter, pore size 0.22 μM, MF-Millipore™) to remove phytoplankton, suspended particles and microbes, so that metabolic rates measured in the incubation could be solely attributed to the animal's microbiota growing inside (e.g. in the digestive system) or outside (e.g. the shell, cuticle or exoskeleton) the macrofauna. All microcosms were equipped with a stirring magnet for continuous water mixing (20 rpm) during

incubation, and with gas tight lids on the top, containing two sampling ports for sample collection and water replacement. Details on the incubations conditions are reported in Table 2.

Table 2. Summary of experimental conditions during the holobiont incubation. CL – the Curonian Lagoon, OE – Öre estuary.

System	Incubated taxa	Incubation temperature	NH_4^+ conc.	NO_3^- conc.
CL	*Chironomus plumosus (chironomid larvae)*	10°C	4.8 μM	26.7 μM
CL	*Dreisena polymorpha (zebra mussel)*	23°C	0.5 μM	0.2 μM
OE	*Limecola balthica (clam)*	12°C	0.4 μM	0.1 μM
OE	*Monoporeia affinis (amphipod)*	12°C	0.4 μM	0.1 μM
OE	*Marenzelleria* spp. *(polychaete)*	12°C	0.4 μM	0.1 μM

Nitrate reduction

The r-IPT was used to assess NO_3^- reduction processes associated with animals, including denitrification, DNRA, and anammox (Thamdrup and Dalsgaard, 2002; Risgaard-Petersen et al., 2003). Three different macrofauna treatments, each with 5 replicates (containing 6 ind. of *C. plumosus*, 1 of *D. polymorpha*, 19–24 ind. of *M. affinis*, 2 ind. of *L. balthica* or 1–2 ind. of *Marenzelleria* spp.) and 1 control (only water) were applied. The first treatment had low $^{15}NO_3^-$ addition to a final concentration of 5.4–21.1 μM, the second treatment had high $^{15}NO_3^-$ addition to a final concentration of 19.0–35.4 μM, and the third treatment had simultaneous $^{15}NH_4^+$ (15 mM $^{15}NH_4Cl$, 98 atom % ^{15}N, Sigma Aldrich) and $^{14}NO_3^-$ additions to final concentrations of 4.5–32.2 and 6.2–26.2 μM, respectively; see more information about tracer concentrations in Papers III–V. The different $^{15}NO_3^-$ concentrations used in treatments 1 and 2 were to explain the IPT assumptions (Risgaard-Petersen et al., 2003). After capping the microcosms, they were incubated in the dark at ambient temperature. The incubation time was set from pilot tests on holobionts respiration rates and by real time monitoring of O_2 concentrations in the microcosms with optodes (FireStingO2, PyroScience GmbH). The rationale was to avoid excess decrease of O_2 that may affect microbial activity (e.g. inhibit nitrification or stimulate denitrification), ultimately leading to underestimated or overestimated in situ rates. During the incubations, water aliquots were subsampled and replaced at three time points (+ time zero = four total incubation times) from each replicate, transferred without headspace into 12 mL exetainers (Labco Ltd) allowing overflow, and fixed with 200 μL of 7 M $ZnCl_2$ for gas measurements.

Slopes of the linear regression of $^{29}N_2$ and $^{30}N_2$ concentrations (see section "Analytical analysis" for more details) versus time were used to calculate rates of denitrification and anammox, using the equations from Thamdrup and Dalsgaard (2002). The slope of the linear regression of $^{15}NH_4^+$ concentration (see section "Analytical analysis" for more details) versus time was used to calculate rates of DNRA according to Bonaglia et al. (2016). The increase of the three ^{15}N species (i.e., $^{29}N_2$, $^{30}N_2$, and $^{15}NH_4^+$) versus time was statistically tested via regression analysis using the whole dataset inclusive of the four time points and only significant ($p < 0.05$) regressions were computed into NO_3^- reduction rates. Rates were then calculated as a function of number or biomass of macrofauna, and corrected with values detected in the controls.

Nitrogen fixation

To determine rates of N_2 fixation, a stock solution of 0.22 μm twice-filtered and $^{30}N_2$-enriched water was prepared using a modified version of the method described in Klawonn et al. (2015). Before starting the incubation, isotopically enriched water was every time gently transferred into 16 microcosms to minimize gas exchange with the atmosphere. Afterwards, animals (6 ind. of *C. plumosus*, 2 of *D. polymorpha*, 3 ind. of *M. affinis*, 2 ind. of *L. balthica* or 2 ind. of *Marenzelleria* spp.) were added in each microcosm, and incubation started when the microcosms were capped. In addition, four microcosms were prepared and incubated as described above, but with unlabelled water to serve as control for isotopic contamination. Microcosms were incubated under the same conditions as described for NO_3^- reduction experiments. Every 12 hours one control and four microcosms with tracer were retrieved and opened. The animals were then collected, measured for their wet weight and stored at –20 °C for later ^{15}N incorporation analysis. Eight freshly sampled animals were always preserved without any incubation to determine the natural $^{15}N/^{14}N$ ratios. N_2 fixation rates were calculated as previously described in Cardini et al. (2019).

Host animal excretion and respiration

Measurements of host animal excretion and respiration were performed in order to determine their contribution to net benthic fluxes of NH_4^+ and O_2 (Paper III, V). Briefly, six 22 mL glass microcosms with different number of animals (4 ind. of *C. plumosus*, 6 ind. of *M. affinis*, 2 ind. of *L. balthica* or 2 ind. of *Marenzelleria* spp. per vial) added to 0.22μm filtered water were incubated; dissolved O_2 were continuously monitored with an optical oxygen meter (FireStingO2, PyroScience GmbH). In addition, two controls for each incubation were added later to correct rates in vials with animals. Incubations were carried out in the dark at ambient temperature and lasted depending on animal activity. At the beginning and at the end of the incubation a 5 ml aliquot was

collected from each vial and filtered into plastic test tubes for later NH_4^+ analyses. At the end of the experiment, animals were recovered and weighed. Excretion and respiration rates were then normalized to the number of animals or biomass corrected with control.

Nitrogen flux and production associated with fiddler crab holobionts

Net N fluxes and ^{15}N probing experiments were used to quantify physiological activity of fiddler crabs and contribution of their associated microbial community to the N cycling processes. A different biogeochemical approach was used due to taxa-specific behaviour (see Paper II). Briefly, crab individuals (1 ind. per microcosm) were incubated in small bottom-capped Plexiglas cylindrical microcosms (total volume 227 ± 3 mL, n=5) filled with unfiltered seawater from the sampling site. In parallel, control microcosms with water alone (n = 3) were prepared in order to correct process rates measured in crab microcosms. All microcosms were equipped with rotating magnets to ensure continuous water mixing (25 rpm). At the beginning and end of the incubations (from each microcosms) aliquots were collected for gas and nutrient analysis. After incubation, crabs from all microcosms were used to determine carapace area, dry weight (at 60 °C for 48 h), and thereafter analysed for isotopic composition.

In addition, ^{15}N tracer slurry incubations, which allow determination of potential rates, were applied to quantify NH_4^+ oxidation to NO_3^- (nitrification) and its reduction to N_2 (denitrification) and NH_4^+ (DNRA). The material for slurry incubation was collected from 22 crab carapaces (for a total area of ~ 60 cm^2) by gentle brushing using a sterile toothbrush while holding single crab individual in separate glass beaker with 0.22-μm-filtered ambient water (500 ml). Afterwards, the homogenized slurries underwent oxic and anoxic incubations to measure different potential N metabolic pathways: 1) nitrification (addition of $^{14}NH_4^+$) and 2) denitrification + DNRA (addition of $^{15}NO_3^-$). Potential nitrification rates were estimated in oxic incubations with samples collected at the beginning and end of incubation for nitrite and nitrate analysis. The NO_3^- reduction processes were measured in 12 mL exetainers (n=24) after additions of $^{15}NO_3^-$ to a final concentration of 100 μM. More details about incubation conditions and experimental design is provided in Paper II. The measured N excretion/production, and NO_3^- reduction rates were normalized for the dry weigh (dw) of crab biomass.

Analytical analysis

Dissolved inorganic nutrients from experiments were GF/F filtered and stored frozen until analysis with a continuous flow analyser (Scan^{++}, Skalar) using standard colorimetric methods (Téguer et al., 1975; Grasshoff, 1983). Total dissolved nitrogen (TDN) was determined with the high

temperature (680 °C) combustion, catalytic oxidation/NDIR method using a analyser with a TN module (TOC 5000 analyser, Shimadzu Corp.). For more detailed information about methods, see papers II and III.

Gasses (O_2, N_2) were measured via the N_2:Ar and O_2:Ar technique by membrane inlet mass spectrometry (MIMS; Kana et al., 1994) and corrected for Ar concentration and solubility based on incubation water temperature and salinity (Colt, 2012). Isotopic composition of produced $^{29}N_2$ and $^{30}N_2$ production were analysed by gas chromatography-isotopic ratio mass spectrometry (GC-IRMS) at the University of Southern Denmark. Briefly, headspace subsamples were injected into a GC extraction line equipped with an ascarite trap, a Porapak R chromatographic column, a copper column heated to 600°C, and a $Mg(ClO_4)_2$ trap (De Brabandere et al., 2015). The extraction line was coupled to an IRMS (Delta V Plus, Thermo Scientific) by means of a Conflo III interface. Samples for $^{15}NH_4^+$ production were analysed by the same GC-IRMS after conversion of NH_4^+ to N_2 (De Brabandere et al., 2015) by the addition of alkaline hypobromite (Warembourg, 1993).

Particulate organic nitrogen (PON) content and its isotopic composition in animal tissues and sediment samples were analyzed by a Flash EA 1112 elemental analyser connected to a Delta V Advantage IRMS (Thermo Scientific) at the University of Sao Paulo (Brazil) and at the Center for Physical Science and Technology (Lithuania). Measured δ values (‰) were corrected using two laboratory standards calibrated against international reference materials (IAEA-600, IAEA-N-2). For more detailed information about method, see Papers II and III. The long-term standard deviation was <0.2‰ for $\delta^{15}N$.

Molecular analysis

Samples for DNA and RNA analysis were collected from different parts of the host body (soft tissue, carapace or whole body) and ambient environment (sediment and water). Biofilm samples (Paper II) was collected from the carapace of randomly selected crabs (n = 3, with total surface area of ~ 8 cm^2) by using swabs (after rinsing in 0.2-μm-filtered seawater). In experiments with zebra mussels (Paper IV), soft tissue of animals (from in the holobiont incubation) and the suspended material from *in situ* water sample were used for nucleic acid extraction. Suspended material was size-fractioned in two size groups, i.e., >10 mm, and 0.22–10 mm (from here on referred to as large and small fraction, respectively) by step-wise filtration of the water as described in Zilius et al. (2020). Whereas in experiments with chironomid larvae (Papers I and III), sediments for molecular analyses were subsampled from the two randomly selected bioturbated cores by collecting approximately 1.5–2 g of subsurface (3–5 cm depth) anoxic sediment and sediments along the burrow wall with a sterile spatula. Anoxic sediments and sediment around burrows were

clearly distinguishable by their color, with a light-brown-to-black transition from the oxidized burrow to the outer, chemically reduced sediment. Chironomid larvae were retrieved from sediments and washed with sterile distilled water (three times). Samples collected in Cananéia (Brazil) were later preserved in RNAlater due to logistic constrains (Zymo Research) whereas samples from the Curonian Lagoon were immediately snap-frozen in liquid N_2. All samples was stored at $-80°C$ until the analysis. In laboratory, nucleic acids (DNA, RNA) were extracted using standard kits (QIAamp Fast DNA Stool Mini Kit and RNA easy Mini Kit, respectively, Qiagen), following the manufacturer's protocol with amended lysis temperature (see Paper I–IV). In addition, extracted RNA purification was performed using the commercial kit (PureLink PCR Purification Kit, Invitrogen) according to manufacturer's instructions. To check whether an RNA sample was free of DNA, a control polymerase chain reaction (PCR) was carried out using universal bacterial primers of 16S rRNA as described in Paper I. Later reverse transcription (RT) was performed with a SuperScript III Reverse Transcriptase (Invitrogen) to obtain complementary DNA (cDNA). The final products were used for 1) 16S rRNA gene amplicon sequencing (Papers I–III), 2) shotgun metagenomic sequencing (Paper II), and 3) functional gene quantification by qPCR (I–IV). 16S rRNA gene sequences amplified from extracted DNA (targeting the V3 region) were used for profiling the microbial community in the environment where samples for N cycling process rates were taken and in macrofaunal hosts, which allowed identification of specify of harboured bacteria. Details on the bioinformatics used are given in Papers I and II. Shotgun-based metagenomics analysis was used to identify microbiome on biofilm–coated carapace. Applied bioinformatics are in details described in Paper II. Briefly, protein annotated sequences were analysed in MEGAN using the database "*acc2interpro-June2018X.abin*" that links accession numbers to the InterPro database and Gene Ontology (GO) categories. The taxonomy and protein data attributed to N cycling were extracted from MEGAN and the average read count for R1 and R2 was used for further analysis. Quantitative polymerase chain reactions (qPCR) were used to quantify the abundance of functional genes and transcripts involved in N-cycling in larvae and adult midges (1) haem-containing nitrite reductase (*nirS*), (2) cytochrome C nitrite reductase (*nrfA*), (3) archaeal and bacterial ammonia monooxygenase (*amoA*-A and *amoA*-B, respectively) and (4) Mo-containing nitrogenase (*nifH*). More details about PCR product purification, quantification and construction of standard curves are provided in Paper I. The abundance and expression of target genes (DNA and RNA samples, respectively) were recalculated to copies per g fresh weight of larvae or expressed per number of 16S rRNA gene copies.

Main statistical methods

Quantitative data for benthic fluxes, process rates and functional genes were visualized using boxplots or bar pots. Differences between treatments (by mean or median) were checked using different statistical analysis depending on the context: parametric (t-test, variance analysis) and nonparametric tests (Kruskal–Wallis, Man–Whitney rank) (Papers I, III–V). In case for significant factors during variance analysis, post hoc pairwise comparisons were performed using the Student–Newman–Keuls (SNK) test. In addition, the relationship between biomass of mixed macrofauna community and benthic fluxes and NO_3^- reduction processes were examined using linear regression. The assumptions, data normality, and homogeneity of variance, were checked using Shapiro–Wilk test and Cochran's test, respectively. In addition, the t-test was used to validate tracer effect on denitrification rates (holobiont incubation). Analyses were performed using SigmaPlot 14.0 software.

A distance-based linear model (distLM) was applied to explain the contribution of macrofauna taxa (metabolism, bioturbation effect) to the variability of specific NO_3^- reduction process and benthic fluxes (Paper V). The biomass of dominant macrofauna taxa was used as a biological predictor. Briefly, the distLM was built on stepwise selection, employing 9999 permutations at a significance level of $p < 0.05$. The resemblance matrices were built on between-sample similarities of Euclidean distance using normalized and logarithmically transformed fluxes and process rates obtained from 18 incubation cores (Clarke and Gorley, 2006). The obtained results were visualized with distance-based redundancy analysis (db-RDA, Anderson et al., 2008), and vectors overlay for analysing predictor variables relationship with response vectors. The analysis was performed using the PRIMER 6 statistical package with the PERMANOVA+ add-on (Primer-E Ltd.; Clarke and Gorley, 2006).

RESULTS AND DISCUSSION

The role of common macrofauna holobionts in benthic ecosystem functioning in this study is supported by findings across a geographical locations: 1) a tropical estuarine system with abundant fiddler crab population (Paper II), 2) north temperate freshwater lagoon with chironomid larvae and zebra mussel populations (Paper I, III and IV), and 3) oligotrophic estuary with three dominant macrofaunal taxa (Paper V). The results of later show how a relatively simple benthic community, hosting three functionally distinct but complementary macrofaunal organisms, actively contributes to benthic N cycling. The contribution includes animal metabolism, burrowing activities, and to a lesser extent processes carried out by holobionts. On the contrary, fiddler crab-associated diazotrophic bacteria actively fix N to environment, largely covering benthic community nutritional needs. The detection of multiple N transformations in chironomid larvae and zebra mussel holobionts suggested a community-associated versatile microbiome, which contributes to the biogeochemical processes.

Nitrogen cycling processes associated with the fiddler crab (*Leptuca thayeri*) holobionts

Biofilm-covered fiddler crabs were collected from an open muddy bank near a tidal creek, where sunlight stimulates the growth of phototrophic microorganisms (Fig. 4). These fiddler crabs are abundant and constantly migrate between burrows and the sediment surface; such vertical and horizontal migrations across contrasting environmental gradients (light regime, salinity, redox conditions, nutrients, organic matter) have the potential to create strong selective pressures on its biofilm-associated prokaryotes.
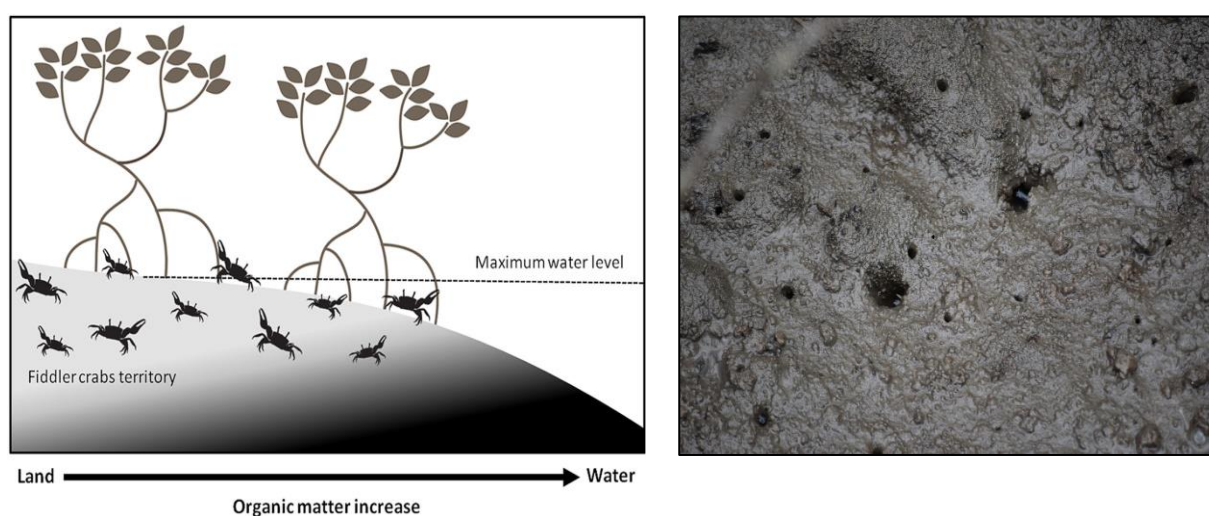

Fig. 4. The distribution of fiddler crabs in coastline according to De Grande et al. (2018) (left panel) and holes of crab burrows in muddy sediments (right panel).

The results show that biofilm-covered crabs actively released NH_4^+ and dissolved organic nitrogen (DON), which corresponded to 35% and 58% of total dissolved N production (DIN+DON) (Fig. 5). The release of DON is an interesting finding since most of decapod crustaceans primarily excrete ammonia (NH_3) or the conjugated acid NH_4^+ (Weihrauch et al., 2017). Nevertheless, it has been shown that some decapods (e.g., shrimps living at lower temperatures than in our study site), can excrete DON, although this never exceeds NH_4^+ excretion (Jiang et al., 2000). In the fiddler crab, the substantial amount of released DON might partly derive from fixed N, which is not assimilated by the crab and its associated microbiota. However, the biochemical mechanisms that promote such DON release should be addressed in future studies.
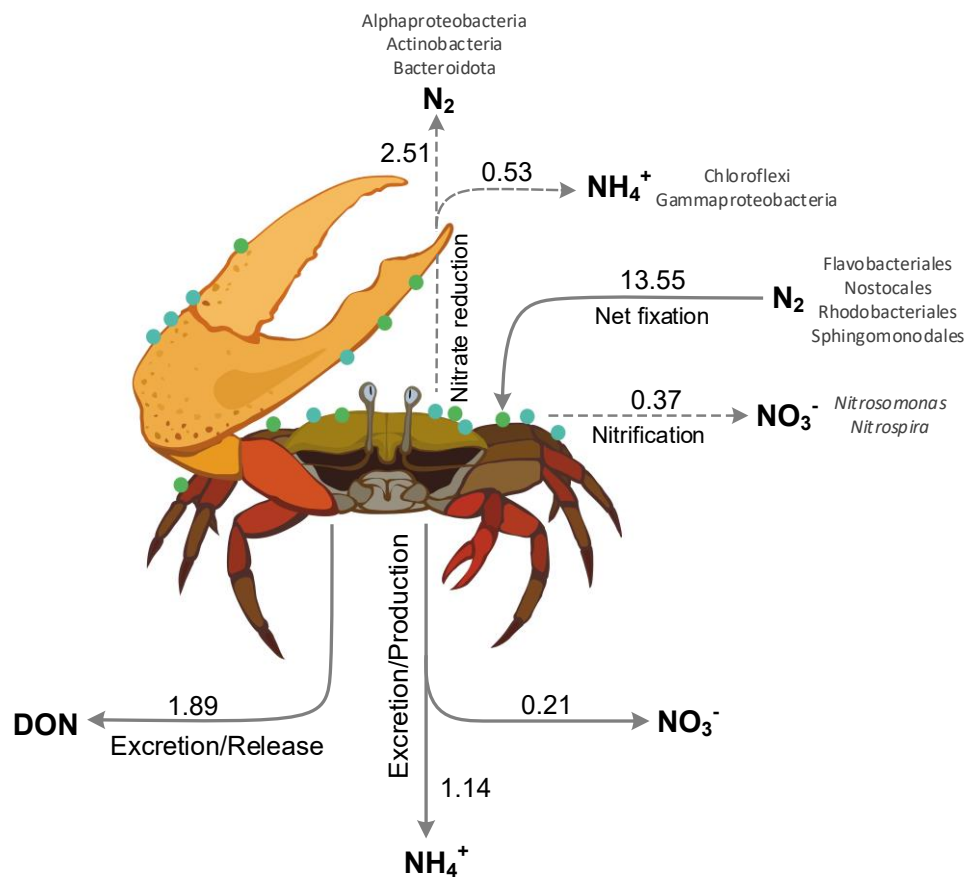

Fig. 5. Flowchart of N cycling by the fiddler crab holobiont. All fluxes were obtained combining data from incubations of single crab holobiont (*in situ* rates, solid lines) and suspended biofilm (potential rates, dashed lines). Note that reported rates are expressed as µmol N crab^{-1} d^{-1}. The main taxonomic groups involved in N cycling as indicated by metagenomics analyses are provided. Drawing by V. Gasiūnaitė. (Paper II)

Net production of NO_3^- and NO_2^- associated with fiddler crab was quantitatively less important, comprising together < 7% of total dissolved N production. The oxic biofilm slurries incubation and measured net NO_x^- flux between crab and water phase support the idea that NO_3^- and NO_2^- production associated with fiddler crabs likely occurs due to nitrification (i.e. the recycling of N through oxidation of NH_4^+ to NO_3^-). However, in our study nitrification and

excretion by the fiddler crab holobiont could only support 8–15% of denitrification potential (Fig. 5). Nevertheless, despite the high potential denitrification rates found in incubations under anaerobic conditions, the metabolic capacity of denitrifiers is likely limited by low NO_3^- background concentrations in the surrounding water ($NO_3^- < 0.5$ µM). In line to previous study, NO_3^- produced in other holobionts during nitrification can partly support denitrification inside the biofilm (Heisterkamp et al., 2013).

Biogeochemical measurements also indicated the metabolic potential for DNRA (0.82 ± 0.05 µmol N gdw^{-1} biofilm d^{-1}) in crab holobionts. Though DNRA genetic potential based on q-PCR was quantitatively similar to that of denitrification (2.42×10^3 and 1.53×10^3 gene copy, respectively; see Paper II), process measurements indicated a much higher expression of the latter, and denitrification (3.89 ± 0.72 µmol N gdw^{-1} biofilm d^{-1}) was a dominant pathway of NO_3^- reduction in the biofilm slurries. Anammox appeared to be a negligible process within the biofilm, probably being suppressed by the fluctuating environmental conditions (temperature, O_2, and nutrient concentrations) experienced by the crab holobionts, which are unfavourable to slow-growing anammox bacteria (Strous et al., 1999).

The negative flux of N_2 measured during the individual fiddler crab incubations indicates a N_2 fixation, which was a dominant metabolic pathways compared to other N cycling processes within holobiont. In addition, depleted ^{15}N stable isotope signatures further point at N_2 fixation as a relevant process within the biofilm (Fig. 6).
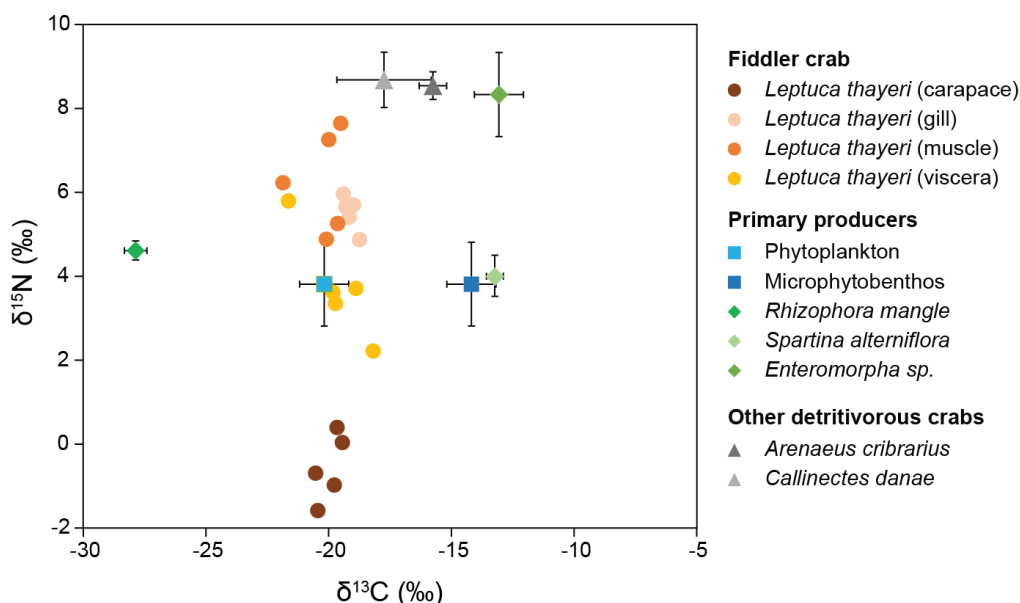

Fig. 6. Signature of N_2 fixation in crab's carapace biofilms stable isotope ratios: biplot of the natural abundance of ^{13}C and ^{15}N isotopes for different samples (carapace, gill, muscle, viscera) from the fiddler crab (*Leptuca thayeri*, n=5), and for different primary producers (as potential sources of detritus) and other detritivores crab species from the Cananéia estuarine system (data from Nagata et al., 2015) (Paper II).

Dinitrogen fixation is a common process in mangrove ecosystems, where the highest activities are found associated with the mangrove rhizosphere (Reis et al., 2017). The presence of N_2-fixing prokaryotes in the mangrove rhizosphere is often explained by a mutualistic relationship between the bacteria and the plant, with roots exuding dissolved carbon required for diazotrophic growth (Nagata et al., 2015). Similarly, although fiddler crabs may take advantage of N_2 fixers residing on their carapace; the depleted ^{15}N signatures in their tissues compared to other detritivorous crab species from the same site may indicate a nutritional relationship between the fiddler crab host and its microbiota (see Paper II).

In the oligotrophic estuarine system of Cananéia, with minimum abundance of 10 crab individuals per square meter (Masunari, 2006), fiddler crabs holobionts can produce 33 μmol m^{-2} d^{-1} of dissolved N which can compensate/reverse total dissolved N (DIN+DON) uptake measured at the sediment-water interface (-71 μmol m^{-2} d^{-1}; Reis et al., 2017). In addition, N_2 fixation associated with fiddler crab carapaces can deliver 135 μmol N m^{-2} d^{-1} which compares to 27% of N_2 fixation in surface microbial mats (500 μmol m^{-2} d^{-1}; Reis et al., 2017). Since the fiddler crabs intermolt and molt cycles last < 150 days (Hopkins, 1982), the labile organic matter of the biofilm–covered carapace is delivered to the benthic system at least 3 times per year and can prime heterotrophy by relieving the very high C:N sediment ratios. Whereas dissimilative processes like denitrification have only little ecological meaning here as they are constrained by low N availability in the water column or within sediments.

Nitrogen cycling in soft-bottom habitat dominated by chironomid larvae (*Chironomus plumosus*) holobionts

Chironomid larvae are the dominant macrofaunal species in the organic-rich sediments of the Curonian Lagoon (Zettler and Daunys, 2007). The presence of this tube-dwelling macrofauna had contrasting effects on benthic metabolism and N cycling pathways (Papers I and III). A density-dependent effect was observed on the net fluxes of O_2 and NO_3^- at the sediment-water interface (p < 0.001), with higher rates at 1800 ind. m^{-2} that at other two densities (0 and 600 ind. m^{-2}). At a density of 1,800 larvae m^{-2}, a realistic density for large areas of the Curonian Lagoon (Zettler and Daunys, 2007), half of the O_2 demand was associated with microbial respiration in the upper oxic layer ($\sim$ 4 mm) and the other half to respiration by the chironomids and in the subsurface burrow network (Fig. 7). Based on results from the individual incubations, 12 to 15% of the total O_2 consumption can be attributed to larvae respiration, and 27 to 38% – to microbial or chemical consumption along the burrow walls. In freshwater sediments, microbial communities consume O_2 mostly for organic matter mineralization or oxidation of reduced compounds (e.g. NH_4^+, Fe^{2+} or Mn^{2+}).
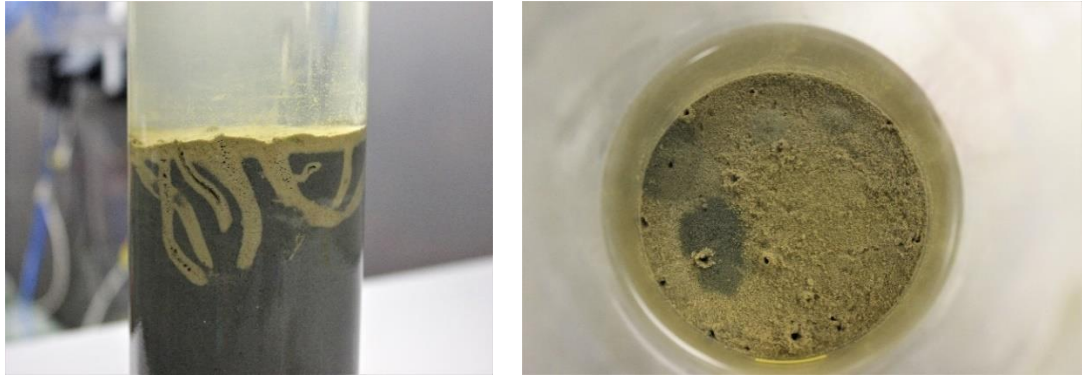
Fig. 7. The bioturbation effects of chironomid larvae, evident in sharp contrast between light-brown oxidized surface and burrow sediment, and black chemically reduced subsurface sediment (photo by A. Mačiūtė). (Paper I)

The finding of a significant ($p < 0.001$) correlation between larvae abundance and net flux of NO_3^- [flux (μmol N m^{-2} h^{-1}) = -0.043 × density + 8.716; R^2=0.96] (Paper III) suggest it increasing consumption in burrows during their intermittent ventilation (Fig. 8). We can assume that NO_3^- pumped into the burrows can either be reduced by microbiota in the burrow walls or in the larvae body through denitrification or DNRA processes.
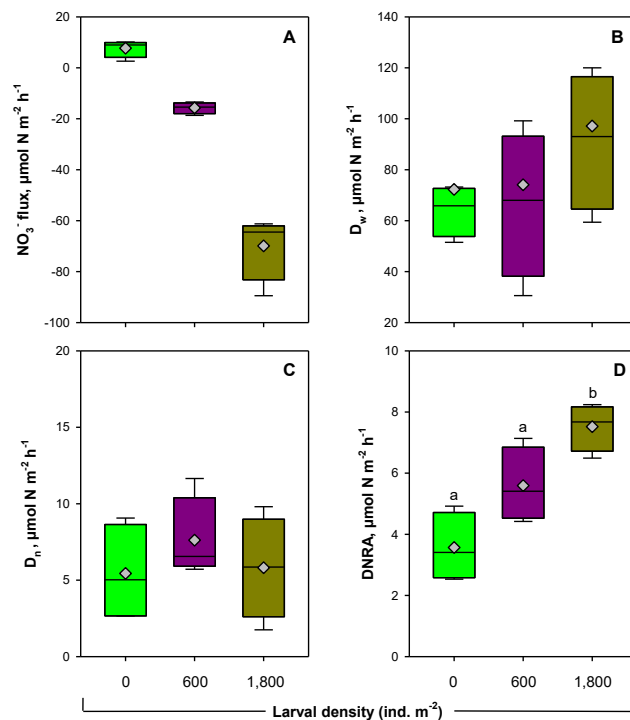

Fig. 8. Net fluxes of nitrates (a), denitrification of water column NO_3^- (b), coupled nitrification-denitrification (c), and dissimilative nitrate reduction to ammonium (d) measured in whole core incubations with different densities of chironomid larvae. Data range (whiskers), upper and lower quartiles (edges), the median (horizontal line), and the mean (grey diamond) are represented for n = 4 replicates. Labelling by letters indicates the outcome of post hoc pairwise comparisons, i.e. bars sharing the same letter are not significantly different ($p > 0.05$). Modified from Paper IV.

The results show that NO_3^- from overlying water was the main source (90%) for denitrification; however, high variability masked significant differences among treatments. DNRA rates increased significantly with larvae density (Kruskal-Wallis, $p = 0.003$), with 43% higher rates (7.5 ± 0.4 μmol N m^{-2} h^{-1}) at 1,800 ind. m^{-2} when compared to the non-bioturbated sediment (3.6 ± 0.6 μmol N m^{-2} h^{-1}). At a density of 1,800 ind. m^{-2}, nearly 7% of NO_3^- reduction was attributed to DNRA process. The dominance of denitrification over DNRA in chironomid reworked sediments might be explained by a relatively low sedimentary C:N ratio in the sediment substrate and by a relatively high NO_3^- availability as electron acceptor (Tiedje et al., 1983). Additionally, low temperature and low salinity in the Curonian Lagoon may create more favourable conditions for denitrifiers than for DNRA bacteria (Giblin et al., 2010).

With increasing bioturbation activity, we expected higher NH_4^+ efflux due to upward transport of pore water during burrow ventilation. However, this was not the case in our microcosms with high larvae densities. The measured NH_4^+ efflux was higher ($p < 0.05$) at 600 ind. m^{-2} density (3.4 ± 2.3 μmol N m^{-2} h^{-1}) than in the 0 (-11.2 ± 0.6 μmol N m^{-2} h^{-1}) and 1800 ind. m^{-2} densities (-10.2 ± 3.8 μmol N m^{-2} h^{-1}). These results are consistent with findings of Benelli et al. (2018), showing that with increasing chironomid larvae densities, NH_4^+ concentration in pore water substantially decreases, ultimately setting the fluxes to zero. This might explain why the NH_4^+ flux was directed towards the sediment at larvae density of 1800 ind. m^{-2}. In chironomid burrows, the NH_4^+ from animal excretion, organic matter mineralization or NO_3^- ammonification might be released to the water column through burrow ventilation (Svenson, 1997). It is difficult to infer how much NH_4^+ was delivered from organic matter mineralization, but we can account for the contribution from the other sources. Excretion of chironomid larvae at 1800 ind. m^{-2} density generated 316.3 μmol N m^{-2} d^{-1}, whereas NO_3^- ammonification in sediments and burrow walls produced 177.6 μmol N m^{-2} d^{-1} through DNRA. All these processes together would likely supply large amounts of NH_4^+, which could be nitrified. Although the burrow network provides an extended oxidised layer of sediment around the burrow walls and an excess of NH_4^+ potentially favourable for nitrifiers (Fig. 7), their transcriptional activity was found barely different from the surrounding environment (Paper I). Overall, our combined data on experimental fluxes estimates and molecular analyses suggest that the presence of chironomids does significantly enhance activity of nitrifiers, similar to what has been reported in previous studies (e.g. Stief and de Beer, 2006; Benelli et al., 2018; Moares et al., 2018).

Our results show that in muddy sediments with densities up to 1800 ind. m^{-2} denitrification and DNRA by the chironomid larvae holobiont accounted for only 0.3–0.4% of NO_3^- reduction in constructed burrows (Fig. 9). These measured rates suggests that the impact of chironomid larvae on denitrification was mainly indirect (related to the altered sediment microbial activity), rather

than via stimulation of NO_3^- reduction in anoxic sections of the animal body. In addition, this study provides the first evidence that microbiota of chironomid larvae are actively involved in N_2 fixation (0.02 µmol N m^{-2} h^{-1}), although its contribution is minor when compared to whole core fluxes in the burrow environment.
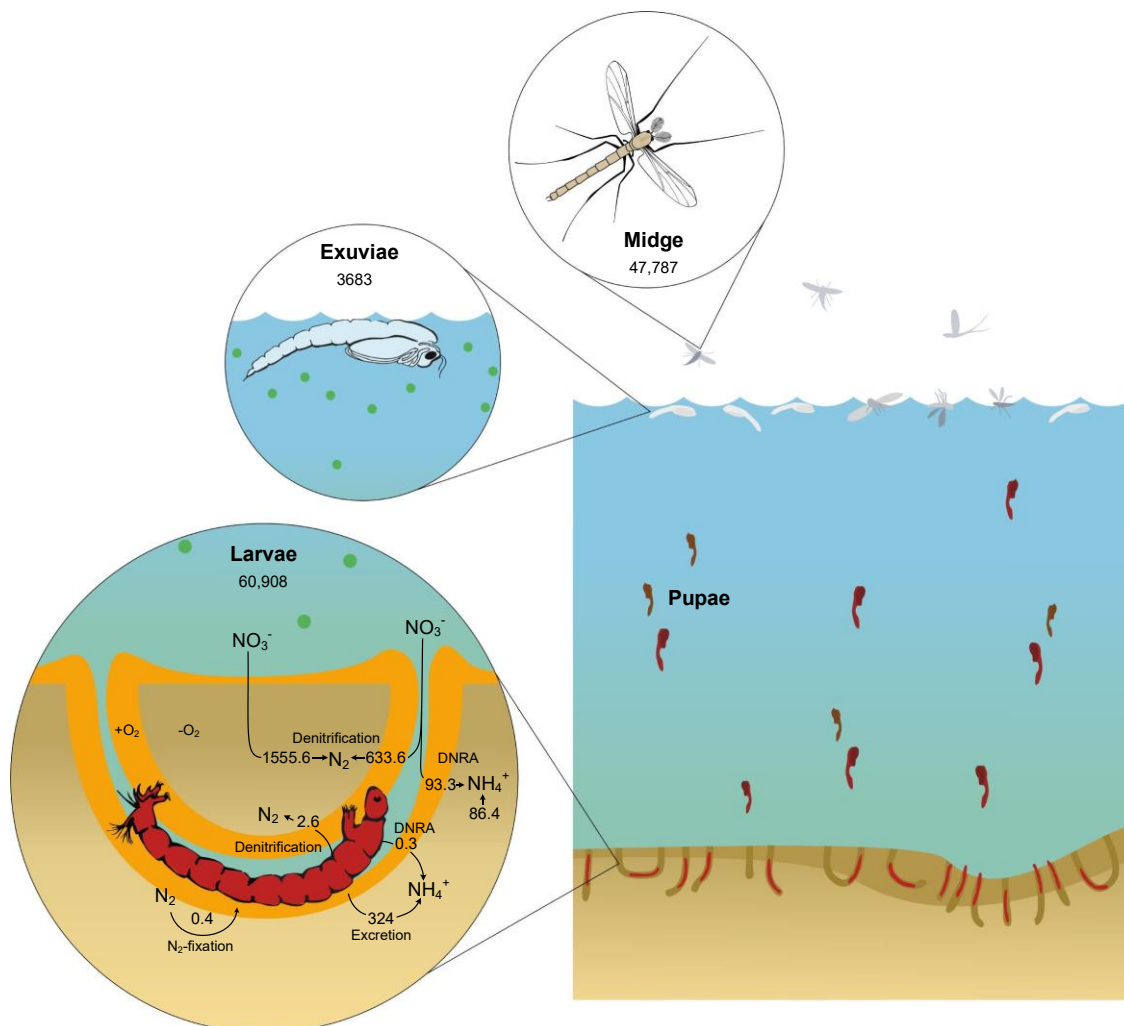

Fig. 9. Flowchart of N-cycling associated with chironomid larvae activities. All fluxes were obtained combining data from incubations of whole core (sediment + larvae) and individual (larvae alone) incubations. Note that rates are reported for sediments inhabited by 1800 larvae per m^2 and are expressed as µmol N m^{-2} d^{-1}. The particulate organic N storage in each life stage is reported in µmol N m^{-2} when presence of 1800 larvae individuals. Drawing by V. Gasiūnaitė (Paper III).

Partitioning nitrogen cycling processes among three common macrofauna holobionts in low biodiversity community

In boreal Öre Estuary, we studied benthic respiration, net N fluxes and N-related microbial processes in sediments colonized by a relatively simple macrofaunal community, hosting three different functional groups. We aimed at understanding how interactions among functionally distinct macrofauna affect specific-pathways of the benthic N cycling. While the effects of

individual functional groups are quite well understood (Mermillod-Blondin and Rosenberg, 2006; Stief, 2013, and references therein), relatively little is known on their aggregated effect in a whole community context. The three taxa investigated comprised 70% of the total macrofauna abundance and 98% of the total biomass in the low diversity benthic community of the Öre Estuary, and explained nearly 30% of variation of the measured biogeochemical processes.

Single animal incubations allowed to quantify the direct contribution of macrofauna to O_2 respiration, which corresponded to nearly 22% of the total benthic O_2 uptake, within the range of 12–25% reported for other marine and coastal systems (Piepenburg et al., 1995; Glud et al., 2003; Paper III). *Marenzelleria* spp. alone accounted for nearly half of macrofaunal community respiration, indicating it as a keystone taxa in benthic metabolism. However, incubations of macrofauna alone remain always challenging due to the stress of animals.

The results of the multivariate analysis (see Fig. 6 in Paper V) applied to unmanipulated community in intact sediments and associated benthic processes suggest that the net O_2 flux was primarily correlated with higher density of clams. It appears that *L. balthica*, like other buried clams, may expel oxic water through the pedal gape and thus maintain an oxic layer at the shell-sediment interface (Camillini et al., 2019), which stimulates microbial and meiofaunal metabolism (Reise, 1983; Karlson et al., 2005). Although clams are semi-mobile subsurface dwelling organisms, and cannot produce comparable effects on solute exchange as polychaetes or amphipods (e.g. Michaud et al., 2005), their biodeposition of faeces may also significantly stimulate the activity of microbial community in surface sediments, ultimately increasing the species role in benthic metabolism (Karlson et al., 2005).

Since surface sediments were oxic and pore water in the upper 10 cm did not have free sulphide (see also Lenstra et al., 2018), most of the O_2 consumption was likely due to organic matter mineralisation or NH_4^+ oxidation to NO_3^- via nitrification. Based on measured NO_x^- effluxes and NO_3^- reduction processes (D_n and $DNRA_n$) we were able to estimate potential nitrification and, thus, mineralization rates within sediments (Fig. 10). As 2 moles of O_2 are used to oxidize 1 mole of NH_4^+ to NO_3^- then nitrification would account for 11% of total O_2 uptake (70.2–206.3 μmol O_2 m^{-2} d^{-1}) in these sediments. Such O_2 demand for nitrification is the highest in relative terms (as % of total O_2 consumption) among those reported in studies in the Baltic Sea using the IPT (< 6%; Karlson et al., 2005; Bonaglia et al., 2014; Bartoli et al., 2021), indicating favourable conditions for nitrifying bacteria. Besides the amount used to oxidize NH_4^+, a residual 67% of total O_2 uptake, corresponding to 949.0 ± 50.4 μmol O_2 m^{-2} d^{-1}, was likely used for organic N ammonification. Assuming a respiratory quotient of 1 (Hargrave and Phillips, 1981) and C:N molar ratio of 10.5 in upper sediments organic mineralization would yield 90.4 ± 1.4 μmol N m^{-2} d^{-1}. Alternatively, macrofaunal community directly via excretion supplied 28.3 ± 4.1 μmol N m^{-2}

d^{-1}, which accounts for ~24% of total NH$_4^+$ production (excretion + ammonification). Macrofauna excretion, on the other hand, was equivalent to 90% of the measured net NH$_4^+$ efflux at the sediment-water interface (Fig. 10). It may consider that most of the NH$_4^+$ excreted by macrofauna was likely transferred to bottom waters, whereas another fraction, primarily regenerated via organic matter ammonification, was oxidized, assimilated or retained within sediments. The results further show that clams alone contributed for up to ~ 60% of the measured excretion by the mixed community. Bivalves like *L. baltica* typically excretes higher amount of NH$_4^+$ when compared to other feeding guilds (e.g. Vanni et al., 2017). Given the fact that this clam has a larger gut it can ingest larger particles and has higher food availability. Additionally, a shift from suspension filtering to deposit feeding for *L. baltica* allows for greater food availability and quality (Olafsson, 1986).
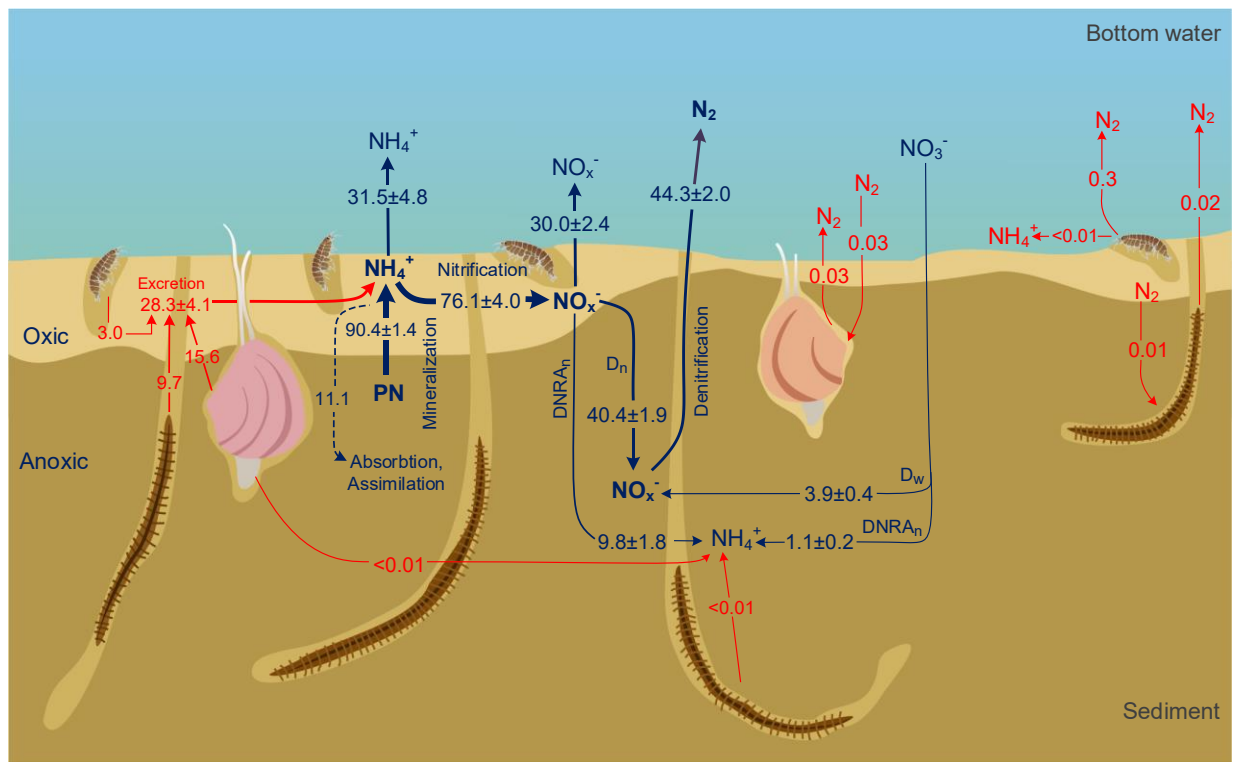

Fig. 10. Flowchart of N cycling in the Öre estuarine sediments hosting the dominant macrofauna species *M. affinis*, *Marenzelleria* spp., and *L. balthica*. Nitrogen transformations were calculated combining measured fluxes and processes in benthic community (unmanipulated whole core incubations = sediment + macrofauna) and macrofauna alone (individual incubations). The animal excretion rates and holobionts-mediated N cycling were calculated based on mean macrofauna biomass in the study area. Equations used to calculate fluxes and process rates are provided in the supplementary material (Table S2, Paper V). Note that rates reported in the figure are expressed as µmol N m^{-2} h^{-1}. Results report means and standard errors based on experiment replicates (n=6 to 18, see the methods for details). Drawing by V. Gasiūnaitė (Paper V).

In the studied habitats, approximately 63% of the regenerated NH$_4^+$ was further oxidized to NO$_x^-$ (Fig. 9). Accordingly, nitrification can rapidly (~6 days) deplete the standing NH$_4^+$ pool in

the upper sediment layer (473 µmol m^{-2}; Bartl., 2019), indicating high turnover rates of N that are maintained by continuous replete from mineralization and/or upward diffusion from deeper layers. Multivariate analysis demonstrated that *M. affinis* primarily stimulated NO_3^- reduction pathways coupled to nitrification (D_n, $DNRA_n$), whereas *Marenzelleria* spp., due to NO_3^- downward transport from bottom water, stimulated the reduction of water column nitrate (D_w). The surface deposit dweller *M. affinis* actively mixes the uppermost sediment layer, and thereby increases solute exchange and sediment oxygenation (Viitasalo-Frösén et al., 2009; Bonaglia et al., 2019). In contrast, *Marenzelleria* spp., capable of construction and bioirrigation of relatively deep burrows, likely facilitated D_w and $DNRA_w$, in deeper layers. Similar effects by amphipods and polychaetes on NO_3^- reduction pathways were previously observed in experimental studies where individual functional groups were analyzed (Tuominen et al., 1999; Karlson et al., 2005; Bonaglia et al., 2013). Although bioturbation can produce contrasting effects on NO_3^- reduction pathways, however, it is largely regulated by NO_3^- availability due to stimulated nitrification or enhanced non-local solute exchange (Bonaglia et al., 2013; Nogaro and Burgin, 2014).

Macrofauna, besides bioturbating sediments and ventilating burrows also host complex microbiomes, which consist of unique assemblages or overlap communities found in the surrounding environment. Our findings show that all three key Baltic macrofauna taxa harboured metabolically diverse microbial communities capable of different N transformations such as denitrification, DNRA and/or N_2 fixation. Scaling up these process rates with the average macrofauna biomass at the study area, we were able to estimate the contribution of holobionts to multiple N-cycling pathways (Fig. 10). The holobionts of whole benthic community, based on biomass estimations, together contributed 1% of denitrification and 0.1% of DNRA measured in sediments, which was estimated to be 0.4 µmol N m^{-2} h^{-1}. The holobiont of clams and polychaetes were also capable for N_2 fixation (0.03 and 0.01 µmol N m^{-2} h^{-1}, respectively) (Fig. 10). Although the holobiont contribution to the N cycling pathways in sediment is marginal in this study, this might be different in other seasons or habitats characterized by much higher macrofauna densities or larger specimens. As the abundance of this soft bottom community can be higher in the other Baltic Sea areas (Gogina and Zettler 2010), we may also expect there higher holobionts contribution to the benthic N cycling. However, it remains questionable to what extent our upscaling reflects *in situ* rates of N transformations in holobionts as we incubated adult macrofauna individuals while the community includes different generation specimens (adults and juveniles). Our main assumption here is that the activity of invertebrate-associated microbes is proportional to the invertebrate biomass and does not vary from juveniles to adults. Notably, the holobionts of *M. affinis* due to their high denitrification rates and abundance can contribute up to ~8% of NO_3^- reduction (3.7 µmol N m^{-2} h^{-1}) if abundance data are used for calculations. To better understand

the biomass- and abundance-specific effects on microbial processes in holobionts, measurements of the appropriate metabolic pathways should be carried out across different host age classes and biotic metrics in future studies.

Nitrogen cycling between different macrofauna holobionts

Single animal incubations allowed to elucidate N cycling associated with common macrofaunal holobionts, and quantify their contribution (Table 3). The highest activity was associated NO_3^- reduction to N_2 through denitrification compared to other N cycling processes simultaneously measured in hosts. Whereas DNRA on average accounted for 14% of the total measured NO_3^- reduction in hosts. Additions of $^{15}NH_4^+ + ^{14}NO_3^-$ revealed measurable $^{29}N_2$ production rates, suggesting the presence of putative anammox; however, this pathway contributed less than 2% of the total N_2 production. N_2 fixation was also found in host animals (Table 3), with substantially higher rates in mollusc holobionts. On average, under our experimental conditions, N_2 fixation was equalled approximately 37% of the denitrification rate. Although higher rates of all N transformations (except for anammox) were found in zebra mussel holobionts, this might be due to the substantially higher incubation temperature (23°C), which enhanced enzymatic activity.

Table 3. The rates of total denitrification (D_{14}), and dissimilative nitrate reduction to ammonium (DNRA), putative anaerobic ammonium oxidation (AAO) and N_2 fixation associated with macrofauna holobionts (individual incubations). Results are represent by mean and standard error based on replicates (Paper III–V)

Holobiont species	Feeding guild of host	Process rates (nmol N g_{dw}^{-1} h^{-1})			
		Denitrification	DNRA	Putative AAO	N_2 fixation
C. plumosus	Deposit feeder/ Filter feeder	9.0 ± 1.1	0.9 ± 0.2	0.19 ± 0.03	0.9 ± 0.3
D. polymorpha	Filter feeder	58.4 ± 28.9	31.2 ± 19.3	0	21.9 ± 4.5
M. affinis	Deposit feeder	26.8 ± 8.9	1.9 ± 0.5	0.11 ± 0.05	0
Marenzelleria spp.	Deposit feeder	1.7 ± 0.1	0.3 ± 0.1	0	6.5 ± 0.9
L. balthica	Filter feeder/ Deposit feeder	7.3 ± 3.0	0.2 ± 0.1	0.02 ± 0.003	11.4 ± 2.5

Denitrification rates associated with *M. affinis* holobionts were at least 66% higher than to those measured at a similar temperature in chironomid larvae (*C. plumosus*). Though added tracer concentration differed between these two experiments, with 2-fold higher in *C. plumosus*, results indicate higher activity of denitrifiers under lower NO_3^- concentration in *M. affinis* holobionts. The possible explanations for different rates might be attributed to variable number of denitrifiers

in hosts as well as their affinity for NO_3^- or quality of available carbon. Since these hosts occupy different niches in sediments and microbial communities display steep vertical zonation in sediments, different microorganisms with unique metabolic features characterize holobionts. Moreover, our finding of higher denitrification rates associated with *D. polymorpha* is not surprising given that transcription of denitrification marker genes, encoding NO_2^- reduction and its derivatives, typically occurs under low O_2 conditions (Härtig and Zumft, 1999), similar to those in macrofaunal gut (Stief and Eller, 2006; Bonaglia et al., 2017).

The finding of relatively high denitrification rates associated with the amphipod *M. affinis* among three Baltic macrofauna was rather surprising due to its body size. Recently, it has been demonstrated that even tiny carcasses of zooplankton can provide anaerobic microniches favourable for denitrifiers or DNRA bacteria in oxic environments (Glud et al., 2015; Stief et al., 2018). Likewise, active NO_3^- reducing bacteria were found on the fiddler crab carapace (Paper II). Although we cannot rule out nitrate reduction in the amphipod intestine, bacteria present on the carapace will benefit from direct access to NO_3^-, which likely is abundant in the burrow environment. The gene copy and transcript numbers of the NO_3^- respiring community were often an order of magnitude lower than that of denitrifying community, indicating lower genetic potential (Paper I–III). The re-occurrence of DNRA confirms that NH_4^+ production, associated with macrofauna, is a complex process driven by both animal excretion and the activity of associated DNRA bacteria (Papers II and III).Measured diazotrophic activity in animal holobionts from the cold boreal estuary was in the range of that observed in other animals from southern eutrophic estuarine systems of the Baltic Sea (21.9–517.1 nmol g_{DW}^{-1} d^{-1}). Though there is evidences of higher diazotrophic activity in filter–feeding hosts, such a feeding mode does not necessarily can favour N_2 fixation; for example *L. baltica* can shift between suspension and deposit feeding (Riisgård and Kamermans, 2001). Due to various feeding modes diazotrophic microorganisms can inhabit different body parts including gills, foot, gut or body surface as has been seen from other N cycling pathways (Heisterkamp et al., 2013). Overall, our finding of diazotrophic activity in holobionts at different coastal sites of the Baltic Sea suggests that this process is widespread across diverse taxa of benthic macrofauna even when N concentrations are not limiting but also highlights a high individual variability.

Holobionts diversity in host invertebrates

The measured biogeochemical rates support the idea that common macrofauna from temperate and boreal estuarine systems act as a host for unique repertoire of microorganisms or inoculated from surrounding environment during feeding or burrowing activities (Bordenstein and Theis, 2015; Poulsen et al., 2014; Ceullar-Gempeler and Leibold, 2018). Interestingly, the microbial

communities found in all studied host invertebrates varying widely across the geographical gradient contributed to N cycling processes. Still questions remain whether the single bacteria group in the community were versatile and capable of different N cycling pathways. Denitrifiers were the most active functional group in most of studied hosts.

The metagenomic analysis revealed that crab biofilm-coated carapace harboured microbial community capable for complete N cycle. Interesting, N_2 fixation was one of the most dominant pathways compared to other N cycling processes associated with fiddler crab microbiota. The most represented taxa within the biofilm was the Cyanobacteria genus *Geitlerinema*, which dominated the community with ~12% of all 16S rRNA gene sequences (see Paper II), suggesting an important role within the assemblage. Other potential N_2 fixers were affiliated with well-known diazotrophic bacterial taxa like Sphingomonadales, Rhodobacteriales and Flavobacteriales. Interestingly, on the crabs' carapace, a N_2-fixing consortium might represent an association arranged along environmental gradients within the biofilm (e.g. light, O_2) and whose strategy is to cooperate in order to enhance diazotrophic activity under N-limiting conditions (Beltrán et al., 2012). The dominance of *Geitlerinema* spp. might be ascribed to its metabolic plasticity allowing it to cope with both high sulphide concentrations, which may build-up in clogged burrows, and air exposure when the crab migrates to the surface (Grim and Dick, 2016).

The NO_3^- respiring microbial phyla on the biofilm-covered crab carapace in our samples were Alphaproteobacteria, Actinobacteria, Bacteroidota, Chloroflexi and Gammaproteobacteria, all common in the marine environment in the marine environment (Jiang et al., 2015). The genuses *Janibacter (Intrasporangiaceae)* and *Aquimarina (Flavobacteriaceae)* were also highly represented in the crab's microbiota and both have the metabolic capacity to reduce NO_3^- (Li et al., 2012; Xu et al., 2015). Most identified bacteria possessed all four genes (*nar/nap, nir, nor* and *nos*) which allow for complete NO_3^- reduction to N_2 as the end product (Zumft, 1997). Whereas the major groups containing the array of genes NapC/NirT/Nrf (therein *nrf*A), responsible for DNRA, were assigned primarily to Chloroflexi (Anaerolineae) and to unclassified Gammaproteobacteria. On the contrary, our combined data of q-PCR suggest that among the studied N cycling pathways in chironomid larvae (Papers I, III), denitrification was a dominant, based on the abundance of *nirS* transcripts. These finding suggest that within each of habitats holobionts could have different genetic potential in contributing N cycling processes.

Phylogenetic analysis revealed that zebra mussels in a eutrophic lagoon host a unique repertoire of active diazotrophs (Paper IV). This finding is in line with a recent study, showing that host invertebrates are able through different mechanisms to select unique assemblages of active bacteria (Weingarten et al., 2019). In zebra mussels, the diazotrophic community was dominated by a large fraction of unknown Bacteria, followed by *Paenibacillus* and a smaller

fraction of unknown Firmicutes. Interestingly, none of these groups were detected in water samples, which were almost completely dominated by Nostocales (83.4%) and Zoogloea (16.6%). These taxa are known to be responsible for most of annual pelagic N_2 fixation (Zilius et al., 2020). Our finding of active N_2 fixation in chironomid larvae holobionts also was rather surprising given the relatively high ambient NH_4^+ concentrations and low temperature (Knapp, 2012). A comparison of gene and transcripts abundance suggests that *nifH* genes were expressed in the microbiota. Previous analyses of 16S rRNA diversity of the microbiome associated with chironomid larvae indicated the prevalence of Proteobacteria and Firmicutes, including diazotrophic taxa (Paper I). Although these bacteria are ubiquitous, they may benefit from the association with chironomid larvae, due to the easy access to electron acceptors (e.g. NO_3^-) or organic substrate needed for energy acquisition (Chaston and Goodrich-Blair, 2010). Further, although it is generally believed that high N concentrations suppress N_2 fixation, heterotrophic diazotrophs may remain metabolically active, as is the case in the Curonian Lagoon waters (Zilius, et al., 2020). N_2 fixing bacteria within the host harboured microbiota may use this process as a strategy to cope with fluctuations of N availability (Cardini et al., 2019) or to successfully compete against other bacteria that more efficiently take up N.

CONCLUSIONS

The only way to understand ecosystem functioning, which is a complex matter, is to use a methodologically integrated approach. The simultaneous analysis of whole benthic community functioning and of the metabolic activity of single macrofauna taxa helps addressing the species role in the community, and identify interspecific interactions. Such complex approach derives from the interaction of different disciplines, including zoology, biogeochemistry, microbial and molecular ecology. Therefore, results from this thesis contribute to the understanding of benthic functioning and, specifically, they address the interactions among microbes and macrofauna. Main outcomes of present research are here reported:

1. The results show that macrofauna-microbes associations (holobionts) are wide spread in estuarine environments across a geographical gradient. Holobionts can simultaneously contribute to multiple N cycling processes, including denitrification, DNRA and N_2 fixation.

2. In a pristine estuarine system, fiddler crab holobionts are hotspots of benthic N cycling, suggesting that this characteristic benthic invertebrate has a potentially relevant role in mangrove ecosystems as a vector of newly fixed N to the surrounding environment.

3. Chironomid larvae impact different N cycling processes. Besides creating O_2 microniches in NH_4^+-rich subsurface sediments via burrow digging and ventilation, chironomid larvae serve themselves as hotspots of microbial communities involved in N cycling. However, such effects are interrupted when chironomid larvae undergoes metamorphosis to flying midges and abandon the sediment.

4. The three dominant macrofaunal taxa in low biodiversity community together alter benthic functioning directly by their impact on microbial respiration and excretion (direct effect), and indirectly by feedbacks to NO_3^- reduction processes. These results suggest that the community has a major role in direct release of NH_4^+ and a minor, but important role in its oxidation via nitrification. However, holobiont role in these host are orders of magnitude lower than sediment rates.

5. Macrofauna hosts harbour distinct microbial communities with different genetic potential in N cycling processes. The findings further suggest that within each of habitats holobionts could be shaped by a different array of environmental conditions forming unique assemblages.

REFERENCES

Altmann, D., P. Stief, R. Amann, and D. de Beer, D. 2004. Nitrification in freshwater sediments as influenced by insect larvae: Quantification by microsensors and fluorescence in situ hybridization, Microbial Ecology 48: 145–153.

Anderson M, R. Gorley, and K. Clarke. 2008. PERMANOVA+ for PRIMER: guide to software and statistical methods. PRIMER-E, Plymouth, pp 214

Arfken, A., B. Song, J.S. Bowman, and M. Piehler. 2017. Denitrification potential of the eastern oyster microbiome using a 16S rRNA gene based metabolic inference approach. PLoS ONE 12(9): e0185071.

Barrera-Alba, J.J., S.M.F. Gianesella, G.A.O. Moser, and F.M.P. Saldanha-Corrêa. 2008. Bacterial and phytoplankton dynamics in a sub-tropical Estuary. Hydrobiologia 598: 229–246.

Bartl, I., D. Hellemann, Ch. Rabouille, K. Schulz, P. Tallberg, S. Hietanen, and M. Voss. 2019. Particulate organic matter controls benthic microbial N retention and N removal in contrasting estuaries of the Baltic Sea. Biogeosciences 16: 3543–3564.

Bartoli, M., D. Nizzoli, M. Zilius, M. Bresciani, A. Pusceddu, S. Bianchelli, K. Sundbäck, A. Razinkovas-Baziukas, and P. Viaroli. 2021. Denitrification, nitrogen uptake, and organic matter quality undergo different seasonality in sandy and muddy sediments of a turbid estuary. Frontiers in Microbiology 11: 612700.

Beltrán, Y., C.M. Centeno, F. García-Oliva, P. Legendre, and L.I. Falcón. 2012. N_2 fixation rates and associated diversity (*nifH*) of microbialite and mat-forming consortia from different aquatic environments in Mexico. Aquatic Microbial Ecology 65: 15–24.

Benelli, S., M. Bartoli, M. Zilius, I. Vybernaite-Lubiene, T. Ruginis, J. Petkuviene, and E.A. Fano. 2018. Microphytobenthos and chironomid larvae attenuate nutrient recycling in shallow-water sediments. Freshwater Biology 63(2): 187–20.

Bianchi, T.S. 2007. Biogeochemistry of estuaries. Oxford University Press: New York, USA.

Bonaglia, S., M. Bartoli, J.S. Gunnarsson, L. Rahm, C. Raymond, O. Svensson, S. Shakeri Yekta, and V. Brüchert. 2013. Effect of reoxygenation and Marenzelleria spp. bioturbation on Baltic Sea sediment metabolism. Marine Ecology Progress Series 482: 43–55.

Bonaglia, S., B. Deutsch, M. Bartoli, H.K. Marchant, and V. Bruchert. 2014. Seasonal oxygen, nitrogen and phosphorus benthic cycling along an impacted Baltic Sea estuary: regulation and spatial patterns. Biogeochemistry 119: 139−160.

Bonaglia, S., I. Klawonn, L. De Brabandere, B. Deutsch, B. Thamdrup, and V. Brüchert. 2016. Denitrification and DNRA at the Baltic Sea oxic–anoxic interface: Substrate spectrum and kinetics. Limnology and Oceanography 61(5): 1900–1915.

Bonaglia, S., V. Brüchert, N. Callac, A. Vicenzi, E.C. Fru, and F.J.A. Nascimento. 2017. Methane fluxes from coastal sediments are enhanced by macrofauna. Scientific Reports 7: 13145.

Bonaglia, S., U. Marzocchi, N. Ekeroth, V. Brüchert, S. Blomqvist, and P.O.J. Hall. 2019. Sulfide oxidation in deep Baltic Sea sediments upon oxygenation and colonization by macrofauna. Marine Biology 166: 149.

Bosch, J.A., J.C. Cornwell, and W.M. Kemp. 2015. Short-term effects of nereid polychaete size and density on sediment inorganic nitrogen cycling under varying oxygen conditions. Marine Ecology Progress Series 524: 155–169.

Bordenstein, S.R., and K.R. Theis. 2015. Host biology in light of the microbiome: ten principles of holobionts and hologenomes. PLoS Biology 13(8): e1002226.

Brydsten, L., and M. Jansson. 1989. Studies of estuarine sediment dynamics using ^{137}Cs from Tjernobyl accident as tracer. Estuarine, Coastal and Shelf Science 28: 249–59.

Caffrey, J.M., J.T. Hollibaugh, and B. Mortazavi. 2016. Living oysters and their shells as sites of nitrification and denitrification. Marine Pollution Bulletin 112(1-2): 86–90

Camillini, N., M. Larsen, and R.N. Glud. 2019. Behavioural patterns of the soft-shell clam *Mya arenaria*: implications for benthic oxygen and nitrogen dynamics. Marine Ecology Progress Series 622: 103–119.

Cardini U, V.N. Bednarz, R.A. Foster, and C. Wild. 2014. Benthic N$_2$ fixation in coral reefs and the potential effects of human-induced environmental change. Ecology and Evolution 4: 1706–1727.

Cardini, U., M. Bartoli, R. Lee, S. Luecker, M. Mooshammer, J. Polzin, M. Weber, and J. Petersen. 2019. Chemosymbiotic bivalves contribute to the nitrogen budget of seagrass ecosystems. The ISME Journal, 13: 3131–3134.

Carstensen, J., D.J. Conley, E. Almroth-Rosell, et al. 2020. Factors regulating the coastal nutrient filter in the Baltic Sea. Ambio 49: 1194–1210.

Chaston, J., Goodrich-Blair, and H. 2010. Common trends in mutualism revealed by model associations between invertebrates and acteria. FEMS Microbiology Reviews 34(1): 41–58.

Christensen, P.B., S. Rysgaard, N.P. Sloth, T. Dalsgaard, and S. Schwærter. 2000. Sediment mineralization, nutrient fluxes, denitrification and dissimilatory nitrate reduction to ammonium in an estuarine fjord with sea cage trout farms. Aquatic Microbial Ecology 21: 73−84.

Clare, D.S., M. Spencer, L.A. Robinson, and C.L.J. Frid. 2016a. Species-specific effects on ecosystem functioning can be altered by interspecific interactions. PLoS ONE 11(11): e01657.

Clare, D.S., M. Spencer, L.A. Robinson, and C.L.J. Frid. 2016b. Species densities, biological interactions and benthic ecosystem functioning: an in situ experiment. Marine Ecology Progress Series 547: 149–161.

Clarke, K., and R. Gorley. 2006. PRIMER v6: User manual/tutorial. PRIMER-E, Plymouth, pp192.

Cuellar-Gempeler, C., and M.A. Leibold. 2018. Multiple colonist pools shape fiddler crab-associated bacterial communities. The ISME Journal 12(3): 825–837.

Colt, J. 2012. Dissolved gas concentration in water: Computation as functions of temperature, salinity and pressure (2nd ed.). London: Elsevier.

Dalsgaard, T., L.P. Nielsen, V. Brotas, et al. 2000. Protocol handbook for NICE—nitrogen cycling in estuaries: a project under the EU research program: Marine Science and Technology (MAST III). National Environmental Research Institute, Silkeborg

Damashek, J., and C.A. Francis. 2018. Microbial nitrogen cycling in estuaries: from genes to ecosystem processes. Estuaries and Coasts 41: 626-660.

De Brabandere, L., S. Bonaglia, M.Y. Kononets, L. Viktorsson, A. Stigebrandt, B. Thamdrup, and P.O.J. Hall. 2015. Oxygenation of an anoxic fjord basin strongly stimulates benthic denitrification and DNRA. Biogeochemistry 126(1-2): 131–152.

De Grandea, F.R., P. Granadoa, F.H.C. Sanches, and T.M. Costac. 2018. Organic matter affects fiddler crab distribution? Results from field and laboratorial trials. Estuarine, Coastal and Shelf Science 212: 138–145.

Dittami, S.M., E. Arboleda, J.C. Auguet, et al. 2021. A community perspective on the concept of marine holobionts: current status, challenges, and future directions. PeerJ 9: e10911.

Ehrnsten, E., X. Sun, C. Humborg, A. Norkko, O.P. Savchuk, C.P. Slomp, K. Timmermann, and B.G. Gustafsson. 2020. Understanding environmental changes in temperate coastal seas: linking models of benthic fauna to carbon and nutrient fluxes. Frontiers in Marine Science 7: 450.

Galloway, J.N., F.J. Dentener, D.G. Capone, E.W. Boyer, R.W. Howarth, S.P. Seitzinger, and C.J. Vöosmarty. 2004. Nitrogen cycles: past, present, and future. Biogeochemistry 70(2): 153–226.

Gamfeldt, L., J.S. Lefcheck, J.E.K. Byrnes, B.J. Cardinale, J.E. Duffy, and J.N. Griffin. 2014. Marine biodiversity and ecosystem functioning: what's known and what's next? Oikos 124: 252–265.

Giblin, A.E., N.B. Weston, G.T. Banta, J. Tucker, and C.S. Hopkinson. 2010.The effects of salinity on nitrogen losses from an oligohaline estuarine sediment. Estuaries and Coasts 33:1054–1068.

Gilbertson, W.W., M. Solan M, and J.I. Prosser. 2012. Differential effects of microorganism–invertebrate interactions on benthic nitrogen cycling. FEMS Microbiology Ecology 82(1): 11–22.

Glud, R.N., J.K. Gundersen, H. Røy, and B.B. Jørgensen. 2003. Seasonal dynamics of benthic O_2 uptake in a semi-enclosed bay: importance of diffusion and fauna activity. Limnology and Oceanography 48(3): 1265–1276.

Glud, R.N., H.-P. Grossart, M. Larsen, K.W. Tang, K.E. Arendt, S. Rysgaard, B. Thamdrup, and T. Gissel Nielsen. 2015. Copepod carcasses as microbial hot spots for pelagic denitrification. Limnology and Oceanography 60: 2026–2036.

Gogina, M., H. Nygård, M. Blomqvist, et al. 2016. The Baltic Sea scale inventory of benthic faunal communities. ICES Journal of Marine Science 73(4): 1196–1213.

Gogina, M., M.L. Zettler. 2010. Diversity and distribution of benthic macrofauna in the Baltic Sea Data inventory and its use for species distribution modelling and prediction. Journal of Sea Research 64: 313–32.

Grasshoff, K. 1982. Determination of nitrate. In K. Grassoff, M. Ehrhardt & K. Kremling (Eds.), Methods of Seawater Analysis. Weinheimm: Verlag Chemie.

Grim, S.L. and G.J. Dick. 2016. Photosynthetic versatility in the genome of *Geitlerinema* sp. PCC 9228 (formerly *Oscillatoria limnetica* 'Solar Lake'), a model anoxygenic photosynthetic cyanobacterium. Frontiers in Microbiology 7: 1546.

Hargrave, B.T. and G.A. Phillips. 1981. Annual in situ carbon dioxide and oxygen flux across a subtidal marine sediment. Estuarine, Costal and Shelf Science 12: 725–737.

Härtig, E., and W.G. Zumft. 1999. Kinetics of nirS expression (cytochrome cd1 nitrite reductase) in *Pseudomonas stutzeri* during the transition from aerobic respiration to denitrification: evidence for a denitrification-specific nitrate- and nitrite-responsive regulatory system. Journal of Bacteriology Research 181(1): 161–166.

Heisterkamp, I.M., A. Schramm, L.H. Larsen, N.B. Svenningsen, G. Lavik, D. de Beer, and P. Stief. 2013. Shell biofilm-associated nitrous oxide production in marine molluscs: processes, precursors and relative importance. Environmental Microbiology 15(7): 1943–55.

Hellemann, D., P. Tallberg, I. Bartl, M. Voss, and S. Hietanen. 2017. Denitrification in an oligotrophic estuary: a delayed sink for riverine nitrate. Marine Ecology Progress Series 583: 63–80.

Herbert, R.A. 1999. Nitrogen cycling in coastal marine ecosystems. FEMS Microbiology Reviews 23(5): 563–590.

Hopkins, P. 1982. Growth and regeneration patterns in the fiddler crab, *Uca pugilator*. Biological Bulletin 163: 301–319.

Hunter, E., H.J. Mills, and J.E. Kostka. 2006. Microbial community diversity associated with carbon and nitrogen cycling in permeable shelf sediments. Applied and Environmental Microbiology 72: 5689–5701.

Jiang, D.-H., A.L. Lawrence, W.H. Neill, and H. Gong. 2000. H. Effects of temperature and salinity on nitrogenous excretion by *Litopenaeus vannamei* juveniles. Journal of Experimental Marine Biology and Ecology 253(2): 193–209.

Jiang, X., H. Dang, and N. Jiao. 2015. Ubiquity and diversity of heterotrophic bacterial *nasA* genes in diverse marine environments. PLoS One 10(2): e0117473.

Kana, T.M., C. Darkangelo, M.D. Hunt, J.B. Oldham, G.E. Bennett, and J.C. Cornwell. 1994. Membrane inlet mass spectrometer for rapid high-precision determination of N_2, O_2, and Ar in environmental water samples. Analytical Chemistry 66(23): 4166–4170.

Karlson, K., S. Hulth, K. Ringdahl, and R. Rosenberg. 2005. Experimental recolonisation of Baltic Sea reduced sediments: survival of benthic macrofauna and effects on nutrient cycling. Marine Ecology Progress Series 294: 35–49.

Kauppi, L., G. Bernard, R. Bastrop, et al. 2018. Increasing densities of an invasive polychaete enhance bioturbation with variable effects on solute fluxes. Scientific Report 8: 7619.

Kessel van M.A.H.J., R.J. Mesman, A. Arshad, et al. 2016. Branchial nitrogen cycle symbionts can remove ammonia in fish gills. Environmental Microbiology Reports 8(5): 590–594.

Klawonn, I., G. Lavik, P. Böning, H. Marchant, J. Dekaezemacker, W. Mohr, and H. Ploug. 2015. Simple approach for the preparation of $^{15-15}N_2$-enriched water for nitrogen fixation assessments: evaluation, application and recommendations. Frontiers in Microbiology 6: 769.

Knapp, A.N. 2012. The sensitivity of marine N_2 fixation to dissolved inorganic nitrogen. Frontiers in Microbiology 3: 374.

König, S., O. Gros, S.E. Heiden, et al. 2016. Nitrogen fixation in a chemoautotrophic lucinid symbiosis. Nature Microbiology 2(1): 16193.

Kristensen, E. 2001. Impact of polychaetes (*Nereis* spp. and *Arenicola marina*) on carbon biogeochemistry in coastal marine sediments. Geochemical Transitions 2: 92–103.

Kristensen, E., G. Penha-Lopes, M. Delefosse, T. Valdemarsen, C.O. Quintana, and G.T. Banta. 2012. What is bioturbation? The need for a precise definition for fauna in aquatic sciences. Marine Ecology Progress Series 446: 285–302.

Laverock, B., K. Tait, J.A. Gilbert, A.M. Osborn, and S. Widdicombe. 2014. Impacts of bioturbation on temporal variation in bacterial and archaeal nitrogen–cycling gene abundance in coastal sediments. Environmental Microbiology Report 6: 113–121.

Lenstra, W.K., M. Egger, N.A.G.M. van Helmond, E. Kritzberg, D.J. Conley, and C.P. Slomp. 2018. Large variations in iron input to an oligotrophic Baltic Sea estuary: impact on sedimentary phosphorus burial. Biogeosciences 15: 6979–6996.

Li, J., L.-J. Long, L.–L. Yang, Y. Xu, F.-Z. Wang, Q.-X. Li, S. Zhang, and W.-J. Li. 2012. *Janibacter alkaliphilus* sp. nov., isolated from coral *Anthogorgia* sp. Antonie van Leeuwenhoek 102(1): 157–62.

Masunari, S. 2006. Distribuição e abundância dos caranguejos *Uca* Leach (Crustacea, Decapoda, Ocypodidae) na Baía de Guaratuba, Paraná, Brasil. Revista Brasileira de Zoologia 23(4): 901–914.

Mermillod-Blondin, F., and R. Rosenberg. 2006. Ecosystem engineering: the impact of bioturbation on biogeochemical processes in marine and freshwater benthic habitats. Aquatic Science 68: 434–442.

Michaud, E., G. Desrosiers, F. Mermillod-Blondin, B. Sundby, and G. Stora. 2005. The functional group approach to bioturbation: II. The effects of the *Macoma balthica* community on fluxes of nutrients and dissolved organic carbon across the sediment–water interface. Journal of Experimental Marine Biology and Ecology 337(2): 178–189.

Moraes, P.C., M. Zilius, S. Benelli, and M. Bartoli. 2018. Nitrification and denitrification in estuarine sediments with tube-dwelling animals. Hydrobiologia 819: 217–230.

Murphy, E.A.K., and M.A. Reidenbach. 2016. Oxygen transport in periodically ventilated polychaete burrows. Marine Biology 163: 208.

Nagata, R.M., M.Z. Moreira, C.R. Pimentel, and A.C. Morandini. 2015. Food web characterization based on $d^{15}N$ and $d^{13}C$ reveals isotopic niche partitioning between fish and jellyfish in a relatively pristine ecosystem. Marine Ecology Progress Series 519: 13–27.

Nielsen, L.P. 1992. Denitrification in sediment determined from nitrogen isotope pairing. FEMS Microbiology Letters 86(4): 357–62.

Nielsen, O.I., B. Gribsholt, E. Kristensen, and N.P. Revsbech. 2004. Microscale distribution of oxygen and nitrate in sediment inhabited by *Nereis diversicolor*: spatial patterns and estimated reaction rates. Aquatic Microbial Ecology 34: 23–32.

Nogaro, G., and A.J. Burgin. 2014. Influence of bioturbation on denitrification and dissimilatory nitrate reduction to ammonium (DNRA) in freshwater sediments. Biogeochemistry 120: 279–294.

Norkko, J., J. Gammal, J.E. Hewitt, et al. 2015. Seafloor Ecosystem Function Relationships: In situ patterns of change across gradients of increasing hypoxic stress. Ecosystems 18: 1424–1439.

Olafsson, E.B. 1986. Density dependence in suspension-feeding and deposit-feeding populations of the bivalve *Macoma balthica*: a field experiment. Journal of Animal Ecology 55: 517–526.

Pelegrí, S.P., and T. Blackburn. 1995. Effect of bioturbation by *Nereis* sp., *Mya Arenaria* and *Cerastoderma* sp. on nitrification and denitrification in estuarine sediments. Ophelia 41: 289–299.

Petersen, J.M., A. Kemper, H. Gruber-Vodicka, et al. 2016. Chemosynthetic symbionts of marine invertebrate animals are capable of nitrogen fixation. Nature Microbiology 2: 16195

Petersen, J. M., and J. Osvatic. 2018. Microbiomes *in Natura*: Importance of invertebrates in understanding the natural variety of animal-microbe interactions. mSystems 3(2): e00179-17.

Piepenburg, D., T.H. Blackburn, C.F. von Dorrienl, J. Gutt, P.O.J. Hall, S. Hulth, M.A. Kendall, K.W. Opalinski, E. Rachor, and M.K. Schmid. 1995. Partitioning of benthic community respiration in the Arctic (northwestern Barents Sea). Marine Ecology Progress Series 118: 199–213.

Pitcher, K.A, and D.A. Soluk. 2018. Fish presence and inter-patch connectivity interactively alter the size of emergent insects in experimental enclosures. Ecosphere 9(3): e02118.

Politi, T., M. Zilius, G. Castaldelli, M. Bartoli, and D. Daunys, 2019. Estuarine macrofauna affects benthic biogeochemistry in a hypertrophic lagoon. Water 11(6): 1186.

Poulsen, M., M.V. Kofoed, L.H. Larsen, A. Schramm, and P. Stief. 2014. *Chironomus plumosus* larvae increase fluxes of denitrification products and diversity of nitrate-reducing bacteria in freshwater sediment. Systematic and Applied Microbiology 37: 51–59.

Quintana, C.O., E. Kristensen, and T. Valdemarsen. 2013. Impact of the invasive polychaete *Marenzelleria viridis* on the biogeochemistry of sandy marine sediments. Biogeochemistry 115(1): 95–109.

Rasigraf, O., N.A.G.M. van Helmond, J. Frank, W.K. Lenstra, M. Egger, C.P. Slomp, and M.S.M. Jetten. 2019. Microbial community composition and functional potential in Bothnian Sea sediments is linked

to Fe and S dynamics and the quality of organic matter. Limnology and Oceanography 65(S1): S113–S133

Ray, N.E., M.C. Henning, and R.W. Fulweiler. 2019. Nitrogen and phosphorus cycling in the digestive system and shell biofilm of the eastern oyster *Crassostrea virginica*. Marine Ecology Progress Series 621: 95–105.

Regnier, P., P. Friedlingstein, P. Ciais, F.T. Mackenzie, N. Gruber, I.A. Janssens, and S. Arndt. 2013. Anthropogenic perturbation of the carbon fluxes from land to ocean. Nature geoscience 6(8): 597–607.

Reis, C.R.G., G.B. Nardoto, and R.S Oliveira. 2017. Global overview on nitrogen dynamics in mangroves and consequences of increasing nitrogen availability for these systems. Plant and Soil 410: 1–19.

Reise, K. 1983. Biotic enrichment of intertidal sediments by experimental aggregates of the deposit-feeding bivalve *Macoma balthica*. Marine Ecology Progress Series 2: 229–236.

Riisgård, H.U., and P. Kamermans. 2001. Switching between deposit and suspension feeding in coastal zoobenthos. In: Reise K. (ed) Ecological Comparisons of Sedimentary Shores. Ecological Studies (Analysis and Synthesis), vol 151. Springer, Berlin, Heidelberg, pp 73-101.

Risgaard-Petersen, N., L.P. Nielsen, S. Rysgaard, T. Dalsgaard, and R.L. Meyer. 2003. Application of the isotope pairing technique in sediments where anammox and denitrification coexist. Limnology and Oceanography-Methods 1: 63–73.

Sánchez, M.I., A.J. Green, and E.M. Castellanos. 2006. Spatial and temporal fluctuations in presence and use of chironomid prey by shorebirds in the Odiel saltpans, south-west Spain. Hydrobiologia 567: 329–340.

Shapira, M. 2016. Gut Microbiotas and Host Evolution: Scaling up symbiosis. Trends in Ecology and Evolution 31: 539–549.

Smyth, A.R., A.E. Murphy, I.C. Anderson, and B. Song. 2018. Differential effects of bivalves on sediment nitrogen cycling in a shallow coastal bay. Estuaries and Coasts 41(4): 1147–1163.

Stief, P., and D. de Beer. 2006. Probing the microenvironment of freshwater sediment macrofauna: Implications of deposit-feeding and bioirrigation for nitrogen cycling. Limnology and Oceanography, 51: 2538–2548.

Stief, P. 2013. Stimulation of microbial nitrogen cycling in aquatic ecosystems by benthic macrofauna: mechanisms and environmental implications. Biogeosciences 10(12): 7829–7846.

Stief, P., A.S.B. Lundgaard, A. Morales-Ramirez, B., Thamdrup, and R.N. Glud. 2017. Fixed-Nitrogen Loss Associated with Sinking Zooplankton Carcasses in a Coastal Oxygen Minimum Zone (Golfo Dulce, Costa Rica). Frontiers in Marine Science 4: 152.

Stief, P., A.S.B. Lundgaard, A.H. Treusch, B. Thamdrup, H.-P. Grossart, and R.N Glud. 2018. Freshwater copepod carcasses as pelagic microsites of dissimilatory nitrate reduction to ammonium. FEMS Microbiology Ecology 94(10): fiy144.

Stief, P., and G. Eller. 2006. The gut microenvironment of sediment-dwelling *Chironomus plumosus* larvae as characterised with O_2, pH, and redox microsensors. Journal of Comparative Physiology B 176: 673–683.

Strous, M., J.A. Fuerst, E.H.M. Kramer, S. Logemann, G. Muyzer, K.T. van de Pas-Schoonen, R. Webb, J. Gijs Kuenen, and M.S.M. Jetten. 1999. Missing lithotroph identified as new planctomycete. Nature 400: 446–449.

Svensson, J.M. 1997. Influence of *Chironomus plumosus* larvae on ammonium flux and denitrification (measured by the acetylene blockage- and the isotope pairing-technique) in eutrophic lake sediment. Hydrobiologia 346: 157–168.

Thamdrup, B., and T. Dalsgaard. 2002. Production of N_2 through anaerobic ammonium oxidation coupled to nitrate reduction in marine sediments. Applied and Environmental Microbiology 68(3): 1312–1318. Tiedje, J.M., A.J. Sexstone, D.D. Myrold, and J.A. Robinson. 1983. Denitrification: Ecological niches, competition and survival. Antonie Leeuwenhoek 48: 569–583.

Tiedje, J.M., A.J. Sexstone, D.D. Myrold, & J.A. Robinson. 1983. Denitrification: Ecological niches, competition and survival. Antonie van Leeuwenhoek 48: 569–583.

Tréguer, P., and P. Le Corre. 1975. Manuel d'analysis des sels nutritifs dans l'eau de mer 2nd ed. pp. 110, Université de Bretagne Occidentale.

Tuominen, L., K. Mäkelä, K.K. Lehtonen, H. Haahti, S. Hietanen, and J. Kuparinen. 1999. Nutrient fluxes, porewater profiles and denitrification in sediment influenced by algal sedimentation and bioturbation by *Monoporeia affinis*. Estuarine, Coastal and Shelf Science 49(1): 83–97.

van der Heide, T., L.L. Govers, J. de Fouw, et al. 2012. A three-stage symbiosis forms the foundation of seagrass ecosystems. Science 336(6087):1432–1434.

van Nugteren, P., L. Moodley, G.J. Brummer, C.H. Heip, P.M. Herman, and J.J. Middelburg. 2009. Seafloor ecosystem functioning: the importance of organic matter priming. Marine Biology 156(11): 2277–2287.

Vanni, M.J., P.B. McIntyre, D. Allen, et al. 2017. A global database of nitrogen and phosphorus excretion rates of aquatic animals. Ecology 98: 1475–1475.

Vasquez-Cardenas, D., C.O. Quintana, F.J.R. Meysman, E. Kristensen, and H.T.S. Boschker. 2016. Species-specific effects of two bioturbating polychaetes on sediment chemoautotrophic bacteria. Marine Ecology Progress Series 549: 55–68.

Viitasalo-Frösén, S., A.O. Laine, and M. Lehtiniemi. 2009. Habitat modification mediated by motile surface stirrers versus semi-motile burrowers: Potential for a positive feedback mechanism in a eutrophied ecosystem. Marine Ecology Progress Series 376: 21–32.

Voss, M., E. Asmala, I. Bartl, et al. 2020. Origin and fate of dissolved organic matter in four shallow Baltic Sea estuaries. Biogeochemistry. Doi:10.1007/s10533-020-00703-5

Wahl, M., F. Goecke, A. Labes, S. Dobretsov, and F. Weinberger. 2012. The second skin: ecological role of epibiotic biofilms on marine organisms. Frontiers in Microbiology 3: 292.

Warembourg, F.R. 1993. Nitrogen fixation in soil and plant systems. In R. Knowles & T.H. Blackburn (Eds.), Nitrogen isotope techniques (pp.127-156). San Diego: Academic Press.

Weihrauch, D., S. Fehsenfeld, and A. Quijada-Rodriguez. 2017. Nitrogen excretion in aquatic crustaceans. In Acid-base balance and nitrogen excretion in invertebrate (eds. Weihrauch, D. & O'Donnell, M.) 1-25 (Springer).

Welsh, D.T., D. Nizzoli, E.A. Fano, and P. Viaroli. 2015. Direct contribution of clams (*Ruditapes philippinarum*) to benthic fluxes, nitrification, denitrification and nitrous oxide emission in a farmed sediment. Estuarine, Coastal and Shelf Science 154: 84–93.

Xu, T. M. Yu, H. Lin, Z. Zhang, J. Liu, and X.-H. Zhan. 2015. Genomic insight into *Aquimarina longa* SW024T: its ultra-oligotrophic adapting mechanisms and biogeochemical functions. BMC Genomics 16: 772.

Yazdani Foshtomi M., F. Leliaert, S. Derycke, A. Willems, M. Vincx, and J. Vanaverbeke. 2018. The effect of bio-irrigation by the polychaete *Lanice conchilega* on active denitrifiers: Distribution, diversity and composition of *nosZ* gene. PLoS ONE 13(2): e0192391.

Zemlys, P., Ch. Ferrarin, G. Umgiesser, S. Gulbinskas, and D. Bellafiore. 2013. Investigation of saline water intrusions into the Curonian Lagoon (Lithuania) and two-layer flow in the Klaipėda Strait using finite element hydrodynamic model. Ocean Science 9(3): 573–584.

Zettler, M.L., and D. Daunys. 2007. Long-term macrozoobenthos changes in a shallow boreal lagoon: Comparison of a recent biodiversity inventory with historical data. Limnologica 37: 170–185.

Zilius, M., I. Vybernaite-Lubiene, D. Vaiciute, J. Petkuviene, P. Zemlys, I. Liskow, M. Voss, and P.A. Bukaveckas. 2018. The influence of cyanobacteria blooms on the attenuation of nitrogen throughputs in a Baltic coastal lagoon. Biogeochemistry 141: 143–165.

Zilius, M., A. Samuiloviene, R. Stanislauskiene, E. Broman, S. Bonaglia, R. Meskys, and A. Zaiko. 2020. Depicting temporal, functional, and phylogenetic patterns in estuarine diazotrophic communities from environmental DNA and RNA. Microbial Ecology. doi:10.1007/s00248-020-01562-1

Zumft, W.G. 1997. Cell biology and molecular basis of denitrification. Microbiology and Molecular Biology Review 61(4): 533–616.

ACKNOWLEDGMENTS

PUBLICATIONS

I

Samuiloviene, A., M. Bartoli, S. Bonaglia, U. Cardini, I. Vybernaite-Lubiene, U. Marzocchi, J. Petkuviene, T. Politi, A. Zaiko, M. Zilius, 2019. The effect of chironomid larvae on nitrogen cycling and microbial communities in soft sediments. *Water* 11: 1931.

The Effect of Chironomid Larvae on Nitrogen Cycling and Microbial Communities in Soft Sediments

Aurelija Samuiloviene [1], **Marco Bartoli** [1,2], **Stefano Bonaglia** [1,3,4], **Ulisse Cardini** [1,5], **Irma Vybernaite-Lubiene** [1], **Ugo Marzocchi** [1,5], **Jolita Petkuviene** [1], **Tobia Politi** [1], **Anastasija Zaiko** [1,6,7] **and Mindaugas Zilius** [1,8,*]

[1] Marine Research Institute, Klaipėda University, 92294 Klaipėda, Lithuania; aurelija.samuiloviene@jmtc.ku.lt (A.S.); irma.lubiene@apc.ku.lt (I.V.-L.); jolita.petkuviene@apc.ku.lt (J.P.); tobia.politi@jmtc.ku.lt (T.P.)

[2] Department of Chemistry, Life science and Environmental Sustainability, Parma University, 43124 Parma, Italy; marco.bartoli@unipr.it

[3] Department of Ecology, Environment and Plant Sciences, Stockholm University, 10691 Stockholm, Sweden; stefano.bonaglia@su.se

[4] Department of Biology, University of Southern Denmark, 5230 Odense, Denmark

[5] Integrative Marine Ecology Department, Stazione Zoologica Anton Dohrn, National Institute of Marine Biology, Ecology and Biotechnology, 8012 Napoli, Italy; ulisse.cardini@szn.it (U.C.); ugomar@bios.au.dk (U.M.)

[6] Coastal and Freshwater Group, Cawthron Institute, 7042 Nelson, New Zealand; anastasija.zaiko@cawthron.org.nz

[7] Institute of Marine Science, University of Auckland, 0941 Warkworth, New Zealand

[8] Department of Life Science and Biotechnology, Ferrara University, 44121 Ferrara, Italy

* Correspondence: mindaugas.zilius@jmtc.ku.lt

Abstract: The combination of biogeochemical methods and molecular techniques has the potential to uncover the black-box of the nitrogen (N) cycle in bioturbated sediments. Advanced biogeochemical methods allow the quantification of the process rates of different microbial processes, whereas molecular tools allow the analysis of microbial diversity (16S rRNA metabarcoding) and activity (marker genes and transcripts) in biogeochemical hot-spots such as the burrow wall or macrofauna guts. By combining biogeochemical and molecular techniques, we analyzed the role of tube-dwelling *Chironomus plumosus* (Insecta, Diptera) larvae on nitrification and nitrate reduction processes in a laboratory experiment with reconstructed sediments. We hypothesized that chironomid larvae stimulate these processes and host bacteria actively involved in N-cycling. Our results suggest that chironomid larvae significantly enhance the recycling of ammonium (80.5 ± 48.7 μmol m^{-2} h^{-1}) and the production of dinitrogen (420.2 ± 21.4 μmol m^{-2} h^{-1}) via coupled nitrification–denitrification and the consumption of water column nitrates. Besides creating oxygen microniches in ammonium-rich subsurface sediments via burrow digging and ventilation, chironomid larvae serve as hot-spots of microbial communities involved in N-cycling. The quantification of functional genes showed a significantly higher potential for microbial denitrification and nitrate ammonification in larvae as compared to surrounding sediments. Future studies may further scrutinize N transformation rates associated with intimate macrofaunal–bacteria associations.

Keywords: chironomid larvae; nitrogen; microbial community; 16S rRNA; functional genes; denitrification; sediment

1. Introduction

Shallow estuarine systems are efficient coastal filters and biogeochemical reactors which regulate organic matter and nutrient loads from land to the sea [1,2]. Their elevated retention of organic sediment fuels high rates of benthic heterotrophic activity and primary production [3]. Such energy and matter flows have positive feedbacks for benthic biodiversity and for the network of ecological interactions that connect physical and biological compartments [3,4]. Thus, estuarine nitrogen (N) cycling is a paradigmatic example of a set of biogeochemical transformations connecting micro- and macro-organisms, modulated by physical environments and undergoing complex regulation and feedbacks [5–7]. Within the estuarine N cycle, permanent N removal via dissimilative processes such as denitrification is of particular interest, as well as undesired dissimilative nitrate reduction to ammonium (DNRA)–N recycling, which is favoured under eutrophic conditions [8,9]. Processes leading to permanent N removal counteract the excessive loads of reactive N to coastal areas, resulting from anthropogenic activities such as agriculture and animal farming and inducing eutrophication, loss of biodiversity and the deterioration of ecosystem health [10,11].

Microbially-mediated N transformations in estuarine sediments are supported and stimulated by a range of macrofauna-related processes, collectively defined as bioturbation [3,12,13]. The multiple paths by which metabolic or feeding strategies and behavioural features of macrofauna affect the physical and biological environment and N-cycling have been scrutinized in many experimental studies. These demonstrated that macrofauna may directly alter inorganic N concentrations as well as the quality and quantity of organic N via respiration, excretion and biodeposition activities [14–21]. Biodeposits from filter-feeding macrofauna, for example, may increase denitrification and ammonification rates [19,22]. Macrofauna are demonstrated to also produce indirect effects on N biogeochemistry via sediment reworking and burrow construction, ventilation or bioirrigation, which may stimulate coupled nitrification–denitrification [14,15,23,24].

Therefore, being involved in N-cycling, macrofauna may facilitate the growth of primary producers or smooth their competition with bacteria for N, resulting in simultaneous high uptake and high loss via denitrification [7,25,26]. Macrofauna may also locally affect microbial communities, creating specific niches such as shallow or deep burrow lining, where peculiar microbiomes develop along the chemical gradients [17,20,27]. Fascinating but less explored is the role of macrofauna as microbial community elevators or transporters, as macrofauna continuously migrate vertically and horizontally across sediments, exposing their associated microbiome to different chemical gradients (e.g., from oxygen (O_2) and nitrate (NO_3^-)-rich to anoxic, ammonium (NH_4^+)-rich). Even less is known about microbial activities occurring within the guts, gills or intestines of macrofauna [28,29]. Substantial densities of symbiotic microbes (e.g., N-fixers, sulphide oxidizers) were detected, for example, in the gills of lucinid bivalves [30]. Even though intimate microbe–macrofauna interactions are likely widespread, they are largely understudied due to methodological limitations or the oversimplification of experimental approaches. Therefore, the cumulative effects of macrofauna and their associated microbiomes are rarely accounted for in biogeochemical studies, and their actual magnitude may be underestimated when assessing ecosystem-wide processes.

The advances of in situ and laboratory approaches based on the use of isotopic tracers have allowed more accurate quantitative assessment of multiple microbial N transformations and their regulation, including ammonification, nitrification and nitrate reduction processes [7–9,16,21]. Integrating biogeochemical approaches with novel molecular tools (such as the metabarcoding of microbial biodiversity or quantification of target functional genes) enables the detailed exploration of macrofaunal–bacterial interactions and of their wider role in benthic ecosystem functioning [18,20,29].

In this study, we analysed the effects of sediment-dwelling *Chironomus plumosus* (Insecta, Diptera) larvae on benthic N transformations combining biogeochemical and functional genomic measurements under controlled conditions. We targeted chironomid larvae—an understudied group compared to other macrofauna—for multiple reasons. They may attain large densities and dominate in organic-rich, chemically reduced sediments, where they may create steep redox gradients across

their burrows [12]. They are suspension feeders and pump large volumes of O_2 and NO_3^--rich water into sediments [31]. Therefore, we hypothesized a substantial stimulation of N-cycling in sediments inhabited by chironomid larvae, as they may alter the sediment's physical structure and host bacteria that catalyse N transformations. To test this hypothesis, we measured inorganic N fluxes in bioturbated sediments in combination with the 16S rRNA metabarcoding of bacterial communities isolated from (1) subsurface, anoxic sediments, (2) burrow wall sediments, and (3) chironomid larvae. We then quantified the representative marker genes involved in N-cycling and their transcripts to better understand whether chironomid larvae and their associated microbiome may contribute to nitrification and/or to NO_3^- reduction.

2. Materials and Methods

2.1. Experimental Setup

In July 2018, muddy sediments with high organic carbon and total N contents (12% and 1.8%, respectively; [2]), water, and chironomid larvae (*C. plumosus*) were collected in the Lithuanian part of the Curonian Lagoon (55°17′51.7″ N, 21°00′36.0″ E) at a water depth of 3 m. In the laboratory, approximately 15 L of sediment was sieved through a 0.5 mm mesh to remove large debris, chironomid larvae and other occasional macrofauna, and gently mixed to a slurry. The homogenized sediment (median grain size = 0.032 μm) was transferred into 10 bottom-capped Plexiglass liners (height = 30 cm, inner diameter = 8 cm) to reconstruct a 10 cm sediment layer in each microcosm. Thereafter, all microcosms were carefully filled with unfiltered water from the sampling site.

Two treatments (five replicates each) were applied to the microcosm cores: sediments without macrofauna (control) and sediments with nine added chironomid larvae per core (corresponding to 1800 ind. m^{-2}). All chironomid larvae added to the cores immediately burrowed in the sediment down to 3–5 cm depth. In each core, a magnetic bar was fixed 10 cm above the sediment surface to stir the water while avoiding sediment resuspension. Then, all the cores were submerged into a 200 L tank, filled with aerated and well-mixed lagoon water (salinity = 0.2, pH = 8.3, dissolved inorganic N conc. ~2 μmol L^{-1}) maintained at ambient temperature (16 ± 0.2 °C). The tank was equipped with two central magnets rotating at 40 rpm, driving the magnet bars inside the cores. Thus, water exchange with the tank was ensured to avoid water column stratification inside the cores and regulate oxygenation. The cores were pre–incubated in the dark for 14 days to attain (1) stable vertical and horizontal chemical gradients after sediment sieving and homogenisation and chironomid larvae addition, and (2) stable bacterial communities within the sediment and along the burrows' walls [32]. During the pre-incubation period, all microcosms were regularly checked for the development of light brown halos along chironomid larvae burrows. About 30% of the tank water was renewed every 2 days to maintain suspended matter, nutrient concentrations and chemical gradients across the sediment–water interface close to in situ conditions. A scheme of the experimental set up is provided in Figure 1.
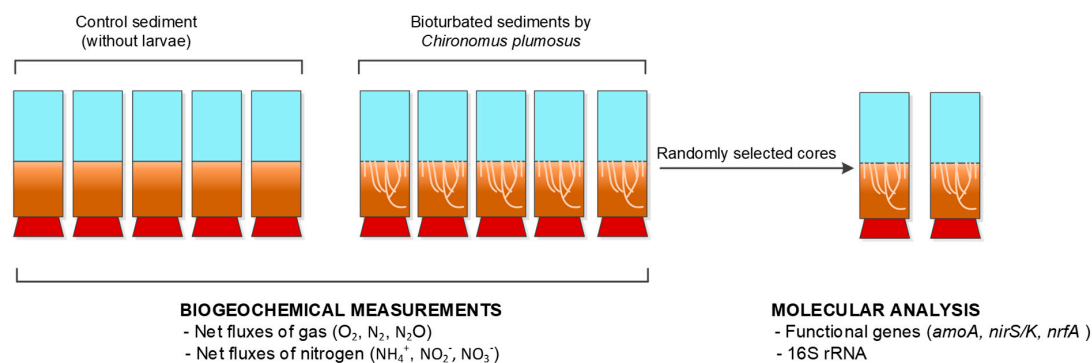

Figure 1. Scheme of the experimental set up.

2.2. Benthic Flux Measurement

After 14 days of pre-incubation, benthic fluxes of dissolved gas (O_2, N_2, N_2O) and inorganic N (NH_4^+, NO_2^- and NO_3^-) were measured in all microcosms during 5 h incubation in dark [33]. Measurements were taken through a gas-tight top lid equipped with an optical sensor spots (PyroScience GmbH, Aachen, Germany) and a sampling port. The incubation was restricted to 5 h to keep oxygen within 20–30% of the initial concentration. At the beginning and at the end of the incubation, 40 mL water samples were collected, with two aliquots immediately transferred into 12 mL exetainers (Labco Limited, Lampeter, UK) and fixed with 7 M $ZnCl_2$ for O_2, N_2, and N_2O measurements. A 10 mL aliquot was filtered (Frisanette GF/F filters), transferred into a plastic test tube and frozen immediately (−20 °C) for later inorganic N analyses. The solute exchange at the sediment–water interface was calculated as follows:

$$F_x = \frac{(C_f - C_i) \times V}{A \times t} \tag{1}$$

where F_x ($\mu mol\ m^{-2}\ h^{-1}$) is the flux of the chemical species x, C_f and C_i ($\mu mol\ L^{-1}$) are the final and initial concentrations of the chemical species x, respectively, V (L) is the water volume in a core, A (m^2) is the surface area of the core sediments, and t (h) is the incubation time.

Dissolved O_2 and N_2 were measured as O_2:Ar and N_2:Ar ratios by membrane inlet mass spectrometry (MIMS, Bay Instruments, Maryland, USA) at Ferrara University, Ferrara, Italy [34]. Ratios were multiplied by theoretical Ar concentration at experimental water temperature and salinity. Nitrous oxide (N_2O) concentrations were determined by headspace analysis on a Thermo Scientific Gas Bench-Precon-IRMS system at UC DAVIS the Stable Isotope Facility, California, USA. Dissolved NH_4^+, NO_2^- and NO_3^- were measured with a continuous flow analyzer (San^{++},Skalar Analitical B.V., Breda, The Netherlands) using standard colorimetric methods [35].

2.3. Oxygen Consumption by Individual Chironomid Larvae

In parallel to sediment core incubations, individual chironomid larvae were incubated in 0.22 μm filtered water to assess the O_2 consumption associated with the animals alone. Briefly, three individuals collected from the same location as above were placed in a Plexiglass chamber (total volume 227 mL) which was partly filled (41 mL) with glass beads (diameter 200–300 μm), and the rest filled with water (186 mL). For this experiment, five chambers with animals plus one chamber with filtered water only (control) were set up.

The chambers were sealed without including any air bubbles and were incubated for approximately 16 h in the dark at in situ temperature. A stirring magnet was placed in each chamber, allowing continuous water mixing during incubation. The concentrations of O_2 in the water were monitored before and after incubation by a pre-calibrated Clark-type oxygen microelectrode (OX-50, Unisense A/S, Aarhus, Denmark). At the end of the incubation, larvae were recovered and weighed. In this experiment, the chironomid larvae wet weight was 0.030 ± 0.003 g (mean ± st. dev.). Oxygen consumption was then calculated as a function of animal wet weight (g WW), according to Bonaglia et al. [36]. The O_2 consumption rates in the experimental chambers with chironomid larvae were corrected for the minimal O_2 consumption in the chamber with filtered water only.

2.4. Nucleic Acid Extraction

At the end of the incubation, sediments for molecular analyses were subsampled from the two randomly selected bioturbated cores (see Figure 1) by collecting approximately 1.5–2 g of subsurface (3–5 cm depth) anoxic sediment and sediments along the burrow wall with a sterile spatula. Anoxic sediments and sediment around burrows were clearly distinguishable by their color, with a light-brown-to-black transition from the oxidized burrow to the outer, chemically reduced sediment. Then, 0.3 g (wet weight) of sediment from each zone was homogenized and equally split for DNA and RNA extractions. Chironomid larvae (n = 6) were retrieved for molecular analyses from sediments

and washed with sterile distilled water (three times). The three types of collected samples—(1) anoxic sediments, (2) oxidized burrow walls, and (3) chironomid larvae—were immediately processed for DNA and RNA extractions. Briefly, DNA was extracted and purified using the QIAamp Fast DNA Stool Mini Kit (Qiagen, Germantown, USA) following the manufacturer's protocol with an amended lysis temperature (temperature was increased to 90 °C to improve bacterial cell rupture).

RNA was extracted with the RNA easy Mini Kit (Qiagen, Germantown, USA) applying additional incubation with lysozyme (20 mg/mL) and mutanolysin (35 μL/1 mL for 90 min at 37 °C). After incubation, 1 mL of Trizol was added and samples was subjected to four cycles of bead beating with glass beads (for 2 min) and rested in the ice (for 3 min) followed by incubation at room temperature (for 5 min). Sediment and cell debris were pelleted by centrifugation at 12,000 rpm for 15 min at 4 °C. The supernatant was transferred to a fresh tube and fixed with 0.2 mL of chloroform, mixed by inversion and left at room temperature for 15 min prior to centrifugation, as described above. The upper aqueous layer containing the RNA was transferred to a new sterile 1.5 mL tube, and RNA cleaning was performed using the RNAeasy Mini Kit (Qiagen, Germantown, USA) according to protocol instructions. The purified DNA and RNA was stored at −80 °C.

2.5. Synthesis of cDNA

Extracted RNA were treated with TURBO DNase (Invitrogen, Carlsbad, USA) according to the manufacturer's instructions. To check whether the RNA sample was free of DNA, a control polymerase chain reaction (PCR) was carried out using universal bacterial primers of 16S rRNA [37]. PCR amplification was undertaken in a total volume of 22 μL using 11 μL of Platinum Green Hot Start 2X Master Mix (Invitrogen, Carlsbad, USA), 0.3 μM of each primer, 1.25 μg μL^{-1} of bovine serum albumin (BSA) and 2 μL of template. Thermocycling conditions were 95 °C for 3 min, followed by 30 cycles of 95 °C for 30 s, 54 °C for 30 s, 72 °C for 45 s, and a final extension of 72 °C for 10 min.

Reverse transcription (RT) was performed with a SuperScript III Reverse Transcriptase (Invitrogen, Carlsbad, USA) following the manufacturer's instructions. Two negative controls lacking either reverse transcriptase or RNA were included. Control PCRs (same as above) were performed to confirm the transcription to complementary DNA (cDNA) and the negative controls using the product of the RT reaction as a template.

2.6. Amplification and Sequencing of 16S rRNA Gene and Bioinformatics

Partial 16S rRNA gene sequences were amplified from extracted DNA using the primer pair Probio Uni/Probio Rev, targeting the V3 region of the 16S rRNA gene sequence [37]. The amplification of the 16S rRNA gene was verified as previously described by Milani et al. [37]. High-throughput sequencing was performed at the DNA sequencing facility of GenProbio srl (Parma University, Parma, Italy) on an Illumina™ MiSeq according to the protocol previously reported in [37]. Metabarcoding reads recovered by paired-end sequencing were merged using the Illumina MiSeq analysis software under the default settings.

Following sequencing, the fastq files were processed using a custom script based on the QIIME software suite [38]. Paired-end read pairs were assembled to reconstruct the complete Probio Uni/Probio_Rev amplicons. Quality filtering retained sequences had a length between 140 and 400 bp and a mean sequence quality score > 20, while sequences with homopolymers > 7 bp and mismatched primers were discarded. Operational taxonomic units (OTUs) were defined at ≥99% sequence homology using uclust [39], and OTUs with less than 10 sequences across datasets were filtered out. All reads were classified to the lowest possible taxonomic rank using QIIME [38] and a reference dataset from the SILVA 132 database [40].

2.7. Quantitative PCR Analyses

Quantitative polymerase chain reactions (qPCR) were used to quantify the abundance and activity of functional genes involved in N-cycling: (1) genes of haem-containing nitrite reductase (*nirS*),

(2) Cu-containing nitrite reductase (*nirK*), (3) ammonia monooxygenase (*amoA*), and (4) cytochrome C nitrite reductase (*nrfA*) (Table 1).

Table 1. List of primers, strains and annealing temperatures used in this study. AOA—ammonia oxidizing archaea, AOB—ammonia oxidizing bacteria.

Gene	Primer	Primer Sequence	Ann. Temp.	Reference Strain
nirS	F3nir R4bcd	SCCGCACCCGGGBCGYGG CGTTGAAYTTRCCGGTSGG	60 °C	*Pseudomonas stutzeri* (DSM 4166)
nirK	F1aCu R3Cu	ATCATGGTSCTGCCGCG GCCTCGATCAGRTTGTGGTT	60 °C	*Achromobcter* sp. (DSM 30128)
AOA-*amoA*	AOA-amoA-f AOA-amoA-r	CTGAYTGGGCYTGGACATC TTCTTCTTTGTTGCCCAGTA	54–60 °C	*Nitrosopumilus maritimus* (NCIMB 15022)
AOB-*amoA*	amoA-1F amoA-2R	GGGGHTTYTACTGGTGGT CCCCTCKGSAAAGCCTTCTTC	63 °C	*Nitrosomonas europaea* (DSM 28437)
nrfA	nrfA-F2aw nrfA-R1	CARTGYCAYGTBGARTA TWNGGCATRTGRCARTC	60 °C	*Citrobacter freundii* (DSM 30039)

Genomic DNA from reference organisms was used to make standard curves and positive controls. Standard curves were constructed using PCR products of the *nirS/K*, *nrfA* and *amoA* genes from the corresponding reference strains (Table 1). For this, the PCR products were purified with the commercial kit (PureLink PCR Purification Kit, Invitrogen, Carlsbad, USA) and their concentration was measured by Qubit 3.0 (Invitrogen, Carlsbad, USA). Obtained products were sequenced at BaseClear B.V (Leiden, The Netherlands) to confirm their identity. Then, serial dilutions were applied to verified products within the range of 10^3–10^7 copies of a gene per reaction and used to calibrate the quantification of target genes in samples.

Quantitative PCR was performed with the StepOnePlus Real Time PCR system (ABI 7900 HT Sequence Detection System, PE Biosystems, Waltham, USA) using optical grade 96-well plates. The PCR reaction was run in the final volume of 20 μL containing 10 μL of SYBR Green master mix, 0.2 μM of forward and reverse primers, 2 mM of $MgCl_2$ (25 mM) and 2 μL of DNA sample (diluted 1/10). The thermocycling conditions were as follows: 50° C for 2 min; initial denaturation at 94 °C for 10 min; 40 cycles at 94 °C (1 min), 60 °C (1 min), 72 °C (1.5 min); and final elongation at 72 °C (5 min). To assess the specificity of amplifications, a melting curve analysis was performed. Each sample was analyzed in triplicate. Triplicate no-template controls were included in each qPCR assay. The abundance and expression of target genes (DNA and RNA samples respectively) were recalculated to copies per g wet weight of a sample (sediment or chironomid larvae).

2.8. Statistical Analysis

The D3 JavaScript library [41] was used to visualize the taxonomic composition of metabarcoding data. Venn diagrams were generated using R package VennDiagram [42] to visualize the proportion of overlapping and unique OTUs within each dataset (anoxic sediments, burrow wall sediments, and chironomid larvae).

Quantitative data (benthic fluxes and abundance and expression of target genes) were visualized using boxplots. Non-parametric Kruskal–Wallis tests were applied to determine the significant difference in benthic net fluxes derived from experimental treatments (control and chironomid larvae microcosms) as well as the difference in the abundance and expression of target genes in anoxic sediments, burrow wall sediments and chironomid larvae. Where relevant, the post-hoc pairwise comparisons were performed using Dunn's test with Bonferroni alpha-correction implemented in the Pairwise Multiple Comparison of Mean Ranks package (PMCMRC, [43]). All analyses were performed in R v3 software [44].

3. Results

3.1. Benthic Fluxes at the Sediment–Water Interface and Animal O_2 Consumption

The presence of chironomid larvae significantly increased benthic metabolism (Kruskal–Wallis test, $p < 0.01$, for O_2 and N_2), reduced NO_3^- efflux and stimulated NH_4^+ recycling (Figure 2). The uptake of O_2 varied from -45.3 to -3125 μmol m^{-2} h^{-1} with 72% higher respiration in the chironomid larvae treatment. The O_2 uptake associated with chironomid larvae was -269 ± 21 μmol g^{-1} WW d^{-1} (range between -329 and -216 μmol g^{-1} WW d^{-1}). When extrapolated to a square meter of sediment containing 1800 individuals, this resulted in a chironomid–associated O_2 uptake of -598 μmol m^{-2} h^{-1}.

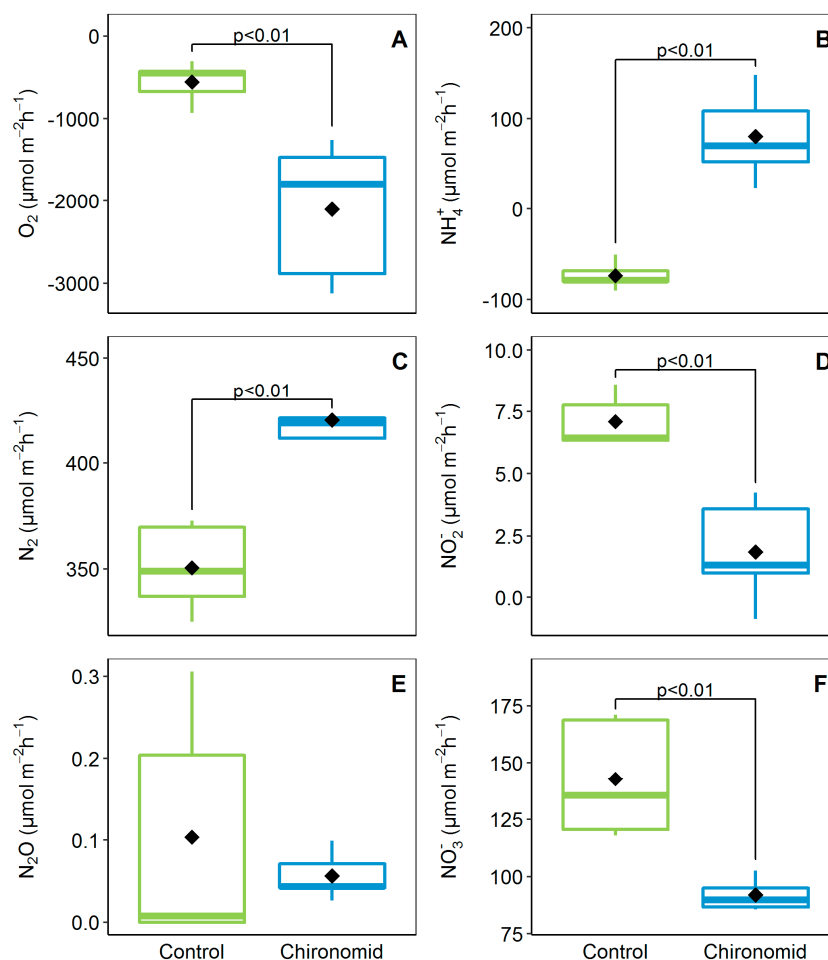**Figure 2.** Benthic net fluxes of dissolved oxygen (**A**), ammonium (**B**), dinitrogen (**C**), nitrite (**D**), nitrous oxide (**E**) and nitrate (**F**) at the sediment–water interface measured in the control and the chironomid larvae microcosms. Each boxplot (n = 5) represents the data range (whiskers), upper and lower quartiles (edges), the median (horizontal line), and the mean (black diamond).

Similar to O_2, net production of N_2 was also higher in the chironomid treatment (420.2 ± 21.4 μmol m^{-2} h^{-1}). We measured N_2O efflux in both treatments, but due to high variability, the difference between the control and the chironomid treatment was not significant (Kruskal–Wallis test, $p > 0.05$; Figure 2). The net flux of N_2O being two orders of magnitude lower than N_2 suggests that complete denitrification was the dominant process.

Chironomid larvae had a significant (Kruskal–Wallis test, $p < 0.01$) effect on nutrient exchange at the sediment–water interface (Figure 2). In the presence of larvae, sediments shifted from a sink (-73.5 ± 14.9 μmol m^{-2} h^{-1}) to source of NH_4^+ (80.5 ± 48.7 μmol m^{-2} h^{-1}). Conversely, the efflux of

the oxidized form of inorganic N decreased when sediments were bioturbated by chironomid larvae. The net fluxes of NO_2^- and NO_3^- were 4 and 2 times lower in the chironomid treatment compared to the control.

3.2. Bacterial Community Composition

An overview of the bacterial community composition using 16S rRNA metabarcoding revealed a prominent difference between sediment samples and chironomid larvae (Figure 3). Of the 35 bacterial phyla detected across all samples, Proteobacteria was the most dominant in sediment samples, followed by Nitrospirae and Chloroflexi. In chironomid larvae, the bacterial community was dominated by three phyla: Firmicutes (40.1%), Proteobacteria (27.6%) and Bacteroidetes (24.4%). No Archea sequences were detected in the samples.
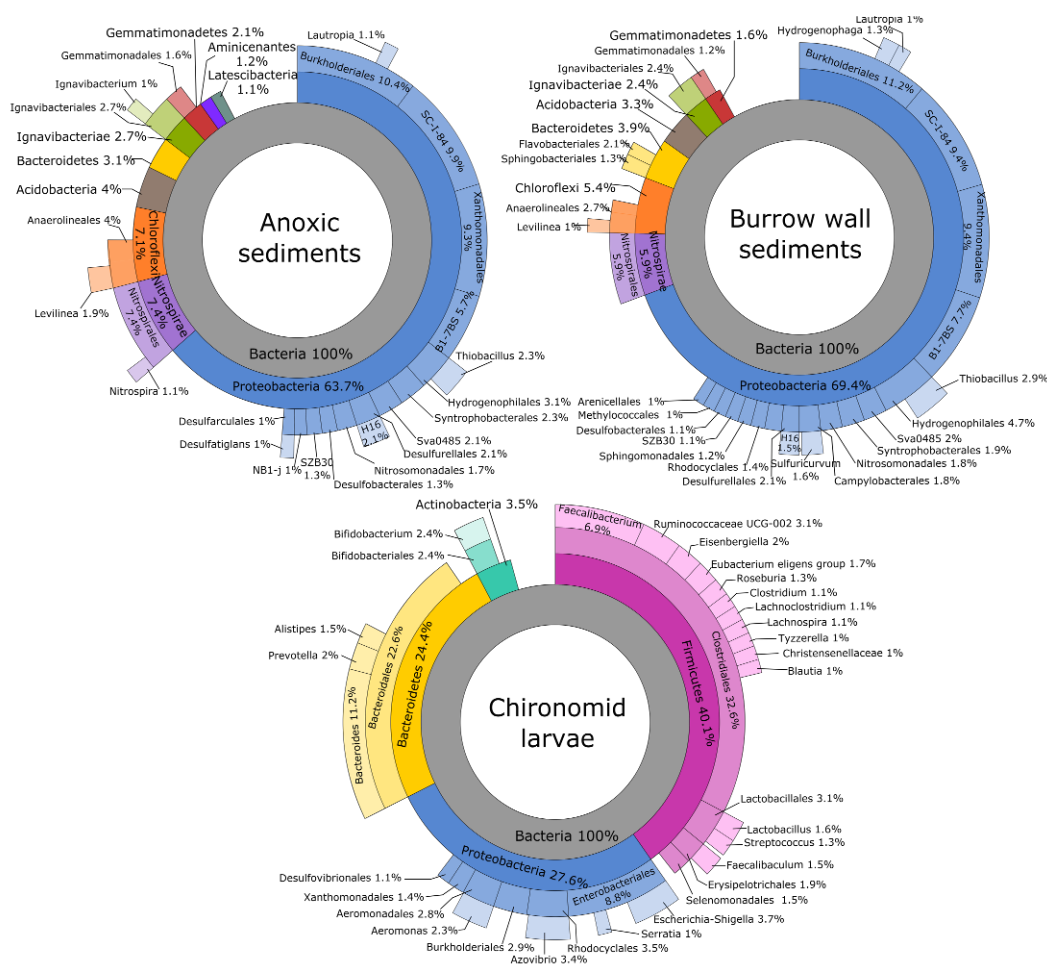

Figure 3. Overview of the bacterial community composition detected using the 16S rRNA marker gene in anoxic sediments, burrow wall sediments and chironomid larvae. The charts show the relative abundance of sequences at different taxonomic levels. To aid in visualization, taxa contributing <0.1% are not shown. The inner circle demonstrates the percentage of taxa assigned at the highest level (Bacteria).

Out of 4841 OTUs detected across three samples, 17.8% were shared between sediments (anoxic sediment and burrow walls) and larvae (Figure 4). These OTUs represented 187 families and 24 phyla. Most of the shared OTUs present in chironomid larvae belonged to Firmicutes (41.4%), Proteobacteria (27.6%), and Bacteroidetes (24.4%). The OTUs detected exclusively in chironomid samples (326 OTUs assigned to 14 families) were dominated by Tenericutes (59.3% of reads), followed by Firmicutes

(15.6%), Saccharibacteria (10.4%), Cyanobacteria and Elusimicrobia (3.8% each), Actinobacteria (3.6%) and Bacteroidetes (1.4%).
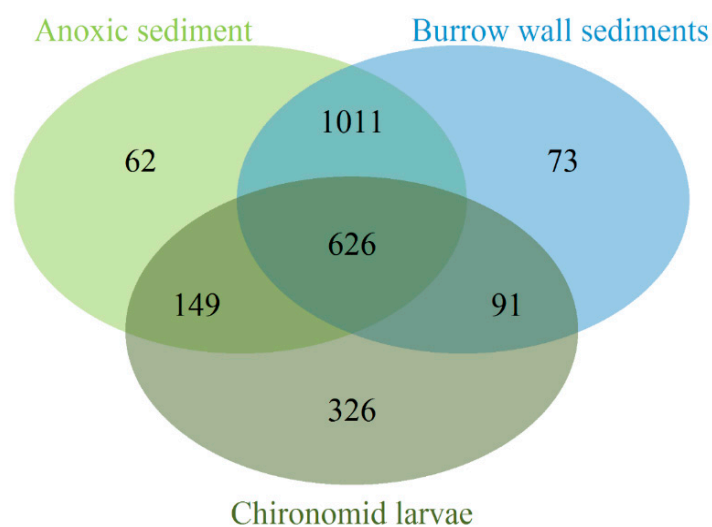

Figure 4. Venn diagram showing the numbers of unique and shared operational taxonomic units (OTUs) in anoxic sediment, burrow wall sediment and chironomid larvae samples (OTU numbers are indicated in the corresponding cross-sections of the diagram).

3.3. Abunadance and Activity of Nitrifying and Denitrifying Genes

Quantitative PCR assays used to quantify the abundance and transcriptional activity of the targeted functional genes associated with the oxidation of NH_4^+ to NO_2^- (*amoA*) and its reduction to nitric oxide (NO; *nirS/nirK*) or to NH_4^+ (*nrfA*) showed that bacterial *amoA* genes were present in all samples, whereas archaeal *amoA* genes were not detected. Significant differences ($p < 0.05$, Kruskal–Wallis test followed by pairwise Dunn's test) were detected only for *nirS* and *nrfA* gene abundance between the anoxic sediment and chironomid larvae samples (Figure 5A,D). Gene transcripts of nitrite reductase genes *nirS* and *nrfA* were detected in significantly lower copy numbers than their relative genes copy numbers ($p < 0.001$, Kruskal–Wallis test). Gene transcripts of bacterial *amoA* genes were detected and quantified from all types of samples at rather consistent rates, similar to DNA copy numbers detected for this gene (Figure 5C), whereas no *nirK* gene transcripts were detected in any type of samples (Figure 5B).
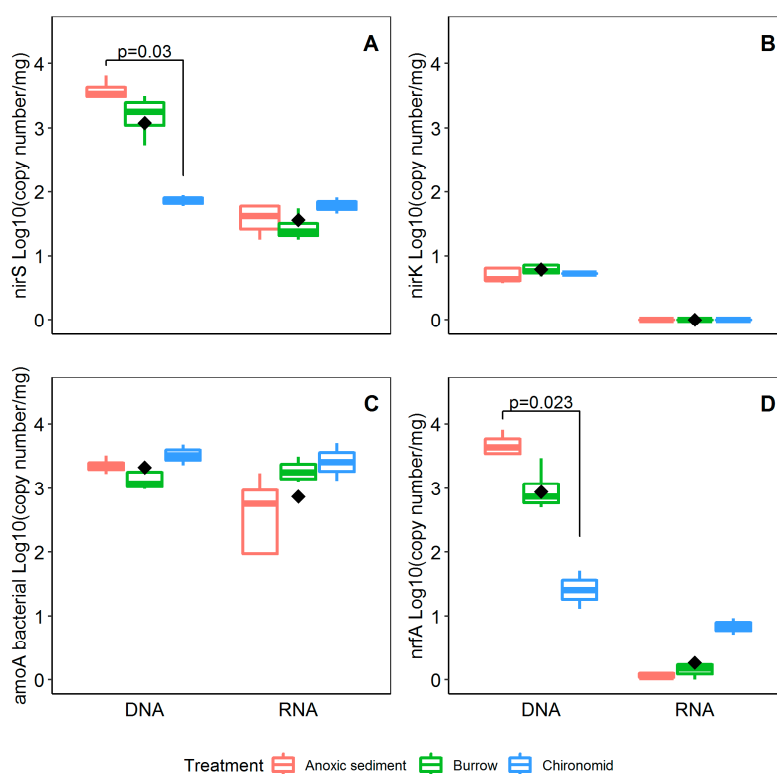
Figure 5. Abundance (DNA) and transcriptional activity (RNA) of the four analyzed target genes—*nirS* (**A**), *nirK* (**B**), *amoA* (**C**) and *nrfA* (**D**)—assessed in the anoxic sediment, burrow wall sediment and chironomid larvae samples. Each boxplot represents the data range (whiskers), upper and lower quartiles (edges), median (horizontal line) and group mean (black diamond). The square brackets indicate significant pairwise difference between treatments (Kruskal–Wallis test followed by pairwise Dunn's test).

4. Discussion

Benthic macrofauna affect the distribution and quality of organic matter and the availability of electron acceptors by burrowing, ventilating and feeding, thus altering microbial communities and their metabolic activity [23,45]. In soft-sediment estuarine environments, it is generally expected that the cumulative effect of burrowing infauna on solute fluxes results in an overall increase of NH_4^+ and N_2 efflux and a decrease of NO_3^- efflux [12,16,29]. The present study aimed at a better understanding of how sediment-dwelling chironomid larvae facilitate solute transport, including electron acceptors (O_2 and NO_3^-), from the overlaying water column to the deep sediment, or vice versa. Furthermore, we were interested in how changes in solute transport in turn may stimulate microbial communities involved in nitrification and NO_3^- reduction processes within the sediment.

Higher N_2 production in the presence of chironomid larvae confirms their stimulatory effect on denitrification, while N_2O production did not change significantly between treatments and was considerably lower than N_2 production. Our results are in line with those of a previous study indicating that with high O_2 availability and low NO_3^- concentrations in the water, the overall N_2O flux from both bioturbated and non-bioturbated sediments is minimal [36]. Stief et al. [46] described higher sedimentary N_2O fluxes associated with the activity of *C. plumosus*, resulting from incomplete microbial denitrification in the larval gut. It was suggested that these N_2O emissions were mainly constrained by the temperature and NO_3^- concentrations [47]. A recent study by Sun et al. [48] revealed that with the presence of nutritional food such as planktonic cyanobacteria, N_2O production in the larval gut can significantly decrease. Cyanobacterial blooms, a common phenomenon in the Curonian Lagoon, may explain why we observed low N_2O production in our study. Alternatively, a large portion of N_2O possibly produced by the larvae [46,47] was likely consumed by sediment-denitrifying bacteria before

reaching the overlying water. However, to confirm these hypotheses, additional measures of N_2O and analyses of functional genes encoding N_2O reduction to N_2 (i.e., *nosZ*) are needed.

As indicated by metabarcoding, the diversity of the bacterial community (numbers of OTUs) was slightly higher in sediment samples (both anoxic and burrow walls) compared to chironomid larvae. The latter had a peculiar composition and was dominated by bacterial groups (Firmicutes/Clostridiales) typical for animals' intestinal microbiota. These bacterial taxa during their fermentative growth, using reduced nicotinamide adenine dinucleotide (NADH) and NO_2^- or NO_3^- as substrates [49], can contribute to the production of NH_4^+ [50]. However, some overlap was present in the composition of the microbial community associated with chironomid larvae and that of the surrounding sediments, which primarily comprised Proteobacteria. This abundant and diverse group includes microbial taxa capable of multiple N transformations, including anammox denitrification, DNRA and N-fixation [51].

Burrow ventilation, including the pumping of NO_3^- through the burrow, is considered one of the main mechanisms by which denitrification is stimulated in sediments reworked by chironomid larvae [14,21,52,53]. However, the degree of stimulation depends on NO_3^- concentration in the overlaying water [14]. In the Curonian Lagoon, NO_3^- concentration varies seasonally, and therefore the effect of chironomid larvae can differ among the seasons. The current study was carried out in summertime, when NO_3^- concentrations were generally low (1.4 μmol L^{-1} on average). In a previous similar incubation experiment performed by Benelli et al. [12], N_2 production was 2.6-fold higher than reported here, likely due to higher dissolved NO_3^- concentrations in spring (109 μmol L^{-1}).

Simple calculations, assuming that two moles of NO_3^- are required to produce one mole of N_2, suggest that the increased uptake of NO_3^- in bioturbated sediment could only explain 41% of the measured N_2 production. This indicates the potential relevance of coupled nitrification–denitrification in sediments bioturbated by chironomid larvae. By constructing burrows and pumping O_2 through them, chironomid larvae create new niches for nitrifiers within the sediments [6,10,15]. Since bacteria require O_2 for NH_4^+ oxidation, respiration (O_2 uptake) is expected to increase alongside nitrification. In the present study, chironomid larvae stimulated respiration by 3.8-fold in comparison to the controls—a stronger effect than that reported earlier by Benelli et al. [12] and by Svensson and Leonardsson [14]. Our extrapolations showed that approximately 28% of the total O_2 consumption was taken up directly by chironomid larvae and 24% by the sediment surface, which leaves approximately 48% of the O_2 consumption related to newly oxidized burrow structures (for example, see the substantial volume of oxidized sediment around larvae borrows in Figure 6). Our estimated 28% of oxygen consumption by larvae is consistent with that reported by Svensson and Leonardsson [14].

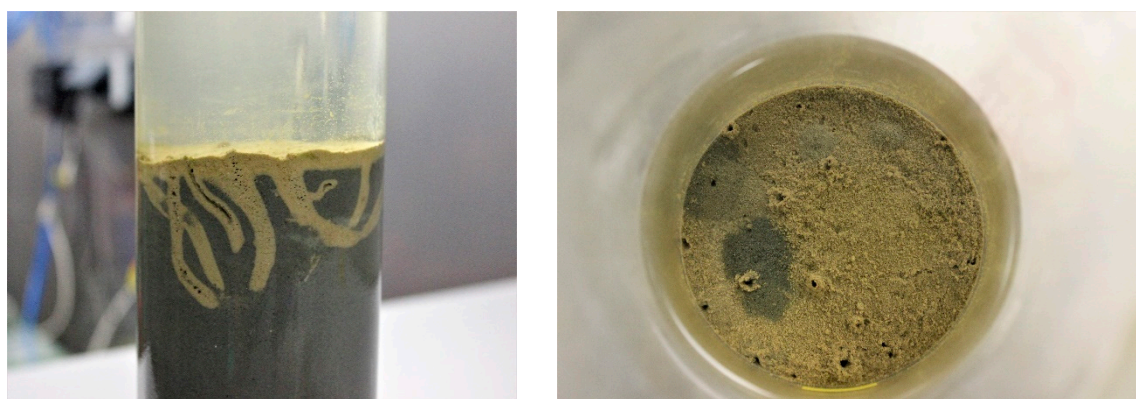**Figure 6.** The bioturbation effects of chironomid larvae, evident in sharp contrast between the light-brown oxidized surface and burrow sediment, and black chemically reduced subsurface sediment (photo by A. Mačiūtė).

However, the degree of stimulation of nitrifiers might be species-specific, as chironomid larvae vary in size, bioturbation mode or grazing pressure on bacteria. Small chironomid species such

as *Chironomus riparius* construct burrows in the upper 1 cm layer where they directly (grazing) or indirectly (burrow ventilation) affect nitrification processes [15]. Larger species, such as *C. plumosus* or *Chironomus* sp., can construct burrows down to 10 cm, significantly extending the niche for nitrifiers and consequently enhancing N-cycling rates [21,54]. Therefore, our findings cannot be generalized for all chironomid species or other macrobenthic invertebrates.

Despite denitrification increasing with the presence of chironomid larvae, its efficiency, expressed as the ratio between the N_2 flux and the sum of N_2 + DIN fluxes, decreased by 20% in bioturbated sediments (from 84% to 65%). The increased NH_4^+ efflux in bioturbated sediments can explain this pattern. Deep-burrowing chironomids are able to increase the upward flux of NH_4^+ from deeper layers (where its pool is considerably higher due to the limited oxidation through nitrification) [12,21,55]. The assumed main source of NH_4^+ in deep sediment pore water is the mineralization of organic matter, as the excretion of NH_4^+ by chironomid larvae rarely exceeds 20% of the immobilized ammonium pool [11,14].

It has never been questioned whether NH_4^+ excretion by chironomid larvae is solely a physiological process or if it could also be attributed to larvae–bacteria associations (e.g., gut microbiomes). Poulsen et al. [29] showed that the *C. plumosus* gut can host NO_3^- reducing microbes, but their targeted functional gene (*nar*) did not allow them to distinguish between nitrite denitrifiers or ammonifiers. Here, we show that the larvae-associated microbial community exhibited transcriptional activity of the *nrfA* gene, which encodes DNRA. This process is strictly anaerobic and may thus potentially occur in the anoxic larvae gut [28]. Therefore, active NO_3^--respiring intestinal bacteria of infauna can act as an alternative source of NH_4^+ in soft-bottom environment.

This was also supported by our functional gene quantification that showed a higher potential for denitrification and DNRA in chironomid larvae rather than in the surrounding sediments. Although *nirS* and *nrfA* genes, encoding NO_2^- reduction to NO and to NH_4^+, respectively, were abundant in anoxic sediment and on the burrow walls, their expression was comparatively low. This indicates that chironomid larvae can provide favourable conditions for bacteria harbouring these genes, facilitating their activity. The expression of *nirS* and *nrfA* genes can be affected by a number of environmental variables, including O_2, temperature, and organic matter availability [56]. This notwithstanding, there is numerous evidence that ingested bacteria can remain active in the larvae gut and carry out NO_3^- reduction [29,46]. In addition, an anoxic gut environment might stimulate NO_3^- reduction by facultative aerobic bacteria [28,29]. A higher *nirS* gene copy number points at denitrification as the dominating pathway of NO_3^- reduction. The differences in the expression of *nirS* or *nrfA* genes can be explained by different bacterial affinity to labile carbon, NO_3^- and sulphide concentration, and temperature [57,58].

The quantification of *amoA*, which encodes the ammonia monooxygenase for the oxidation of NH_4^+ to NO_2^-, revealed that its abundance and activity was primarily associated with ammonium oxidizing bacteria (AOB) in burrows and chironomid larvae. This is likely due to the simultaneous availability of O_2 and NH_4^+, which is favourable for AOB. Surprisingly, relatively high copy numbers of *amoA* were associated with the larval body. Since nitrification is an aerobic process and is unexpected in the anoxic environment of larvae gut and intestine, the active nitrifying bacteria might have been located on the external biofilm of the chironomid body, thus having direct access to NH_4^+ and O_2-enriched pore water, within the larvae-ventilated burrow.

5. Conclusions

The present study confirms that tube-dwelling invertebrates such as *C. plumosus* may have a considerable influence on N-cycling in estuarine sediments. Combining biogeochemical (flux measurements) and molecular (metabarcoding, functional gene analysis) approaches allowed the precise identification of N transformation hot-spots (burrow lining, macrofauna gut) and the quantification of their contribution to in-sediment N-cycling processes. Chironomid larvae stimulated nitrification, denitrification and NH_4^+ production, while increased N recycling reduced denitrification efficiency.

Chironomid larvae produced visible, direct effects on the volume of oxidized sediments, creating new suboxic niches via burrowing and ventilation. They harboured a unique and active array of bacteria compared to those found in the surrounding environment. Interestingly, active functional genes involved in contrasting processes such as nitrification and NO_3^- reduction were detected both in sediments and the larvae microbiome, suggesting the co-occurrence of adjacent oxic and anoxic niches also within the larvae. Our study suggests that overlooked invertebrate–bacteria associations could be a significant component of N-cycling in benthic environments. Future studies should further scrutinize microbially mediated N processes in isolated macrofauna to partition nitrification and denitrification processes associated with intimate animal–bacteria interactions.

Conflicts of Interest: The authors declare no conflict of interest.

References

1. Asmala, E.; Carstensen, J.; Conley, D.J.; Slomp, C.P.; Stadmark, J.; Voss, M. Efficiency of the coastal filter: Nitrogen and phosphorus removal in the Baltic Sea. *Limnol. Oceanogr.* **2017**, *62*, S222–S238. [CrossRef]
2. Zilius, M.; Vybernaite-Lubiene, I.; Vaiciute, D.; Petkuviene, J.; Zemlys, P.; Liskow, I.; Voss, M.; Bartoli, M.; Bukaveckas, P.A. The influence of cyanobacteria blooms on the attenuation of nitrogen throughputs in a Baltic coastal lagoon. *Biogeochemistry* **2018**, *141*, 143–165. [CrossRef]
3. Bianchi, T.S. *Biogeochemistry of Estuaries*; Oxford University Press: New York, NY, USA, 2007.
4. Brinson, M.M.; Christian, R.R.; Blum, L.K. Multiple states in the sea-level induced transition from terrestrial forest to estuary. *Estuaries* **1995**, *18*, 648–659. [CrossRef]
5. Kristensen, E. Organic matter diagenesis at the oxic/anoxic interface in coastal marine sediments, with emphasis on the role of burrowing animals. *Hydrobiologia* **2000**, *426*, 1–24. [CrossRef]
6. Mermillod-Blondin, F.; Rosenberg, R.; François-Carcaillet, F.; Norling, K.; Mauclaire, L. Influence of bioturbation by three benthic infaunal species on microbial communities and biogeochemical processes in marine sediment. *Aquat. Microb. Ecol.* **2004**, *36*, 271–284. [CrossRef]
7. Magri, M.; Benelli, S.; Bondavalli, C.; Bartoli, M.; Christian, R.R.; Bodini, A. Benthic N pathways in illuminated and bioturbated sediments studied with network analysis. *Limnol. Oceanogr.* **2018**, *63*, S68–S84. [CrossRef]
8. An, S.; Gardner, W.S. Dissimilatory nitrate reduction to ammonium (DNRA) as a nitrogen link, versus denitrification as a sink in a shallow estuary (Laguna Madre/Baffin Bay, Texas). *Mar. Ecol. Prog. Ser.* **2002**, *237*, 41–50. [CrossRef]
9. Bonaglia, S.; Deutsch, B.; Bartoli, M.; Marchant, H.K.; Brüchert, V. Seasonal oxygen, nitrogen and phosphorus benthic cycling along an impacted Baltic Sea estuary: Regulation and spatial patterns. *Biogeochemistry* **2014**, *119*, 139–160. [CrossRef]
10. Vybernaite-Lubiene, I.; Zilius, M.; Saltyte-Vaisiauske, L.; Bartoli, M. Recent trends (2012–2016) of N, Si, and P export from the Nemunas River Watershed: Loads, unbalanced stoichiometry, and threats for downstream aquatic ecosystems. *Water* **2018**, *10*, 1178. [CrossRef]
11. Carstensen, J.; Conley, D.J.; Bonsdorff, E.; Gustafsson, B.G.; Hietanen, S.; Janas, U.; Jilbert, T.; Maximov, A.; Norkko, A.; Norkko, J.; et al. Hypoxia in the Baltic Sea: Biogeochemical cycles, benthic fauna, and management. *Ambio* **2014**, *43*, 26–36. [CrossRef]
12. Benelli, S.; Bartoli, M.; Zilius, M.; Vybernaite–Lubiene, I.; Ruginis, T.; Petkuviene, J.; Fano, E.A. Microphytobenthos and chironomid larvae attenuate nutrient recycling in shallow-water sediments. *Freshw. Biol.* **2018**, *63*, 187–201. [CrossRef]

13. Kristensen, E.; Penha-Lopes, G.; Delefosse, M.; Valdemarsen, T.; Quintana, C.O.; Banta, G.T. What is bioturbation? The need for a precise definition for fauna in aquatic sciences. *Mar. Ecol. Prog. Ser.* **2012**, *446*, 285–302. [CrossRef]

14. Svensson, J.E.; Leonardson, L.G. Effects of bioturbation by tube-dwelling chironomid larvae on oxygen uptake and denitrification in eutrophic lake sediments. *Freshw. Biol.* **1996**, *35*, 289–300. [CrossRef]

15. Stief, P.; Beer, D.D. Probing the microenvironment of freshwater sediment macrofauna: Implications of deposit-feeding and bioirrigation for nitrogen cycling. *Limnol. Oceanogr.* **2006**, *51*, 2538–2548. [CrossRef]

16. Bonaglia, S.; Nascimento, F.A.; Bartoli, M.; Klawonn, I.; Brüchert, V. Meiofauna increases bacterial denitrification in marine sediments. *Nat. Commun.* **2014**, *5*, 5133. [CrossRef] [PubMed]

17. Laverock, B.; Tait, K.; Gilbert, J.A.; Osborn, A.M.; Widdicombe, S. Impacts of bioturbation on temporal variation in bacterial and archaeal nitrogen–cycling gene abundance in coastal sediments. *Environ. Microbiol. Rep.* **2014**, *6*, 113–121. [CrossRef] [PubMed]

18. Foshtomi, M.Y.; Braeckman, U.; Derycke, S.; Sapp, M.; Van Gansbeke, D.; Sabbe, K.; Willems, A.; Vincx, M.; Vanaverbeke, J. The link between microbial diversity and nitrogen cycling in marine sediments is modulated by macrofaunal bioturbation. *PLoS ONE* **2015**, *10*, e0130116.

19. Welsh, D.T.; Nizzoli, D.; Fano, E.A.; Viaroli, P. Direct contribution of clams (*Ruditapes philippinarum*) to benthic fluxes, nitrification, denitrification and nitrous oxide emission in a farmed sediment. *Estuar. Coast. Shelf Sci.* **2015**, *154*, 84–93. [CrossRef]

20. Foshtomi, M.Y.; Leliaert, F.; Derycke, S.; Willems, A.; Vincx, M.; Vanaverbeke, J. The effect of bio-irrigation by the polychaete *Lanice conchilega* on active denitrifiers: Distribution, diversity and composition of *nosZ* gene. *PLoS ONE* **2018**, *13*, e0192391.

21. Moraes, P.C.; Zilius, M.; Benelli, S.; Bartoli, M. Nitrification and denitrification in estuarine sediments with tube-dwelling benthic animals. *Hydrobiologia* **2018**, *819*, 217–230. [CrossRef]

22. Murphy, A.E.; Kolkmeyer, R.; Song, B.; Anderson, I.C.; Bowen, J. Bioreactivity and Microbiome of Biodeposits from Filter-Feeding Bivalves. *Microb. Ecol.* **2019**, *77*, 343–357. [CrossRef]

23. Stief, P. Stimulation of microbial nitrogen cycling in aquatic ecosystems by benthic macrofauna: Mechanisms and environmental implications. *Biogeosciences* **2013**, *10*, 7829–7846. [CrossRef]

24. Laverock, B.; Gilbert, J.A.; Tait, K.; Osborn, A.M.; Widdicombe, S. Bioturbation: Impact on the marine nitrogen cycle. *Biochem. Soc. Trans.* **2011**, *39*, 315–320. [CrossRef]

25. Gilbertson, W.W.; Solan, M.; Prosser, J.I. Differential effects of microorganism–invertebrate interactions on benthic nitrogen cycling. *FEMS Microbiol. Ecol.* **2012**, *82*, 11–22. [CrossRef]

26. Bartoli, M.; Nizzoli, D.; Viaroli, P. Microphytobenthos activity and fluxes at the sediment-water interface: Interactions and spatial variability. *Aquat. Ecol.* **2003**, *37*, 341–349. [CrossRef]

27. Moulton, O.M.; Altabet, M.A.; Beman, J.M.; Deegan, L.A.; Lloret, J.; Lyons, M.K.; Nelson, J.A.; Pfister, C.A. Microbial associations with macrobiota in coastal ecosystems: Patterns and implications for nitrogen cycling. *Front. Ecol. Environ.* **2016**, *14*, 200–208. [CrossRef]

28. Stief, P.; Eller, G. The gut microenvironment of sediment-dwelling *Chironomus plumosus* larvae as characterised with O$_2$, pH, and redox microsensors. *J. Comp. Physiol. B* **2006**, *176*, 673–683. [CrossRef]

29. Poulsen, M.; Kofoed, M.V.; Larsen, L.H.; Schramm, A.; Stief, P. Chironomus plumosus larvae increase fluxes of denitrification products and diversity of nitrate-reducing bacteria in freshwater sediment. *Syst. Appl. Microbiol.* **2014**, *37*, 51–59. [CrossRef]

30. Petersen, J.M.; Kemper, A.; Gruber-Vodicka, H.; Cardini, U.; van der Geest, M.; Kleiner, M.; Silvia Bulgheresi, S.; Mußmann, M.; Herbold, C.; Seah, B.K.B.; et al. Chemosynthetic symbionts of marine invertebrate animals are capable of nitrogen fixation. *Nat. Microbiol.* **2016**, *2*, 16196. [CrossRef]

31. Hölker, F.; Vanni, M.J.; Kuiper, J.J.; Meile, C.; Grossart, H.P.; Stief, P.; Adrian, R.; Lorke, A.; Dellwig, O.; Brand, A.; et al. Tube-dwelling invertebrates: Tiny ecosystem engineers have large effects in lake ecosystems. *Ecol. Monogr.* **2015**, *85*, 333–351. [CrossRef]

32. Stocum, E.T.; Plante, C.J. The eect of artificial defaunation on bacterial assemblages of intertidal sediments. *J. Exp. Mar. Biol. Ecol.* **2006**, *337*, 147–158. [CrossRef]

33. Dalsgaard, T.; Nielsen, L.P.; Brotas, V.; Viaroli, P.; Underwood, G.; Nedwell, D.; Dong, L.D.; Sundbäck, K.; Rysgaard, S.; Miles, A.; et al. *Protocol Handbook for NICE-Nitrogen Cycling in Estuaries: A Project under the EU Research Programme: Marine Science and Technology (MAST III)*; Ministry of Environment and Energy National Environmental Research Institute: Silkeborg, Denmark, 2000; pp. 1–62.

34. Kana, T.M.; Darkangelo, C.; Hunt, M.D.; Oldham, J.B.; Bennett, G.E.; Cornwell, J.C. Membrane inlet mass spectrometer for rapid high-precision determination of N_2, O_2, and Ar in environmental water samples. *Anal. Chem.* **1994**, *66*, 4166–4170. [CrossRef]

35. Grassshoff, K. Determination of nitrate. In *Methods of Seawater Analysis*; Grassoff, K., Ehrhardt, M., Kremling, K., Eds.; Verlag Chemie: Weinheimm, Germany, 1982; p. 143.

36. Bonaglia, S.; Brüchert, V.; Callac, N.; Vicenzi, A.; Fru, E.C.; Nascimento, F.J.A. Methane fluxes from coastal sediments are enhanced by macrofauna. *Sci. Rep.* **2017**, *7*, 13145. [CrossRef]

37. Milani, C.; Hevia, A.; Foroni, E.; Duranti, S.; Turroni, F.; Lugli, G.A.; Sanchez, B.; Martín, R.; Gueimonde, M.; van Sinderen, D.; et al. Assessing the fecal microbiota: An optimized ion torrent 16S rRNA gene-based analysis protocol. *PLoS ONE* **2013**, *8*, e68739. [CrossRef]

38. Caporaso, J.G.; Kuczynski, J.; Stombaugh, J.; Bittinger, K.; Bushman, F.D.; Costello, E.K.; Fierer, N.; Peña, A.G.; Goodrich, J.K.; Gordon, J.I.; et al. QIIME allows analysis of high-throughput community sequencing data. *Nat. Methods* **2010**, *7*, 335–336. [CrossRef]

39. Edgar, R.C. Search and clustering orders of magnitude faster than BLAST. *Bioinformatics* **2010**, *26*, 2460–2461. [CrossRef]

40. Quast, C.; Pruesse, E.; Yilmaz, P.; Gerken, J.; Schweer, T.; Yarza, P.; Peplies, J.; Glöckner, F.O. The SILVA ribosomal RNA gene database project: Improved data processing and web-based tools. *Nucleic Acids Res.* **2012**, *41*, D590–D596. [CrossRef]

41. Data-Driven Documents. Available online: https://d3js.org (accessed on 22 July 2019).

42. Chen, H.; Boutros, P.C. VennDiagram: A package for the generation of highly-customizable Venn and Euler diagrams in R. *BMC Bioinform.* **2011**, *12*, 35. [CrossRef]

43. Pohlert, T. *The Pairwise Multiple Comparison of Mean Ranks Package (PMCMR)*; R Package, 2014; p. 27.

44. R-Project. R: A Language and Environment for Statistical Computing [Online]. R Foundation for Statistical Computing: Vienna, Austria. 2014. Available online: http://www.R-project.org (accessed on 22 July 2019).

45. Welsh, D.T. It's a dirty job but someone has to do it: The role of marine benthic macrofauna in organic matter turnover and nutrient recycling to the water column. *Chem. Ecol.* **2003**, *19*, 321–342. [CrossRef]

46. Stief, P.; Poulsen, M.; Nielsen, L.P.; Brix, H.; Schramm, A. Nitrous oxide emission by aquatic macrofauna. *Proc. Natl. Acad. Sci. USA* **2009**, *106*, 4296–4300. [CrossRef]

47. Stief, P.; Schramm, A. Regulation of nitrous oxide emission associated with benthic invertebrates. *Freshw. Biol.* **2010**, *55*, 1647–1657. [CrossRef]

48. Sun, X.; Hu, Z.; Jia, W.; Duan, C.; Yang, L. Decaying cyanobacteria decrease N_2O emissions related to diversity of intestinal denitrifiers of *Chironomus plumosus*. *J. Limnol.* **2015**, *74*. [CrossRef]

49. Cabello, P.; Roldán, M.D.; Castillo, F.; Moreno-Vivián, C. Nitrogen cycle. In *Encyclopaedia of Microbiology*, 3rd ed.; Schaechter, M., Ed.; Academic Press: London, UK, 2009.

50. Baggs, E.; Phillipot, L. Nitrous oxide production in the terrestrial environment. In *Nitrogen Cycling in Bacteria: Molecular Analysis*; Moir, J.W.B., Ed.; Caister Academic Press: Norfolk, UK, 2011.

51. Rasigraf, O.; Schmitt, J.; Jetten, M.S.M.; Lüke, C. Metagenomic potential for and diversity of N-cycle driving microorganisms in the Bothnian Sea sediment. *Microbiol. Open.* **2017**, *6*, e475. [CrossRef]

52. Svensson, J.M. Influence of *Chironomus plumosus* larvae on ammonium flux and denitrification (measured by the acetylene blockage- and the isotope pairing-technique) in eutrophic lake sediment. *Hydrobiologia* **1997**, *346*, 157–168. [CrossRef]

53. Pelegrí, S.P.; Blackburn, T.H. Nitrogen cycling in lake sediments bioturbated by *Chironomus plumosus* larvae, under different degrees of oxygenation. *Hydrobiologia* **1996**, *325*, 231–238. [CrossRef]

54. Xing, X.; Liu, L.; Yan, W.; Wu, T.; Zhao, L.; Wang, X. Bioturbation effects of Chironomid larvae on nitrogen release and ammonia-oxidizing bacteria abundance in sediments. *Water* **2018**, *10*, 512. [CrossRef]

55. Nogaro, G.; Mermillod-Blondin, F.; Montuelle, B.; Boisson, J.C.; Gibert, J. Chironomid larvae stimulate biogeochemical and microbial processes in a riverbed covered with fine sediment. *Aquat. Sci.* **2008**, *70*, 156–168. [CrossRef]

56. Song, B.; Lisa, J.A.; Tobias, C.R. Linking DNRA community structure and activity in a shallow lagoonal estuarine system. *Front. Microbiol.* **2014**, *5*, 460. [CrossRef]

57. Herbert, R.A. Nitrogen cycling in coastal marine ecosystems. *FEMS Microbiol. Rev.* **1999**, *23*, 563–590. [CrossRef]

58. Burgin, A.J.; Hamilton, S.K. Have we overemphasized the role of denitrification in aquatic ecosystems? A review of nitrate removal pathways. *Front. Ecol. Environ.* **2007**, *5*, 89–96. [CrossRef]

II

Zilius, M., S. Bonaglia, E. Broman, V. G. Chiozzini, A. Samuiloviene, F.J.A. Nascimento, U. Cardini, M. Bartoli, 2020. N_2 fixation dominates nitrogen cycling in a mangrove fiddler crab holobiont. *Scientific Report* 10, 13966.

SCIENTIFIC REPORTS

natureresearch

Check for updates

OPEN

N₂ fixation dominates nitrogen cycling in a mangrove fiddler crab holobiont

Mindaugas Zilius[1,2✉], Stefano Bonaglia[1,3,4], Elias Broman[3,5], Vitor Gonsalez Chiozzini[6], Aurelija Samuiloviene[1], Francisco J. A. Nascimento[3,5], Ulisse Cardini[1,7] & Marco Bartoli[1,8]

Mangrove forests are among the most productive and diverse ecosystems on the planet, despite limited nitrogen (N) availability. Under such conditions, animal-microbe associations (holobionts) are often key to ecosystem functioning. Here, we investigated the role of fiddler crabs and their carapace-associated microbial biofilm as hotspots of microbial N transformations and sources of N within the mangrove ecosystem. 16S rRNA gene and metagenomic sequencing provided evidence of a microbial biofilm dominated by Cyanobacteria, Alphaproteobacteria, Actinobacteria, and Bacteroidota with a community encoding both aerobic and anaerobic pathways of the N cycle. Dinitrogen (N_2) fixation was among the most commonly predicted process. Net N fluxes between the biofilm-covered crabs and the water and microbial N transformation rates in suspended biofilm slurries portray these holobionts as a net N_2 sink, with N_2 fixation exceeding N losses, and as a significant source of ammonium and dissolved organic N to the surrounding environment. N stable isotope natural abundances of fiddler crab carapace-associated biofilms were within the range expected for fixed N, further suggesting active microbial N_2 fixation. These results extend our knowledge on the diversity of invertebrate-microbe associations, and provide a clear example of how animal microbiota can mediate a plethora of essential biogeochemical processes in mangrove ecosystems.

Among coastal ecosystems, mangrove forests are of great importance as they account for three quarters of the tropical coastline and provide different ecosystem services[1,2]. Mangrove ecosystems generally act as a net sink of carbon, although they release organic matter to the sea in the form of dissolved refractory macromolecules, leaves, branches and other debris[3,4]. In pristine environments, mangroves are among the most productive eco-systems on the planet, despite growing in tropical waters that are often nutrient depleted[5]. The refractory nature of the organic matter produced and retained in mangroves can slow the recycling of nutrients, particularly of nitrogen (N)[3,6]. Nitrogen limitation in such systems may be overcome by microbial dinitrogen (N_2) fixation when combined with high rates of bioturbation by macrofauna[7,8].

Bioturbation by macrofauna affect N availability and multiple N-related microbial processes through sediment reworking, burrow construction and bioirrigation, feeding and excretion[9]. Macrofauna mix old and fresh organic matter, extend oxic–anoxic sediment interfaces, increase the availability of energy-yielding electron acceptors and increase N turnover via direct excretion[10,11]. Thus, macrofauna may alleviate N limitation by priming the remineralization of refractory N, reducing plants-microbe competition[12,13]. Such activity ultimately promotes N-recycling, plant assimilation and high N retention, as well as favours it loss by stimulating coupled nitrifica-tion and denitrification[14].

Mangrove sediments are highly bioturbated by decapods such as crabs[15]. Crab populations continuously rework sediment by constructing burrows, creating new niches, transporting or selectively grazing on sediment microbial communities[15–18]. In addition, crabs can affect organic matter turnover by assimilating leaves and producing finely fragmented faeces, or by carrying them into their burrows[19,20]. Therefore, crabs are considered

[1]Marine Research Institute, Klaipėda University, Klaipeda, Lithuania. [2]Department of Life Sciences and Biotechnology, University of Ferrara, Ferrara, Italy. [3]Department of Ecology, Environment and Plant Sciences, Stockholm University, Stockholm, Sweden. [4]Department of Biology, University of Southern Denmark, Odense, Denmark. [5]Baltic Sea Centre, Stockholm University, Stockholm, Sweden. [6]Oceanographic Institute, University of São Paulo, São Paulo, Brazil. [7]Integrative Marine Ecology Department, Stazione Zoologica Anton Dohrn, National Institute of Marine Biology, Ecology and Biotechnology, Napoli, Italy. [8]Department of Chemistry, Life Science and Environmental Sustainability, University of Parma, Parma, Italy. ✉email: mindaugas.zilius@jmtc.ku.lt
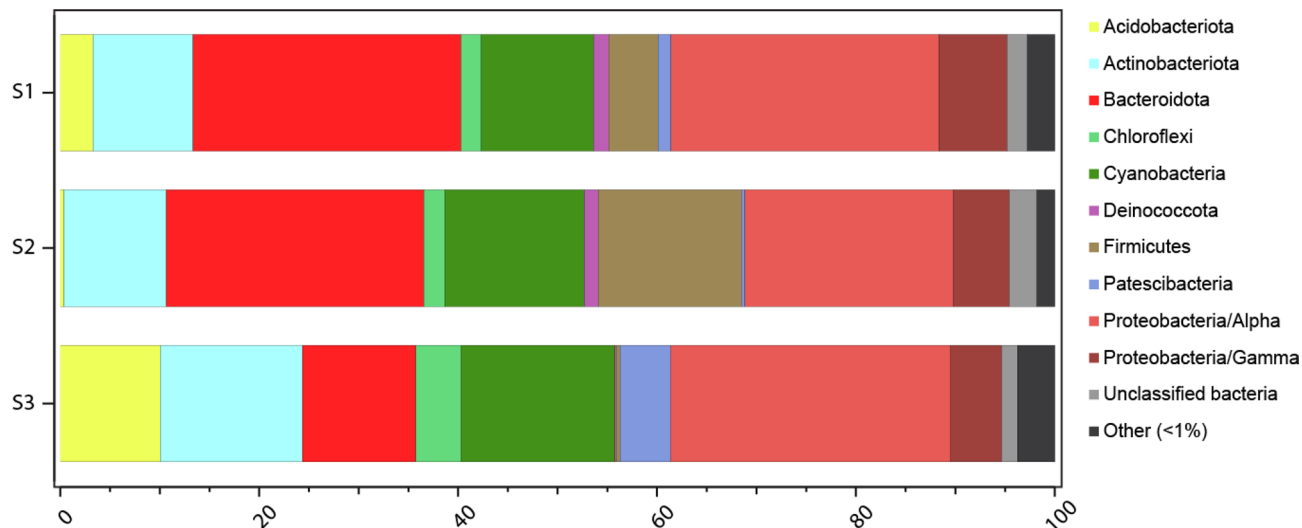
Figure 1. Systematic diversity of the crab's carapace microbiota: Relative abundance of bacterial phyla and Proteobacteria classes obtained by 16S rRNA gene sequencing. Taxa contributing < 1% are not shown.

important ecosystem engineers shaping biogeochemical processes in intertidal muddy banks of mangroves[21–23]. In contrast to burrowing polychaetes or amphipods, the abundant Ocipodid crabs, mainly represented by fiddler crabs, do not permanently ventilate their burrows. These crabs may temporarily leave their burrows for surface activities[18], or otherwise plug their burrow entrance during tidal inundation in order to trap air[24]. A recent study by Cuellar-Gempeler and Leibold[17] showed that these crabs can be associated with a diverse microbial community, either on their carapace or in their gut.

The exoskeleton of living animals, such as shells or carapaces, offers a habitat for microbial biofilms which are actively involved in different N-cycling pathways such as nitrification, denitrification and dissimilatory nitrate reduction to ammonium (DNRA)[25–30]. Colonizing the carapace of crabs may be advantageous for specific bacteria, because of host activities such as respiration, excretion, feeding and horizontal and vertical migrations[31]. However, the ecological interactions between fiddler crabs and bacteria, their regulation and significance as well as their implications at scales spanning from the single individual to the ecosystem are not well understood[16,32].

Prior manipulative laboratory experiments have explored the density-dependent effects of macrofauna on selected N processes (e.g., *Corophium* density vs. sedimentary denitrification rates[33]). So far studies have addressed the three dimensional redox environment created by active burrowers, supported by microelectrode[34] and later by planar optode measurements[35]. More recently, the increasing synergy between biogeochemical approaches and molecular techniques have opened new avenues of research on N-cycling at the scale of a single macrofauna individual and its associated microbial community, i.e., the holobiont[36–38].

Here, we hypothesized that the fiddler crab holobiont (here *Leptuca thayeri*) may represent a N-cycling hotspot and specifically a N source for bioturbated mangrove ecosystems. To assess this hypothesis, we integrated molecular techniques and N-related biogeochemical measurements on crabs collected from a protected Brazilian mangrove system with a low inorganic N background. Such habitat is representative of the most pristine mangrove forests worldwide[39]. 16S rRNA gene amplicon and metagenomic sequencing allowed to explore the taxonomic and functional diversity of the crabs' carapace microbiota. This was complemented by qPCR assays that allowed to quantify the abundance of relevant functional genes regulating nitrate (NO_3^-) production and consumption. Additionally, net N fluxes and ^{15}N probing experiments were used to quantify microbial N transformations and animal excretion, allowing for a mechanistic understanding of holobiont N-cycling.

Results

Systematic diversity of the crab's carapace microbiota. The 16S rRNA gene amplicon sequencing with subsequent DADA2 analysis yielded 1913 amplicon sequence variants (ASVs). Shannon's H alpha diversity in the 16S rRNA gene data was 5.5 ± 0.1 (mean ± standard error, n = 3). The analysis showed that the dominating prokaryotic phyla on the biofilm-covered carapace were Alphaproteobacteria ($25.3 \pm 2.2\%$) and Bacteroidota ($21.4 \pm 5.0\%$) followed by Cyanobacteria ($13.6 \pm 1.2\%$) and Actinobacteria ($11.5 \pm 1.4\%$) (Fig. 1). Most of these sequences were attributed to the Cyanobacteria order Cyanobacteriales, followed by Alphaproteobacteria orders Sphingomonadales and Rhodobacterales, and the Bacteroidota order Flavobacteriales (Supplementary Fig. 1, Supplementary Information 1). The ASVs with the highest relative abundance belonged to the Cyanobacteria genus *Geitlerinema* PCC-7105 (12.3 ± 1.1; Supplementary Fig. 1). The top Bacteroidota ASVs included unclassified *Flavobacteriaceae* sequences ($6.6 \pm 1.7\%$) and the genus *Hoppeia* ($5.2 \pm 1.5\%$) belonging to the same family. Top Alphaproteobacteria genera included *Erythrobacter* and *Paracoccus* (8.0 ± 3.0 and $2.5 \pm 0.4\%$, respectively). Shotgun metagenomic sequencing yielded on average 9,433,482 sequences (R1 and R2) that could be classified for microbial taxa based on functional genes classified against NCBI NR and imported into MEGAN. The analysis returned results similar to the ones obtained by 16S rRNA gene amplicon sequencing, with a commu-
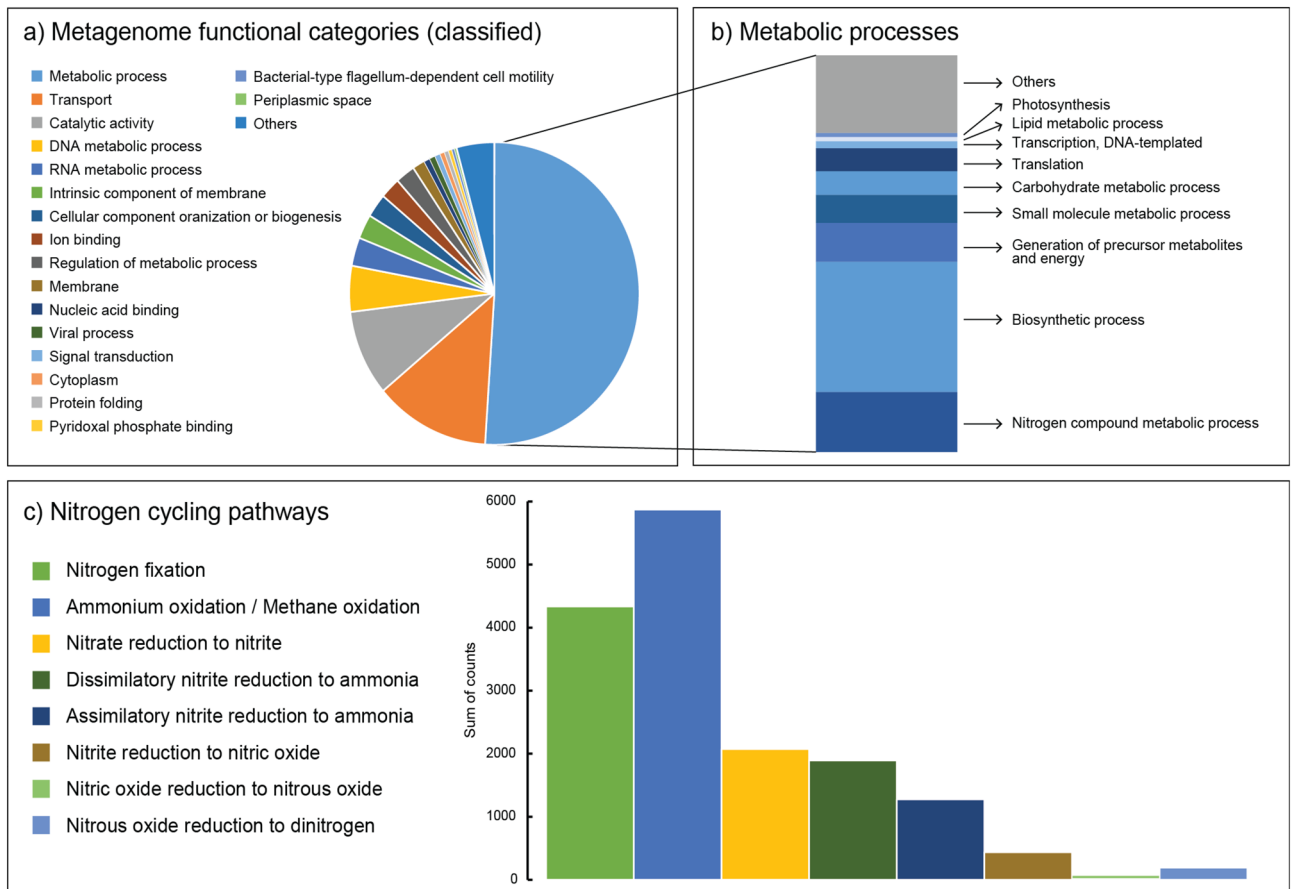
Figure 2. Functional profiling of the crab's carapace microbiota using metagenomics: (**a**) Gene Ontology functional categories of metagenome sequences (%) that constituted the majority of the metagenomic data (45.3% classified reads) with (**b**) a breakdown of the subcategories (%) among the classified metabolic processes and (**c**) metabolic processes of the nitrogen cycle (5% of the "Nitrogen compound metabolic process" subcategory). Pathways consist of the sum of counts for related proteins. The analysis was limited to functional categories > 0.1%.

nity dominated by Alphaproteobacteria, Cyanobacteria, Bacteroidetes (Bacteroidota in the SILVA database), and Actinobacteria, despite the comparison between these two datasets presents limitations and many bacteria remain unclassified in the metagenomic database.

N-cycling functional diversity of the crab's carapace microbiome. Most of the metagenome reads were attributed to the Gene Ontology categories: metabolic processes, transport, and catalytic activity (Fig. 2a). Among metabolic processes, the main subcategories were those related to aerobic respiration, central carbon cycling, peptidases, and housekeeping genes, but also pathways involving N compounds (Fig. 2b). Browsing of the proteins involved in N-cycling (according to the KEGG nitrogen metabolism reference pathway: https://www.genome.jp/kegg-bin/show_pathway?map00910) revealed that the microbial community was capable of all N-cycling pathways, including N_2 fixation, ammonium (NH_4^+) oxidation (and potentially methane oxidation), NO_3^- reduction to nitrites (NO_2^-) and assimilatory NO_2^- reduction to NH_4^+, dissimilatory NO_2^- reduction to NH_4^+, NO_2^- reduction to nitric oxide (NO) and subsequent reduction to nitrous oxide (N_2O) and to N_2 (Fig. 2c). The studied N-cycling pathways represented 0.32% of all the classified proteins, 0.75% of the "Metabolic processes" category, and 5% of the "Nitrogen compound metabolic process" subcategory. A full list of all classified proteins is provided in Supplementary Information 2. Unclassified sequences attributed to the *nifH/frxC* protein family were included in the N_2 fixation category (sequences classified to specific *frxC* family proteins were not included). Major prokaryotic groups that could be taxonomically classified and attributed to these processes were indicated to be Alphaproteobacteria (24% of all N-cycling related sequences), Cyanobacteria (20%), Bacteroidetes (9%), Actinobacteria (6%), Chloroflexi (2%) and Gammaproteobacteria (2%) (Supplementary Information 2). In more detail, these phyla constituted e.g. taxonomic orders Sphingomonadales, Rhodobacterales, Flavobacteriales, and Nostocales (Supplementary Information 2). Our identified prokaryotes harboured a large array of metabolic features, carrying marker genes for up to 5 different N-cycling pathways (e.g., Alphaproteobacteria). For example, NO_3^- reduction pathways in biofilms were carried out by Alphaproteobacteria, Actinobacteria, Bacteroidetes, Cyanobacteria, Chloroflexi and Gammaproteobacteria, as shown in the metagenome data (Supplementary Information 2).

Functional gene	Copy number in sample	
nirS	$1.53 \pm 0.13 \times 10^3$	$n=3$
nirK	0.14×10^3	$n=3$
nrf	2.42×10^3	$n=3$
amoA-archaeal	$0.08 \pm 0.04 \times 10^3$	$n=3$
amoA-bacterial	Not detected	$n=3$

Table 1. Abundance of functional marker genes associated with N-cycling on the fiddler crab carapace. Note that *nirK* and *nrfA* was detected only in two of three samples. Average and standard errors are given.

Measure	Rates µmol N g_{dw}^{-1} crab d^{-1}	
N_2	-12.98 ± 2.93	$n=5$
NH_4^+	1.10 ± 0.21	$n=5$
NO_2^-	0.07 ± 0.01	$n=5$
NO_3^-	0.21 ± 0.03	$n=5$
DON	1.81 ± 2.17	$n=5$
TDN	3.18 ± 2.14	$n=5$

Table 2. Nitrogen fluxes associated with fiddler crab individuals incubated in microcosms. Average and standard errors are given. Total dissolved nitrogen was calculated as sum of NH_4^+, NO_2^-, NO_3^- and DON.

Abundance of key N-cycling genes. qPCR assays confirmed the genetic potential of the microbial community to produce or reduce NO_3^- on the carapace. Functional *nrfA* and *nirS/K* genes, involved in NO_2^- reduction to NH_4^+ and NO were simultaneously present on the biofilm-covered carapace (Table 1). The relative abundance of biofilm associated *nirS* and *nrfA* were $6.7 \pm 3.1 \times 10^{-5}$ and 10.5×10^{-5} per 16S rRNA gene copy, respectively. Contrarily, NH_4^+ oxidation to NO_2^- had considerably lower capacity, contributed solely by archaea ($2.1 \pm 0.2 \times 10^{-6}$ per 16S rRNA gene copy). Bacterial *amoA* was not detected on carapace by qPCR.

Net N fluxes associated with fiddler crab holobiont. Biofilm-covered crabs actively released NH_4^+ and dissolved organic nitrogen (DON) which corresponded to 34% and 57% of total dissolved N production (DIN + DON) in the microcosms with crabs, respectively (Table 2). Net production of NO_3^- and NO_2^- was quantitatively less important, comprising together < 9% of total dissolved N production. Net N_2 fluxes in the microcosms were negative, indicating the dominance of N_2 fixation over denitrification.

Microbial NO_3^- reduction and production in the biofilm. Anoxic slurry incubations of biofilms collected from multiple crab carapaces revealed that the dominant process was denitrification with 3.89 ± 0.72 µmol N g_{dw}^{-1} biofilm d^{-1}, while DNRA was considerably lower (0.82 ± 0.05 µmol N g_{dw}^{-1} biofilm d^{-1}) (Fig. 3). Anammox was a negligible process in the biofilm, as $^{29}N_2$ production was always below the detection limit (data not shown). In the oxic biofilm slurries, NO_3^- increased from 6.4 to 20.6 µmol N l^{-1}, which corresponded to 0.56 ± 0.01 µmol N g_{dw}^{-1} biofilm d^{-1} of potential nitrification rate.

Natural abundance of stable isotopes. The $\delta^{13}C$ values were similar among all crab tissues, while $\delta^{15}N$ values varied among samples with lowest values found in carapace biofilm samples (Fig. 4, Supplementary Information 3). Plotting natural abundances in a biplot together with values recorded in the literature for multiple primary producers and other crab species from the same site (data from Nagata et al.[40]) shows that crab tissues (gill, muscle and viscera) are depleted with regards to ^{15}N as compared to other crab species (Fig. 4).

Discussion
Using multiple lines of evidence integrating biogeochemical measurements, stable isotope probing, 16S rRNA gene and metagenomic sequencing and qPCR of functional genes, we constructed a flowchart of holobiont N-cycling (Fig. 5). Combining evidence from potential and measured fluxes with the key microbial players presumably responsible of N transformations within the biofilm, we show that fiddler crab holobionts are hotspots of benthic N-cycling, acting as relevant sources of fixed N to their surrounding environment.

The crab microbiota fix atmospheric N_2. The highest measured rates were attributed to negative N_2 fluxes, suggesting N_2 fixation as the dominant process. N_2 fixation was also one of the most dominant metabolic processes compared to other N-cycling pathways within the metagenome, and depleted ^{15}N stable isotope signatures further point at N_2 fixation as a relevant process within the biofilm. Dinitrogen fixation is a common process in mangrove ecosystems, where the highest activities are found associated with the mangrove rhizosphere[39]. The presence of N_2 fixing prokaryotes in the mangrove rhizosphere is often explained by a mutualistic relation-
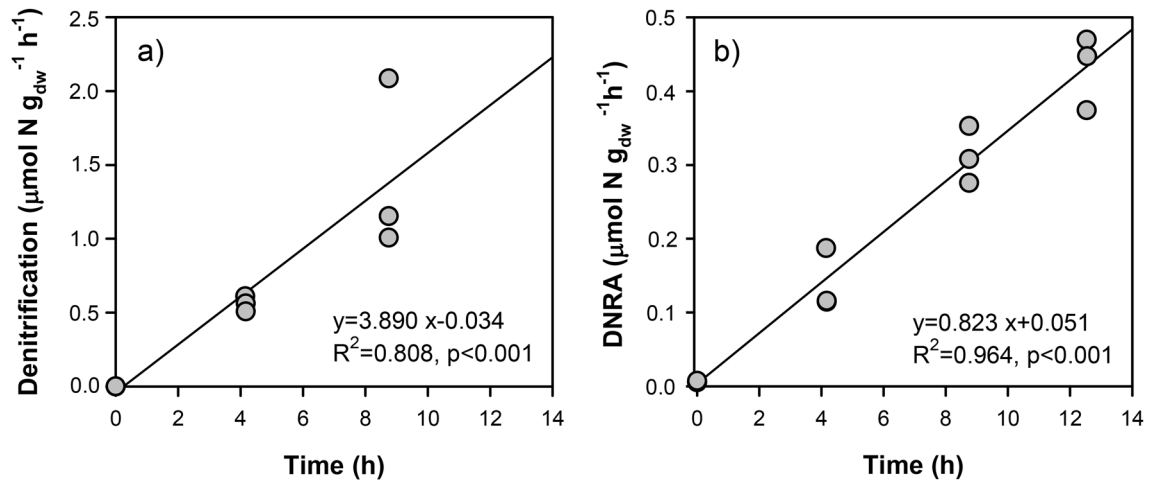
Figure 3. Nitrate reduction processes in crab carapace biofilm slurries: (**a**) production of N_2 via denitrification and (**b**) production of NH_4^+ via dissimilative nitrate reduction to ammonia (DNRA). Biofilm slurries were amended with $^{15}NO_3^-$ and incubated over a period of 12 h, and represent potential rates. Note that production of N_2 is not shown for the last time point as it exceeded the measuring rage of the instrument. Both potential rates are expresses as micromoles of N per g dry weight of suspended biofilm.
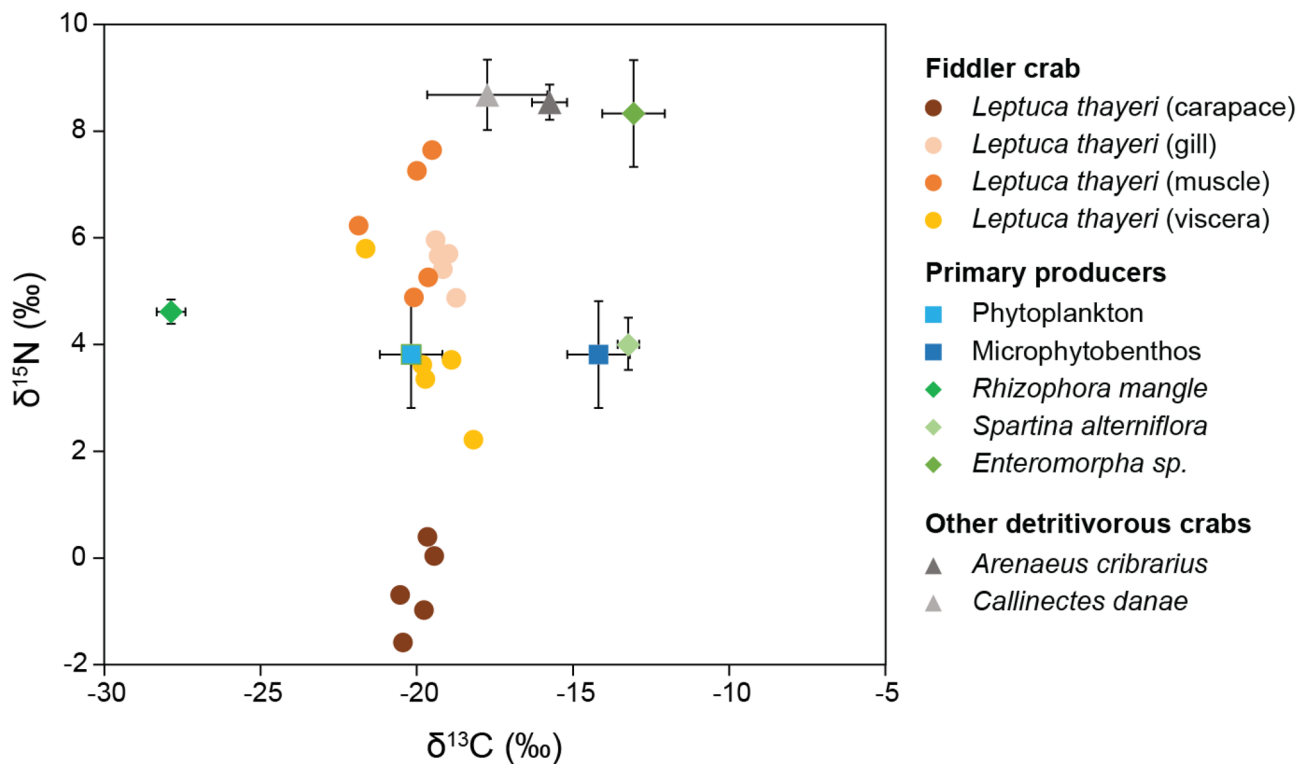

Figure 4. Signature of N_2 fixation in crab's carapace biofilms stable isotope ratios: biplot of the natural abundance of ^{13}C and ^{15}N isotopes for different samples (carapace, gill, muscle, viscera) from the fiddler crab (*Leptuca thayeri*, n = 5), and for different primary producers (as potential sources of detritus) and other detritivores crab species from the Cananéia estuarine system (data from Nagata et al.[40]).

ship between the bacteria and the plant, with roots exuding dissolved carbon required for diazotrophic growth[41]. Similarly, although it remains speculative whether fiddler crabs take advantage of N_2 fixers residing on their carapace, the depleted ^{15}N signatures in their tissues compared to other detritivores crab species from the same site may indicate a nutritional relationship between the fiddler crab host and its microbiota. Additionally, the alpha diversity of the crab biofilm prokaryotic community (Shannon's H ~ 5.5) was within the lower range of prokaryotic diversity reported in previous studies focusing on sediments[42,43], suggesting the occurrence of selection processes on the crab's carapace.
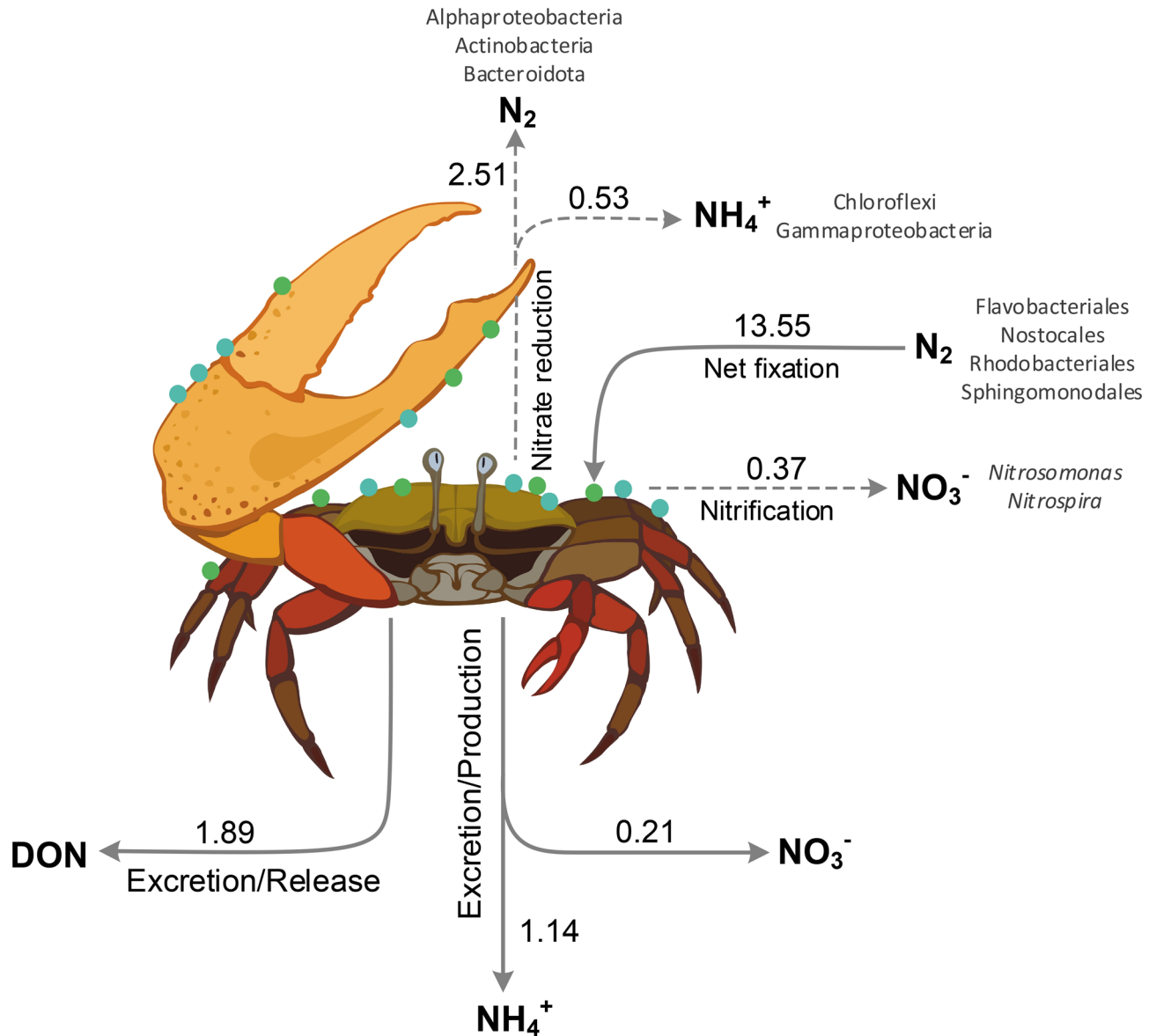
Figure 5. Flowchart of N-cycling by the fiddler crab holobiont: all fluxes were obtained combining data from incubations of single crab holobiont (in situ rates, solid lines) and suspended biofilm (potential rates, dashed lines). Note that reported rates differ from those in Table 2 as they were normalized per mean dry weight of crab's biofilm or per mean dry weight of incubated fiddler crab and are expressed as µmol N crab^{-1} d^{-1}. The main taxonomic groups involved in N-cycling as indicated by metagenomics analyses are provided. Drawing by V. Gasiūnaitė.

Biofilm-covered fiddler crabs were collected from an open muddy bank near a tidal creek, where sunlight stimulates the growth of unique phototrophic microorganisms, different from those found landward[44]. These fiddler crabs constantly migrate between burrows and the sediment surface and such vertical and horizontal migrations across contrasting environmental gradients (light regime, salinity, redox conditions, nutrients, organic matter) have the potential to create strong selective pressures on its biofilm-associated prokaryotes, although prior studies found that the fiddler crabs' carapace was colonized by multiple microbial pools from the burrow walls[17,18].

The most represented taxa within the biofilm was the Cyanobacteria genus *Geitlerinema*, which dominated the community with ~ 12% of all 16S rRNA gene sequences (see Supplementary Fig. 1) suggesting an important role within the assemblage. *Geitlerinema* contains biofilm-forming species that are capable of photosynthetic anoxygenic N$_2$ fixation[45]. Due to its environmental plasticity, *Geitlerinema* spp. photosystem machinery may reduce oxygen production allowing oxygen-sensitive processes such as N$_2$ fixation to operate in its cell or in neighbouring bacteria[45]. Other potential N$_2$ fixers in our dataset were affiliated to well-known diazotrophic bacterial taxa like Sphingomonadales, Rhodobacteriales and Flavobacteriales. For example, *Erythrobacter* (the top alphaproteobacterial ASVs, Supplementary Fig. 1) is suspected to be diazotrophic[46] and forms facilitative consortia with N$_2$-fixing cyanobacteria[47]. Similarly, on the crabs' carapace, a N$_2$-fixing consortium (Fig. 5) might

represent an association arranged along environmental gradients within the biofilm (e.g. light, oxygen) and whose strategy is to cooperate in order to enhance diazotrophic activity under N-limiting conditions[48,49]. The dominance of *Geitlerinema* spp. might be ascribed to its metabolic plasticity allowing it to cope with both high sulphide concentrations, which may build-up in clogged burrows, and air exposure when the crab leaves to the surface[45].

Nitrogen is both assimilated and lost. Nitrification (i.e. the recycling of N through oxidation of NH_4^+ to NO_3^-) doesn't appear to play an important role on the crab's carapace (Fig. 5). Accordingly, nitrifying bacteria affiliated to *Nitrospira* and *Nitrosomonas* represented only a minor fraction of the biofilm bacterial community. The low abundance of these microbial taxa is also a common feature across different benthic environments[50,51]. Sequences encoding proteins such as *amoA* and likely *pmoA*, responsible for NH_4^+ and methane oxidation, were present in the metagenome. However, it is difficult to discriminate the relevance of nitrification from the metagenomic dataset, as both monooxygenases are membrane-bound and evolutionary-related enzymes, thus frequently annotated together[52]. Additionally, our measured potential rates of nitrification were low, further indicating limited nitrification (Fig. 5).

Sequences encoding key enzymes for both assimilative and dissimilative (denitrification and DNRA) NO_3^- reduction process were detected in our metagenome, indicating the metabolic potential for both these processes to occur on the carapace. Though DNRA genetic potential was quantitatively similar to that of denitrification, process measurements indicated a much higher expression of the latter, and denitrification was a dominant pathway of NO_3^- reduction in the biofilm slurries (Fig. 5). Nevertheless, despite the high potential denitrification rates found in our incubations under anaerobic conditions, the metabolic capacity of denitrifiers is likely limited by low NO_3^- background concentrations in the surrounding water ($NO_3^- < 0.5$ μM). A previous study showed that NO_3^- produced during nitrification can partly support denitrification inside the biofilm[28]. However, in our study nitrification and excretion by the fiddler crab holobiont could only support 8–15% of denitrification potential. Furthermore, the high potential of assimilatory NO_2^- reduction to NH_4^+ in the biofilm likely promotes competition for NO_3^- between the different microbial populations. Therefore, the predominance of potential denitrification over DNRA in our biofilm slurry incubations might be explained by the C:N ratio or by NO_2^- concentrations[53].

The major groups likely involved in dissimilative processes in our samples were Alphaproteobacteria, Actinobacteria, Bacteroidota, Chloroflexi and Gammaproteobacteria, taxa which frequently harbour these proteins in the marine environment[54]. The genuses *Janibacter* (*Intrasporangiaceae*) and *Aquimarina* (*Flavobacteriaceae*) were highly represented in the crab's microbiota and both have the metabolic capacity to reduce NO_3^-[55,56]. Most identified bacteria possess all four genes (*nar/nap*, *nir*, *nor* and *nos*) which allow for complete NO_3^- reduction to N_2 as the end product[57]. The genus *Blastomonas* (Sphingomonadales), also highly represented, include members known for their chemotrophic lifestyle, capable of using NO_3^- and its reduction products as electron acceptors[51,58–61]. Furthermore, the phylogenetic assignment of *nar* and *nir* genes indicates that the cyanobacterium *Geitlerinema* spp. may be involved in both N_2 fixation and dissimilative NO_3^- reduction. On the other hand, the major groups containing the array of genes NapC/NirT/Nrf (therein *nrf*A), responsible for DNRA, were assigned primarily to Chloroflexi (Anaerolineae) and to unclassified Gammaproteobacteria.

The transcription of most marker genes encoding for NO_3^- reduction and its derivatives typically occurs under low oxygen conditions[62], which we may also expect within the crab's biofilm. However, temporal oxygen fluctuation on the carapace is inevitable when the host leaves its burrow to the surface and it is exposed to air and oxygen production via photosynthesis by associated phototrophs (e.g. Nostocales). Oxygen rise should supress the metabolic capacity of anaerobic bacteria, and especially of those that are respiring NO_3^-. However, Marchant et al.[63] demonstrated that in dynamic environments with strong oxygen oscillations such as permeable sediments subject to daily tidal inundations, the transcription of denitrification genes happens both under oxic and anoxic conditions, suggesting that in the short time (hours) terminal reductases are not immediately suppressed and the electron flow continues. The occurrence of anoxic niches within the biofilm would further allow the microbial community to physiologically dispose of excess reducing equivalents[63,64]. Aerobic denitrification, on the other hand, is unlikely to occur under these conditions as indicated by the low number of reads of the key marker gene—periplasmic nitrate reductase (*nap*; review by[65])—in our samples. Similarly, anammox appeared to be a negligible process within the biofilm, probably being suppressed by the fluctuating environmental conditions (temperature, O_2, and nutrient concentrations) experienced by the crab holobionts, which are unfavourable to slow-growing anammox bacteria[66]. This is also the case in mangrove sediments where the contribution of anammox to N removal is usually of minor importance[67].

Overall, we speculate that dissimilative processes like denitrification have little ecological meaning here as they are constrained by low N availability in the water column or within sediments. Furthermore, the presence of both assimilative and dissimilative NO_3^- reduction processes within the biofilm (see Fig. 3) suggests strong competition for N between denitrifiers and other bacteria/microalgae. As potential rates generally overestimate in situ rates due to high substrate availability, we argue that the biofilm tends to recycle and relocate N via coupled dissimilative and assimilative processes, avoiding permanent N losses and acting as a net N_2 sink and as a source of particulate and dissolved N to the environment.

Host excretion further releases N. As a matter of fact, we show significant DON release by the fiddler crab and associated microbiota (Fig. 5). This is an interesting finding since most of decapod crustaceans primarily excrete ammonia (NH_3) or the conjugated acid NH_4^+[68]. Nevertheless, it has been shown that some decapods (e.g., shrimps living at lower temperatures than in our study site), can excrete DON, although this never exceeds NH_4^+ excretion[69]. In the fiddler crab, the significant amount of released DON might partly derive from fixed N which is not assimilated by the crab and its associated bacteria or microalgae. The biochemical mechanisms

that promote such DON release should be addressed in future studies. Furthermore, it has rarely been questioned whether NH_4^+ excretion by animals is solely a physiological process or if it might also be attributed to invertebrate-bacteria associations[70]. For example, Samuiloviene et al.[38] found active transcription of *nrfA* gene (encoding for DNRA) in tube dwelling chironomid larvae, suggesting the presence of active ammonifiers. In our study, the results from both qPCR and metagenomic analyses corroborate the presence of ammonifiers within the biofilm, which can potentially contribute up to 46% of net NH_4^+ production by the fiddler crab holobiont.

The crab holobiont contributes to the ecosystem N budget. N_2 fixation was one of the most dominant pathways compared to other N-cycling processes associated with fiddler crab microbiota, suggesting that this characteristic benthic invertebrate has a potentially relevant role in mangrove ecosystems as a vector of newly fixed N to the surrounding environment. The study area is a system where N_2 fixation is an important conduit for bioavailable N[39]. Therefore, fixed N is an essential element in mangrove food webs, including detritus-feeding fiddler crabs. On the other hand, by selective grazing on bacteria or microalgae[15,71,72] these crabs can redistribute or reduce N_2 fixation in mangrove forests. Measured dissolved N production by the host, which likely comes from crab excretion, exudation of newly fixed N or its turnover within the biofilm, together with that associated to crab faeces—not measured here—can enrich with N the surrounding benthic system. Moreover, as the fiddler crabs intermolt and molt cycles last < 150 days[73], the labile organic matter of the biofilm-covered carapace is delivered to the benthic system at least 3 times per year and can prime heterotrophy by relieving the very high C:N sediment ratios.

In a wider ecosystem context, considering a minimum abundance of 10 crab individuals per square meter[74], fiddler crabs can produce 33 μmol m^{-2} d^{-1} of dissolved N which compensate/reverse dissolved N uptake measured at the sediment–water interface (-71 μmol m^{-2} d^{-1};[39]). In addition, N_2 fixation associated with fiddler crabs can deliver 135 μmol N m^{-2} d^{-1} which compares to 27% of N_2 fixation in surface microbial mats (500 μmol m^{-2} d^{-1};[39]). Unlike most bioturbating invertebrates, fiddler crabs temporally leave their burrows while feeding, mating or for territorial defence, moving to the surface sediment during low tide[24,75,76]. During high tide the crabs plug their burrows with sediment, residing either in a formed air chamber or crawling deeper to the flooded part of the burrow[23,77,78]. Because of crab respiration (~7 μmol O_2 crab^{-1} h^{-1}, data not shown) or oxidation of end-metabolic compounds (e.g., NH_4^+, H_2S), oxygen is gradually consumed in the burrows[79], promoting NO_3^- reduction processes and transient accumulation of NH_4^+, despite these latter processes likely having little quantitative relevance at the ecosystem level.

Conclusion

Mangroves ecosystems are increasingly challenged by anthropogenic activities, which may result in pressure to these ecosystems in terms of increasing nutrient or organic matter loading[80]. Under the pristine conditions of Cananéia region[39], crab's biofilm microbiota may be dominated by diazotrophic members, contributing fixed N to the environment, and possibly to the host. Conversely, if exposed to eutrophic conditions, fiddler crab holobionts may experience changes in the biofilm composition and metabolic repertoire, with a suppression of the energy-costly process of N_2 fixation and an increase of dissimilative losses of excess N. Future studies should extend this combined molecular and biogeochemical approach to other study areas along environmental gradients, in order to verify to which degree fiddler crab carapace microbiota is environmentally assembled vs determined by host factors.

Material and methods

Study site.   Specimens of the Atlantic mangrove fiddler crab (*Leptuca thayeri,* Rathbun 1900) were collected in their burrows during low tide from a muddy bank nearby a small channel (25°2′55.50″, 47°58′31.24″) located in the estuarine system of Cananéia, on the south coast of Brazil. During the sampling event surface (0.5 m depth) water temperature in the channel was 19.5 °C, salinity was 26.2 and dissolved oxygen concentration was 184.4 μM. This pristine estuarine system receives seasonally variable nutrient inputs depending on rainfalls, however, dissolved inorganic nitrogen (DIN) concentration in the system rarely exceeds > 4 μM of DIN[81]. The estuarine system, extending over an area of 110 km², is part of the Cananéia–Iguape complex and is characterized by the presence of mangroves, restingas, inland seas and islands (Cananéia, Cardoso, Comprida, and Iguape). The region is part of the Cananéia–Iguape–Paranaguá Environmental Protection Area, and is recognized by UNESCO as part of the Biosphere Reserve. The estuarine system is connected to the South Atlantic Ocean by the Cananéia and Icapara inlets located, respectively, to the south and north of the system. Water circulation in the estuary channels is driven by a daily tidal flow and inflow of freshwater from continental drainage of several small rivers up to 6 m³ s^{-1} during dry season[82]. The intertidal stands are composed by *Spartina* meadows at the outermost portion, followed by *Laguncularia racemosa* in two stages of development. *Rhizophora* mangle followed by *Avicennia schaueriana* occupy the inner parts of the mangrove forests[83].

DNA extraction.   Samples for DNA analysis were collected in the field from the carapace of randomly selected crabs (n = 3, with total surface area of ~ 8 cm²) by using swabs (after rinsing in 0.2-μm-filtered seawater), which were later preserved in RNAlater (Zymo Research). In the laboratory, DNA was extracted from three samples using the QIAamp Fast DNA Stool Mini Kit (QIAGEN). The lysis temperature was increased to 90 °C to improve the bacterial cell rupture. The final extracted DNA was subsampled for (1) 16S rRNA gene amplicon sequencing, (2) shotgun metagenomic sequencing, and (3) functional gene quantification by qPCR. Metagenome sequencing was carried out in one pooled sample (n = 3) to get sufficient amount of DNA for shotgun sequencing.

16S rRNA gene amplicon sequencing. 16S rRNA gene sequences were amplified from extracted DNA using the primer pair Probio Uni and/Probio Rev, targeting the V3 region of the 16S rRNA gene sequence as described previously by Milani et al.[84]. High-throughput sequencing was performed at the DNA sequencing facility of GenProbio srl (www.genprobio.com) on an Illumina MiSeq with the length of 250×2 bp, according to the protocol previously reported in Milani et al.[84]. Sequencing yielded 144,418 paired-end reads (range 102,813–185,876) and the fastq data was analysed according to the DADA2 pipeline[85] using the DADA2 1.12.1 package with R. Default settings were used with some exceptions, during quality trimming: truncLen = c(150,150), maxEE = 5, truncQ = 2, m, trimLeft = c(21, 22). This allowed to keep high quality reads and remove leftover primers from the sequences. FastQC 0.11.8 was used to manually check the quality of the trimmed reads[86]. During merging of the reads: minOverlap = 10, and during chimera removal: allowOneOff = TRUE, minFoldParentOverAbundance = 4. Sequences were classified against the SILVA 138 database[87], and chloroplast sequences were removed. The final amplicon sequence variant (ASV) data was normalized as relative abundance (%). Shannon's H alpha diversity was calculated in the software Explicet 2.10.15[88] after sub-sampling to the lowest sample size (88,457 counts). A full list of all ASVs, taxonomic classifications and sequence counts are available in Supplementary Information 1.

Shotgun metagenomic sequencing. Shotgun-based metagenomics analysis was performed on Illumina NextSeq with sequence length of 150×2 bp. Raw sequencing data consisted of 17.8 million paired-end reads and was manually checked for quality using FastQC[86]. Illumina adapters had been removed by the sequencing facility, and that no remains of PhiX control sequences were left was checked by mapping reads against the PhiX genome (NCBI Reference Sequence: NC_001422.1) using Bowtie2 2.3.4.3[89]. Reads were quality trimmed using Trimmomatic 0.36[90] with the following parameters: LEADING:20 TRAILING:20 MINLEN:50. FastQC was used to check the quality of the trimmed reads. The trimmed data consisted of 17.4 million paired-end reads, with an average quality Phred score of 33 per base, and an average read length of 144 bp. Because low merging rate of the pairs, ~ 37% with PEAR 0.9.10[91], the quality trimmed forward (R1) and reverse (R2) read-pairs were annotated separately. Protein annotation against the NCBI NR database was conducted by using the aligner Diamond 0.9.10[92] in combination with BLASTX 2.6.0+[93] with an e-value threshold of 0.001. The data was imported into the software MEGAN 6.15.2[94] and analysed for taxonomy, using default lowest common ancestor (LCA) settings, with the NCBI accession numbers linked to NCBI taxa (MEGAN supplied database: prot_acc2tax-Nov2018X1.abin). Protein annotated sequences were analysed in MEGAN using the supplied database acc2interpro-June2018X.abin that links accession numbers to the InterPro database and Gene Ontology (GO) categories. The taxonomy and protein data attributed to N-cycling were extracted from MEGAN and the average read count for R1 and R2 was used for further analysis. In total, 9.0–9.2 million sequences were classified to taxonomy, and 4.9–5.0 million sequences to proteins (range of R1 and R2 data). To link taxonomy with protein classifications the "read name-to-taxonomy" and "read name-to-protein" tables were extracted from MEGAN using the inbuilt functions of the software. These tables were combined based on identical read names. A full list of taxonomy, related N-cycling proteins, and sequence counts are available in Supplementary Information 2.

Functional gene quantification. Quantitative polymerase chain reactions (qPCR) were used to quantify the abundance of bacterial 16S rRNA gene and functional genes involved in N-cycling on the crab carapace: (1) genes of haem-containing nitrite reductase (*nirS*), (2) Cu-containing nitrite reductase (*nirK*), (3) bacterial and archaeal ammonia monooxygenase (*amoA*) and (4) cytochrome C nitrite reductase (*nrfA*). The primers and reference strains were used according to Samuiloviene et al.[38]. Quantitative PCR was performed with the StepOnePlus Real Time PCR system (ABI 7900 HT Sequence Detection System, PE Biosystems) using optical grade 96-well plates. The PCR reaction was run with a final volume of 20 µl containing 10 µl of SYBR Green master mix, 0.2 µM of forward and reverse primers, 2 mM of $MgCl_2$ (25 mM) and 2 µl of DNA sample (diluted 1/10). The thermocycling conditions were as follows: 50 °C for 2 min; initial denaturation at 94 °C for 10 min; 40 cycles at 94 °C (1 min), 60 °C (1 min), 72 °C (1.5 min); and final elongation at 72 °C (5 min). To assess the specificity of amplifications, a melting curve analysis was performed in the range of 60–95 °C, with 0.3 °C increment. Each sample was analysed in triplicates. Triplicate no-template controls were also included in each qPCR assay. The abundance of target functional genes was expressed per number of 16S rRNA gene copy.

Individual microcosm incubations. In the laboratory, collected fiddler crabs (n = 50) were left overnight in three aquaria (volume 20 l) with ambient water, continuous aeration and temperature control fixed at 19 °C for further experimental activities. Afterwards, single intermolt fiddler crab individuals were transferred into Plexiglas microcosms (n = 5, i.d. 4 cm, height ~ 20 cm, volume = 227 ± 3 ml) filled with unfiltered seawater from the sampling site. In parallel, control microcosms with water alone (n = 3) were prepared in order to correct process rates measured in crab microcosms. All microcosms were equipped with rotating magnets to ensure continuous water mixing (25 rpm) and were initially submersed, with the top open, in an incubation tank. Dark incubations started when microcosms top opening was closed with gas tight lids and lasted for < 6 h. At the beginning (from the incubation tank, in quadruplicate) and end of the incubations (from each microcosms) 50 ml aliquots were transferred to 12 ml exetainers (Labco Ltd) and fixed with 100 µl of 7 M $ZnCl_2$ for N_2:Ar measurements. In addition, two aliquots of 20 ml were collected, filtered (GF/F filters) and transferred into PE tubes and glass vials for inorganic and organic N analyses, respectively. Filtered water samples for spectrophotometric analyses were immediately frozen at − 20 °C until analysis (see details below). After incubation, crabs from all microcosms were used to determine carapace area, dry weight (at 60 °C for 48 h), and thereafter analysed for isotopic composition. The measured N excretion/production rates were normalized for the dry weigh (dw) crab biomass.

Biofilm slurry incubations. ^{15}N tracer slurry incubations, which allow determination of potential rates, have commonly been used to investigate benthic N transformations[95]. The material for slurry incubation was collected from 22 crab carapaces (for a total area of ~ 60 cm^2) by gentle brushing using a sterile toothbrush while holding single crab individual in separate glass beaker with 0.22-μm-filtered ambient water (500 ml). The final concentration of the scratched material, suspended in 500 ml water, corresponded to 28.39 ± 0.34 g$_{dw}$ biofilm l^{-1} (at 60 °C for 48 h). The homogenized slurry, composed of material from carapace and 0.22-μm-filtered ambient water, was subsampled for oxic and anoxic incubations to measure different potential N metabolic pathways: (1) nitrification, (2) denitrification + DNRA, and (3) anammox. Potential nitrification rates were estimated by oxic incubation in Erlenmeyer flasks (n = 4) of 20 ml of the biofilm slurry enriched with ^{14}NH$_4^+$ to a final concentration of 100 μM and maintained on table shaker at 19 °C. Water samples (5 ml) were collected at the beginning and at the end of the dark incubation, that lasted ~ 21 h. Samples were centrifuged, and the GF/F filtered supernatant was analysed for combined nitrite and nitrate concentrations (NO$_x^-$ = NO$_2^-$ + NO$_3^-$). Rates were expresses as NO$_x^-$ amount produced per individual crab, taking into account the mean dry weight of biofilm per carapace. Potential NO$_3^-$ reduction processes (denitrification, DNRA and anammox) were measured in anoxic incubations. For this incubation biofilm slurries were transferred into 12 ml exetainers (n = 24) without air bubbles and continuously suspended on a rotating shaker. An overnight preincubation was necessary to consume all dissolved oxygen and ^{14}NO$_3^-$. Dissolved oxygen concentrations were monitored in additional 20 ml glass scintillation vials (n = 2) equipped with optical sensor spots (PyroScience GmbH). Thereafter, half of the exetainers was added with ^{15}NO$_3^-$ to a final concentration of 100 μM whereas the remaining exetainers were added with ^{15}NH$_4^+$ + ^{14}NO$_3^-$ to a final concentration 100 μM. After the various additions, microbial activity was immediately terminated in three replicates of each treatment by adding 100 μl of 7 M ZnCl$_2$. The other exetainers were maintained on the rotating shaker and incubated in the dark at 19 °C for 12 h. Every four hours three replicates from each treatment were retrieved and microbial activity terminated by adding 100 μl of 7 M ZnCl$_2$. This was followed by determination of isotopic composition of produced ^{15}N–N$_2$ and ^{15}N–NH$_4^+$ with the protocol explained below.

Analytical procedures and rates calculation.   Dissolved inorganic N concentrations were measured with a continuous flow analyser (Technicon AutoAnalyzer II, SEAL Analytical) using colorimetric methods[96]. NO$_3^-$ was calculated as the difference between NO$_x^-$ and NO$_2^-$. Dissolved NH$_4^+$ was analysed using the method by Treguer and Le Corre[94]. Net N$_2$ fluxes were measured via the N$_2$:Ar technique by membrane inlet mass spectrometry (MIMS) at Ferrara University (Bay Instruments[97];) and corrected for Ar concentration and solubility based on incubation water temperature and salinity[98]. Isotopic samples for ^{29}N$_2$ and ^{30}N$_2$ production were analysed by gas chromatography-isotopic ratio mass spectrometry (GC-IRMS) at the University of Southern Denmark. Briefly, headspace subsamples were injected into a GC extraction line equipped with an ascarite trap, a Porapak R chromatographic column, a copper column heated to 600 °C, and a Mg(ClO$_4$)$_2$ trap[99]. The extraction line was coupled to an isotope ratio mass spectrometer (IRMS, Thermo Delta V Plus, Thermo Scientific) by means of a Conflo III interface. Samples for ^{15}NH$_4^+$ production were analysed by the same GC-IRMS after conversion of NH$_4^+$ to N$_2$[97] by the addition of alkaline hypobromite[100]. Slopes of the linear regression of ^{29}N$_2$ and ^{30}N$_2$ concentration against time were used to calculate production rates of labelled N$_2$–p^{29}N$_2$ and p^{30}N$_2$, respectively. Since p^{29}N$_2$ was not significant in ^{15}NH$_4^+$ + ^{14}NO$_3^-$ treatment, we deduced that anammox rate was negligible. Denitrification potential rate was calculated from the equations reported in the Thamdrup and Dalsgaard[101]. The slope of the linear regression of ^{15}NH$_4^+$ concentration against time was used to calculate the production rate of labelled NH$_4^+$–p^{15}NH$_4^+$. Potential DNRA rate was calculated according to Bonaglia et al.[102]. These NO$_3^-$ reduction rates were thus corrected for the actual ^{15}N enrichment, and for individual specimen taking into account mean dry weight of biofilm per carapace.

Organic C and total N content and their isotopic composition in different crab tissues (~ 1 mg) were analyzed with a mass spectrometer (IRMS, Thermo Delta V, Thermo Scientific) coupled with elemental analyzer (ECS-4010, Costech Instruments) at the University of Sao Paulo. Before measurements samples were acidified with 1 M HCl to remove carbonates. C and N content was presented in percentage and their isotopic signatures were expressed in the form of δ ‰, according to the following equation:

$$\delta = \left[R_{sample}/R_{reference} \right) - 1 \right] \times 1000$$

where R$_{sample}$ is the isotopic ratio in the sample and R$_{reference}$ is the isotopic ratio in the reference standard (Vienna Pee Dee Belminite (V-PDB) and atmospheric N$_2$, respectively).

Data availability
The raw sequence data supporting this study have been uploaded online and are available at the NCBI BioProject PRJNA549720.

References
1. Lee, S. Y. *et al.* Reassessment of mangrove ecosystem services. *Glob. Ecol. Biogeogr.* **23**, 726–743 (2014).
2. Kathiresan, K. & Bingham, B. L. Biology of mangroves and mangrove ecosystems. *Adv. Mar. Biol.* **40**, 81–251 (2001).
3. Dittmar, T., Hertkorn, N., Kattner, G. & Lara, R. J. Mangroves, a major source of dissolved organic carbon to the oceans. *Glob. Biogeochem. Cycles* **20**(1), GB1012. https://doi.org/10.1029/2005GB002570 (2006).

4. Kristensen, E., Bouillon, S., Dittmard, T. & Marchande, C. Organic carbon dynamics in mangrove ecosystems: A review. *Aquat. Bot.* **89**, 201–219 (2008).
5. Reef, R., Feller, I. C. & Lovelock, C. E. Nutrition of mangroves. *Tree Physiol.* **30**(9), 1148–1160 (2010).
6. Woolfe, K. J., Dale, P. J. & Brunskill, G. J. Sedimentary C/S relationships in a large tropical estuary: evidence for refractory carbon inputs from mangroves. *Geo-Mar. Lett.* **15**(3–4), 140–144 (1995).
7. Woitchik, A. F. *et al.* Nitrogen enrichment during decomposition of mangrove leaf litter in an east African coastal lagoon (Kenya): relative importance of biological nitrogen fixation. *Biogeochemistry* **39**(1), 15–35 (1997).
8. Zuberer, D. & Silver, W. S. Biological dinitrogen fixation (acetylene reduction) associated with Florida mangroves. *Appl. Environ. Microbiol.* **35**(3), 567–575 (1978).
9. Kristensen, E. *et al.* What is bioturbation? The need for a precise definition for fauna in aquatic sciences. *Mar. Ecol. Prog. Ser.* **446**, 285–302 (2012).
10. Welsh, D. T. It's a dirty job but someone has to do it: the role of marine benthic macrofauna in organic matter turnover and nutrient recycling to the water column. *Chem. Ecol.* **19**, 321–342 (2003).
11. Stief, P. Stimulation of microbial nitrogen cycling in aquatic ecosystems by benthic macrofauna: mechanisms and environmental implications. *Biogeosciences* **10**(12), 7829–7846 (2013).
12. Gilbertson, W. W., Solan, M. & Prosser, J. I. Differential effects of microorganism–invertebrate interactions on benthic nitrogen cycling. *FEMS Microbiol. Ecol.* **82**, 11–12 (2012).
13. Laverock, B., Gilbert, J. A., Tait, K., Osborn, A. M. & Widdicombe, S. Bioturbation: impact on the marine nitrogen cycle. *Biochem. Soc. Trans.* **39**, 315–320 (2011).
14. Magri, M. *et al.* Benthic N pathways in illuminated and bioturbated sediments studied with network analysis. *Limnol. Oceanogr.* **63**, S68–S84. https://doi.org/10.1002/lno.10724 (2018).
15. Kristensen, E. Mangrove crabs as ecosystem engineers; with emphasis on sediment processes. *J. Sea Res.* **59**, 30–43 (2008).
16. Booth, J. M., Fusi, M., Marasco, R., Mbobo, T. & Daffonchioco, D. Fiddler crab bioturbation determines consistent changes in bacterial communities across contrasting environmental conditions. *Sci. Rep.* **9**, 3749. https://doi.org/10.1038/s41598-019-40315-0 (2019).
17. Cuellar-Gempeler, C. & Leibold, M. A. Multiple colonist pools shape fiddler crab-associated bacterial communities. *ISME J.* **12**(3), 825–837 (2018).
18. Reinsel, K. A. Impact of fiddler crab foraging and tidal inundation on an intertidal sandflat: season-dependent effects in one tidal cycle. *J. Exp. Mar. Biol. Ecol.* **313**, 1–17 (2004).
19. Nordhaus, I., Diele, K. & Wolff, M. Activity patterns, feeding and burrowing behaviour of the crab *Ucides cordatus* (Ucididae) in a high intertidal mangrove forest in North Brazil. *J. Exp. Mar. Biol. Ecol.* **374**, 104–112 (2009).
20. Nordhaus, I. & Wolff, M. Feeding ecology of the mangrove crab *Ucides cordatus* (Ocypodidae): food choice, food quality and assimilation efficiency. *Mar. Biol.* **151**, 1665–1681 (2007).
21. Fanjul, E., Bazterrica, M. C., Escapa, M., Grela, M. A. & Iribarne, O. Impact of crab bioturbation on benthic flux and nitrogen dynamics of Southwest Atlantic intertidal marshes and mudflats. *Estuar. Coast. Shelf Sci.* **92**, 629–638 (2011).
22. Quintana, C. O. *et al.* Carbon mineralization pathways and bioturbation in coastal Brazilian sediments. *Sci. Rep.* **5**, 16122. https://doi.org/10.1038/srep16122 (2015).
23. Thongtham, N. & Kristensen, E. Physical and chemical characteristics of mangrove crab (*Neoepisesarma versicolor*) burrows in the Bangrong mangrove forest, Phuket, Thailand; with emphasis on behavioural response to changing environmental conditions. *Vie et Milieu* **53**, 141–151 (2003).
24. De la Iglesia, H. O., Rodríguez, E. M. & Dezi, R. E. Burrow plugging in the crab *Uca uruguayensis* and its synchronization with photoperiod and tides. *Physiol. Behav.* **55**(5), 913–919 (1994).
25. Arfken, A., Song, B., Bowman, J. S. & Piehler, M. Denitrification potential of the eastern oyster microbiome using a 16S rRNA gene based metabolic inference approach. *PLoS ONE* **12**(9), e0185071. https://doi.org/10.1371/journal.pone.0185071 (2017).
26. Caffrey, J. M., Hollibaugh, J. T. & Mortazavi, B. Living oysters and their shells as sites of nitrification and denitrification. *Mar. Pollut. Bull.* **112**(1–2), 86–90 (2016).
27. Glud, R. N. *et al.* Copepod carcasses as microbial hot spots for pelagic denitrification. *Limnol. Oceanogr.* **60**, 2026–2036 (2015).
28. Heisterkamp, I. M. *et al.* Shell biofilm-associated nitrous oxide production in marine molluscs: processes, precursors and relative importance. *Environ. Microbiol.* **15**(7), 1943–1955 (2013).
29. Ray, N. E., Henning, M. C. & Fulweiler, R. W. Nitrogen and phosphorus cycling in the digestive system and shell biofilm of the eastern oyster *Crassostrea virginica*. *Mar. Ecol. Prog. Ser.* **621**, 95–105 (2019).
30. Stief, P. *et al.* Freshwater copepod carcasses as pelagic microsites of dissimilatory nitrate reduction to ammonium. *FEMS Microbiol. Ecol.* **94**(10), fiy144. https://doi.org/10.1093/femsec/fiy144 (2018).
31. Wahl, M., Goecke, F., Labes, A., Dobretsov, S. & Weinberger, F. The second skin: ecological role of epibiotic biofilms on marine organisms. *Front. Microbiol.* **3**, 292. https://doi.org/10.3389/fmicb.2012.00292 (2012).
32. Foshtomi, M. Y. *et al.* The link between microbial diversity and nitrogen cycling in marine sediments is modulated by macrofaunal bioturbation. *PLoS ONE* **10**, e0130116. https://doi.org/10.1371/journal.pone.0130116 (2015).
33. Pelegri, S. P., Nielsen, L. P. & Blackburn, T. H. Denitrification in estuarine sediment stimulated by the irrigation activity of the amphipod *Corophium volutator*. *Mar. Ecol. Prog. Ser.* **105**(3), 285–290 (1994).
34. Stief, P. & Beer, D. D. Probing the microenvironment of freshwater sediment macrofauna: Implications of deposit-feeding and bioirrigation for nitrogen cycling. *Limnol. Oceanogr.* **51**, 2538–2548 (2006).
35. Pischedda, L., Cuny, P., Esteves, J. L., Pogiale, J. C. & Gilbert, F. Spatial oxygen heterogeneity in a *Hediste diversicolor* irrigated burrow. *Hydrobiologia* **680**, 109–124 (2012).
36. Poulsen, M., Kofoed, M. V., Larsen, L. H., Schramm, A. & Stief, P. *Chironomus plumosus* larvae increase fluxes of denitrification products and diversity of nitrate-reducing bacteria in freshwater sediment. *Syst. Appl. Microbiol.* **37**, 51–59 (2014).
37. Petersen, J. M. *et al.* Chemosynthetic symbionts of marine invertebrate animals are capable of nitrogen fixation. *Nat. Microbiol.* **2**, 16196. https://doi.org/10.1038/nmicrobiol.2016.195 (2016).
38. Samuiloviene, A. *et al.* The effect of chironomid larvae on nitrogen cycling and microbial communities in soft sediments. *Water* **11**, 1931. https://doi.org/10.3390/w11091931 (2019).
39. Reis, C. R. G., Nardoto, G. B. & Oliveira, R. S. Global overview on nitrogen dynamics in mangroves nd consequences of increasing nitrogen availability for these systems. *Plant Soil* **410**, 1–19 (2017).
40. Nagata, R. M., Moreira, M. Z., Pimentel, C. R. & Morandini, A. C. Food web characterization based on d15N and d13C reveals isotopic niche partitioning between fish and jellyfish in a relatively pristine ecosystem. *Mar. Ecol. Progr. Ser.* **519**, 13–27 (2015).
41. Alfaro-Espinoza, G. & Ullrich, M. S. Bacterial N2-fixation in mangrove ecosystems: insights from a diazotroph–mangrove interaction. *Front. Microbiol.* **6**, 445. https://doi.org/10.3389/fmicb.2015.00445 (2015).
42. Jiménez, M.F.S.-S., Cerqueda-García, D., Montero-Muñoz, J. L., Aguirre-Macedo, M. L. & García-Maldonado, J. Q. Assessment of the bacterial community structure in shallow and deep sediments of the Perdido Fold Belt region in the Gulf of Mexico. *PeerJ* **6**, e5583. https://doi.org/10.7717/peerj.5583 (2018).
43. Wang, Y. *et al.* Comparison of the levels of bacterial diversity in freshwater, intertidal wetland, and marine sediments by using millions of Illumina tags. *Appl. Environ. Microbiol.* **78**(23), 8264–8271 (2012).

44. Dias, A. C. F. *et al.* The bacterial diversity in a Brazilian non-disturbed mangrove sediment. *Antonie Van Leeuwenhoek* **98**, 541–551 (2010).
45. Grim, S. L. & Dick, G. J. Photosynthetic versatility in the genome of *Geitlerinema* sp. PCC (formerly *Oscillatoria limnetica* 'Solar Lake'), a model anoxygenic photosynthetic cyanobacterium. *Front. Microbiol.* **7**, 1546. https://doi.org/10.3389/fmicb.2016.01546 (2016).
46. Zehr, J. P., Church, M. J. & Moisander, P. H. Diversity, distribution and biogeochemical significance of nitrogen-fixing micro-organisms in anoxic and suboxic ocean environments. In *Past and Present Water Column Anoxia. Nato Science Series: IV: Earth and Environmental Sciences* (ed. Neretin, L.) 64, 337–369 (Springer, Berlin, 2006).
47. Brauer, V. S. *et al.* Competition and facilitation between the marine nitrogen-fixing cyanobacterium Cyanothece and its associated bacterial community. *Front. Microbiol.* **7**, 795. https://doi.org/10.3389/fmicb.2014.00795 (2015).
48. Beltrán, Y., Centeno, C. M., García-Oliva, F., Legendre, P. & Falcón, L. I. N$_2$ fixation rates and associated diversity (*nifH*) of microbialite and mat-forming consortia from different aquatic environments in Mexico. *Aquat. Microb. Ecol.* **65**, 15–24 (2012).
49. Wong, H. L., Smith, D.-L., Visscher, P. T. & Burns, B. P. Niche differentiation of bacterial communities at a millimeter scale in Shark Bay microbial mats. *Sci. Rep.* **5**, 15607. https://doi.org/10.1038/srep15607 (2015).
50. Rasigraf, O., Schmitt, J., Jetten, M. S. M. & Lüke, C. Metagenomic potential for and diversity of N-cycle driving microorganisms in the Bothnian Sea sediment. *Microbiol. Open* **6**(4), 1. https://doi.org/10.1002/mbo3.475 (2017).
51. Zhang, S. *et al.* Responses of bacterial community structure and denitrifying bacteria in biofilm to submerged macrophytes and nitrate. *Sci. Rep.* **6**, 36178. https://doi.org/10.1038/srep36178 (2016).
52. Holmes, A. J., Costello, A., Lidstrom, M. E. & Murrell, J. C. Evidence that particulate methane monooxygenase and ammonia monooxygenase may be evolutionarily related. *FEMS Microbiol. Lett.* **132**(3), 203–208 (1995).
53. Kraft, B. *et al.* Nitrogen cycling. The environmental controls that govern the end product of bacterial nitrate respiration. *Science* **345**, 676–679 (2014).
54. Jiang, X., Dang, H. & Jiao, N. Ubiquity and diversity of heterotrophic bacterial *nasA* genes in diverse marine environments. *PLoS ONE* **10**(2), e0117473. https://doi.org/10.1371/journal.pone.0117473 (2015).
55. Xu, T. *et al.* Genomic insight into *Aquimarina longa* SW024T: its ultra-oligotrophic adapting mechanisms and biogeochemical functions. *BMC Genom.* **16**, 772. https://doi.org/10.1186/s12864-015-2005-3 (2015).
56. Li, J. *et al. Janibacter alkaliphilus* sp. nov., isolated from coral *Anthogorgia* sp. *Antonie Van Leeuwenhoek* **102**(1), 157–162 (2012).
57. Zumft, W. G. Cell biology and molecular basis of denitrification. *Microbiol. Mol. Biol. R.* **61**(4), 533–616 (1997).
58. Elifantz, H., Horn, G., Ayon, M., Cohen, Y. & Minz, D. *Rhodobacteraceae* are the key members of the microbial community of the initial biofilm formed in Eastern Mediterranean coastal seawater. *FEMS Microbiol. Ecol.* **85**(2), 348–357 (2013).
59. Glaeser, S. P. & Kämpfer, P. The family *Sphingomonadaceae*. In *The Prokaryotes* (eds Rosenberg, E. *et al.*) 641–707 (Springer, Berlin, 2014).
60. Katayama, Y., Hiraishi, A. & Kuraishi, H. *Paracoccus thiocyanatus* sp. nov., a new species of thiocyanate-utilizing facultative chemolithotroph, and transfer of *Thiobacillus versutus* to the genus *Paracoccus* as *Paracoccus versutus* comb. nov. with emendation of the genus. *Microbiology* **141**, 1469–1477 (1995).
61. Kraft, B., Tegetmeyer, H. E., Meier, D., Geelhoed, J. S. & Strous, M. Rapid succession of uncultured marine bacterialand archaeal populations in a denitrifying continuous culture. *Environ. Microbiol.* **16**(10), 3275–3286 (2014).
62. Härtig, E. & Zumft, W. G. Kinetics of *nirS* expression (cytochrome cd1 nitrite reductase) in *Pseudomonas stutzeri* during the transition from aerobic respiration to denitrification: evidence for a denitrification-specific nitrate- and nitrite-responsive regulatory system. *J. Bacteriol. Res.* **181**(1), 161–166 (1999).
63. Marchant, H. K. *et al.* Denitrifying community in coastal sediments performs aerobic and anaerobic respiration simultaneously. *ISME J.* **11**, 1799–1812 (2017).
64. Patureau, D., Zumstein, E., Delgenes, J. P. & Moletta, R. Aerobic denitrifiers isolated from diverse natural and managed ecosystems. *Microb. Ecol.* **39**(2), 145–152 (2000).
65. Ji, B. *et al.* Aerobic denitrification: a review of important advances of the last 30 years. *Biotechnol. Bioproc. E* **20**(4), 643–651 (2015).
66. Strous, M. *et al.* Missing lithotroph identified as new planctomycete. *Nature* **400**, 446–449 (1999).
67. Luvizotto, D. M. *et al.* The rates and players of denitrification, dissimilatory nitrate reduction to ammonia (DNRA) and anaerobic ammonia oxidation (anammox) in mangrove soils. *An. Acad. Bras. Ciênc.* **91**, e20180373. https://doi.org/10.1590/0001-37652 01820180373 (2018).
68. Weihrauch, D., Sandra Fehsenfeld, S. & Quijada-Rodriguez, A. Nitrogen excretion in aquatic crustaceans. In *Acid–Base Balance and Nitrogen Excretion in Invertebrate* (eds Weihrauch, D. & O'Donnell, M.) 1–25 (Springer, Berlin, 2017).
69. Jiang, D.-H., Lawrence, A. L., Neill, W. H. & Gong, H. Effects of temperature and salinity on nitrogenous excretion by *Litopenaeus vannamei* juveniles. *J. Exp. Mar. Biol. Ecol.* **253**(2), 193–209 (2000).
70. Cardini, U. *et al.* Chemosymbiotic bivalves contribute to the nitrogen budget of seagrass ecosystems. *ISME J.* **13**, 3131–3134 (2019).
71. Citadin, M., Costa, T. M. & Netto, S. A. The response of meiofauna and microphytobenthos to engineering effects of fiddler crabs on a subtropical intertidal sandflat. *Aust. Ecol.* **41**(5), 572–579 (2016).
72. Dyea, A. H. & Lasiak, T. A. Assimilation efficiencies of fiddler crabs and deposit-feeding gastropods from tropical mangrove sediments. *Comp. Biochem. Phys. Part A* **87**(2), 341–344 (1987).
73. Hopkins, P. Growth and regeneration patterns in the fiddler crab, *Uca pugilator. Biol. Bull.* **163**, 301–319 (1982).
74. Masunari, S. Distribuição e abundância dos caranguejos Uca Leach (Crustacea, Decapoda, Ocypodidae) na Baía de Guaratuba, Paraná, Brasil. *Rev. Bras. Zool.* **23**(4), 901–914 (2006).
75. Fusi, M. *et al.* Thermal sensitivity of the crab *Neosarmatium africanum* in tropical and temperate mangroves on the east coast of Africa. *Hydrobiologia* **803**(1), 251–263 (2017).
76. Hemmi, J. M. & Zeil, J. Burrow surveillance in fiddler crabs I. Description of behaviour. *J. Exp. Biol.* **206**, 3935–3950 (2003).
77. Christy, J. H. Predation and the reproductive behavior of fiddler crabs (Genus *Uca*). In *Evolutionary Ecology of Social and Sexual Systems—Crustaceans as Model Organisms* (eds Duffy, E. J. & Thiel, M.) 211–231 (Oxford University Press, Oxford, 2007).
78. Teal, J. M. Respiration of crabs in Georgia salt marshes and its relation to their ecology. *Physiol. Zool.* **32**, 1–14 (1959).
79. Michaels, R. E. & Zieman, J. C. Fiddler crab (*Uca* spp.) burrows have little effect on surrounding sediment oxygen concentrations. *J. Exp. Mar. Biol. Ecol.* **444**, 104–113 (2013).
80. Alongi, D. M. Impact of global change on nutrient dynamics in mangrove forests. *Forests* **9**(10), 596. https://doi.org/10.3390/f9100596 (2018).
81. Barrera-Alba, J. J., Gianesella, S. M. F., Moser, G. A. O. & Saldanha-Corrêa, F. M. P. Bacterial and phytoplankton dynamics in a sub-tropical Estuary. *Hydrobiologia* **598**, 229–246 (2008).
82. Bérgamo, A. L. *Característica da hidrografia, circulação e transporte de sal: Barra de Cananéia, sul do Mar de Cananéia e Baía do Trapandé (Master in Physical Oceanography)* (Universidade de São Paulo, São Paulo, Instituto Oceanográfico, 2000).
83. Cunha-Lignon, M. Dinâmica do Manguezal no Sistema Cananéia-Iguape, Estado de São Paulo—Brasil. Dissertação (Master in Biological Oceanography). Instituto Oceanográfico, Universidade de São Paulo, São Paulo (2001).
84. Milani, C. *et al.* Assessing the fecal microbiota: an optimized ion torrent 16S rRNA gene-based analysis protocol. *PLoS ONE* **8**, e68739. https://doi.org/10.1371/journal.pone.0068739 (2013).

85. Callahan, B. J. *et al.* DADA2: high-resolution sample inference from Illumina amplicon data. *Nat. Methods* **13**(7), 581–583 (2016).
86. Andrews, S. *FastQC: A Quality Control Tool for High Throughput Sequence Data*. Available online at https://www.bioinformatics.babraham.ac.uk/projects/fastqc (2010).
87. Quast, C. *et al.* The SILVA ribosomal RNA gene database project: Improved data processing and web-based tools. *Nucleic Acids Res.* **41**, D590–D596. https://doi.org/10.1093/nar/gks1219 (2012).
88. Robertson, C. E. *et al.* Explicet: graphical user interface software for metadata-driven management, analysis and visualization of microbiome data. *Bioinformatics* **29**(23), 3100–3101 (2013).
89. Langmead, B. & Salzberg, S. L. Fast gapped-read alignment with Bowtie 2. *Nat. Methods* **9**, 357. https://doi.org/10.1038/nmeth.1923 (2012).
90. Bolger, A. M., Lohse, M. & Usadel, B. Trimmomatic: a flexible trimmer for Illumina sequence data. *Bioinformatics* **30**, 2114–2120 (2014).
91. Zhang, J., Kobert, K., Flouri, T. & Stamatakis, A. PEAR: a fast and accurate Illumina paired-end reAd mergeR. *Bioinformatics* **30**, 614–620 (2014).
92. Buchfink, B., Xie, C. & Huson, D. H. Fast and sensitive protein alignment using DIAMOND. *Nat. Methods* **12**, 59–60. https://doi.org/10.1038/nmeth.3176 (2015).
93. Altschul, S. F., Gish, W., Miller, W., Myers, E. W. & Lipman, D. J. Basic local alignment search tool. *J. Mol. Biol. Res.* **215**, 403–410 (1990).
94. Huson, D. H. & Mitra, S. Introduction to the analysis of environmental sequences: metagenomics with MEGAN. *Methods Mol. Biol.* **856**, 415–429 (2012).
95. Risgaard-Petersen, N. *et al.* Anaerobic ammonium oxidation in an estuarine. *Aquat. Microb. Ecol.* **36**, 293–304 (2004).
96. Tréguer, P. & Le Corre, P. *Manuel d'analysis des sels nutritifs dans l'eau de mer* 2nd edn, 110 (Université de Bretagne Occidentale, Brest, 1975).
97. Kana, T. M. *et al.* Membrane inlet mass spectrometer for rapid high-precision determination of N_2, O_2, and Ar in environmental water samples. *Anal. Chem.* **66**, 4166–4170 (1994).
98. Colt, J. *Dissolved gas concentration in water: computation as functions of temperature, salinity and pressure* 2nd edn. (Elsevier, Amsterdam, 2012).
99. De Brabandere, L. *et al.* Oxygenation of an anoxic fjord basin strongly stimulates benthic denitrification and DNRA. *Biogeochemistry* **126**(1–2), 131–152 (2015).
100. Warembourg, F. R. Nitrogen fixation in soil and plant systems. In *Nitrogen Isotope Techniques* (eds Knowles, R. & Blackburn, T. H.) 127–156 (Academic Press, Cambridge, 1993).
101. Thamdrup, B. & Dalsgaard, T. Production of N_2 through anaerobic ammonium oxidation coupled to nitrate reduction in marine sediments. *Appl. Environ. Microbiol.* **68**(3), 1312–1318 (2002).
102. Bonaglia, S. *et al.* Denitrification and DNRA at the Baltic Sea oxic–anoxic interface: substrate spectrum and kinetics. *Limnol. Oceanogr.* **61**(5), 1900–1915 (2016).

Acknowledgements

Author contributions

M.Z. and M.B. conceived the ideas and designed methodology; M.Z. performed invertebrate sampling; M.Z. and V.G.C. carried out the incubation experiments; S.B. and V.G.C. carried out the mass spectrometric, spectrophotometric analyses and crab measurements; A.S. and E.B. performed molecular analysis. M.Z., U.C., F.J.A.N., M.B., E.B. and S.B. led the data analysis and wrote the manuscript. All authors contributed to the discussion and interpretation of the data, and to the writing of the manuscript.

Competing interests

Additional information

Supplementary information is available for this paper at https://doi.org/10.1038/s41598-020-70834-0.

Correspondence and requests for materials should be addressed to M.Z.

Reprints and permissions information is available at www.nature.com/reprints.

III

Politi, T., R. Barisevičiūtė, M. Bartoli, S. Bonaglia, U. Cardini, G. Castaldelli, A. Kančauskaitė, U. Marzocchi, J. Petkuviene, A. Samuiloviene, I. Vybernaite-Lubiene, A. Zaiko, M. Zilius. 2021. A bioturbator, a holobiont, and a vector: The multifaceted role of *Chironomus plumosus* in shaping N-cycling. *Freshwater Biology* 66(6), 1036–1048.

ORIGINAL ARTICLE

Freshwater Biology **WILEY**

A bioturbator, a holobiont, and a vector: The multifaceted role of *Chironomus plumosus* in shaping N-cycling

Tobia Politi[1] | Rūta Barisevičiūtė[2] | Marco Bartoli[1,3] | Stefano Bonaglia[1,4,5] |
Ulisse Cardini[1,6] | Giuseppe Castaldelli[7] | Akvilė Kančauskaitė[1] | Ugo Marzocchi[1,6] |
Jolita Petkuviene[1] | Aurelija Samuiloviene[1] | Irma Vybernaite-Lubiene[1] |
Anastasija Zaiko[1,8,9] | Mindaugas Zilius[1,7] (ID)

[1]Marine Research Institute, Klaipeda University, Klaipeda, Lithuania

[2]State Research Institute, Center for Physical Sciences and Technology, Vilnius, Lithuania

[3]Department of Chemistry, Life science and Environmental Sustainability, Parma University, Parma, Italy

[4]Department of Ecology, Environment and Plant Sciences, Stockholm University, Stockholm, Sweden

[5]Department of Marine Sciences, University of Gothenburg, Gothenburg, Sweden

[6]Integrative Marine Ecology Department, Stazione Zoologica Anton Dohrn, National Institute of Marine Biology, Ecology and Biotechnology, Napoli, Italy

[7]Department of Life Science and Biotechnology, Ferrara University, Ferrara, Italy

[8]Coastal and Freshwater Group, Cawthron Institute, Nelson, New Zealand

[9]Institute of Marine Science, University of Auckland, Auckland, New Zealand

Correspondence
Tobia Politi, Marine Research Institute of Klaipeda University, Universiteto al. 17, 92294 Klaipeda, Lithuania.
Email: tobia.politi@jmtc.ku.lt

Funding information
Lietuvos Mokslo Taryba; European Social Fund, Grant/Award Number: 09.3.3-LMT-K-712-01-0069; Klaipėda University

Abstract

1. Tube-dwelling chironomid larvae are among the few taxa that can withstand and thrive in the organic-rich sediments typical of eutrophic freshwater ecosystems. They can have multiple effects on microbial nitrogen (N) cycling in burrow environments, but such effects cease when chironomid larvae undergo metamorphosis into flying adults and leave the sediment.

2. Here we investigated the ecological role of *Chironomus plumosus* by exploring the effect of its different life stages (as larva and adult midge) on microbial N transformations in a shallow freshwater lagoon by means of combined biogeochemical and molecular approaches. Results suggest that sediment bioturbation by chironomid larvae produce contrasting effects on nitrate (NO_3^-)-reduction processes.

3. Denitrification was the dominant pathway of NO_3^- reduction (>90%), primarily fuelled by NO_3^- from bottom water. In addition to pumping NO_3^--rich bottom water within the burrows, chironomid larvae host microbiota capable of NO_3^- reduction. However, the contribution of larval microbiota is lower than that of microbes inhabiting the burrow walls. Interestingly, dinitrogen fixation co-occurred with NO_3^- reduction processes, indicating versatility of the larvae's microbial community.

4. Assuming all larvae (averaging 1,800 ind./m^2) leave the sediment following metamorphosis into flying adults, we estimated a displacement of 47,787 μmol of organic N/m^2 from the sediment to the atmosphere during adult emergence. This amount of particulate organic N is similar to the entire N removal stimulated by larvae denitrification over a period of 20 days.

5. Finally, the detection of N-cycling marker genes in flying adults suggests that these insects retain N-cycling microbes during metamorphosis and migration to the aerial and terrestrial ecosystems. This study provides evidence that chironomids have a multifaceted role in shaping the N cycle of aquatic ecosystems.

KEYWORDS
chironomid larvae, denitrification, functional genes, metamorphosis, nitrogen cycling, nitrogen fixation

1 | INTRODUCTION

Few macrofauna taxa are able to thrive in the highly reduced conditions typical of eutrophic freshwater sediments. Those that manage to colonise these environments exhibit behavioural and physiological adaptations, such as frequent burrow ventilation and low basal metabolism (minimal excretion or shift to alternative respiration pathways) to help them deal with low oxygen (O_2) levels in sediments. Chironomid larvae are among those few taxa that withstand such harsh conditions (Hamburger et al., 1995; Zettler & Daunys, 2007). They have a peculiar regulation of respiratory metabolism (Brodersen et al., 2008), shifting from aerobic to glycogen metabolism during periods of O_2 shortage (Hamburger et al., 1995). In eutrophic and low biodiverse benthic environments, chironomid larvae can reach densities of up to 11,000 ind./m^2 (Hölker & Vanni, 2015; McLachlan, 1977). They act as keystone species in benthic communities, actively bioturbating sediments and stimulate various biogeochemical processes (Benelli et al., 2018; Hölker et al., 2015).

Tube-dwelling chironomid larvae create U-shaped burrow structures within surface sediments. Although the depth of reworked sediment varies among chironomid species (Brennan & McLachlan, 1979; Stief & de Beer, 2006), the burrow network is generally characterised by steep vertical redox gradients. During intermittent ventilation of burrows, O_2- and/or nitrate (NO_3^-)-rich bottom water is pumped downwards, whereas reduced metabolites, e.g. ammonium (NH_4^+), are transported upwards (Gautreau et al., 2020; Moraes et al., 2018; Roskosch et al., 2012). This, in turn, stimulates oxidation processes and enhances microbial nitrogen (N) cycling pathways, including denitrification and nitrification (Benelli et al., 2018; Pelegrí & Blackburn, 1996; Svensson, 1997). Burrows also increase the spatial and biogeochemical heterogeneity of sediments (Lewandowski et al., 2007), creating a mosaic of microniches, in which the abundance and activity of microbial communities often exceed those of surrounding, non-bioturbated sediments (Laverock et al., 2014).

Recent studies demonstrate that chironomid larvae are hosts for a diverse bacterial community involved in different N-cycling pathways (Poulsen et al., 2014; Samuiloviene et al., 2019; Stief et al., 2009, 2010; Sun et al., 2015). Ingested bacteria can also remain active and continue their metabolic activity inside the body of their host (Poulsen et al., 2014; Stief et al., 2009). Stief and Eller (2006), by means of microsensor profiling, found that the larva's intestine is consistently anoxic and enriched with NO_3^-, thus possibly acting as a hotspot for NO_3^- reduction. Recent studies have revealed active transcription of functional genes encoding multiple NO_3^- reduction pathways in the larval body (Poulsen et al., 2014; Samuiloviene et al., 2019). While phylogenetic analyses of functional genes seemed to indicate that NO_3^- reducing bacteria originated from the surrounding sediments (Poulsen et al., 2014; Stief et al., 2009), a recent analysis of the microbial diversity associated with chironomid larvae found distinct phylotypes as compared to those found along the burrow walls or in the anoxic sediments (Samuiloviene et al., 2019).

In the present study, we explored the effect of different life stages (larvae and adults) of *Chironomus plumosus* (Diptera, Insecta) on microbial N transformations in the shallow freshwater Curonian Lagoon (south-east Baltic Sea). Chironomids, with their multifaceted ecological role in aquatic ecosystems, provide an opportunity to investigate coupled redox processes and specialised microbial communities involved in N-cycling. We hypothesise that chironomids differentially affect N transformations across their life stages, with a substantial contribution to N export from sediments during emergence. While the role of *C. plumosus* in stimulating sediment microbial communities through bioturbation is well known (Johnson et al., 1989; Samuiloviene et al., 2019), we here consider its role, together with associated microbiota, as a discrete ecological unit, i.e. a holobiont (Bordenstein & Theis, 2015). Another aspect investigated here, which distinguishes *C. plumosus* from other bioturbating species, is its metamorphosis from burrowing larvae to flying adults. Such a process, with the consequent organic N export, may be an alternative to N removal via sedimentary denitrification or anaerobic ammonium oxidation (anammox). In this study, we employed whole sediment core and individual larvae incubations, quantification of functional genes and N content analysis both in larvae and following their emergence as flying adults to better understand the multifaceted role of chironomids in benthic N-cycling.

2 | METHODS

2.1 | Experimental setup

In April 2019, the upper layer (top 10 cm) of muddy sediments (organic carbon = 12.1%, median grain size = 0.035 mm) were collected in the central part of the eutrophic Curonian Lagoon (55°17.2388′N, 21°01.2898′E, depth *c.* 3.0 m). Sediments were sieved (0.5 mm mesh) to remove large debris and to retrieve a sufficient amount of chironomid larvae (fourth instar). A scheme of the experimental workflow, setup, and analysis is provided in Appendix S1. Microcosms set up for whole core incubations were prepared following an experimental design previously described in Benelli et al. (2018). Briefly, 12 bottom-capped Plexiglas microcosms (height = 30 cm, inner diameter = 8 cm) were reconstructed with a 10-cm sediment layer and *c.* 17-cm water column in each. Three different densities of larvae were applied: only sediment (0 ind./m^2), low (600 ind./m^2) and high (1,800 ind./m^2), by adding none, three, and nine larvae per core, respectively. A few minutes later, when larvae had dug into the sediment, all microcosms were equipped with Teflon-coated stirring bars, submerged, and pre-incubated in a temperature-controlled (10 ± 0.2°C) tank containing 200 L of unfiltered, aerated and well-stirred lagoon water. The microcosms were pre-incubated for 15 days to allow for the establishment of stable vertical and horizontal chemical gradients and the growth of microbial communities in subsurface oxic and suboxic niches (Stocum & Plante, 2006). About 30% of the tank water was renewed with fresh lagoon water every 4 days to maintain suspended matter, nutrient concentrations and chemical gradients

across the sediment–water interface as close as possible to in situ conditions.

2.2 | Whole core incubations

After a 15-day preincubation period, net fluxes of dissolved gas (O_2, N_2), dissolved organic N (DON) and inorganic N (NH_4^+, NO_2^- and NO_3^-) were measured in microcosms during dark incubations (c. 10 hr), following the protocol previously described by Samuiloviene et al. (2019). At the beginning and end of the incubation, 40-ml water aliquots were collected from each microcosm, transferred into 12-ml exetainers (Labco Ltd) allowing overflow for two volumes before fixing with 200 μl of 7 M $ZnCl_2$ for further gas measurements. A second 40-ml water aliquot was filtered (Frisenette GF/F filters) into a plastic test tube and frozen immediately at −20°C for later dissolved N analyses (see Section 2.5). After the first incubation, microcosms were left submerged with the top open overnight, allowing to equilibrate concentration gradients across the sediment–water interface, before starting the second incubation for denitrification measurements using the isotope pairing technique (IPT; Nielsen, 1992). The original IPT calculations from Nielsen (1992) were used, as the overestimation of denitrification due to anammox was assumed negligible, given its low reported rates (<4% of total N_2 production) in the lagoon sediments (Zilius, 2011). Briefly, ^{15}N labelled NO_3^- from a stock solution (20 mM $Na^{15}NO_3$, 98 atom % ^{15}N, Sigma Aldrich) was added to the water column of each core to reach a final concentration of 24 μM. To calculate the isotopic enrichment, water samples for NO_3^- analysis were collected prior to and after the isotope addition. The cores were then capped and incubated in the dark as described for flux measurements. At the end of the incubation, the water and sediment phase were gently mixed to a slurry. Thereafter, 20-ml aliquots of the slurry were transferred into 12-ml exetainers (Labco Ltd) allowing twice overflow and fixed with 200 μl of 7 M $ZnCl_2$. An additional 40-ml subsample was collected and treated with 2 g of KCl for the determination of the exchangeable NH_4^+ pool and the $^{15}NH_4^+$ fraction. Thereafter, production of $^{29}N_2$, $^{30}N_2$, and $^{15}NH_4^+$ was measured in the samples. After the second incubation, sediments from all cores were carefully sieved (0.5 mm mesh size) to count larval abundance and to estimate their wet and dry biomass (g).

2.3 | Incubations of individual larvae

Incubations of individual larvae were used to assess N-fluxes (e.g. excretion, denitrification, dissimilative nitrate reduction to ammonium [DNRA], and N_2 fixation) associated with the chironomid larvae holobionts (i.e. the assemblage of the host and its associated microbial community). Incubations were carried out in small bottom-capped Plexiglas cylindrical microcosms (total volume 227 ± 3 ml) partly filled (15 ml) with sterilised glass beads (Ø 1–1.3 mm) to provide a comparable natural habitat. Smaller glass beads were avoided

as they could be ingested by the larvae. The rest of the volume was filled with 0.2-μm twice-filtered, aerated lagoon water and amended with different isotopes (see Sections 2.3.1 and 2.3.2 for details). Filtration was necessary to remove phytoplankton, spores, and free-living and particle-associated bacteria (99.9% of living particles, verified by flow cytometry) and to target only microbial processes carried out by the larval microbiota growing on the animal cuticle and in its digestive system. A stirring magnet was placed in each chamber, allowing continuous water mixing (20 rpm) during incubation. All microcosms were capped with gas-tight lids containing two sampling ports for sample collection and water replacement.

2.3.1 | Nitrate reduction in larvae

The revised IPT was used to assess NO_3^- reduction processes associated with larvae, including denitrification, DNRA, and anammox (Nielsen, 1992; Thamdrup & Dalsgaard, 2002). Three different treatments, each with four replicates (containing six larvae each) and one control (only water), were applied (see scheme in Appendix S1). The treatments were as follows: (1) low $^{15}NO_3^-$ addition to a final concentration of 21 μM; (2) high $^{15}NO_3^-$ addition to a final concentration of 35 μM; and (3) $^{15}NH_4^+$ (15 mM $^{15}NH_4Cl$, 98 atom % ^{15}N, Sigma Aldrich) and $^{14}NO_3^-$ additions to final concentrations of 18 and 13 μM, respectively. The different $^{15}NO_3^-$ concentrations of treatments 1 and 2 were used to validate the IPT assumptions (Risgaard-Petersen et al., 2003). To calculate the degree of isotopic enrichment, water samples for NH_4^+ and NO_3^- analysis were collected prior to and after the isotope addition. The microcosms were incubated in the dark for 18 hr at 10 ± 0.2°C. Every 6 hr, water aliquots were subsampled from each replicate, transferred into 12-ml exetainers (Labco Ltd) and fixed with 200 μl of 7 M $ZnCl_2$ for gas measurements. In addition, we monitored dissolved O_2 during the incubation with a microelectrode (OX-50, Unisense A/S) in order to adjust the incubation time and prevent O_2 from changing > 20% of the initial concentration (360 μM). We used the slope of linear regressions of $^{29}N_2$ and $^{30}N_2$ concentrations versus time to calculate rates of denitrification and anammox with the equations from Thamdrup and Dalsgaard (2002). Similarly, the slope of linear regressions of $^{15}NH_4^+$ concentration versus time was used to calculate rates of DNRA according to Bonaglia et al. (2016). All NO_3^- reduction rates were expressed as a function of the number of animals, and corrected against the controls.

2.3.2 | Nitrogen fixation

Filtered water was enriched with ^{15}N-N_2 using a modified version of the method described in Marzocchi et al. (2021). Briefly, two 2-L glass bottles (Shott) were filled with 0.22-μm twice-filtered in situ water and sealed with black butyl septa and screw caps, with a hollow needle in the septum to prevent the formation of air bubbles. Thereafter, 10 ml of $^{30}N_2$ gas (99 atom % ^{15}N, Cambridge Isotope Laboratories) were injected into the bottles with a second hollow

needle in the septum to allow replacement of the liquid and the formation of a $^{30}N_2$ headspace. The procedure was repeated with additional 20 ml of gas without the second needle in the septum, to create over-pressure within the bottles and increase the dissolution of the gas. To favour the $^{30}N_2$ dissolution the bottles were shaken on a table shaker for 1 hr. This procedure resulted in a final ^{15}N-atom % of $c.$ 40% (determined by membrane inlet mass spectrometry [MIMS], see Section 2.5 for more details). Before starting the incubation, the bottles were opened and the water was gently transferred into 16 microcosms to minimise gas exchange with the atmosphere. Afterwards, 6 larvae were added to each microcosm, and incubation started when microcosms were sealed. In addition, four microcosms were prepared and incubated as described above, but with unlabelled water to serve as control for isotopic contamination. Microcosms were incubated under the same conditions as described in Section 2.3.1. Every 12 hr, one control and four microcosms with tracer were retrieved and opened. Thereafter, the larvae were collected, measured for their wet weight, and stored at −20°C for subsequent analyses. Eight freshly sampled larvae were preserved without any incubation to determine the natural $^{15}N/^{14}N$ ratios. Finally, the larvae were freeze-dried for 48 hr and analysed for particulate organic N (PON) content (%) and isotopic ratio ($\delta^{15}N$). Nitrogen fixation rates were calculated as described in Cardini et al. (2019).

2.3.3 | Excretion and respiration

Chironomid larvae excretion and respiration were assessed in parallel with isotopic measurements. Briefly, eight 22-ml glass microcosms containing 0.22-μm twice-filtered water, six with four larvae and two without larvae (control) were set up. The microcosms were sealed without leaving a headspace and incubated for approximately 4.5 hr in the dark at 10 ± 0.3°C. The concentrations of O_2 were monitored in all microcosms continuously with oxygen optodes (FireStingO2, PyroScience GmbH). At the beginning and at the end of the incubation, a 5-ml aliquot was collected from each vial and filtered (Frisenette GF/F filters) into plastic test tubes for later NH_4^+ analyses. At the end of the experiment, larvae were recovered and weighed. Excretion and respiration rates were then normalised to experimental larval densities and corrected against the controls.

2.4 | Chironomid larvae emergence

This experiment was designed to estimate the export of PON and functional marker genes (*amoA*, *nirS*, *nrfA*, and *nifH*) with the emerging adult midges. Briefly, a glass cylinder (internal diameter 20 cm, height 20 cm) was filled with homogenised surface sediment slurry to reconstruct a 10-cm sediment layer. Unfiltered lagoon water and 30 chironomid larvae were then added. The microcosm with chironomids was left in the dark for 15 days, with continuous water aeration, and with the overlying water being renewed every 4 days.

After this period, 6 larvae were collected via sterile 20-ml cut-off syringes and the cylinder was capped by a glass funnel, to which a plastic test tube was attached in order to collect emerging chironomids. Thereafter, temperature was increased by 5°C (from 10 to 15°C) to stimulate the emergence process. After 2 days, the first six adult midges and pulpal exuviae (i.e. the remains of the exoskeleton) individuals were collected in sterile test tubes. All individuals were immediately snap-frozen in liquid N_2 and stored at −80°C until further processing. Half of the collected larvae, adult midges and exuviae were used to quantify PON, while the other half was used for functional genes analysis (except for exuviae).

2.5 | Analytical methods

Dissolved gases (N_2, O_2) were quantified from N_2:Ar and O_2:Ar ratios measured by MIMS at Ferrara University (Bay Instruments; Kana et al., 1994) and corrected for Ar concentration and solubility based on temperature and salinity (Colt, 2012). The ^{15}N-atom % in the dissolved N_2 pool from the N_2 fixation experiment was also estimated using MIMS. Isotopic samples for $^{29}N_2$ and $^{30}N_2$ production were analysed by gas chromatography (GC)–isotopic ratio mass spectrometry (IRMS) at the University of Southern Denmark. Briefly, headspace subsamples were injected into a GC extraction line equipped with an ascarite trap, a Porapak R chromatographic column, a copper column heated to 600°C, and a $Mg(ClO_4)_2$ trap (De Brabandere et al., 2015). The extraction line was coupled to an IRMS (Delta V Plus, Thermo Scientific) by means of a Conflo III interface. Samples for $^{15}NH_4^+$ production were analysed by the same technique (GC-IRMS) after conversion of NH_4^+ to N_2 by the addition of alkaline hypobromite (Warembourg, 1993). Particulate organic N and its isotopic composition in *C. plumosus* (larvae, adult midge and exuviae) were analysed by a Flash EA 1112 elemental analyser connected to a Delta V Advantage IRMS (Thermo Scientific). Measured δ values (‰) were corrected using two laboratory standards calibrated against international reference materials (IAEA-600, IAEA-N-2). The long-term standard deviation was <0.2‰ for $\delta^{15}N$. Dissolved inorganic N concentrations (NH_4^+, NO_2^- and NO_x^-) were measured with a continuous flow analyser (San^{++}, Skalar) using standard colorimetric methods (Grassoff et al., 1983). Nitrate was calculated as the difference between NO_x^- and NO_2^-. Total dissolved N was analysed by the high temperature (680°C) catalytic oxidation/nondispersive infrared method using a TOC 5000 analyser (Shimadzu Corp.) with a TN module. Dissolved organic N was calculated as difference between total dissolved N and dissolved inorganic N (sum of NH_4^+, NO_2^-, and NO_3^-).

2.6 | Nucleic acid extraction

At the end of the individual incubations (Appendix S1), 24 chironomid larvae from four microcosms (six larvae per microcosm) from the high $^{15}NO_3^-$ treatment were isolated into sterilised 1.5-ml tubes, immediately snap-frozen in liquid N_2 and stored at −80°C. Before nucleic

acid extraction, the six larvae from each microcosm were pooled producing a total of four samples. In addition, samples of larvae ($n = 3$) and of emerged adults ($n = 3$) from the chironomid larvae emergence experiment were processed to analyse gene export from the sediment to the atmosphere. Individual samples were homogenised using a tissue grinder with a sterile grinding pestle (Coyote Bioscience Co Ltd) and divided equally for DNA and RNA extraction. Briefly, DNA was extracted and purified using the QIAamp Fast DNA Stool Mini Kit (QIAGEN) following the manufacturer's protocol with amended lysis temperature (temperature was increased to 90°C to improve bacterial cell rupture). RNA was extracted with the RNAeasy Mini Kit (QIAGEN) applying additional incubation with lysozyme (20 mg/ ml) and mutanolysin (250 U/ml) for 90 min at 37°C. After incubation, samples were treated following the protocol reported in Samuiloviene et al. (2019). Additional RNA cleaning was performed using the RNAeasy Mini Kit (QIAGEN) according to the manufacturer's instructions. The purified DNA and RNA were stored at −80°C until further analyses. Extracted RNA was treated with TURBO DNase (Invitrogen) according to the manufacturer's instructions. To check whether an RNA sample was free of DNA, a control polymerase chain reaction (PCR) was carried out using universal bacterial primers of 16S rRNA as described in Samuiloviene et al. (2019). Reverse transcription was performed with a SuperScriptIII Reverse Transcriptase (Invitrogen) following manufacturer's instructions. Two negative controls (without reverse transcriptase or RNA) were included. Control PCRs (same as above) were performed to confirm the transcription to complementary DNA (cDNA) and the negative controls using the product of the reverse transcription reaction as a template.

2.7 | Quantitative PCR analyses

Quantitative PCR (qPCR) was used to quantify the abundance of functional genes and transcripts involved in N-cycling in holobionts of larvae and adult midges, targeting: (1) haem-containing nitrite reductase (*nirS*); (2) cytochrome C nitrite reductase (*nrfA*); (3) archaeal and bacterial ammonia monooxygenase (*amoA-A* and *amoA-B*, respectively); and (4) Mo-containing nitrogenase (*nifH*; Appendix S2). Genomic DNA from reference organisms was used to make standard curves, and as positive controls. Standard curves were constructed using PCR products of the marker genes from the corresponding reference strains (Appendix S2). For this, the PCR products were purified with the commercial kit (PureLink PCR Purification Kit, Invitrogen) and their concentration was measured by Qubit 3.0 (Invitrogen). Obtained products were sequenced at BaseClear B.V to confirm their identity. Quantitative PCR was performed with the StepOnePlus Real Time PCR system (ABI 7900 HT Sequence Detection System, PE Biosystems). Briefly, the PCR was run on a final volume of 20 μl containing 10 μl of SYBR Green master mix, 0.2 μM of forward and reverse primers, 2 mM of $MgCl_2$, and 2 μl of DNA sample (diluted 1/10). The thermocycling conditions were adjusted as in Samuiloviene et al. (2019). To assess the specificity of amplifications, a melting curve analysis was performed in the range of 60–95°C, with 0.3°C

increments. Each sample was analysed in triplicate. In addition, triplicate template-free controls were included in each qPCR assay. The abundance and expression of target genes (DNA and RNA samples, respectively) were recalculated to copies per g fresh weight of larvae.

2.8 | Statistical analysis

Quantitative data for benthic fluxes, NO_3^--reduction processes, and functional genes were visualised using boxplots. Non-parametric Kruskal–Wallis tests were applied to determine: (1) the effect of larvae densities on benthic net fluxes and NO_3^--reduction processes (whole core incubations); (2) the effect of tracers on denitrification rates (individual incubations); and (3) differences between copy and transcript numbers. Post hoc pairwise comparisons were performed using Student–Newman–Keuls (SNK) test implemented in the Pairwise Multiple Comparison of Mean Ranks package (PMCMRC 19; Pohlert, 2014). The effect of incubation conditions on gene transcription was tested using the non-parametric Mann–Whitney rank test. The significance level was set at $\alpha = 0.05$. All analyses were performed in R v3.5.3 software (R-project, 2014) and SigmaPlot 14.0 software was used for graphical visualisations. Averages, standard errors, and number of replicates are reported in the text.

3 | RESULTS

3.1 | Oxygen and nitrogen exchange at the sediment–water interface

The presence of chironomid larvae enhanced solute exchange at the sediment–water interface (except for NO_2^-, Figure 1). However, the effect of chironomid larvae varied among the different densities, and depended on measured solute. The total uptake of O_2 was in the range of −1,190 and −2,617 μmol O_2 m^{-2} hr^{-1} (Figure 1a), and significantly (Kruskal–Wallis, $p < 0.001$) increased with the chironomid density [O_2 uptake = −0.627 × density + 1,347; $r^2 = 0.95$]. Total O_2 uptake was on average *c.* 40% higher at 1,800 ind./m^2 than at the other two densities. The O_2 respiration associated with chironomid larvae alone in individual incubations was −0.181 ± 0.008 μmol O_2 ind.$^{-1}$ hr^{-1}. The measured net flux of N_2 indicated a prevalence of denitrification over N_2 fixation in all studied microcosms (Figure 1b). The net N_2 flux at the sediment–water interface was also chironomid density-dependent [net N_2 flux = 0.075 × density + 54.71; $Rr^2 = 0.82$], with significantly (SNK test, $p < 0.05$) higher N_2 production at the highest chironomid density (196.0 ± 10.2 μmol N m^{-2} hr^{-1}). The net flux of NH_4^+ varied from −19.1 to 8.7 μmol N m^{-2} hr^{-1} without a clear correlation with chironomid larvae density (Figure 1c), with significantly higher (SNK test, $p < 0.05$) values at the low density (3.4 ± 2.3 μmol N m^{-2} hr^{-1}). The net flux of NO_2^- was marginal compared to the other solutes and varied between −0.66 and −1.73 μmol N m^{-2} hr^{-1} among the different densities (Kruskal–Wallis, $p > 0.05$). Net NO_3^- fluxes were one
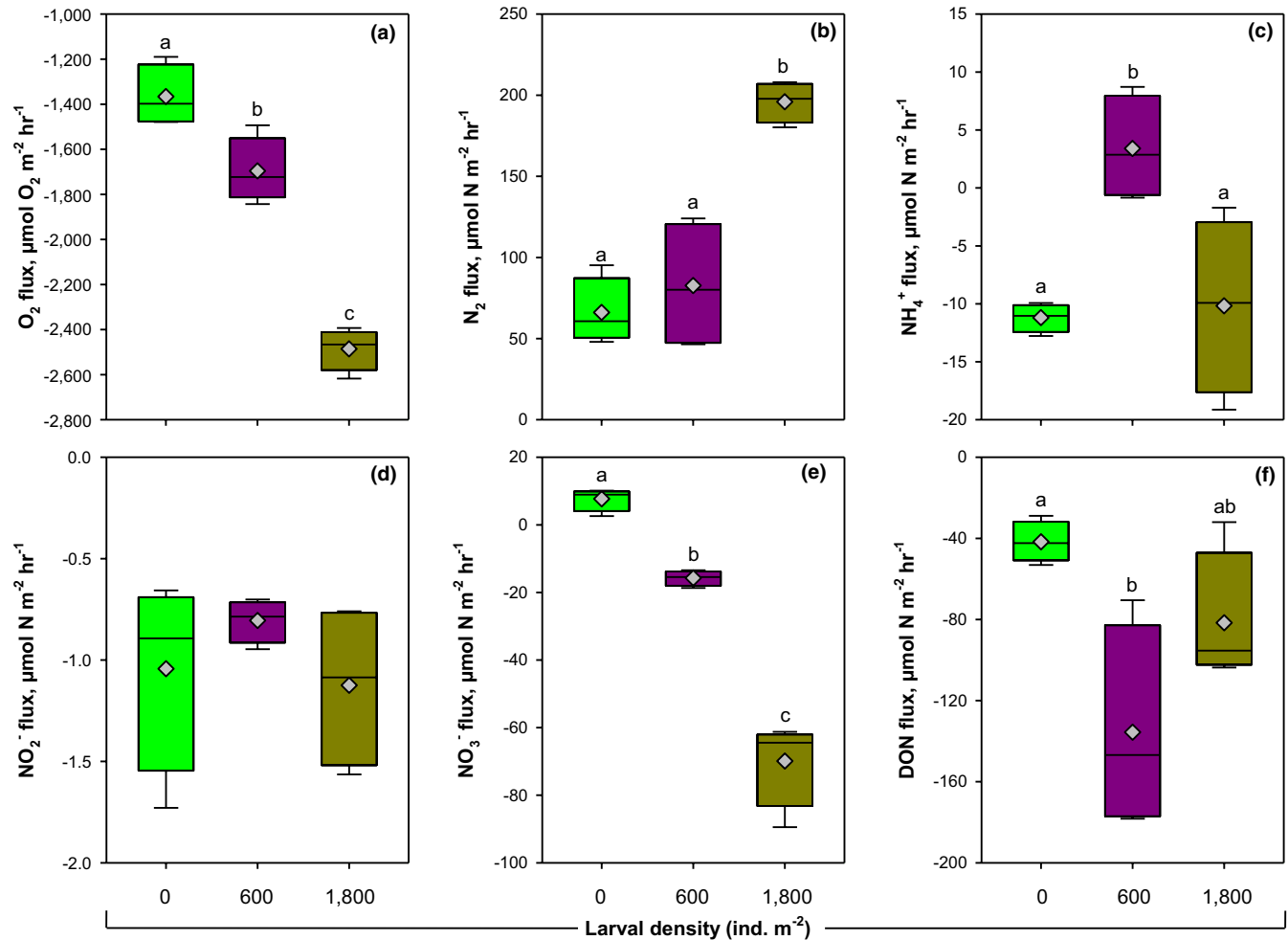
FIGURE 1 Net fluxes of dissolved oxygen (a), dinitrogen (b), ammonium (c), nitrite (d), nitrate (e), and dissolved organic nitrogen (f) at the sediment–water interface measured in whole core incubations with different densities of chironomid larvae. Data range (whiskers), upper and lower quartiles (edges), the median (horizontal line), and the mean (grey diamond) are represented for $n = 4$ replicates. Labelling by letters indicates the outcome of post hoc pairwise comparisons, i.e. bars sharing the same letter are not significantly different ($p > 0.05$)

order of magnitude higher than those of NO_2^-. The presence of larvae reversed the direction of the NO_3^- flux, which increased proportionally with the density of chironomid larvae (flux = $-0.043 \times$ density + 8.716; $r^2 = 0.96$). Nitrate uptake was significantly higher at the highest larvae density (-69.9 ± 6.6 µmol N m^{-2} hr^{-1}, SNK test, $p < 0.05$). Although we determined a stimulation of DON uptake in the presence of chironomid larvae, DON fluxes were higher in the low-density treatment (-135.9 ± 25.4 µmol N m^{-2} hr^{-1}) compared to the other two treatments (SNK test, $p < 0.05$).

## 3.2 | Denitrification and DNRA in whole core incubations

The presence of chironomid larvae selectively stimulated NO_3^- reduction. The highest total denitrification rate (D_{tot}; 97.2 ± 12.6 µmol N m^{-2} hr^{-1}) was observed at 1,800 ind./m^2 (Figure 2a). Rates of total denitrification tended to increase with the density of chironomid larvae, although such trend was not statistically

significant ($p > 0.05$). Denitrification in sediments was primarily (c. 90%) fuelled from overlaying water (D_w), while the contribution of coupled nitrification–denitrification (D_n) was of minor importance (Figure 2b,c). D_w varied between 30.5 and 120.0 µmol N m^{-2} hr^{-1} with 30% higher rates in presence of 1,800 ind./m^2 than in the other two densities. D_n rates ranged between 1.8 and 11.7 µmol N m^{-2} hr^{-1}, with high variability in sediments both with and without larvae. In contrast, DNRA rates increased significantly with larvae density (Kruskal–Wallis, $p = 0.003$), with 43% higher rates (7.5 ± 0.4 µmol N m^{-2} hr^{-1}) at 1,800 ind./m^2 when compared to the non-bioturbated sediment (3.6 ± 0.6 µmol N m^{-2} hr^{-1}; Figure 2d). At high larval density, nearly 7% of NO_3^- reduction was attributed to DNRA process.

3.3 | N-cycling associated with chironomid holobionts

Mean denitrification rates were 1.5 ± 0.4 and 1.4 ± 0.1 nmol N ind.$^{-1}$ day^{-1} at low and high $^{15}NO_3^-$ levels, respectively, indicating

FIGURE 2 Total denitrification (a), denitrification of water column NO_3^- (b), coupled nitrification-denitrification (c), and dissimilative nitrate reduction to ammonium (d) measured in whole core incubations with different densities of chironomid larvae. Data range (whiskers), upper and lower quartiles (edges), the median (horizontal line), and the mean (grey diamond) are represented for $n = 4$ replicates. Labelling by letters indicates the outcome of post hoc pairwise comparisons, i.e. bars sharing the same letter are not significantly different ($p > 0.05$)
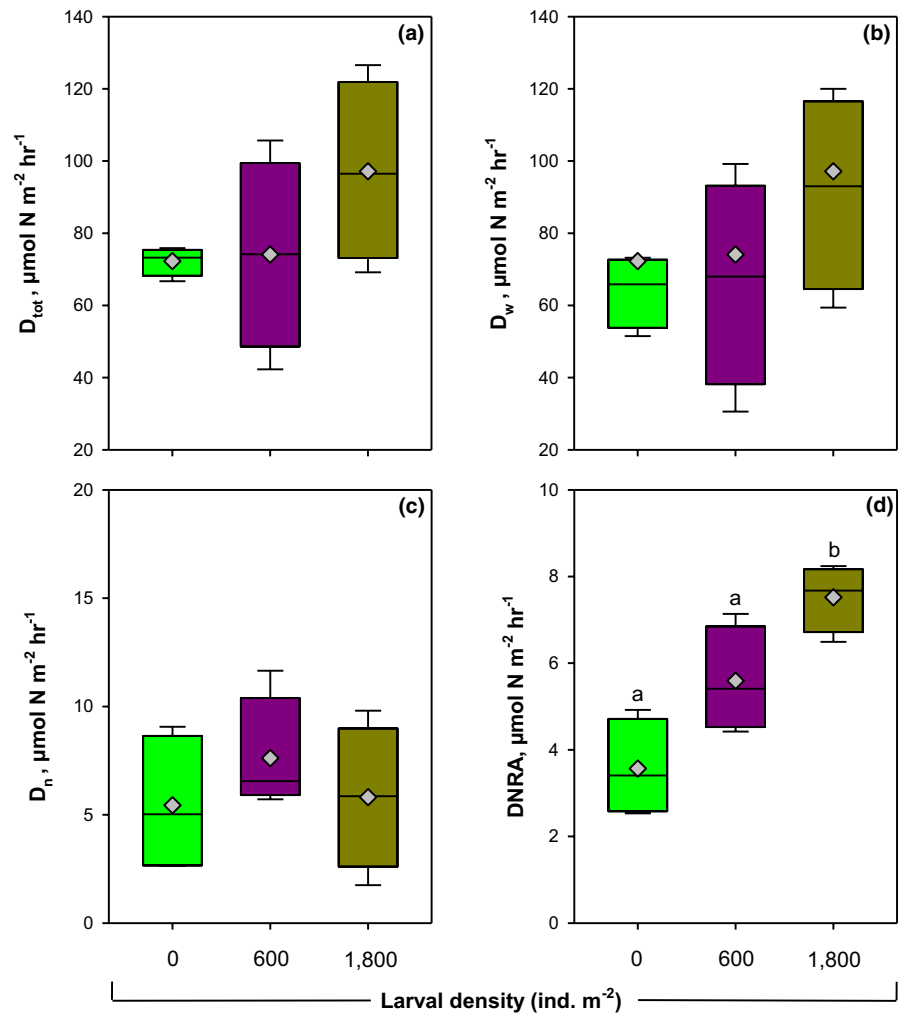
independence of tracer concentrations (Kruskal–Wallis, $p = 0.841$). This validates the proper application of the IPT in the present experiment. Dissimilative nitrate reduction to ammonium accounted for 10% of the total measured NO_3^- reduction and averaged 0.18 ± 0.04 nmol N ind.$^{-1}$ day^{-1}. NH_4^+ production via larvae excretion was the most important inorganic N flux with 175.7 ± 20.2 nmol N ind.$^{-1}$ day^{-1}. Additions of $^{15}NH_4^+ + ^{14}NO_3^-$ revealed measurable $^{29}N_2$ production rates, suggesting the presence of putative anammox (0.03 ± 0.01 nmol N ind.$^{-1}$ day^{-1}). However, this pathway contributed only 2% of the total N_2 production. N_2 fixation accounted for 0.2 ± 0.1 nmol N ind.$^{-1}$ day^{-1}.

3.4 | Nitrogen storage across different life stages of a chironomid holobiont

The PON content in chironomid larvae, measured just before their emergence, was 33.84 ± 1.04 μmol N per individual, which corresponded to 8.4% of their dry body weight (6.75 ± 0.20 mg; Table 1). Adult midges and the residual pulpal exuviae contained 78 and 4% of N that was measured in the larvae, respectively. The missing amount (18%) was putatively excreted during metamorphosis. Upscaling

TABLE 1 Particulate organic nitrogen (PON) storage and relative abundance in individuals during the different stages of *Chironomid plumosus* metamorphosis

Life stage	PON storage in tissues (μmol N/g$_{dw}$)	Relative amount (%)
Larvae	33.84 ± 1.04	8.4
Exuviae	2.05 ± 0.00	9.7
Adult midge	26.55 ± 0.19	7.0

Note: Average and standard errors are given based on three replicates.

these values to estimate the amount of N effectively leaving the sediment with the emerging adult midges, we estimated a sediment efflux of PON of 15,929 and 47,787 μmol N/m^2 at densities of 600 and 1,800 ind./m^2, respectively.

3.5 | Microbiota involved in N-cycling in chironomid larvae and adult midges

Both the larvae and the flying adult midges associated bacteria contained *nirS*, *nrfA*, and *nifH* genes, while bacterial and archaeal

Functional genes	Copy number ($\times 10^3$ g^{-1})			
	Burrowing larvae		Flying adults	
	DNA	RNA	DNA	RNA
nirS	321.65 ± 14.32	38.82 ± 6.73	4.25 ± 0.68	Not detected
nrfA	0.25 ± 0.05	0.05 ± 0.01	0.37 ± 0.01	0.32 ± 0.06
nifH	16.88 ± 0.26	0.09 ± 0.02	6.70 ± 0.41	0.07 ± 0.02
amoA-AOA	Not detected	Not detected	Not detected	Not detected
amoA-AOB	Not detected	Not detected	Not detected	Not detected

TABLE 2 Abundance of functional marker genes in different life stages of *Chironomus plumosus*

Note: Average and standard errors are given based on three replicates.

Abbreviations: AOA, ammonia oxidising archaea; AOB, ammonia oxidising bacteria.

amoA were not detected by qPCR assays (Table 2). Results showed that copy and transcript numbers of *nirS* were greater than those of *nrfA* and *nifH* in larvae and adult midges (except *nirS* transcripts in adult midges). Only transcripts of *nrfA* and *nifH* were found in adult midges, the former, surprisingly, at the same copy number as in larvae (0.07×10^3 copy/g). Quantitative PCR assays of chironomid holobionts from individual incubations confirmed the presence of bacterial *amoA*, *nrfA*, *nirS*, and *nifH* genes in larvae (Figure 3). The abundance of their transcripts, varied across samples, and no significant differences (Kruskal–Wallis, $p > 0.05$) with DNA copy numbers were detected. Furthermore, the number of *nirS* and *nrfA* transcripts in larvae from individual incubations with $^{15}NO_3^-$ tracer did not significantly differ (Mann–Whitney rank, $p = 0.100$, $p = 0.143$ and $p = 0.250$ for *nirS*, *nrfA*, and *nifH*, respectively) from the results obtained from burrowed individuals, indicating a negligible effect of incubation conditions on transcriptional activity.

4 | DISCUSSION

4.1 | Effects of bioturbating chironomid larvae on benthic metabolism

Due to their high densities in organic-rich sediments of the Curonian Lagoon, chironomid larvae can substantially affect benthic metabolism, in particular O_2 and NO_3^- respirations. As our results showed, O_2 demand increased with larval density, probably due to both the response of microbial communities to the increased sediment–water interface (i.e. burrow walls) and to the direct respiration of larvae. We estimated that at a realistic density of 1,800 larvae/m^2, half of the O_2 demand was associated to microbial respiration in the upper oxic layer (*c.* 4 mm) and the other half to the respiration in the subsurface burrow network, including the chironomids themselves. Based on results from the individual incubations, 12–15% of the total O_2 consumption can be attributed to the larval respiration, and 27–38% to microbial or chemical consumption along the burrow walls. In freshwater sediments, microbial communities consume O_2 mostly for organic matter mineralisation or microbial oxidation of reduced compounds (e.g. NH_4^+ or Fe^{2+}) (Hedrich et al., 2011; Moraes

et al., 2018). Intermittent burrow ventilation by the larvae creates a temporal oscillation in redox conditions that can substantially increase the metabolic rates of associated anaerobic bacteria, thus stimulating organic matter degradation (Aller, 1994). This notion was confirmed in our study by the significant correlation between larval abundance and NO_3^- reduction rates. Notably, chironomid larvae stimulated NO_3^- reduction thorough DNRA. However, rates of NO_3^- ammonification were considerably lower (<10%) than rates of denitrification. Here, the dominance of denitrification over DNRA may be explained by a relatively low C/N ratio in the sediment substrate and by a relatively high NO_3^- availability, (Tiedje et al., 1983). Additionally, low temperature and low salinity in the Curonian Lagoon create conditions that may be more favourable for denitrifiers than for DNRA bacteria (Giblin et al., 2010).

In the present study, we measured fluxes of N_2 across the sediment–water interface independently via the IPT and the N_2:Ar methods (Robertson et al., 2019). As expected, results from the two approaches matched well only for non-bioturbated sediments whereas the IPT rates were generally lower in the presence of chironomid larvae. A possible explanation may be the violation of the assumption of homogeneous mixing of $^{15}NO_3^-$ and $^{14}NO_3^-$ in the denitrification zone, which is likely to be along burrow structures and inside the larvae, where zones of nitrification and denitrification overlap (Van Luijn et al., 1996). Similar N_2 fluxes extrapolated from the IPT and N_2:Ar techniques in control sediments confirmed that N_2 fixation rates were negligible.

By combining our results from the whole core (sediment + larvae) and individual incubations (larvae alone), we constructed a conceptual scheme of chironomid-driven N-cycling in sediments inhabited by 1,800 larvae per m^2 (Figure 4). We assumed that NO_3^- in water pumped into the burrows can either be reduced by microbiota in the burrow walls or in the larval body through denitrification or DNRA. Previous studies have shown that the chironomid larvae gut can host NO_3^--reducing microbes (Poulsen et al., 2014; Samuiloviene et al., 2019), but specific rates have not yet been quantified. Based on our results, denitrification and DNRA by the chironomid larvae holobiont can account for only 0.3–0.4% of NO_3^- reduction in sediment core incubations. We have also demonstrated that 31% of total NO_3^- reduction through denitrification and DNRA is attributed to

FIGURE 3 Abundance (DNA) and transcriptional activity (RNA) of the analysed target functional genes—*amoA-B* (a, nitrification), *nrfA* (b, DNRA), *nifH* (c, N$_2$ fixation) and *nirS* (d, denitrification)— assessed in the chironomid larvae. Each boxplot represents the data range (whiskers), upper and lower quartiles (edges), and median (horizontal line; *n* = 3–4)
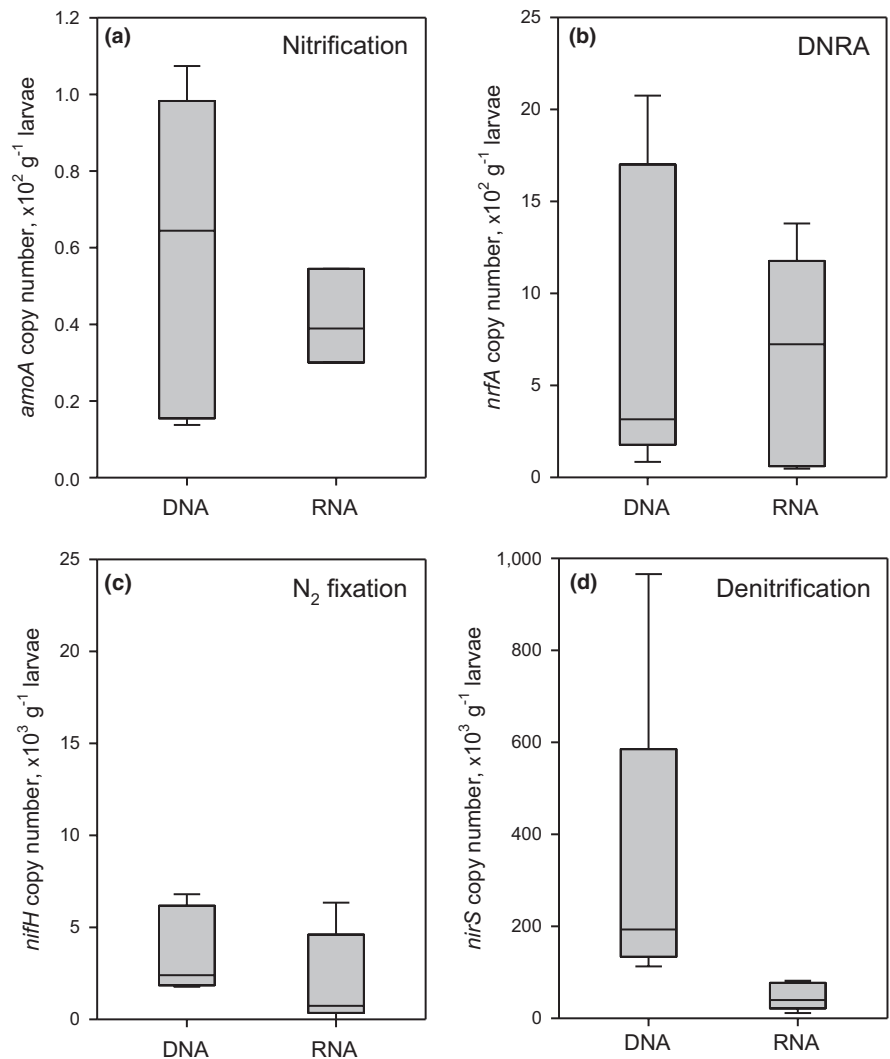
processes occurring in burrow walls. Additionally, our study provides the first evidence that larval microbiota are actively involved in N$_2$ fixation, although its contribution is minor when compared to whole core fluxes in the sediment environment. The ecological relevance of this process under different environmental conditions and the nature of the symbiotic relationship deserve future attention.

With increasing bioirrigation activity, we expected higher NH$_4^+$ efflux due to enhanced upward transport of pore water. However, this was not the case in our microcosms with high larval densities. Our results are consistent with findings of Benelli et al. (2018), showing that with increasing chironomid larval densities, NH$_4^+$ concentration in pore water and fluxes substantially decreases, ultimately resulting in no net flux into or out of the sediment. This might explain why the NH$_4^+$ flux was directed towards the sediment at larval densities of 1,800 ind./m^2. In chironomid burrows, NH$_4^+$ from animal excretion, organic matter mineralisation, or NO$_3^-$ ammonification might be released to the water column through burrow ventilation (Svensson, 1997). While it is difficult to infer how much NH$_4^+$ was delivered from organic matter mineralisation, we can estimate the contribution from the other sources. Excretion of chironomid larvae at 1,800 ind./m^2 density generated 316.3 μmol N/

day, whereas NO$_3^-$ ammonification in the sediments and burrow walls produced 177.6 μmol N m^{-2} day^{-1} through DNRA. These processes together can thus supply large amounts of NH$_4^+$ which can be nitrified in oxic sediment layers. Although the burrow network provides an extended oxidised layer of sediment around the burrow walls and an excess of NH$_4^+$ potentially favourable for nitrifiers, the transcriptional activity of nitrifying organisms (as determined from *amoA* abundances) was minimally different from the surrounding environment (Samuiloviene et al., 2019). Overall, our combined data of experimental flux estimates and molecular analyses suggest that the presence of chironomids does not stimulate the growth and activity of nitrifiers, as has been reported in previous studies (Benelli et al., 2018; Moraes et al., 2018; Stief & de Beer, 2006).

4.2 | Role of chironomid larvae holobionts in N-transformations

Our combined biogeochemical (rates) and molecular (gene transcripts) assessment of the chironomids' role in N-cycling has allowed us to shed new light on the functioning of their holobionts. Our
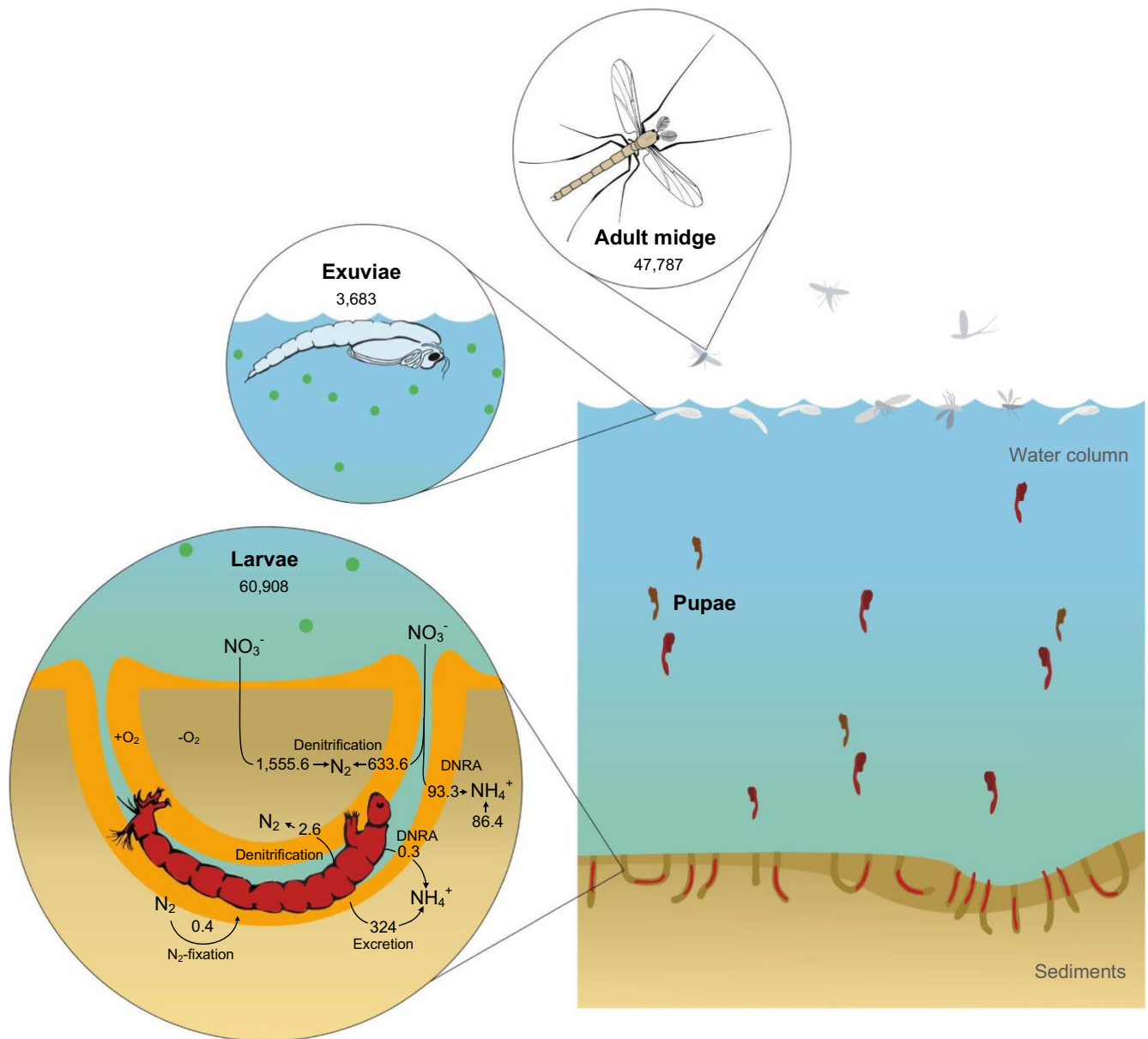
FIGURE 4 Flowchart of N-cycling associated with chironomid activities. All fluxes were obtained combining data from whole core (sediment + larvae) incubations and individual (larvae alone) incubations. Note that rates are reported for sediments inhabited by 1,800 larvae/m^2 and are expressed as μmol N m^{-2} day^{-1}. The particulate organic N storage in each life stage is reported in μmol N/m^2 and refers to a population with density 1,800 ind./m^2. Drawing by V. Gasiūnaitė

results show that the larvae microbial community was metabolically diverse and capable of different N transformations, including nitrification, denitrification, DNRA, and N$_2$ fixation. Among these pathways, denitrification was dominant, based on the abundance of *nirS* transcripts and individual incubation measurements. The transcription of denitrification marker genes, encoding NO$_2^-$ reduction and its derivatives, typically occurs under low O$_2$ conditions, which are common in the larval gut (Härtig & Zumft, 1999; Stief & Eller, 2006). Thus, at least part of the bacteria ingested during larvae feeding remain active in the larval gut, which is intermittently flushed with NO$_3^-$-rich pore water. In our study, chironomid larvae holobionts collected in spring had a substantially higher number of *nirS* transcripts as compared to those reported in summertime (Samuiloviene

et al., 2019), suggesting decreased activity of denitrifiers under lower NO$_3^-$ concentrations typical of the summer period (Zilius et al., 2018). Our study confirms that NH$_4^+$ production associated with chironomid larvae is driven by both animal excretion and the activity of associated ammonifiers. Our results also suggest that NH$_4^+$ production via DNRA is of minor importance as compared to that produced through larval excretion (<1% of total animal production).

Our finding of active N$_2$ fixation in chironomid larvae holobionts was rather surprising given the relatively high ambient NH$_4^+$ concentrations and low temperature (Knapp, 2012). A comparison of gene and transcripts abundance suggests that *nifH* genes were expressed in the microbiota. Previous analyses of 16S rRNA diversity of the microbiome associated with chironomid larvae indicated the

prevalence of Proteobacteria and Firmicutes, including diazotrophic taxa (Samuiloviene et al., 2019). Although these bacteria are ubiquitous, they may benefit from the association with chironomid larvae, due to the easy access to electron acceptors (e.g. NO_3^-) or organic substrate needed for energy acquisition (Chaston & Goodrich-Blair, 2010). Further, although it is generally believed that high N concentrations suppress N_2 fixation, heterotrophic diazotrophs may remain metabolically active, as is the case in the Curonian Lagoon waters (Zilius, Samuiloviene, et al., 2020). Nitrogen-fixing bacteria within the larval microbiota may use this process as a strategy to cope with fluctuations of N availability (Cardini et al., 2019) or to successfully compete against other bacteria that more efficiently take up N. Detection of N_2 fixation in chironomid larvae holobionts implies that diazotrophs actively involved in this process may be widespread across diverse taxa of benthic macrofauna even when N concentrations are not limiting (Cardini et al., 2019).

While we have not directly measured nitrification rates associated with chironomid larvae holobionts, our finding of low *amoA* transcript numbers suggests a low nitrifying activity (Zilius, Bonaglia, et al., 2020). Since this pathway is strictly aerobic, we assume that the involved nitrifying bacteria were growing as epibionts on the cuticle of chironomid larvae, benefiting from direct access to NH_4^+ and O_2 in the burrow environment. Gene transcripts of *amoA* were not found in larvae retrieved from burrows, again indicating a limited genetic potential for nitrification.

4.3 | Chironomids as vectors: flying adult midges export particulate N from the lagoon system

In contrast to other burrowing macrofauna, *C. plumosus* has a complex life cycle that includes complete metamorphosis from eggs, to burrowing larvae, pupae, and flying adult midges. This allows organic matter transfer through the different stages and its further export from the aquatic to the terrestrial realm at the adult stage (Gratton et al., 2008). In the late spring, millions of emerging midges leave the lagoon sediments, exporting bioaccumulated N. At 1,800 ind./m², a realistic density for large areas of the Curonian Lagoon (Zettler & Daunys, 2007), adult midge emergence may result in the displacement of 47,787 μmol of PON/m² to the atmosphere (Figure 4). This amount is comparable to the amount of N lost via denitrification in bioturbated sites over *c.* 20 days and represents an important N export from the lagoon ecosystem, not accounted for in previous budgets (Zilius et al., 2018). Thus, the emerged midges contribute to reducing excess N loading in lagoon sediments, while at the same time importing bioavailable N to the adjacent terrestrial ecosystems. However, caution should be taken when extrapolating these experimentally derived values to the entire ecosystem, since predation (e.g. by fish or water birds) or larval mortality can strongly regulate the abundance of emerging chironomid larvae (Pitcher & Soluk, 2018; Sánchez et al., 2006). Further, it is unclear how much of this PON is returned to the lagoon ecosystem via released eggs or die-off of midges.

To the best of our knowledge, the presence and activity of N-cycling bacteria in adult midges has never been investigated. Quantification of RNA transcripts in adult midges by qPCR suggested activity of ammonifiers (*nrfA*) and diazotrophs (*nifH*). However, it remains unclear which factors constrain the metabolic activity of these prokaryotes and for how long these processes will remain active in the terrestrial and aerial environment. Further studies are required to investigate the metagenome of chironomids during the different life stages to understand shifts in microbial community structure and function that are likely to occur throughout the larval development.

5 | CONCLUSION

The results of this study suggest that *C. plumosus* produces distinct effects on the different pathways of benthic N-cycling. We demonstrate for the first time that the larvae, as holobionts, affect N-cycling processes such as denitrification, DNRA, and N_2 fixation thanks to the metabolic repertoire of their microbiota. Such a finding is corroborated by our analyses of abundance and transcription of N-cycling functional genes. However, larvae-associated rates of dominant benthic processes, such as denitrification, are orders of magnitude lower than sediment rates, at least in the hypertrophic conditions of the Curonian Lagoon system. The effects of chironomid larvae on benthic N-cycling ends with their emergence as flying adults, when a large amount of particulate N is exported from the sediments to the terrestrial and aerial ecosystem. Notably, the emerged adult midges still host prokaryotes with genes encoding several N-cycling pathways, but the ecological relevance of such association and its long-term fate requires further investigation.

AUTHOR CONTRIBUTIONS

M.Z., U.C., and S.B. conceived the ideas and designed methodology; T.P. performed invertebrate sampling; M.Z., T.P., J.P., and I.V.-L. carried out the incubation experiments; I.V.-L., J.P., R.B., S.B., and U.M. carried out the mass spectrometric, spectrophotometric analyses and larvae measurements; A.S. and A.K.

performed molecular analysis. U.C., U.M., R.B., A.S., A.Z., and S.B. led the data analysis; M.Z., T.P., M.B., and A.Z. wrote the first draft of the manuscript. All authors contributed to the discussion and interpretation of data, and revised and approved the manuscript for submission.

ORCID

Mindaugas Zilius [iD] https://orcid.org/0000-0002-2390-6636

REFERENCES

Aller, R. C. (1994). Bioturbation and remineralization of sedimentary organic matter: Effects of redox oscillation. *Chemical Geology*, *114*(3–4), 331–345. https://doi.org/10.1016/0009-2541(94)90062-0

Benelli, S., Bartoli, M., Zilius, M., Vybernaite-Lubiene, I., Ruginis, T., Petkuviene, J., & Fano, E. A. (2018). Microphytobenthos and chironomid larvae attenuate nutrient recycling in shallow-water sediments. *Freshwater Biology*, *63*, 187–201. https://doi.org/10.1111/fwb.13052

Bonaglia, S., Klawonn, I., De Brabandere, L., Deutsch, B., Thamdrup, B., & Brüchert, V. (2016). Denitrification and DNRA at the Baltic Sea oxic–anoxic interface: Substrate spectrum and kinetics. *Limnology and Oceanography*, *61*(5), 1900–1915. https://doi.org/10.1002/lno.10343

Bordenstein, S. R., & Theis, K. R. (2015). Host biology in light of the microbiome: Ten principles of holobionts and hologenomes. *PLoS Biology*, *13*(8), e1002226. https://doi.org/10.1371/journal.pbio.1002226

Brennan, A., & McLachlan, A. J. (1979). Tubes and tube-building in a lotic chironomid (Diptera) community. *Hydrobiologia*, *67*(2), 173–178. https://doi.org/10.1007/BF00126716

Brodersen, K. P., Pedersen, O., Walker, I. R., & Jensen, M. T. (2008). Respiration of midges (Diptera; Chironomidae) in British Columbian lakes: Oxy-regulation, temperature and their role as palaeo-indicators. *Freshwater Biology*, *53*, 593–602. https://doi.org/10.1111/j.1365-2427.2007.01922.x

Cardini, U., Bartoli, M., Lücker, S., Mooshammer, M., Polzin, J., Lee, R. W., … Petersen, J. M. (2019). Chemosymbiotic bivalves contribute to the nitrogen budget of seagrass ecosystems. *The ISME Journal*, *13*, 3131–3134. https://doi.org/10.1038/s41396-019-0486-9

Chaston, J., & Goodrich-Blair, H. (2010). Common trends in mutualism revealed by model associations between invertebrates and bacteria. *FEMS Microbiology Reviews*, *34*(1), 41–58. https://doi.org/10.1111/j.1574-6976.2009.00193.x

Colt, J. (2012). *Dissolved gas concentration in water: Computation as functions of temperature, salinity and pressure* (2nd ed.). Elsevier.

De Brabandere, L., Bonaglia, S., Kononets, M. Y., Viktorsson, L., Stigebrandt, A., Thamdrup, B., & Hall, P. O. J. (2015). Oxygenation of an anoxic fjord basin strongly stimulates benthic denitrification and DNRA. *Biogeochemistry*, *126*(1–2), 131–152. https://doi.org/10.1007/s10533-015-0148-6

Gautreau, E., Volatier, L., Nogaro, G., Gouze, E., & Mermillod-Blodin, F. (2020). The influence of bioturbation and water column oxygenation on nutrient recycling in reservoir sediments. *Hydrobiologia*, *847*(4), 1027–1040. https://doi.org/10.1007/s10750-019-04166-0

Giblin, A. E., Weston, N. B., Banta, G. T., Tucker, J., & Hopkinson, C. S. (2010). The effects of salinity on nitrogen losses from an oligohaline estuarine sediment. *Estuaries and Coasts*, *33*, 1054–1068. https://doi.org/10.1007/s12237-010-9280-7

Grassoff, M., Ehrhardt, M., & Kremling, K. (1983). *Methods of seawater analysis* (2nd ed.). Verlag Chemie.

Gratton, C., Donaldson, J., & Vander Zanden, M. J. (2008). Ecosystem linkages between lakes and the surrounding terrestrial landscape in northeast Iceland. *Ecosystems*, *11*(5), 764–774. https://doi.org/10.1007/s10021-008-9158-8

Hamburger, K., Dall, P. C., & Lindegaard, C. (1995). Effects of oxygen deficiency on survival and glycogen content of *Chironomus anthracinus* (Diptera, Chironomidae) under laboratory and field conditions. *Hydrobiologia*, *297*(3), 187–200. https://doi.org/10.1007/BF00019284

Härtig, E., & Zumft, W. G. (1999). Kinetics of nirS expression (cytochrome cd1 nitrite reductase) in *Pseudomonas stutzeri* during the transition from aerobic respiration to denitrification: Evidence for a denitrification-specific nitrate- and nitrite-responsive regulatory system. *Journal of Bacteriology Research*, *181*(1), 161–166. https://doi.org/10.1128/JB.181.1.161-166.1999

Hedrich, S., Schlömann, M., & Johnson, D. B. (2011). The iron-oxidizing proteobacteria. *Microbiology*, *157*(6), 1551–1564. https://doi.org/10.1099/mic.0.045344-0

Hölker, F., Vanni, M. J., Kuiper, J. J., Meile, C., Grossart, H.-P., Stief, P., … Lewandowski, J. (2015). Tube-dwelling invertebrates: Tiny ecosystem engineers have large effects in lake ecosystems. *Ecological Monographs*, *85*(3), 333–351. https://doi.org/10.1890/14-1160.1

Johnson, R. K., Boström, B., & van de Bund, W. (1989). Interactions between *Chironomus plumosus* (L.) and the microbial community in surficial sediments of a shallow, eutrophic lake. *Limnology and Oceanography*, *34*(6), 992–1003. https://doi.org/10.4319/lo.1989.34.6.0992

Kana, T. M., Darkangelo, C., Hunt, M. D., Oldham, J. B., Bennett, G. E., & Cornwell, J. C. (1994). Membrane inlet mass spectrometer for rapid high-precision determination of N_2, O_2, and Ar in environmental water samples. *Analytical Chemistry*, *66*(23), 4166–4170. https://doi.org/10.1021/ac00095a009

Knapp, A. N. (2012). The sensitivity of marine N_2 fixation to dissolved inorganic nitrogen. *Frontiers in Microbiology*, *3*, 374. https://doi.org/10.3389/fmicb.2012.00374

Laverock, B., Tait, K., Gilbert, J. A., Osborn, A. M., & Widdicombe, S. (2014). Impacts of bioturbation on temporal variation in bacterial and archaeal nitrogen–cycling gene abundance in coastal sediments. *Environmental Microbiology Report*, *6*, 113–121. https://doi.org/10.1111/1758-2229.12115

Lewandowski, J., Laskov, C., & Hupfer, M. (2007). The relationship between *Chironomus plumosus* burrows and the spatial distribution of pore-water phosphate, iron and ammonium in lake sediments. *Freshwater Biology*, *52*(2), 331–343. https://doi.org/10.1111/j.1365-2427.2006.01702.x

Marzocchi, U., Bonaglia, S., Zaiko, A., Quero, G. M., Vybernaite-Lubiene, I., Politi, T., … Cardini, U. (2021). Zebra mussel holobionts fix and recycle nitrogen in lagoon sediments. *Frontiers in Microbiology*, *11*, 610269. https://doi.org/10.3389/fmicb.2020.610269

McLachlan, A. J. (1977). Density and distribution in laboratory populations of midge larvae (Chironomidae: Diptera). *Hydrobiologia*, *55*(3), 195–199. https://doi.org/10.1007/BF00017550

Moraes, P. C., Zilius, M., Benelli, S., & Bartoli, M. (2018). Nitrification and denitrification in estuarine sediments with tube-dwelling animals. *Hydrobiologia*, *819*, 217–230. https://doi.org/10.1007/s10750-018-3639-3

Nielsen, L. P. (1992). Denitrification in sediment determined from nitrogen isotope pairing. *FEMS Microbiology Letters*, *86*(4), 357–362. https://doi.org/10.1111/j.1574-6968.1992.tb04828.x

Pelegrí, S. P., & Blackburn, T. H. (1996). Nitrogen cycling in lake sediments bioturbated by *Chironomus plumosus* larvae, under different degrees of oxygenation. *Hydrobiologia*, *325*, 231–238. https://doi.org/10.1007/BF00014989

Pitcher, K. A., & Soluk, D. A. (2018). Fish presence and inter-patch connectivity interactively alter the size of emergent insects in experimental enclosures. *Ecosphere*, *9*(3), e02118. https://doi.org/10.1002/ecs2.2118

Pohlert, T. (2014). The Pairwise Multiple Comparison of Mean Ranks Package (PMCMR). R Package, p. 27–44.

Poulsen, M., Kofoed, M. V., Larsen, L. H., Schramm, A., & Stief, P. (2014). *Chironomus plumosus* larvae increase fluxes of denitrification products and diversity of nitrate-reducing bacteria in freshwater sediment. *Systematic and Applied Microbiology*, 37, 51–59. https://doi.org/10.1016/j.syapm.2013.07.006

Risgaard-Petersen, N., Nielsen, L. P., Rysgaard, S., Dalsgaard, T., & Meyer, R. L. (2003). Application of the isotope pairing technique in sediments where anammox and denitrification coexist. *Limnology and Oceanography-Methods*, 1, 63–73. https://doi.org/10.4319/lom.2003.1.63

Robertson, E. K., Bartoli, M., Brüchert, V., Dalsgaard, T., Hall, P. O. J., Hellemann, D., ... Conley, D. J. (2019). Application of the isotope pairing technique in sediments: Use, challenges, and new directions. *Limnology and Oceanography: Methods*, 17(2), 112–136. https://doi.org/10.1002/lom3.10303

Roskosch, A., Hette, N., Hupfer, M., & Lewandowski, J. (2012). Alteration of *Chironomus plumosus* ventilation activity and bioirrigation-mediated benthic fluxes by changes in temperature, oxygen concentration, and seasonal variations. *Freshwater Science*, 31(2), 269–281. https://doi.org/10.1899/11-043.1

R-project. (2014). *R: A language and environment for statistical computing.* Retrieved from http://www.R-project.org

Samuiloviene, A., Bartoli, M., Bonaglia, S., Cardini, U., Vybernaite-Lubiene, I., Marzocchi, U., ... Zilius, M. (2019). The effect of chironomid larvae on nitrogen cycling and microbial communities in soft sediments. *Water*, 11, 1931. https://doi.org/10.3390/w1109193

Sánchez, M. I., Green, A. J., & Castellanos, E. M. (2006). Spatial and temporal fluctuations in presence and use of chironomid prey by shorebirds in the Odiel saltpans, south-west Spain. *Hydrobiologia*, 567, 329–340. https://doi.org/10.1007/s10750-006-0060-0

Stief, P., & Beer, D. D. (2006). Probing the microenvironment of freshwater sediment macrofauna: Implications of deposit-feeding and bioirrigation for nitrogen cycling. *Limnology and Oceanography*, 51, 2538–2548. https://doi.org/10.4319/lo.2006.51.6.2538

Stief, P., & Eller, G. (2006). The gut microenvironment of sediment-dwelling *Chironomus plumosus* larvae as characterised with O_2, pH, and redox microsensors. *Journal of Comparative Physiology B*, 176, 673–683. https://doi.org/10.1007/s00360-006-0090-y

Stief, P., Polerecky, L., Poulsen, M., & Schramm, A. (2010). Control of nitrous oxide emission from *Chironomus plumosus* larvae by nitrate and temperature. *Limnology and Oceanography*, 2, 872–884. https://doi.org/10.4319/lo.2010.55.2.0872

Stief, P., Poulsen, M., Nielsen, L. P., Brix, H., & Schramm, A. (2009). Nitrous oxide emission by aquatic macrofauna. *Proceedings of the National Academy of Sciences of the United States of America*, 106, 4296–4300. https://doi.org/10.1073/pnas.0808228106

Stocum, E. T., & Plante, C. J. (2006). The effect of artificial defaunation on bacterial assemblages of intertidal sediments. *Journal of Experimental Marine Biology and Ecology*, 337(2), 147–158. https://doi.org/10.1016/j.jembe.2006.06.012

Sun, X., Hu, Z., Jia, W., Duan, C., & Yang, L. (2015). Decaying cyanobacteria decrease N_2O emissions related to diversity of intestinal denitrifiers of *Chironomus plumosus*. *Journal of Limnology*, 74(2), 261–271. https://doi.org/10.4081/jlimnol.2014.1072

Svensson, J. M. (1997). Influence of *Chironomus plumosus* larvae on ammonium flux and denitrification (measured by the acetylene blockage- and the isotope pairing-technique) in eutrophic lake sediment. *Hydrobiologia*, 346, 157–168. https://doi.org/10.1023/A:1002974201570

Thamdrup, B., & Dalsgaard, T. (2002). Production of N_2 through anaerobic ammonium oxidation coupled to nitrate reduction in marine sediments. *Applied and Environmental Microbiology*, 68(3), 1312–1318. https://doi.org/10.1128/AEM.68.3.1312-1318.2002

Tiedje, J. M., Sexstone, A. J., Myrold, D. D., & Robinson, J. A. (1983). Denitrification: Ecological niches, competition and survival. *Antonie van Leeuwenhoek*, 48, 569–583. https://doi.org/10.1007/BF00399542 pmid:6762848

Van Luijn, F., Boers, P. C., & Lijklema, L. (1996). Comparison of denitrification rates in lake sediments obtained by the N_2 flux method, the ^{15}N isotope pairing technique and the mass balance approach. *Water Research*, 30(4), 893–900. https://doi.org/10.1016/0043-1354(95)00250-2

Warembourg, F. R. (1993). Nitrogen fixation in soil and plant systems. In R. Knowles & T. H. Blackburn (Eds.), *Nitrogen isotope techniques* (pp. 127–156). Academic Press.

Zettler, M. L., & Daunys, D. (2007). Long-term macrozoobenthos changes in a shallow boreal lagoon: Comparison of a recent biodiversity inventory with historical data. *Limnologica*, 37, 170–185. https://doi.org/10.1016/j.limno.2006.12.004

Zilius, M. (2011). Oxygen and nutrient exchange at the sediment water interface in the eutrophic boreal lagoon (Baltic Sea). Doctoral dissertation, PhD dissertation, Klaipėda University.

Zilius, M., Bonaglia, S., Broman, E., Chiozzini, V. G., Samuiloviene, A., Nascimento, F. J. A., ... Bartoli, M. (2020). N_2 fixation dominates nitrogen cycling in a mangrove fiddler crab holobiont. *Scientific Report*, 10, 13966. https://doi.org/10.1038/s41598-020-70834-0

Zilius, M., Samuiloviene, S., Stanislauskienė, R., Broman, E., Bonaglia, S., Meškys, R., & Zaiko, A. (2020). Depicting temporal, functional and phylogenetic patterns in estuarine diazotrophic communities from environmental DNA and RNA. *Microbial Ecology*, 81(1), 36–51. https://doi.org/10.1007/s00248-020-01562-1

Zilius, M., Vybernaite-Lubiene, I., Vaiciute, D., Petkuviene, J., Zemlys, P., Liskow, I., ... Bukaveckas, P. A. (2018). The influence of cyanobacteria blooms on the attenuation of nitrogen throughputs in a Baltic coastal lagoon. *Biogeochemistry*, 141(2), 143–165. https://doi.org/10.1007/s10533-018-0508-0

SUPPORTING INFORMATION

Additional supporting information may be found online in the Supporting Information section.

IV

Marzocchi, U., S. Bonaglia, A. Zaiko, G. Marina Quero, I. Vybernaite-Lubiene, T. Politi, A. Samuiloviene, M. Zilius, M. Bartoli, U. Cardini. 2021. Zebra mussel holobionts fix and recycle nitrogen in lagoon sediments. *Frontiers in Microbiology* 11, 610269.

Zebra Mussel Holobionts Fix and Recycle Nitrogen in Lagoon Sediments

Ugo Marzocchi[1,2,3*], Stefano Bonaglia[2,4,5,6], Anastasija Zaiko[2,7,8], Grazia M. Quero[1,9], Irma Vybernaite-Lubiene[2], Tobia Politi[2], Aurelija Samuiloviene[2], Mindaugas Zilius[2,10], Marco Bartoli[2,11] and Ulisse Cardini[1,2*]

[1] Integrative Marine Ecology Department, Stazione Zoologica Anton Dohrn, National Institute of Marine Biology, Ecology and Biotechnology, Naples, Italy, [2] Marine Research Institute, Klaipėda University, Klaipėda, Lithuania, [3] Center for Water Technology (WATEC), Department of Biology, Aarhus University, Aarhus, Denmark, [4] Department of Ecology, Environment and Plant Sciences, Stockholm University, Stockholm, Sweden, [5] Nordcee, Department of Biology, University of Southern Denmark, Odense, Denmark, [6] Department of Marine Sciences, University of Gothenburg, Gothenburg, Sweden, [7] Coastal and Freshwater Group, Cawthron Institute, Nelson, New Zealand, [8] Institute of Marine Science, University of Auckland, Auckland, New Zealand, [9] Institute for Biological Resources and Marine Biotechnologies, National Research Council of Italy, Ancona, Italy, [10] Department of Life Sciences and Biotechnology, University of Ferrara, Ferrara, Italy, [11] Department of Chemistry, Life science and Environmental Sustainability, Parma University, Parma, Italy

Bivalves are ubiquitous filter-feeders able to alter ecosystems functions. Their impact on nitrogen (N) cycling is commonly related to their filter-feeding activity, biodeposition, and excretion. A so far understudied impact is linked to the metabolism of the associated microbiome that together with the host constitute the mussel's holobiont. Here we investigated how colonies of the invasive zebra mussel (*Dreissena polymorpha*) alter benthic N cycling in the shallow water sediment of the largest European lagoon (the Curonian Lagoon). A set of incubations was conducted to quantify the holobiont's impact and to quantitatively compare it with the indirect influence of the mussel on sedimentary N transformations. Zebra mussels primarily enhanced the recycling of N to the water column by releasing mineralized algal biomass in the form of ammonium and by stimulating dissimilatory nitrate reduction to ammonium (DNRA). Notably, however, not only denitrification and DNRA, but also dinitrogen (N_2) fixation was measured in association with the holobiont. The diazotrophic community of the holobiont diverged substantially from that of the water column, suggesting a unique niche for N_2 fixation associated with the mussels. At the densities reported in the lagoon, mussel-associated N_2 fixation may account for a substantial (and so far, overlooked) source of bioavailable N. Our findings contribute to improve our understanding on the ecosystem-level impact of zebra mussel, and potentially, of its ability to adapt to and colonize oligotrophic environments.

Keywords: *Dreissena polymorpha*, nitrogen, denitrification, DNRA, nitrogen fixation, *nifH*, Curonian Lagoon

INTRODUCTION

Microbial symbionts may drive speciation and evolution (Shropshire and Bordenstein, 2016), but their relevance in organismal ecology has only recently gained widespread recognition (Dittami et al., 2020). Huge progress has been made in this research field thanks to rapidly advancing molecular tools (Petersen and Osvatic, 2018). However, molecular methods alone cannot

overcome the major challenge of understanding how host-microbe associations, otherwise known as holobionts (Bordenstein and Theis, 2015), contribute to the functioning of the ecosystems they inhabit (see nested ecosystem concept – Pita et al., 2018). Interdisciplinary approaches combining molecular and geochemical investigations are thus urgently needed to investigate the role of complex and diverse host-microbe associations *in natura* (Petersen and Osvatic, 2018; Beinart, 2019). Historically, most ecological research into biological invasions has focused on detrimental species interactions such as predation and competition. However, microbial associates may play an important role by facilitating niche adaptations and allowing their host to occupy otherwise inaccessible habitats (Shapira, 2016). Recent research shows that associations between bivalves and bacteria are paramount in regulating benthic biogeochemical processes (Smyth et al., 2013; Benelli et al., 2017; Bonaglia et al., 2017; Cardini et al., 2019), with microbes contributing to the metabolic potential and impact of the holobiont, in particular concerning carbon (C) and nitrogen (N) cycling (Petersen et al., 2016; Arfken et al., 2017; Konig et al., 2017). Still, little is known on microbiomes of invasive bivalve holobionts and their role in phenotypic plasticity and colonization potential of the invader, and ultimately its ecosystem-level impact (e.g., alteration of biogeochemical processes).

Zebra mussels (*Dreissena polymorpha*, Pallas 1771) are filter-feeding bivalves native to the Ponto-Caspian region, which successfully invaded several regions in Europe and North America, where they significantly altered community structure and ecosystem functioning (Strayer et al., 1999). Their rapid colonization rates together with proficient filter-feeding activity have been linked with the decline in chlorophyll-a, and increase in water transparency and total phosphorous (P) (Caraco et al., 1997), which may result in an overall shift of the trophic state of the colonized freshwater ecosystems (Kumar et al., 2016). The impact of zebra mussel on N cycling is manifold and includes enhanced release of ammonium (NH_4^+) from digested algal biomass (Lavrentyev et al., 2000), stimulation of benthic nitrification (Bruesewitz et al., 2008) and denitrification (Bruesewitz et al., 2006), and release of P to the water column (Benelli et al., 2019) potentially stimulating pelagic dinitrogen (N_2) fixation. The nature and extent of such impacts may however be seasonal (Bruesewitz et al., 2006) and depend upon intrinsic features of the water body such as morphometry (Higgins and Zanden, 2010) and sediment organic matter content. An additional level of complexity in unraveling the overall impact of zebra mussel on N cycling is the distinction between its ability to alter key microbial transformation indirectly (via stimulating the activity of pelagic and benthic communities) and directly, via the hosted microbiome (e.g., Svenningsen et al., 2012). Although the indirect impact has been extensively documented, the role of its microbiome remains largely unexplored both in terms of metabolic repertoire and magnitude of the N transformations. Unraveling the diverse impacts of zebra mussel on nutrient cycling is pivotal to achieve a comprehensive understanding of its invasiveness and role as ecosystem engineer.

In this study, a combination of biogeochemical and molecular approaches was employed to investigate the impact of zebra mussel on N cycling in the sediment of the largest European lagoon (Curonian Lagoon, SE Baltic Sea). Both a "benthic community" (i.e., intact sediment + zebra mussel colony) and a "holobiont" (i.e., zebra mussel alone) incubations were conducted to quantitatively assess the effect of the zebra mussel holobiont on N cycling and to discern it from its effect on sediment processes.

MATERIALS AND METHODS

Site Description and Samples Collection
Sediment and zebra mussel specimens were collected in June 2018 at a fine-sand site (median grain size 0.238 mm) from a shallow area (1.2 m depth) of the oligohaline Curonian Lagoon (55°20′25.9″N, 21°11′24.4″E). The Curonian Lagoon, is a micro-tidal, low-energy system, characterized by a reduced vertical mixing in particularly in the summer months when the discharge from tributaries and wind intensity are at minimum (Ferrarin et al., 2008; Mezine et al., 2019). At the time of sampling, water temperature was 22.5°C, salinity was 0.2, concentration of dissolved organic and inorganic nitrogen (i.e., DON and DIN) was 57.2 ± 0.7 (Mean ± SEM) and 1.8 ± 0.1 μM, respectively. Height intact cores were collected by hand using Plexiglas liners (i.d.: 8.4 cm, length: 30 cm). Four cores included sediments with an overlying colony of zebra mussels and four cores included bare sediments without mussels or other visible macrofauna. Each liner contained approximately 10 cm of sediment overlaid by 16 cm of water. Additional *in situ* water and zebra mussel specimens were collected for single animal incubations and molecular analyses (see details below). Within 1 h, the samples were transported to the laboratory in cool box filled with *in situ* water. At the laboratory, intact cores were submerged overnight in a temperature-controlled tank (23 ± 0.2°C, 200 L) containing unfiltered, aerated *in situ* water. Homogeneous water conditions were kept in each core via magnetic stirring bar (40 rpm). The following day, intact sediment cores with and without mussel colonies were incubated to assess the impact of zebra mussels on (i) sediment nutrients and oxygen fluxes, and subsequently on (ii) nitrate (NO_3^-) reduction processes (benthic community). A second set of incubations was conducted to assess the diversity and relevance of N transformations associated with zebra mussel specimens and their microbiome (holobiont incubations).

Benthic Community Incubations
After a preincubation of 15 h, the water in the tank was partly renewed. Thereafter, the top of each core was sealed with a Plexiglas lid without leaving a head-space and net fluxes of O_2, DIN (i.e., NH_4^+, NO_3^-, NO_2^-), DON, and phosphate (PO_4^{3-}) between the benthic compartment and the water were measured in dark, while keeping the water stirring on, as described in Samuiloviene et al. (2019). Incubations lasted for less than 4 h to limit the change in water column O_2 concentration to ≤20% as this is a prerequisite to maintain a linear rate of change in nutrients concentration over time (Dalsgaard et al., 2000).

Oxygen concentration was monitored throughout the incubation with an optical O_2 meter (FireStingO2, PyroScience GmbH). At the start and at the end of each incubation, 30 mL of water were collected from each core, filtered (Frisenette GF/F filters) and stored into 12 mL Polyethylene vials for later determination of DIN. An additional 40 mL aliquot was filtered into a 20 mL glass vials for DON and PO_4^{3-} determination. Water samples were stored frozen ($-20°C$) until analyses.

Following the flux measurements, microcosms were left submerged with the top open overnight before starting the NO_3^- reduction [i.e., denitrification and dissimilatory nitrate reduction to ammonium (DNRA)] measurements via $^{15}NO_3^-$ tracer as described by Dalsgaard et al. (2000). Briefly, $^{15}NO_3^-$ was added to the water of each core from a stock solution (20 mM, 99 atom % $Na^{15}NO_3$; Sigma-Aldrich) to a final ^{15}N enrichment of approximately 60% ($^{14+15}NO_3^-$ concentration 6.9 μM). The cores were then closed and incubated for 1.5–3 h in the dark. At the end of the incubation, the mussels were removed, and the water and the sediment were gently mixed to a slurry. Thereafter, 20 mL aliquots of the slurry were transferred into 12 mL exetainers (Labco Ltd.) and 200 μL of 7 M $ZnCl_2$ were added to stop microbial activity. An additional 40 mL subsample was collected for $^{15}NH_4^+$ determination. Rates of total denitrification (D_{tot}) and its components i.e., denitrification of NO_3^- from the water (D_w) and denitrification coupled to nitrification (D_n), were calculated from the fluxes of $^{29}N_2$ and $^{30}N_2$ according to Nielsen (1992). Overestimation of denitrification due to anaerobic ammonium oxidation (anammox) (Risgaard-Petersen et al., 2003) was assumed negligible, since anammox has been previously reported to be marginal in the lagoon sediment (Zilius, 2011). Rates of DNRA were calculated from the $^{15}NH_4^+$ production, D_{tot}, and denitrification of $^{15}NO_3^-$ as in Risgaard-Petersen and Rysgaard (1995). At the end of the incubation, sediment from all cores was carefully sieved (0.5 mm mesh-size) to assess the mussel density and to determine their shell-free dry weight (SFDW) after drying the soft tissue at $60°C$ to a constant weight.

Inorganic nutrient (i.e., NO_x^-, NO_2^-, NH_4^+, PO_4^{3-}) concentrations were measured with a 5-channel continuous flow analyzer (San^{++}, Skalar) using standard colorimetric methods (Grasshoff et al., 1983). Nitrate concentration was calculated as the difference between NO_x^- and NO_2^-. Total dissolved nitrogen (TDN) was analyzed by the high temperature ($680°C$) combustion, catalytic oxidation/NDIR method using a Shimadzu TOC 5000 analyzer with a TN module. Dissolved organic nitrogen (DON) was calculated as difference between TDN and DIN. Samples for $^{29}N_2$ and $^{30}N_2$ were analyzed by gas chromatography-isotopic ratio mass spectrometry (GC-IRMS, Thermo Delta V Plus). Samples for $^{15}NH_4^+$ were analyzed by the same technique (GC-IRMS) after conversion of NH_4^+ to N_2 by the addition of alkaline hypobromite (Warembourg, 1993).

Zebra Mussel Holobiont Incubations

To determine rates of N transformation (i.e., denitrification, DNRA, anammox, and N_2-fixation), associated with the zebra mussel holobiont, a series of ^{15}N isotope incubations were carried out with individual specimens in the absence of sediment. Prior to the incubation, the biofilm on the mussels' shell was carefully removed using a toothbrush and mussels were then rinsed in 0.2 μm double-filtered water. Incubations were performed in bottom-capped Plexiglas cylindrical microcosms (total volume 227 ± 3 mL). The microcosms were filled with 0.2 μm double-filtered aerated *in situ* water amended with ^{15}N tracers (see the details below). A stirring magnet allowed for continuous water mixing (40 rpm) during the incubation. Microcosms were capped with gas-tight lids provided with two sampling ports for sample collection and water replacement.

Nitrate Reduction

Rates of denitrification, DNRA and anammox were estimated following the revised isotope-pairing technique (r-IPT) (Thamdrup and Dalsgaard, 2002; Risgaard-Petersen et al., 2003). Three treatments were prepared: (1) low $^{15}NO_3^-$ addition (final concentration 6.2 μM), (2) high $^{15}NO_3^-$ addition (final concentration 19.1 μM) and (3) $^{15}NH_4^+ + {}^{14}NO_3^-$ (final concentration 6.3 + 5.3 μM, respectively). Treatments 1 and 2 were used to measure rates of denitrification and DNRA. The different tracer concentrations in treatments 1 and 2 allowed to validate the main assumption of IPT, (i.e., tracer concentration-independency of rates). Treatment 3 allowed to measure anammox. Each treatment included five microcosms: four containing one mussel and one control with filtered water only. To calculate the degree of isotopic enrichment, water samples for NH_4^+ and NO_3^- analysis were collected prior and after to the isotope addition. Microcosms were incubated in the dark for 8 h at $23 \pm 0.3°C$. Every 3 h aliquots were subsampled from each replicate/control, transferred into 12 mL exetainers (Labco, United Kingdom) and poisoned with 200 μL of 7 M $ZnCl_2$ for later N_2 and NH_4^+ isotopic determination as described above. Significance of the increase in 15N species (i.e., $^{29}N_2$, $^{30}N_2$, and $^{15}NH_4^+$) over time was tested via regression analysis using the whole datasets (including all data points) for denitrification ($p < 0.05$) and DNRA ($p < 0.10$), respectively. Production rates were calculated from single incubations (time series) and normalized per grams of biomass (SFDW).

N₂ Fixation

To determine rates of N_2 fixation, a stock solution of $^{30}N_2$-enriched filtered water was prepared using a modified version of the protocol described in Klawonn et al. (2015) (see **Supplementary Material**). Before starting the incubation, the stock solution was gently transferred into four microcosms to minimize gas exchange with the atmosphere. After the mussels were added, the top lids were closed and incubated in the dark for 12 h. Four additional microcosms were prepared and incubated as above but with unlabeled water to serve as a control for isotopic contamination. At the end of the incubation, the mussels were collected and dissected for SFDW determination. Mussel tissues were then stored at $-20°C$ for later ^{15}N incorporation analysis. In addition, ten non-incubated specimens were dissected and store as above for later determination of the natural $^{15}N/^{14}N$

ratios. Prior to the isotopic analysis, mussels' tissues were freeze-dried for 48 h, ground to fine powder and weighed into tin capsules. Samples were analyzed for N elemental composition (%) and isotope ratios ($\delta^{15}N$) by continuous flow isotope ratio mass spectrometry (IRMS, Isoprime, GV Instruments Ltd.) coupled with elemental analyzer (Costech Instruments). $^{15}N_2$ incorporation rates were calculated as in Montoya et al. (1996). $^{15}N_2$ incorporation was considered significant for those samples that showed an atom % excess that was higher than two times the standard deviation of the atom % of the unlabeled samples.

Molecular Analyses of the Prokaryotic Communities

Nucleic Acids Extraction and Sequencing

Analysis of 16S rRNA gene and of the *nifH* gene expression were conducted to characterize the N_2-fixing community in the mussel's microbiome and its possible relationship with the N_2-fixing community in the water via filter-feeding activity. Nucleic acids were extracted from the soft tissue of zebra mussels (from in the holobiont incubation) and from the suspended material from *in situ* water sample. Suspended material was size-fractioned in two size groups, i.e., >10 μm, and 0.22–10 μm (from here on referred to as *large* and *small* fraction, respectively) by step-wise filtration of the water as described in Zilius et al. (2020). All samples were collected and analyzed in triplicates. Samples was snap-frozen in liquid nitrogen and stored at −80°C until DNA and RNA extraction. DNA was extracted using the QIAamp Fast DNA Stool Mini Kit (QIAGEN) with increased lysis temperature to 90°C to improve the bacterial cell rupture. RNA was extracted using the RNAeasy Mini Kit (QIAGEN) as in Zilius et al. (2020) and treated with TURBO DNase (Invitrogen). Complementary DNA (cDNA) was synthesized using SuperScriptIII Reverse Transcriptase (Invitrogen), RNaseOUT Ribonuclease Inhibitor (Invitrogen) and random primers. Two negative controls without either reverse transcriptase or RNA were included to assess the potential contamination with residual DNA. Partial 16S rRNA gene sequences were amplified using primer pair Probio_Uni (5′-CCTACGGGRSGCAGCAG-3′) and Probio_Rev (5′-ATTACCGCGGCTGCT-3′), targeting the V3 region of the 16S rRNA gene sequence as described by Milani et al. (2013). High-throughput sequencing was performed at the DNA sequencing facility of GenProbio srl[1] on an Illumina™ MiSeq with the length of 250 × 2 bp, according to the protocol reported in Milani et al. (2013).

The cDNA-based amplification of *nifH* gene was performed using a nested PCR approach (Zehr and Turner, 2001) with nifH3 and nifH4 primers in the first PCR round followed by second amplification round with nifH1 and nifH2 primers with Illumina indices. Nested PCR conditions were set as in Zilius et al. (2020). Only single bands of appropriate size (359 bp) were detected after the second round of amplification. PCR products were purified from the gel (Thermo Scientific GeneJET Gel Extraction Kit), quantified (Qubit 3.0 Fluorometer) and the sequencing library was constructed following the two-step tailed

PCR amplicon procedure, as described in Kozich et al. (2013). Paired-end sequences (2 × 250 bp) were generated on an Illumina MiSeq® instrument using the TruSeq® SBS kit. Sequence data were automatically demultiplexed using MiSeq Reporter (v2), and forward and reverse reads were assigned to samples. Raw sequence data for the 16S rRNA and *nifH* dataset were bioinformatically processed as described in Zilius et al. (2020). Briefly, primers from the raw sequence reads (with Illumina adapters removed by sequencing facility) were trimmed using cutadapt v2.10 (Martin, 2011), with no primer mismatch allowed. The bioinformatics pipeline was run using DADA2 package implemented in R (Callahan et al., 2016). Quality filtering and denoising of the trimmed fastq files were performed using the following parameters: "truncLen = c(150,150), maxEE = c(2,6), truncQ = 2, ndmaxN = 0." Singletons were discarded, and the remaining paired-end reads were merged with a minimum overlap of 65 bp and 1 mismatch allowed in the overlap region. Chimera removal was performed using the default (consensus) method and the resulting de-noised amplicon sequence variants (ASV) were used for taxonomic classification against the SILVA 132 database for 16S rRNA (Quast et al., 2013) and *nifH* Sequence Database (Gaby and Buckley, 2014). Sequences are available in the NCBI/SRA database under accession number PRJNA658818.

Statistical Analyses on the Sequencing Data

The de-noised ASV tables and assigned taxonomy of *nifH* and 16S datasets were imported in RStudio (R Core Team, 2018), combined into two phyloseq objects and processed for data analysis (McMurdie and Holmes, 2013). Rarefaction curves were plotted for both 16S and *nifH* datasets using ggrare function in R (package *ranacapa*; Kandlikar et al., 2018). ASV tables for 16S and *nifH* were rarefed to the lowest number of reads (9,395 and 51,180 for the 16S and *nifH* dataset, respectively) (R package *phyloseq*). For 16S, alpha diversity indices (ASV richness, Shannon index, Simpson index and Pielou's evenness) were calculated using the R package *vegan* (Oksanen et al., 2019) and number of shared ASVs visualized with Venn diagram (package *venn*; Dusa, 2020). For *nifH*, only ASV richness was calculated. A Kruskal–Wallis test was used to assess differences in 16S and *nifH* ASV richness between water and zebra mussel samples (R package *phyloseq*). Differences in community composition were assessed using the Analysis of Similarity (ANOSIM) based on a Bray–Curtis similarity matrix implemented in *vegan*. PCoA was performed to explore and visualize similarities among the different samples, basing on the same Bray–Curtis similarity matrix, for both the 16S and *nifH* genes datasets. A heatmap with hierarchical clustering was plotted to visualize differences in the abundance of the top 70 16S rRNA gene ASVs (>0.01% across the dataset) using the R packages *Heatplus* (Ploner, 2020), *ggplot2* (Wickham, 2009), and *vegan*. Finally, to gain further information on the identity of unknown Bacteria and unknown Firmicutes identified in the *nifH* dataset for zebra mussel samples, blastn (search in nucleotide databases using a nucleotide query) and blastx (search in protein databases using a translated nucleotide query) (Altschul et al., 1990) analyses were performed against GenBank database (released version 237, May 2020).

---

[1]www.genprobio.com

RESULTS

Respiration and Nutrient Fluxes in Benthic Community Incubations

Mussel total biomass varied between 0.6 and 1.0 g $_{(SFDW)}$ per core, corresponding to an average areal biomass ($\pm$SD) of 134 ± 38 g $_{(SFDW)}$ m^{-2} and a density of 30–64 mussels per colony. Mean benthic O_2 consumption was fivefold higher in the presence of the mussels (S + ZM) compared to the bare sediment (S) (**Figure 1A**). Bare sediment was a net sink for all the measured nutrients (**Figure 1B**). The presence of mussels reversed the fluxes resulting in the net efflux of all the analyzed species. Net NH_4^+ flux accounted for the largest share of the whole DIN efflux. For all measured parameters the difference between net fluxes in S + ZM and S was significant (Mann–Whitney U test, $p < 0.05$).

Rates of DNRA were significantly higher (+72%) in cores with mussels compared to the bare sediment (Mann–Whitney U test, $p < 0.03$) (**Figure 2**). D_w tended to be higher in the presence of the mussels compared to the bare sediment (Mann–Whitney U test, $p = 0.06$). D_n showed an opposite trend with lower rates in the presence of mussels, although the difference was not significant (Mann–Whitney U test, $p = 0.23$). The D_n:D_w ratio was lower with the mussels compared to the bare sediment (Mann–Whitney U test, $p < 0.02$). Overall denitrification ($D_n + D_w$) was unaltered by the presence of the mussel (Mann–Whitney U test, $p = 0.66$).
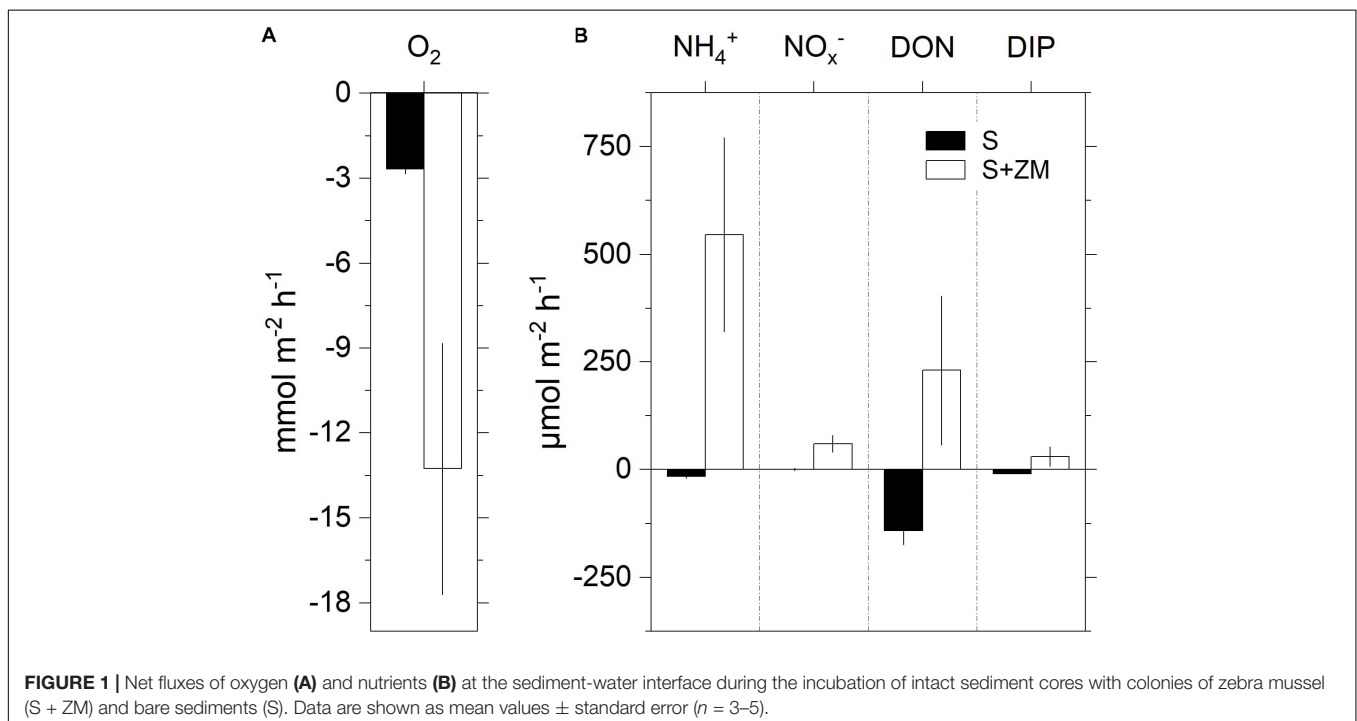
N Cycling Associated With the Zebra Mussel Holobiont

The average biomass of the incubated specimens was 37 ± 10 (SD) mg $_{(SFDW)}$. Regression analysis showed a significant

increase in $^{15}NH_4^+$ and ^{15}N-N_2 (i.e., $^{29}N_2$, $^{30}N_2$) in the DNRA and denitrification incubations, respectively (**Supplementary Table 1**). Biomass-normalized rates of DNRA spanned between zero and 192 nmol N g $_{(SFDW)}^{-1}$ h^{-1} (average $\pm$ SEM, 31.2 ± 19.3 nmol N g $_{(SFDW)}^{-1}$ h^{-1}) (**Figure 3**). Rates of denitrification ranged between zero and 260 nmol N g $_{(SFDW)}^{-1}$ h^{-1} (average $\pm$ SEM, 58.4 ± 28.9 nmol N g $_{(SFDW)}^{-1}$ h^{-1}). No anammox activity was detected within the timespan of the incubation (results not shown). N_2 fixation was detected in all tested animals (**Supplementary Table 2**) at rates ranging between 7.8 and 30 nmol N-N_2 g $_{(SFDW)}^{-1}$ h^{-1} (average $\pm$ SEM, 21.9 ± 4.5 nmol N g $_{(SFDW)}^{-1}$ h^{-1}). On average, under our experimental conditions, N_2 fixation was equal to 37% of the denitrification rate.

Water Column and Mussel-Associated Microbial Communities

After denoising and eukaryote sequence removal, the complete 16S rDNA dataset comprised 447,071 good quality sequence reads from the nine analyzed samples representing 2,705 bacterial ASVs. Rarefaction curves (**Supplementary Figure 1**) evidenced that the sequencing effort was sufficient to describe bacterial diversity. The normalized ASV richness (after rarefying the sequences at an even depth of 9,395) was significantly higher in zebra mussel compared to both size fractions of the water samples (Kruskal–Wallis, $p < 0.01$) (**Supplementary Figure 2**). Shannon and Simpson diversity and Pielou's evenness indices showed significantly higher values in the large compared to the small fraction of water samples. Shannon diversity tended to be higher in zebra mussel samples, although no significant difference with water samples was observed ($p < 0.05$). Zebra mussel and water

FIGURE 1 | Net fluxes of oxygen **(A)** and nutrients **(B)** at the sediment-water interface during the incubation of intact sediment cores with colonies of zebra mussel (S + ZM) and bare sediments (S). Data are shown as mean values $\pm$ standard error (n = 3–5).
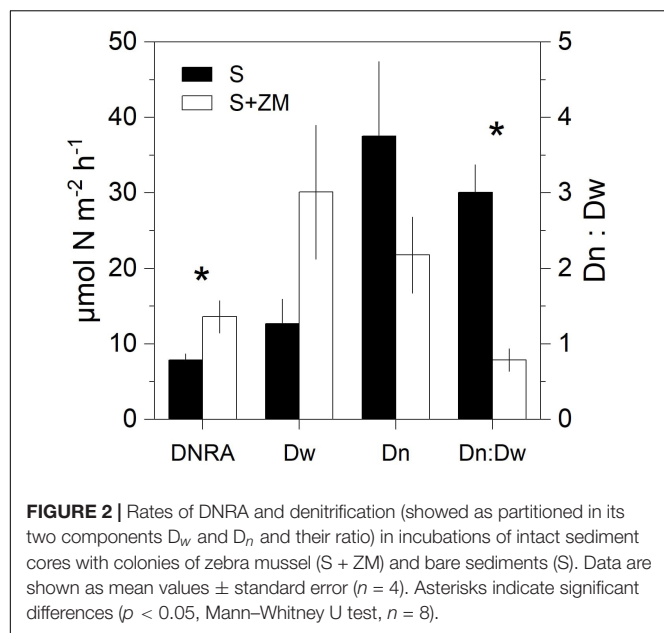
FIGURE 2 | Rates of DNRA and denitrification (showed as partitioned in its two components D_w and D_n and their ratio) in incubations of intact sediment cores with colonies of zebra mussel (S + ZM) and bare sediments (S). Data are shown as mean values ± standard error ($n = 4$). Asterisks indicate significant differences ($p < 0.05$, Mann–Whitney U test, $n = 8$).
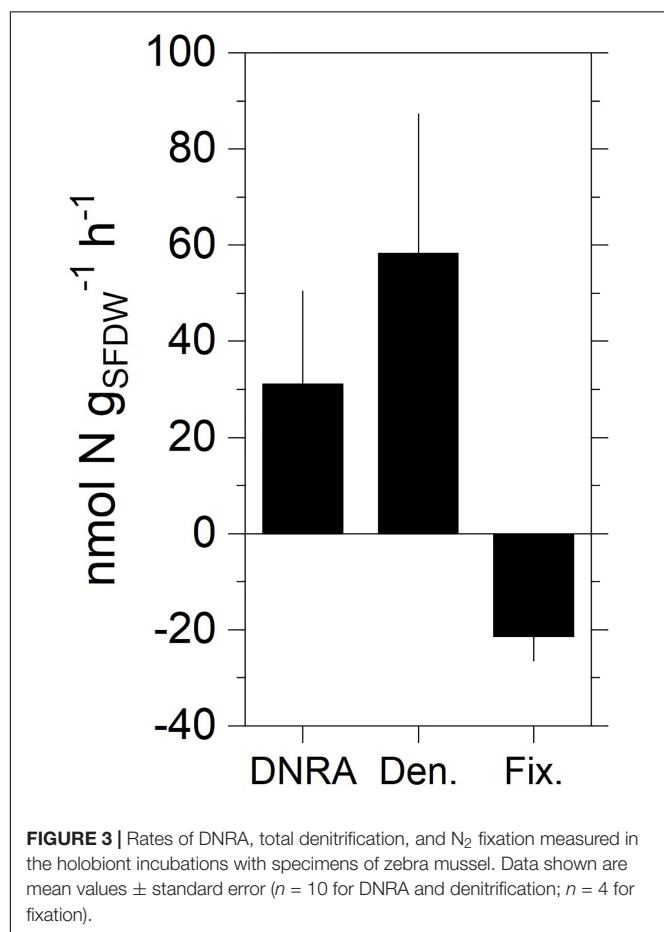

FIGURE 3 | Rates of DNRA, total denitrification, and N_2 fixation measured in the holobiont incubations with specimens of zebra mussel. Data shown are mean values ± standard error ($n = 10$ for DNRA and denitrification; $n = 4$ for fixation).

samples (small and large fractions) shared 13.3% of the detected ASVs ($n = 359$), while 1,074 ASVs (39.7%) were exclusively associated with zebra mussels (**Supplementary Figure 3**).

The three types of samples showed distinct relative abundances of major prokaryotic taxa (**Figure 4A**) (ANOSIM, global $R = 0.88$; $p < 0.01$) and grouped separately when analyzed by PCoA (**Supplementary Figure 4A**). Zebra mussels were characterized by high abundances of Tenericutes (average, 25%), that were basically undetectable in water samples. Beta- (average, 12.8%) and Gammaproteobacteria (average, 6.5%), and Bacteroidetes (average, 22.5%) accounted for a considerable fraction in zebra mussel samples, while a general lower presence of Cyanobacteria (average, 4.3%) and Actinobacteria (average, 3.8%) was observed in comparison to both types of water samples. The Tenericutes phylum was almost entirely represented by members of the genus *Mycoplasma*, with relative abundances up to 40% of the overall community. In the large fraction of the water samples, Cyanobacteria clearly dominated the community (average, 67.8%), while in the small fraction, a more even community structure was observed, represented by Cyanobacteria (average, 24.7%), Bacteroidetes (average, 20.6%), and Actinobacteria (average, 16.9%), Alpha- (12.6%) and Betaproteobacteria (7.8%).

The heatmap visualization of the most abundant (>0.1%) ASVs, supported the taxonomic differentiation of the microbial communities between two water fractions and zebra mussel samples (**Figure 4B**). In particular, the zebra mussel microbial community was characterized by a pool of taxa mainly including *Mycoplasma* and Mycoplasmataceae (eight ASVs, average, 3% of zebra mussel reads), Spirochaetaceae (three ASVs, average 0.5%), Burkholderiaceae (two ASVs, average 0.6%), *Lacihabitans* (1), Sphingomonadaceae (1), *Dechloromonas* (1), *Hydrogenophaga* (1), *Flavobacterium* (1), and three unidentified Proteobacteria. Water samples were characterized by the presence of numerous Cyanobacteria and freshwater taxa (e.g., *Limnohabitans*, *Polynucleobacter*).

Water Column and Mussel-Associated Active Diazotrophic Communities

The *nifH* dataset comprised a total of 2,045,435 good quality reads (on average, 227,270 reads per sample, ranging from 51,180 in a zebra mussel sample to 389,159 in a large fraction water sample), representing 360 *nifH* ASVs. Rarefaction curves for *nifH* (**Supplementary Figure 5**) confirmed the adequate diversity coverage at the attained sequencing depth. After rarefying at 51,180 sequence depth, a total of 344 ASVs were retained for the downstream analyses. No statistically significant difference in ASV richness was observed between the two water fractions and zebra mussel samples (Kruskal–Wallis rank sum test, $p = 0.707$) (**Supplementary Figure 6**). Diazotrophic communities significantly differed among the three type of samples (**Figure 5**; ANOSIM, global $R = 0.543$; $p = 0.006$) and grouped separately when analyzed by PCoA (**Supplementary Figure 4B**). In zebra mussel samples, the diazotrophic community was dominated by a large fraction of unknown Bacteria (54.4%), followed by *Paenibacillus* (33.2%) and a smaller fraction of unknown Firmicutes (12.2%). Interestingly, none of these groups were detected in water samples, which were almost completely dominated by Nostocales (83.4%) and *Zoogloea* (16.6%). More
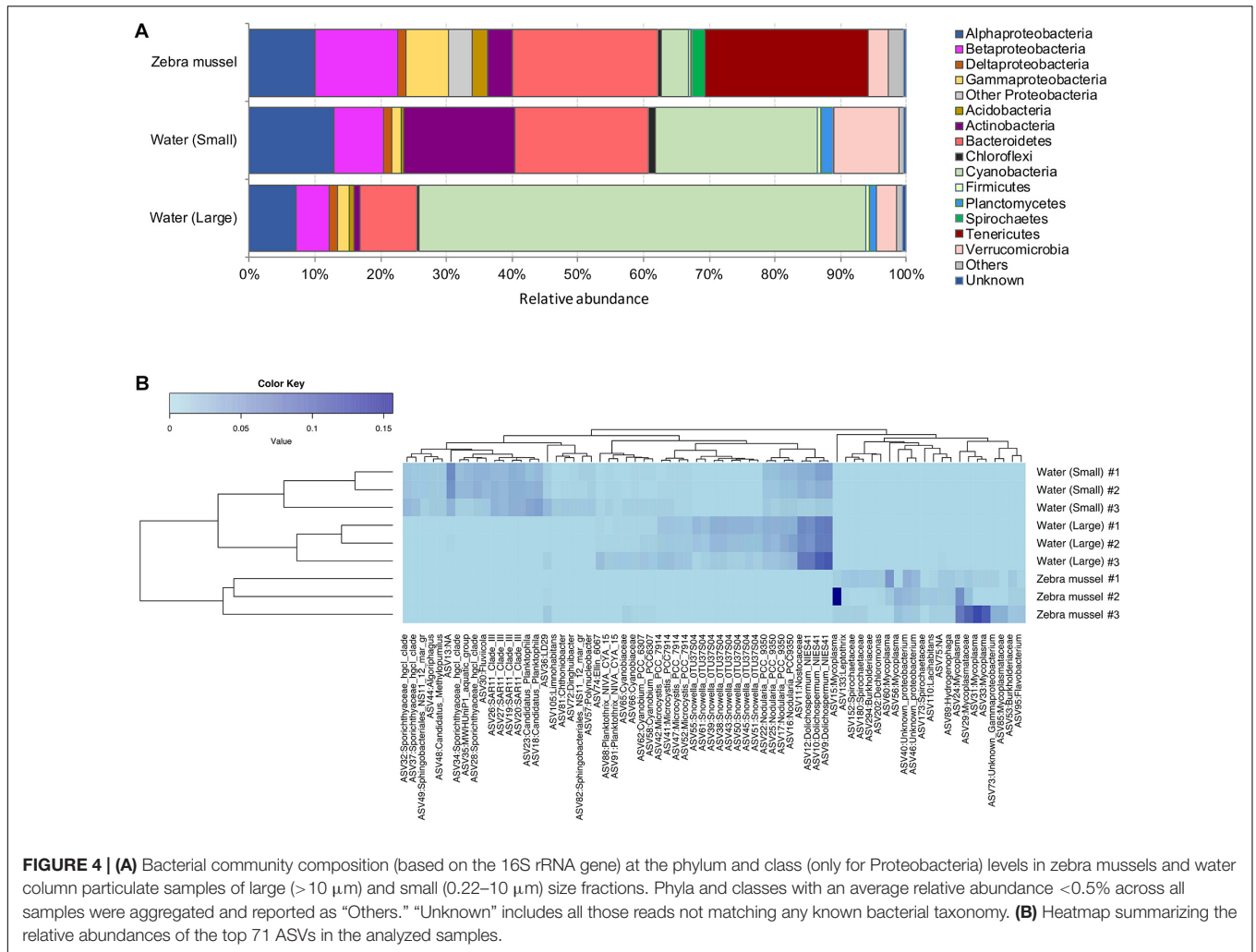
FIGURE 4 | (A) Bacterial community composition (based on the 16S rRNA gene) at the phylum and class (only for Proteobacteria) levels in zebra mussels and water column particulate samples of large (>10 μm) and small (0.22–10 μm) size fractions. Phyla and classes with an average relative abundance <0.5% across all samples were aggregated and reported as "Others." "Unknown" includes all those reads not matching any known bacterial taxonomy. **(B)** Heatmap summarizing the relative abundances of the top 71 ASVs in the analyzed samples.
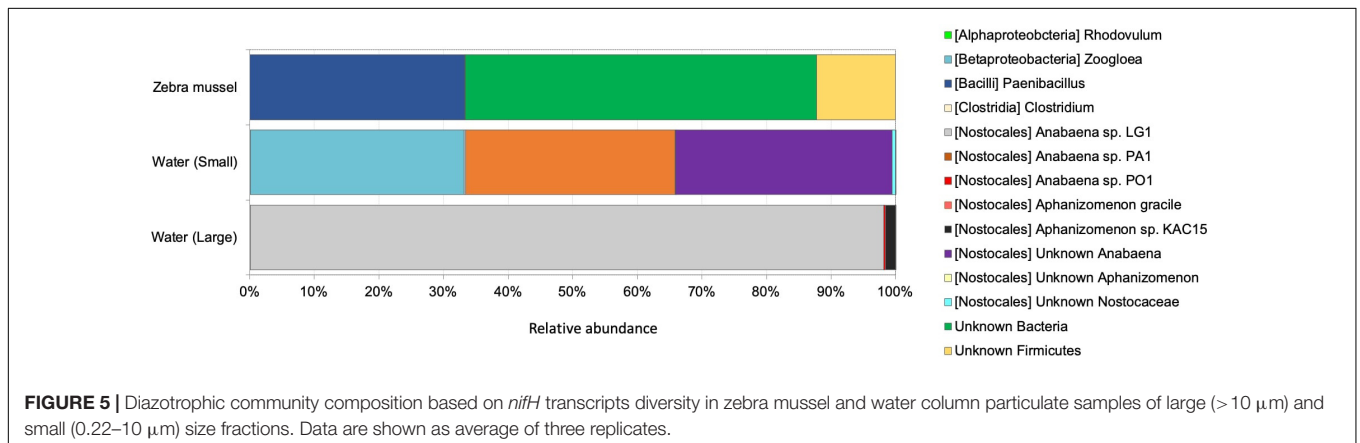
FIGURE 5 | Diazotrophic community composition based on *nifH* transcripts diversity in zebra mussel and water column particulate samples of large (>10 μm) and small (0.22–10 μm) size fractions. Data are shown as average of three replicates.

specifically, the small fraction of the water samples was dominated by *Anabaena* (66.2%) and *Zoogloea* (33.1%), while the large fraction of water samples by *Anabaena* (98.4%).

After blastn analyses, all ASV sequences identified as unknown Firmicutes matched with *nifH* sequences belonging to Clostridia, although weakly (<79% of similarity, 99% query coverage).

Protein sequence similarity search analyses based on translated proteins (i.e., blastx) also indicated, that such ASVs were loosely related to Clostridia (90–92% of similarity, 99% query coverage). Blastn analyses performed on ASV identified as unknown Bacteria matched, although at low similarities (75–82%), mostly with *Azotobacter*, *Paenibacillus*, and Clostridia. Results from

blastx indicated that most of the ASVs identified as unknown Bacteria were highly related to Clostridia and *Paenibacillus* (80.5–93.5%). Some of the ASVs, showed similarities up to 91.5% with queries belonging to the phylum Bacteroidetes.

DISCUSSION

Impact of Zebra Mussel on Benthic N Cycling

Although it is well documented that benthic macroinvertebrates alter vital sediment processes such as N turnover through irrigation and bioturbation (e.g., Stief, 2013), animal-bacterial associations and their role on biogeochemical cycling remain largely unresolved. Here, we quantitatively assessed how a model invasive bivalve (the zebra mussel) alters benthic N cycling both directly (e.g., via excretion of DIN and DON) and indirectly via stimulating microbial activity both at the sedi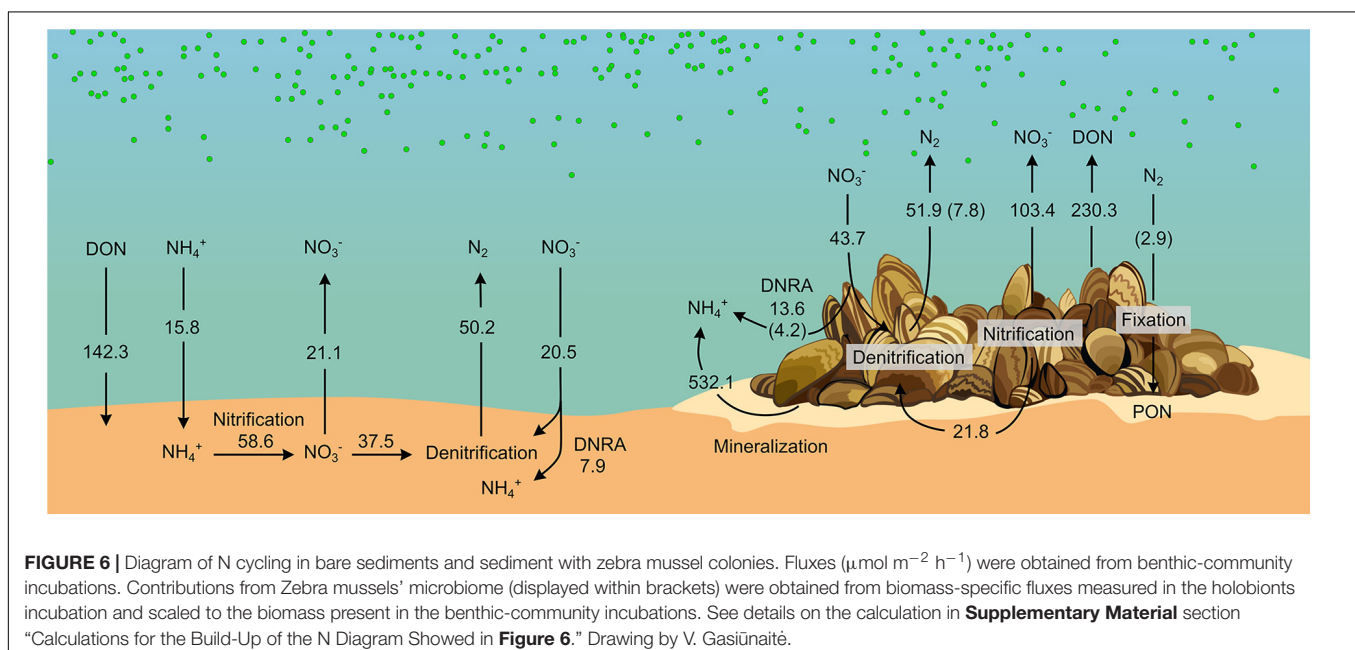ment level and through its microbiome. **Figure 6** summarizes rates of N fluxes measured in the benthic community incubations, and the biomass-specific rates measured in the holobiont incubations after extrapolation using the densities from the benthic community experiment. As evidenced, the presence of zebra mussels turned the benthic compartment from a sink to a source of all measured nutrients. In particular, NH_4^+ was the most prominent dissolved N species released into the water. Enhanced benthic release of NH_4^+ has been consistently reported in the presence of zebra mussels (James et al., 1997; Lavrentyev et al., 2000; Conroy et al., 2005; Ruginis et al., 2014) and other filter feeders (Mazouni et al., 1996; Bartoli et al., 2003; Nizzoli et al., 2006). The increase in NH_4^+ efflux can be sustained by three mechanisms: (i) mineralized algal biomass from filter-feeding activity of the mussel, (ii) stimulation of DNRA activity, and (iii) inhibition of nitrification due to

the colony physical presence and consequent limitation of the O_2 transport into the sediment (Zaiko et al., 2010). The proximity of the NH_4^+: DIP ratio (i.e., 18) to the Redfield ratio calculated from the fluxes in the benthic-community incubations suggests that NH_4^+ most likely originates from mineralization of algae biomass by zebra mussel. Accordingly, enhanced rates of DNRA measured in the benthic-community incubations with the mussels could only contribute 1.0% of the enhanced NH_4^+ efflux. Net fluxes of NO_3^- in the whole-community incubations suggest a stimulation of nitrification by zebra mussel rather than its inhibition. Assuming that the drop in D_n measured in the presence of zebra mussel is caused by the suppression of nitrification, the resulting release of NH_4^+ would, however, only contribute to 4% of the overall sediment efflux of NH_4^+. Our data therefore indicate that the most prominent impact of zebra mussel on DIN dynamics is via the recycling of fixed N through mineralization of pelagic algae and other particulate organic matter either being egested as biodeposits or retained within the mussels' colony.

The net release of DON in the presence of the mussel might be sustained by the mussels' egestion/excretion or derive from exudates by settled phytoplankton aggregates within the colony. Recently, it has been shown that other dreissenids excrete dissolved organic matter with relatively low C to N ratio indicating high proportion of organic N compounds (DeVilbiss and Guo, 2017). The biochemical mechanisms at the basis of such DON release, the conditions that promote it, and its environmental relevance remain, however, poorly understood in filter-feeders.

Contrary to what previously reported from the upper Mississippi River (Bruesewitz et al., 2006, 2008) and from a freshwater Lithuanian lake (Ruginis et al., 2014), zebra mussels did not increase overall benthic denitrification in our incubations. Rather, the presence of the mussels altered

FIGURE 6 | Diagram of N cycling in bare sediments and sediment with zebra mussel colonies. Fluxes (μmol m^{-2} h^{-1}) were obtained from benthic-community incubations. Contributions from Zebra mussels' microbiome (displayed within brackets) were obtained from biomass-specific fluxes measured in the holobionts incubation and scaled to the biomass present in the benthic-community incubations. See details on the calculation in **Supplementary Material** section "Calculations for the Build-Up of the N Diagram Showed in **Figure 6**." Drawing by V. Gasiūnaitė.

the balance between D_w and D_n favoring the former over the latter. Denitrification was previously reported from zebra mussels holobiont incubations, possibly occurring in the gut (Svenningsen et al., 2012). However, our holobiont incubations showed that such contribution accounted only for 15% of the denitrification rates measured in the benthic-community incubations (**Figure 6**), suggesting that the impact of zebra mussel on denitrification was mainly indirect (related to the altered sediment microbial activity), rather than via stimulation of NO_3^- reduction in anoxic sections of the animal body.

On the contrary, DNRA activity in the holobiont incubation accounted for a major fraction (i.e., 74% = 4.2 μmol m^{-2} h^{-1}, **Figure 6**) of the increment in DNRA measured in the benthic-community incubation in the presence of the mussels (i.e., +5.7 μmol m^{-2} h^{-1}, **Figures 2**, **6**), indicating a dominant effect of the mussels' microbiome in stimulating DNRA. DNRA bacteria have a competitive advantage over denitrifiers when the organic carbon to NO_3^- ratio is high (Tiedje, 1988). Such conditions are plausibly met in the anoxic section of the mussels' gut. Accordingly, DNRA to denitrification ratio was higher in holobiont incubations (i.e., 0.58) compared to the benthic-community incubation (i.e., 0.16–0.26), suggesting a relatively more favorable niche for DNRA activity in the animal's gut compared to the surrounding sedimentary environment.

Increase in NO_3^- efflux and D_w and simultaneous decrease in D_n are compatible with the thinning of the sediment oxic layer as due to the accumulation of labile phytodetritus (Marzocchi et al., 2018). Similarly, the biodeposition of labile organic carbon by zebra mussel (in the form of feces and pseudo-feces) has been shown to enhance benthic respiration causing the thinning of the sediment oxic layer (Bruesewitz et al., 2008). Such a decrease of the O_2 penetration depth shortens the diffusional path for water-NO_3^- to reach the denitrification zone, hence, enhancing D_w. At the same time, the contraction of the oxic portion of the sediment diminishes the sediment volume suitable for nitrification, favoring the diffusion of sediment NH_4^+ to the water and thus partially decoupling nitrification and denitrification. Moreover, nitrification activity occurring at shallower depths is expected to favor the diffusion of NO_3^- to the water, further contributing to the decrease in D_n. Assuming that the drop in D_n is caused by a preferential release of NO_3^- to the water, the so generated NO_3^- would account for 33% of the measured net NO_x^- effluxes in the benthic-community incubation. The accumulation of biodeposits by zebra mussel was visually observed during our incubations, providing a plausible, additional, mechanism by which zebra mussel impacts benthic N dynamics via altering the architecture of the habitat.

N_2 Fixation by Zebra Mussel Holobionts

This study is the first, to our knowledge, to report N_2 fixation associated with zebra mussel holobionts. Our incubations show that if unaccounted, this process can lead to 6 and ~60% overestimation of the benthic community and holobiont-associated net N_2 fluxes, respectively. At the lagoon level, N_2 fixation has been traditionally attributed to pelagic cyanobacterial activity (Lesutienė et al., 2014; Bartoli et al., 2018; Zilius et al., 2020) and reported to occur seasonally (spring and winter) in undisturbed sediments (Zilius et al., 2018). Dinitrogen fixation associated with the zebra mussel (and more in general in mussel-colonized sediment) has not been accounted so far in estimations of the lagoon's N mass balance (Zilius et al., 2018). The zebra mussel is a dominant benthic organism in the Curonian Lagoon sediment where it has been reported at densities ranging between 40 and 57,000 individuals per square meter (median 12,600) (Daunys et al., 2006). Scaled-up to these abundances, N_2 fixation rates derived from our incubations can account for 0.01 to 19.9 μmol of fixed N m^{-2} h^{-1} (median 4.4 μmol N m^{-2} h^{-1}), respectively. In summer, cyanobacterial-driven N_2 fixation has been reported at rates between 0.9 and 209.4 μmol m^{-2} h^{-1} (median 33.7 μmol^{-2} h^{-1}; Zilius et al., 2018). Thus, zebra mussel holobionts could possibly contribute a substantial (and so far disregarded) input of N to the lagoon, offsetting the attenuation of the N load via denitrification, and therefore mitigating summer N limitation of the lagoonal system (Vybernaite-Lubiene et al., 2018). Considering maximum densities of 100,000 individuals per square meters reported from zebra mussel-colonized riverine sediments (Svenningsen et al., 2012), its impact could potentially alter N pathways at a scale significantly exceeding that assumed from our experiments and calculations. Further studies are needed to assess the overall relevance of N_2 fixation driven by zebra mussels holobionts, its variation under diverse environmental conditions and its seasonal patterns.

The analysis of the microbiome associated with zebra mussels showed that comparatively few ASVs were shared with the waterborne microbial community. The detected high diversity of mussel-associated assemblages (with many taxa not observed in water samples) is consistent with previous findings of specific and diverse bacterial communities associated with bivalves (Lokmer et al., 2016; Cleary and Polonia, 2018; Vezzulli et al., 2018; Mathai et al., 2020). Tenericutes, and more specifically *Mycoplasma*, abundant in the zebra mussel samples, are typical constituents of the core bivalve gut microbiome (Pierce, 2016; Aceves et al., 2018; Pierce and Ward, 2018, 2019), including zebra mussels (Mathai et al., 2020). These obligate cell-associated bacteria are commonly found within a number of eukaryotic hosts and, although previously considered as parasites or even a sign of infection, are now assumed to be involved in mutually beneficial interactions with the host (Fraune and Zimmer, 2008; Holm and Heidelberg, 2016; van de Water et al., 2018). However, no diazotrophic activity has been attributed to any taxa of the Tenericutes phylum (Dos Santos et al., 2012; Albright et al., 2019). On the other hand, the *Flavobacterium* genus, commonly identified in or isolated from bivalves (Pujalte et al., 1999; Aceves et al., 2018; Pierce and Ward, 2019), and fairly abundant in zebra mussel samples from our incubations, includes some species carrying nitrogenase genes. Several studies confirmed the ability of *Flavobacterium* isolates to perform N_2 fixation, although this has been demonstrated mainly in plants (Giri and Pati, 2004; Kampfer et al., 2015). A number of other potential diazotrophs were detected in zebra mussel samples in our study. Along with Tenericutes, Spirochetes are well-documented common members of bivalve

gut microbiome (Margulis and Hinkle, 1992). This taxon dominates the microbiome of other eukaryotic organisms in different environments (Lilburn et al., 2001; van de Water et al., 2016) and has been shown to exhibit diazotrophic activity. Burkholderiaceae are among the most well-known N_2-fixing bacterial groups in plants (Sprent et al., 2017). Species of this family occupy diverse ecological niches and can be found in soil and water, and in association – even symbiosis – with plants, animals, and fungi (Coenye, 2014). Species of the genus *Leptothrix*, belonging to the Burkholderiaceae family, are commonly found in lakes, lagoons, and swamps, and species of this genus have been studied and isolated as root endophytes in plants (López-López et al., 2010; Li et al., 2011). Finally, members of both *Hydrogenophaga* (i.e., *Hydrogenophaga pseudoflava*) and *Dechloromonas* have shown the ability to fix N_2 (Willems et al., 1989; Salinero et al., 2009), although this has been observed so far only in plants, and to our knowledge no indications of diazotrophic activity carried out by these taxa have been reported in bivalves.

The diversity of active diazotrophs in zebra mussels, as characterized by *nifH* gene transcription analysis, also differed substantially from that of water samples. Unlike pelagic diazotrophs, which were mainly represented by Cyanobacteria, *nifH* transcript diversity of the mussels was dominated by *Paenibacillus* and other taxa closely related to Clostridia and Bacteroidetes. Such taxa have been previously described as diazotrophs, although, a few evidences have suggested – so far – their association with bivalves. *Paenibacillus* (phylum Firmicutes) is a genus widely known to include N_2-fixing species in soil, and recent studies highlighted its frequent detection and potential role in N_2 fixation in aquatic environments (Yu et al., 2018; Pang et al., 2019; Tang et al., 2019). However, to our knowledge, this is the first study reporting its association with benthic invertebrates. On the contrary, Clostridiales have been described as the most frequently detected sequences in the microbiome of Unionidae mussels (Weingarten et al., 2019), which co-exist with zebra mussels in the Curonian Lagoon (Benelli et al., 2019). Besides, Clostridiales are common in the gut microbiome of vertebrates (Colston and Jackson, 2016). In addition, several members of the Clostridiales are euryhaline, may thus perform N_2 fixation in the wide range of conditions as those found in estuarine environments (Herbert, 1975). Finally, many Bacteroidetes bacteria possess nitrogenase genes, and are thus capable of N_2 fixation (Inoue et al., 2015); however, to the best of our knowledge, studies reporting associations between bivalves and members of Bacteroidetes and/or describing the role of this taxon in N_2 fixation in aquatic invertebrates are missing.

CONCLUSION

Our results show that zebra mussels favor the recycling of N via algal mineralization and by stimulating DNRA activity both in the sediment and via its microbiome. In addition, the mussels mediate a so far overlooked input of nitrogen via N_2 fixation. Diazotrophic activity is likely sustained by a unique mussel-associated microbial community, which differs

substantially from the N_2-fixing community in the water column. Further investigations are needed to assess whether the association of zebra mussels with diazotrophs is a transient interaction or a stable symbiosis, as well as potential fluxes of energy and matter between the microbiome and the host. The capability to host diazotrophic bacteria might be particularly advantageous for zebra mussels to facilitate their establishment and spread in nutrient-poor environments and might therefore represent an important factor in determining their high invasiveness and adaptive capacity. It may also provide an advantage in eutrophic estuaries such as the Curonian Lagoon, which typically display pronounced seasonal variations in inorganic N availability.

DATA AVAILABILITY STATEMENT

The datasets presented in this study can be found in online repositories. The names of the repository/repositories and accession number(s) can be found below: https://www.ncbi.nlm.nih.gov/, PRJNA658818.

AUTHOR CONTRIBUTIONS

SB, MB, MZ, and UC conceived and designed the study. UM contributed to the concept. SB, IV-L, TP, AS, MZ, MB, and UC performed the experiments. UM, SB, IV-L, TP, and AS conducted the chemical analyses. UM, SB, and MZ analyzed the geochemical data. AS carried out the nucleic acid extraction and amplicon sequencing. AZ and GQ performed the bioinformatic and statistical analysis on the sequencing data. UM, GQ, and UC wrote the first draft of the manuscript. All authors contributed to draft revisions, read, and approved the final version.

FUNDING

ACKNOWLEDGMENTS

SUPPLEMENTARY MATERIAL

The Supplementary Material for this article can be found online at: https://www.frontiersin.org/articles/10.3389/fmicb.2020.610269/full#supplementary-material

REFERENCES

Aceves, A. K., Johnson, P., Bullard, S. A., Lafrentz, S., and Arias, C. R. (2018). Description and characterization of the digestive gland microbiome in the freshwater mussel Villosa nebulosa (Bivalvia: Unionidae). *J. Mollus. Stud.* 84, 240–246. doi: 10.1093/mollus/eyy014

Albright, M. B. N., Timalsina, B., Martiny, J. B. H., and Dunbar, J. (2019). Comparative Genomics of Nitrogen Cycling Pathways in Bacteria and Archaea. *Microbial. Ecol.* 77, 597–606. doi: 10.1007/s00248-018-1239-4

Altschul, S. F., Gish, W., Miller, W., Myers, E. W., and Lipman, D. J. (1990). Basic Local Alignment Search Tool. *J. Mol. Biol.* 215, 403–410.

Arfken, A., Song, B., Bowman, J. S., and Piehler, M. (2017). Denitrification potential of the eastern oyster microbiome using a 16S rRNA gene based metabolic inference approach. *PLoS One* 12:e0185071. doi: 10.1371/journal.pone.0185071

Bartoli, M., Naldi, M., Nizzoli, D., Roubaix, V., and Viaroli, P. (2003). Influence of Clam Farming on Macroalgal Growth: A Microcosm Experiment. *Chem. Ecol.* 19, 147–160. doi: 10.1080/0275754031000119906

Bartoli, M., Zilius, M., Bresciani, M., Vaiciute, D., Vybernaite-Lubiene, I., Petkuviene, J., et al. (2018). Drivers of Cyanobacterial Blooms in a Hypertrophic Lagoon. *Front. Mar. Sci.* 5:434. doi: 10.3389/fmars.2018.00434

Beinart, R. A. (2019). The Significance of Microbial Symbionts in Ecosystem Processes. *Msystems* 4, e127–e119.

Benelli, S., Bartoli, M., Racchetti, E., Moraes, P. C., Zilius, M., Lubiene, I., et al. (2017). Rare but large bivalves alter benthic respiration and nutrient recycling in riverine sediments. *Aquat. Ecol.* 51, 1–16. doi: 10.1007/s10452-016-9590-3

Benelli, S., Bartoli, M., Zilius, M., Vybernaite-Lubiene, I., Ruginis, T., Vaiciute, D., et al. (2019). Stoichiometry of regenerated nutrients differs between native and invasive freshwater mussels with implications for algal growth. *Freshw. Biol.* 64, 619–631. doi: 10.1111/fwb.13247

Bonaglia, S., Bruchert, V., Callac, N., Vicenzi, A., Fru, E. C., and Nascimento, F. J. A. (2017). Methane fluxes from coastal sediments are enhanced by macrofauna. *Sci. Rep.* 7:13145.

Bordenstein, S. R., and Theis, K. R. (2015). Host Biology in Light of the Microbiome: Ten Principles of Holobionts and Hologenomes. *PLoS Biol.* 13:e1002226. doi: 10.1371/journal.pbio.1002226

Bruesewitz, D. A., Tank, J. L., and Bernot, M. J. (2008). Delineating the effects of zebra mussels (Dreissena polymorpha) on N transformation rates using laboratory mesocosms. *J. N. Am. Benthol. Soc.* 27, 236–251. doi: 10.1899/07-031.1

Bruesewitz, D. A., Tank, J. L., Bernot, M. J., Richardson, W. B., and Strauss, E. A. (2006). Seasonal effects of the zebra mussel (Dreissena polymorpha) on sediment denitrification rates in Pool 8 of the Upper Mississippi River. *Can. J. Fish Aquat. Sci.* 63, 957–969. doi: 10.1139/f06-002

Callahan, B. J., McMurdie, P. J., Rosen, M. J., Han, A. W., Johnson, A. J. A., and Holmes, S. P. (2016). DADA2: High-resolution sample inference from Illumina amplicon data. *Nat. Methods* 13, 581–583. doi: 10.1038/nmeth.3869

Caraco, N. F., Cole, J. J., Raymond, P. A., Strayer, D. L., Pace, M. L., Findlay, S. E. G., et al. (1997). Zebra mussel invasion in a large, turbid river: Phytoplankton response to increased grazing. *Ecology* 78, 588–602. doi: 10.1890/0012-9658(1997)078[0588:zmiial]2.0.co;2

Cardini, U., Bartoli, M., Lücker, S., Mooshammer, M., Polzin, J., Lee, R. W., et al. (2019). Chemosymbiotic bivalves contribute to the nitrogen budget of seagrass ecosystems. *ISME J.* 13, 3131–3134. doi: 10.1038/s41396-019-0486-9

Cleary, D. F. R., and Polonia, A. R. M. (2018). Bacterial and archaeal communities inhabiting mussels, sediment and water in Indonesian anchialine lakes. *Antonie van Leeuwenhoek* 111, 237–257. doi: 10.1007/s10482-017-0944-1

Coenye, T. (2014). "The Family Burkholderiaceae," in *The Prokaryotes: Alphaproteobacteria and Betaproteobacteria*, eds E. Rosenberg, E. F. DeLong, S. Lory, E. Stackebrandt, and F. Thompson (Berlin: Springer), 759–776. doi: 10.1007/978-3-642-30197-1_239

Colston, T. J., and Jackson, C. R. (2016). Microbiome evolution along divergent branches of the vertebrate tree of life: what is known and unknown. *Mol. Ecol.* 25, 3776–3800. doi: 10.1111/mec.13730

Conroy, J. D., Edwards, W. J., Pontius, R. A., Kane, D. D., Zhang, H., Shea, J. F., et al. (2005). Soluble nitrogen and phosphorus excretion of exotic freshwater mussels (Dreissena spp.): potential impacts for nutrient remineralisation in western Lake Erie. *Freshw. Biol.* 50, 1146–1162. doi: 10.1111/j.1365-2427.2005.01392.x

Dalsgaard, T., Nielsen, L. P., Brotas, V., Viaroli, P., Undewood, G. J. C., Nedwell, D. B., Sundbäck, K. et al. (2000). "Protocol handbook for NICE - Nitrogen Cycling in Estuaries," in *A Project Under the EU Research "Programme: Marine Science and Technology (MAST III)*. (Denmark: National Environmental Research Institute).

Daunys, D., Zemlys, P., Olenin, S., Zaiko, A., and Ferrarin, C. (2006). Impact of the zebra mussel Dreissena polymorpha invasion on the budget of suspended material in a shallow lagoon ecosystem. *Helgoland Mar. Res.* 60, 113–120. doi: 10.1007/s10152-006-0028-5

DeVilbiss, S. E., and Guo, L. (2017). Excretion of organic matter and nutrients from invasive quagga mussels and potential impact on carbon dynamics in Lake Michigan. *J. Great Lakes Res.* 43, 79–89. doi: 10.1016/j.jglr.2017.03.002

Dittami, S., Arboleda, E., Auguet, J., Bigalke, A., Briand, E., Cárdenas, P., et al. (2020). A community perspective on the concept of marine holobionts: current status, challenges, and future directions. Preprint. doi: 10.2147/cciden.s7712

Dos Santos, P. C., Fang, Z., Mason, S. W., Setubal, J. C., and Dixon, R. (2012). Distribution of nitrogen fixation and nitrogenase-like sequences amongst microbial genomes. *BMC Genomics* 13:162. doi: 10.1186/1471-2164-13-162

Dusa, A. (2020). *venn: Draw Venn Diagrams R package*. Austria: R Core Team.

Ferrarin, C., Razinkovas, A., Gulbinskas, S., Umgiesser, G., and Bliudziute, L. (2008). Hydraulic regime-based zonation scheme of the Curonian Lagoon. *Hydrobiologia* 611, 133–146. doi: 10.1007/s10750-008-9454-5

Fraune, S., and Zimmer, M. (2008). Host-specificity of environmentally transmitted Mycoplasma-like isopod symbionts. *Environ. Microbiol.* 10, 2497–2504. doi: 10.1111/j.1462-2920.2008.01672.x

Gaby, J. C., and Buckley, D. H. (2014). A comprehensive aligned nifH gene database: a multipurpose tool for studies of nitrogen-fixing bacteria. *Database* 2014:bau001.

Giri, S., and Pati, B. R. (2004). A comparative study on phyllosphere nitrogen fixation by newly isolated Corynebacterium sp. & Flavobacterium sp. and their potentialities as biofertilizer. *Acta Microbiol. Immunol. Hung.* 51, 47–56. doi: 10.1556/amicr.51.2004.1-2.3

Grasshoff, K., Ehrhardt, M., Kremling, K., and Almgren, T. (eds) (1983). *Methods of seawater analysis*, 2nd Edn. Weinheim: Verlag Chemie.

Herbert, R. A. (1975). Heterotrophic Nitrogen-Fixation in Shallow Estuarine Sediments. *J. Exp. Mar. Biol. Ecol.* 18, 215–225. doi: 10.1016/0022-0981(75)90106-9

Higgins, S. N., and Zanden, M. J. V. (2010). What a difference a species makes: a meta–analysis of dreissenid mussel impacts on freshwater ecosystems. *Ecol. Monogr.* 80, 179–196. doi: 10.1890/09-1249.1

Holm, J. B., and Heidelberg, K. B. (2016). Microbiomes of Muricea californica and M. fruticosa: Comparative Analyses of Two Co-occurring Eastern Pacific Octocorals. *Front. Microbiol.* 7:917. doi: 10.3389/fmicb.2016.00917

Inoue, J., Oshima, K., Suda, W., Sakamoto, M., Iino, T., Noda, S., et al. (2015). Distribution and Evolution of Nitrogen Fixation Genes in the Phylum Bacteroidetes. *Microbes Environ.* 30, 44–50. doi: 10.1264/jsme2.me14142

James, W. F., Barko, J. W., and Eakin, H. L. (1997). Nutrient regeneration by the zebra mussel (Dreissena polymorpha). *J. Freshw. Ecol.* 12, 209–216. doi: 10.1080/02705060.1997.9663528

Kampfer, P., Busse, H. J., McInroy, J. A., Xu, J., and Glaeser, S. P. (2015). Flavobacterium nitrogenifigens sp. nov., isolated from switchgrass (Panicum virgatum). *Int. J. Syst. Evol. Microbiol.* 65, 2803–2809. doi: 10.1099/ijs.0.000330

Kandlikar, G. S., Gold, Z. J., Cowen, M. C., Meyer, R. S., Freise, A. C., Kraft, N. J. B., et al. (2018). ranacapa: An R package and Shiny web app to explore environmental DNA data with exploratory statistics and interactive visualizations. *F1000Res* 7:1734. doi: 10.12688/f1000research.16680.1

Klawonn, I., Lavik, G., Boning, P., Marchant, H. K., Dekaezemacker, J., Mohr, W., et al. (2015). Simple approach for the preparation of N-15-15(2)-enriched water for nitrogen fixation assessments: evaluation, application and recommendations. *Front. Microbiol.* 6:769. doi: 10.3389/fmicb.2015.00769

Konig, S., Gros, O., Heiden, S. E., Hinzke, T., Thurmer, A., Poehlein, A., et al. (2017). Nitrogen fixation in a chemoautotrophic lucinid symbiosis. *Nat. Microbiol.* 2:16193.

Kozich, J. J., Westcott, S. L., Baxter, N. T., Highlander, S. K., and Schloss, P. D. (2013). Development of a Dual-Index Sequencing Strategy and Curation Pipeline for Analyzing Amplicon Sequence Data on the MiSeq Illumina Sequencing Platform. *Appl. Environ. Microb.* 79, 5112–5120. doi: 10.1128/aem.01043-13

Kumar, R., Varkey, D., and Pitcher, T. (2016). Simulation of zebra mussels (Dreissena polymorpha) invasion and evaluation of impacts on Mille Lacs Lake, Minnesota: An ecosystem model. *Ecol. Model* 331, 68–76. doi: 10.1016/j.ecolmodel.2016.01.019

Lavrentyev, P. J., Gardner, W. S., and Yang, L. Y. (2000). Effects of the zebra mussel on nitrogen dynamics and the microbial community at the sediment-water interface. *Aquat. Microb. Ecol.* 21, 187–194. doi: 10.3354/ame021187

Lesutienė, J., Bukaveckas, P. A., Gasiūnaitė, Z. R., Pilkaitytė, R., and Razinkovas-Baziukas, A. (2014). Tracing the isotopic signal of a cyanobacteria bloom through the food web of a Baltic Sea coastal lagoon. *Estuar. Coastal Shelf Sci.* 138, 47–56. doi: 10.1016/j.ecss.2013.12.017

Li, Y. H., Liu, Q. F., Liu, Y., Zhu, J. N., and Zhang, Q. (2011). Endophytic bacterial diversity in roots of Typha angustifolia L. in the constructed Beijing Cuihu Wetland (China). *Res. Microbiol.* 162, 124–131. doi: 10.1016/j.resmic.2010.09.021

Lilburn, T. G., Kim, K. S., Ostrom, N. E., Byzek, K. R., Leadbetter, J. R., and Breznak, J. A. (2001). Nitrogen fixation by symbiotic and free-living spirochetes. *Science* 292, 2495–2498. doi: 10.1126/science.1060281

Lokmer, A., Kuenzel, S., Baines, J. F., and Wegner, K. M. (2016). The role of tissue-specific microbiota in initial establishment success of Pacific oysters. *Environ. Microbiol.* 18, 970–987. doi: 10.1111/1462-2920.13163

López-López, A., Rogel, M. A., Ormeño-Orrillo, E., Martínez-Romero, J., and Martínez-Romero, E. (2010). Phaseolus vulgaris seed-borne endophytic community with novel bacterial species such as Rhizobium endophyticum sp. nov. *Syst. Appl. Microbiol.* 33, 322–327. doi: 10.1016/j.syapm.2010.07.005

Margulis, L., and Hinkle, G. (1992). "Large Symbiotic Spirochetes: Clevelandina, Cristispira, Diplocalyx, Hollandina, and Pillotina," in *The Prokaryotes: A Handbook on the Biology of Bacteria: Ecophysiology, Isolation, Identification, Applications*, eds A. Balows, H. G. Trüper, M. Dworkin, W. Harder, and K.-H. Schleifer (New York: Springer), 3965–3978. doi: 10.1007/978-1-4757-2191-1_59

Martin, M. (2011). Cutadapt removes adapter sequences from high-throughput sequencing reads. *EMBnet J.* 17:200.

Marzocchi, U., Thamdrup, B., Stief, P., and Glud, R. N. (2018). Effect of settled diatom-aggregates on benthic nitrogen cycling. *Limnol. Oceanogr.* 63, 431–444. doi: 10.1002/lno.10641

Mathai, P. P., Magnone, P., Dunn, H. M., and Sadowsky, M. J. (2020). Water and sediment act as reservoirs for microbial taxa associated with invasive dreissenid mussels. *Sci. Total Environ.* 703:134915. doi: 10.1016/j.scitotenv.2019.134915

Mazouni, N., Gaertner, J. C., DeslousPaoli, J. M., Landrein, S., and dOedenberg, M. G. (1996). Nutrient and oxygen exchanges at the water-sediment interface in a shellfish farming lagoon (Thau, France). *J. Exp. Mar. Biol. Ecol.* 205, 91–113. doi: 10.1016/s0022-0981(96)02594-4

McMurdie, P. J., and Holmes, S. (2013). phyloseq: An R Package for Reproducible Interactive Analysis and Graphics of Microbiome Census Data. *PLoS One* 8:e61217. doi: 10.1371/journal.pone.0061217

Mezine, J., Ferrarin, C., Vaiciute, D., Idzelyte, R., Zemlys, P., and Umgiesser, G. (2019). Sediment Transport Mechanisms in a Lagoon with High River Discharge and Sediment Loading. *Water* 11:1970. doi: 10.3390/w11101970

Milani, C., Hevia, A., Foroni, E., Duranti, S., Turroni, F., Lugli, G. A., et al. (2013). Assessing the Fecal Microbiota: An Optimized Ion Torrent 16S rRNA Gene-Based Analysis Protocol. *PLoS One* 8:e68739. doi: 10.1371/journal.pone.0068739

Montoya, J. P., Voss, M., Kahler, P., and Capone, D. G. (1996). A Simple, High-Precision, High-Sensitivity Tracer Assay for N(inf2) Fixation. *Appl. Environ. Microb.* 62, 986–993. doi: 10.1128/aem.62.3.986-993.1996

Nielsen, L. P. (1992). Denitrification in Sediment Determined from Nitrogen Isotope Pairing. *Fems Microbiol. Ecol.* 86, 357–362. doi: 10.1111/j.1574-6941.1992.tb01771.x

Nizzoli, D., Welsh, D. T., Fano, E. A., and Viaroli, P. (2006). Impact of clam and mussel farming on benthic metabolism and nitrogen cycling, with emphasis on nitrate reduction pathways. *Mar. Ecol. Prog. Ser.* 315, 151–165. doi: 10.3354/meps315151

Oksanen, J., Guillaume, F., Friendly, B., Friendly, M., Kindt, R., Legendre, P., et al. (2019). *vegan: Community Ecology Package. R package version 2.5-6*. Austria: R Core Team.

Pang, J., Yamato, M., Soda, S., Inoue, D., and Ike, M. (2019). Nitrogen-Cycling Functional Genes in Brackish and Freshwater Sediments in Yodo River in Japan. *J. Water Environ. Technol.* 17, 109–116. doi: 10.2965/jwet.18-074

Petersen, J. M., and Osvatic, J. (2018). Microbiomes In Natura: Importance of Invertebrates in Understanding the Natural Variety of Animal-Microbe Interactions. *Msystems* 3, 179–117e.

Petersen, J. M., Kemper, A., Gruber-Vodicka, H., Cardini, U., van der Geest, M., Kleiner, M., et al. (2016). Chemosynthetic symbionts of marine invertebrate animals are capable of nitrogen fixation. *Nat. Microbiol.* 2:16195.

Pierce, M. L. (2016). *The Microbiome of the Eastern Oyster, Crassostrea virginica (Gmelin, 1791): Temporal and Spatial Variation, Environmental Influences, and its Impact on Host Physiology.* Ph D thesis, Chicago: University of Illinois, 1279.

Pierce, M. L., and Ward, J. E. (2018). Microbial Ecology of the Bivalvia, with an Emphasis on the Family Ostreidae. *J. Shellf. Res.* 37, 793–806. doi: 10.2983/035.037.0410

Pierce, M. L., and Ward, J. E. (2019). Gut Microbiomes of the Eastern Oyster (Crassostrea virginica) and the Blue Mussel (Mytilus edulis): Temporal Variation and the Influence of Marine Aggregate-Associated Microbial Communities. *Msphere* 4:19.

Pita, L., Rix, L., Slaby, B. M., Franke, A., and Hentschel, U. (2018). The sponge holobiont in a changing ocean: from microbes to ecosystems. *Microbiome* 6:46.

Ploner, A. (2020). *Heatplus: Heatmaps with row and/or column covariates and colored clusters*. Austria: R package.

Pujalte, M. J., Ortigosa, M., Macian, M. C., and Garay, E. (1999). Aerobic and facultative anaerobic heterotrophic bacteria associated to Mediterranean oysters and seawater. *Int. Microbiol.* 2, 259–266.

Quast, C., Pruesse, E., Yilmaz, P., Gerken, J., Schweer, T., Yarza, P., et al. (2013). The SILVA ribosomal RNA gene database project: improved data processing and web-based tools. *Nucl. Acids Res.* 41, D590–D596.

R Core Team (2018). *R: A language and environment for statistical computing*. Vienna: R Foundation for Statistical Computing.

Risgaard-Petersen, N., and Rysgaard, S. (1995). "Nitrate reduction in sediments and waterlogged soil measured by 15N techniques," in *Methods in Applied Soil Microbiology and Biochemistry*, eds K. Alef and P. Nannipieri (Cambridge: Academic Press), 287–295.

Risgaard-Petersen, N., Nielsen, L. P., Rysgaard, S., Dalsgaard, T., and Meyer, R. L. (2003). Application of the isotope pairing technique in sediments where anammox and denitrification co-exist. *Limnol. Oceanogr. Meth.* 2, 315–315. doi: 10.4319/lom.2004.2.315

Ruginis, T., Bartoli, M., Petkuviene, J., Zilius, M., Lubiene, I, Laini, A., et al. (2014). Benthic respiration and stoichiometry of regenerated nutrients in lake sediments with Dreissena polymorpha. *Aquat. Sci.* 76, 405–417. doi: 10.1007/s00027-014-0343-x

Salinero, K. K., Keller, K., Feil, W. S., Feil, H., Trong, S., Di Bartolo, G., et al. (2009). Metabolic analysis of the soil microbe Dechloromonas aromatica str. RCB: indications of a surprisingly complex life-style and cryptic anaerobic pathways for aromatic degradation. *BMC Genomics* 10:351. doi: 10.1186/1471-2164-10-351

Samuiloviene, A., Bartoli, M., Bonaglia, S., Cardini, U., Vybernaite-Lubiene, I., Marzocchi, U., et al. (2019). The Effect of Chironomid Larvae on Nitrogen Cycling and Microbial Communities in Soft Sediments. *Water* 11:1931. doi: 10.3390/w11091931

Shapira, M. (2016). Gut Microbiotas and Host Evolution: Scaling Up Symbiosis. *Trends Ecol. Evolut.* 31, 539–549. doi: 10.1016/j.tree.2016.03.006

Shropshire, J. D., and Bordenstein, S. R. (2016). Speciation by Symbiosis: the Microbiome and Behavior. *Mbio* 7:e01785.

Smyth, A. R., Geraldi, N. R., and Piehler, M. F. (2013). Oyster-mediated benthic-pelagic coupling modifies nitrogen pools and processes. *Mar. Ecol. Prog. Ser.* 493, 23–30. doi: 10.3354/meps10516

Sprent, J. I., Ardley, J., and James, E. K. (2017). Biogeography of nodulated legumes and their nitrogen-fixing symbionts. *N. Phytol.* 215, 40–56. doi: 10.1111/nph.14474

Stief, P. (2013). Stimulation of microbial nitrogen cycling in aquatic ecosystems by benthic macrofauna: mechanisms and environmental implications. *Biogeosciences* 10, 7829–7846. doi: 10.5194/bg-10-7829-2013

Strayer, D. L., Caraco, N. F., Cole, J. J., Findlay, S., and Pace, M. L. (1999). Transformation of freshwater ecosystems by bivalves: a case study of zebra mussels in the Hudson River. *BioScience* 49, 19–27. doi: 10.1525/bisi.1999.49.1.19

Svenningsen, N. B. I, Heisterkamp, M., Sigby-Clausen, M., Larsen, L. H., Nielsen, L. P., Stief, P., et al. (2012). Shell Biofilm Nitrification and Gut Denitrification Contribute to Emission of Nitrous Oxide by the Invasive Freshwater Mussel Dreissena polymorpha (Zebra Mussel). *Appl. Environ. Microb.* 78, 4505–4509. doi: 10.1128/aem.00401-12

Tang, W. Y., Wang, S., Fonseca-Batista, D., Dehairs, F., Gifford, S., Gonzalez, A. G., et al. (2019). Revisiting the distribution of oceanic N-2 fixation and estimating diazotrophic contribution to marine production. *Nat. Commun.* 10:831.

Thamdrup, B., and Dalsgaard, T. (2002). Production of N-2 through anaerobic ammonium oxidation coupled to nitrate reduction in marine sediments. *Appl. Environ. Microb.* 68, 1312–1318. doi: 10.1128/aem.68.3.1312-1318.2002

Tiedje, J. (1988). Ecology of denitrification and dissimilatory nitrate reduction to ammonium. *Environ. Microbiol. Anaerob.* 717, 179–244.

van de Water, J. A. J. M., Melkonian, R., Junca, H., Voolstra, C. R., Reynaud, S., Allemand, D., et al. (2016). Spirochaetes dominate the microbial community associated with the red coral Corallium rubrum on a broad geographic scale. *Sci. Rep.* 6:27277.

van de Water, J. A. J. M., Voolstra, C. R., Rottier, C., Cocito, S., Peirano, A., Allemand, D., et al. (2018). Seasonal Stability in the Microbiomes of Temperate Gorgonians and the Red Coral Corallium rubrum Across the Mediterranean Sea. *Microbial. Ecol.* 75, 274–288. doi: 10.1007/s00248-017-1006-y

Vezzulli, L., Stagnaro, L., Grande, C., Tassistro, G., Canesi, L., and Pruzzo, C. (2018). Comparative 16SrDNA Gene-Based Microbiota Profiles of the Pacific Oyster (Crassostrea gigas) and the Mediterranean Mussel (Mytilus galloprovincialis) from a Shellfish Farm (Ligurian Sea, Italy). *Microbial. Ecol.* 75, 495–504. doi: 10.1007/s00248-017-1051-6

Vybernaite-Lubiene, I., Zilius, M., Saltyte-Vaisiauske, L., and Bartoli, M. (2018). Recent Trends (2012-2016) of N, Si, and P Export from the Nemunas River Watershed: Loads, Unbalanced Stoichiometry, and Threats for Downstream Aquatic Ecosystems. *Water* 10:1178. doi: 10.3390/w10091178

Warembourg, F. R. (1993). "Nitrogen fixation in soil and plant systems," in *Nitrogen isotope techniques*, eds R. Knowles and T. H. Blackburn (San Diego: Academic Press), 127–156. doi: 10.1016/b978-0-08-092407-6.50010-9

Weingarten, E. A., Atkinson, C. L., and Jackson, C. R. (2019). The gut microbiome of freshwater Unionidae mussels is determined by host species and is selectively retained from filtered seston. *PLoS One* 14:e0224796. doi: 10.1371/journal.pone.0224796

Wickham, H. (2009). *ggplot2*. New York: Springer-Verlag.

Willems, A., Busse, J., Goor, M., Pot, B., Falsen, E., Jantzen, E., et al. (1989). Hydrogenophaga, a New Genus of Hydrogen-Oxidizing Bacteria That Includes Hydrogenophaga-Flava Comb-Nov (Formerly *Pseudomonas*-Flava), Hydrogenophaga-Palleronii (Formerly *Pseudomonas*-Palleronii), Hydrogenophaga-Pseudoflava (Formerly *Pseudomonas*-Pseudoflava and *Pseudomonas*-Carboxydoflava), and Hydrogenophaga-Taeniospiralis (Formerly *Pseudomonas*-Taeniospiralis)N. *Int. J. Syst. Bacteriol.* 39, 319–333. doi: 10.1099/00207713-39-3-319

Yu, T. T., Li, M., Niu, M. Y., Fan, X. B., Liang, W. Y., and Wang, F. P. (2018). Difference of nitrogen-cycling microbes between shallow bay and deep-sea sediments in the South China Sea. *Appl. Microbiol. Biot.* 102, 447–459. doi: 10.1007/s00253-017-8594-9

Zaiko, A., Paskauskas, R., and Krevs, A. (2010). Biogeochemical alteration of the benthic environment by the zebra mussel Dreissena polymorpha (Pallas). *Oceanologia* 52, 649–667. doi: 10.5697/oc.52-4.649

Zehr, J. P., and Turner, P. J. (2001). Nitrogen fixation: Nitrogenase genes and gene expression. *Method Microbiol.* 30, 271–286. doi: 10.1016/s0580-9517(01)30049-1

Zilius, M. (2011). *Oxygen and nutrient exchange at the sediment–water interface in the eutrophic boreal lagoon (Baltic Sea)*. Ph D thesis. Klaipėda: Klaipėda University.

Zilius, M., Samuiloviene, A., Stanislauskiene, R., Broman, E., Bonaglia, S., Meskys, R., et al. (2020). Depicting Temporal, Functional, and Phylogenetic Patterns in Estuarine Diazotrophic Communities from Environmental DNA and RNA. *Microbial. Ecol.* Preprint.

Zilius, M., Vybernaite-Lubiene, I., Vaiciute, D., Petkuviene, J., Zemlys, P., Liskow, I., et al. (2018). The influence of cyanobacteria blooms on the attenuation of nitrogen throughputs in a Baltic coastal lagoon. *Biogeochemistry* 141, 143–165. doi: 10.1007/s10533-018-0508-0

V

Zilius, M., M. Bartoli, U. Marzocchi, U. Cardini, S. Bonaglia, D. Daunys, G. Castaldelli. Partitioning benthic nitrogen cycle processes among three common macrofauna holobionts. *Biogeochemistry* (resubmitted after revisions).

1

2

3

4

5

6 **PARTITIONING BENTHIC NITROGEN CYCLE PROCESSES AMONG THREE**

7 **COMMON MACROFAUNA HOLOBIONTS**

8

9

10 Mindaugas Zilius[1,2]*, Darius Daunys[1], Marco Bartoli[1,3], Ugo Marzocchi[1,4,5], Stefano Bonaglia[1,6,7],

11 Ulisse Cardini[8], Giuseppe Castaldelli[2]

12

13

14

15

16

17

18 [1] Marine Research Institute, Klaipeda University, 92294 Klaipeda, Lithuania

19 [2] Department of Life Science and Biotechnology, Ferrara University, 44121 Ferrara, Italy

20 [3] Department of Chemistry, Life science and Environmental Sustainability, Parma University, 43124 Parma,

21 Italy

22 [4] Center for Electromicrobiology, Section for Microbiology, Department of Biology, Aarhus University, 8000

23 Aarhus, Denmark

24 [5] Center for Water Technology (WATEC), Department of Biology, Aarhus University, 8000 Aarhus, Denmark

25 [6] Department of Marine Sciences, University of Gothenburg, Box 461, 40530 Gothenburg, Sweden

26 [7] Department of Biology, University of Southern Denmark, 5230 Odense, Denmark

27 [8] Integrative Marine Ecology Department, Stazione Zoologica Anton Dohrn, National Institute of Marine

28 Biology, Ecology and Biotechnology, 8012 Napoli, Italy

29

30

31

32 *Corresponding author:

33 E-mail: mindaugas.zilius@jmtc.ku.lt

34 Tel.: +370 46 398818

Abstract

The effects of single macrofauna taxa on benthic nitrogen (N) cycling have been extensively studied, whereas how macrofaunal communities affect N-related processes remains poorly explored. In this study, we characterized benthic N-cycling in bioturbated sediments of the oligotrophic Öre Estuary (northern Baltic Sea). Solute fluxes and N transformations (N_2 fixation, denitrification and dissimilative nitrate reduction to ammonium [DNRA]) were measured in sediments and macrofauna-associated microbes (holobionts) to partition the role of three dominant taxa (the filter feeder *Limnecola balthica*, the deep deposit feeder *Marenzelleria* spp., and the surface deposit feeder *Monoporeia affinis*) in shaping N-cycling. In the studied area, benthic macrofauna comprised a low diversity community with dominance of the three taxa, which are widespread and dominant in the Baltic. The biomass of these three taxa in the benthic macrofaunal community explained up to 30% of variation in measured biogeochemical processes, confirming their important role in ecosystem functioning. The results also show that these taxa significantly contributed to the benthic metabolism and N-cycling (direct effect) as well as to sediments bioturbation with positive feedback to dissimilative nitrate reduction (indirect effect). Taken together, these functions promoted a reuse of nutrients at the benthic level, limiting net losses (e.g. denitrification) and effluxes to bottom water. Finally, the detection of multiple N transformations in dominating macrofauna holobionts suggested a community-associated versatile microbiome, which actively contributes to the biogeochemical processes. The present study highlights hidden and interactive effects among microbes and macrofauna, which should be considered analysing benthic functioning.

1. Introduction

The community of benthic invertebrates sustains ecosystem functioning in shallow coastal areas via functional group-specific mechanisms such as benthic-pelagic coupling (e.g. filter feeders) or sediment reworking and bioirrigation with oxygen (O_2)-rich bottom water (e.g. deposit feeders) (Lohrer et al. 2004; Karlson et al. 2005; Kristensen et al. 2014; Bonaglia et al. 2019). Filter and deposit feeders generally dominate the benthic communities (e.g. Gogina et al. 2016). Filter feeders like bivalves may favour the transport of pelagic primary production to the sediment, promote water transparency and enhance the regeneration of nutrients to the water column, sustaining primary production (Nakamura et al. 2000; Naldi et al. 2020). Surface or deep burrowing deposit feeders, like polychaetes, increase the rates of mineralization via injection of O_2 or sulphate to subsurface sediments, removal of pore water metabolites and sediment reworking (Kristensen 2001; Quintana et al. 2013, 2018). The latter, by mixing old, refractory organic matter with recently settled labile particles, stimulates mineralization via priming effects (van Nugteren et al. 2013). By constructing and ventilating burrows, macrofauna alter redox conditions due to the transport of electron acceptors and metabolic end-products (Kristensen 2001; Hedman et al. 2011; Kristensen et al. 2014; Kauppi et al. 2018; Bonaglia et al. 2019) and increase coupling between aerobic and anaerobic horizons (Nielsen et al. 2004; Pischedda et al. 2008; Kristensen et al. 2012). Therefore, macrofauna may stimulate an array of reactions and processes regulating benthic functioning. Macrofauna may also select and host unique microbiomes, which can contribute to carbon, sulphur and nitrogen (N) biogeochemical cycling (König et al. 2016; Cardini et al. 2019; Zilius et al. 2020; Marzocchi et al. 2021).

Most studies on macrofauna-mediated benthic functioning were based on abundant species (Thrush et al. 2006; Smyth et al. 2018), and on intact or reconstructed microcosms where different abundance levels of macrofauna taxa were manipulated (Karlson et al. 2005, 2007b; Braeckman et al. 2010; Gilbertson et al. 2012; Bonaglia et al. 2014; Benelli et al. 2018; Kauppi et al. 2018; Samuiloviene et al. 2019). Alternatively, inferential multivariate statistical approaches were used to analyse the relationships between benthic communities and functional processes (Norkko et al. 2015; Villnäs et al. 2018; Politi et al. 2019). However, *emerging* properties of natural communities, which are unpredictable from the analysis of single organisms and *emerge* when analyzing different, interacting species, still remain poorly explored and understood (Gamfeldt et al. 2014; Kaupi et al. 2018). A fascinating example of emerging property comes from the common association between seagrass, lucinid bivalves and sulphide-oxidizing bacteria, which results both in enhanced plant production due to sulphide detoxification and increased N availability, and in increased invertebrates and microbes fitness due to roots radial O_2 loss and sulphide accumulation (van der Heide et al. 2012; Cardini et al. 2019). Such emerging properties may either amplify or buffer the biogeochemical

102   effects of a single species or functional group (Clare et al. 2016a), since interactions may lead to non-
103   additive effects.

104   The simultaneous analysis of whole benthic community functioning and of the metabolic activity
105   of single macrofauna taxa may help addressing the species role in the community, and may identify
106   interspecific interactions. The contribution of macrofauna to benthic functioning can occur in multiple
107   ways: 1) directly, via their own metabolic rates (Welsh et al. 2015; Smyth et al. 2018), 2) indirectly
108   via reworking of sediments, which stimulates microbial communities (Laverock et al. 2014; Bonaglia
109   et al. 2013, 2014; Vasquez-Cardenas et al. 2016; Samuiloviene et al. 2019), and 3) via ecological
110   interactions (predation, competition, facilitation) with other macrofauna (Clare et al. 2016a, b) or with
111   microbes (Zilius et al. 2020; Marzocchi et al. 2021). The latter aspect is understudied but has
112   potentially important implications for the functioning of benthic ecosystems. Macrofauna hosts and
113   their associated microbes form holobionts, which are biological and functional units capable of
114   performing multiple processes (Dittami et al. 2021). Recent biogeochemical studies revealed for
115   example how macrofauna-microbe holobionts might contribute to various processes of benthic N
116   cycle, increasing its import, recycling and bioavailability to primary producers (Zilius et al. 2020;
117   Marzocchi et al. 2021). Increasing synergy between molecular tools and the use of stable isotope
118   probing have allowed large improvements in our understanding of elements cycling in holobionts and
119   benthic macrofauna bioturbated sediments (Poulsen et al. 2014; Vasquez-Cardenas et al. 2016;
120   Cardini et al. 2019; Zilius et al. 2020; Marzocchi et al. 2021; Politi et al. 2021).

121   In particular, benthic microbial N-cycling is largely affected by macrofaunal activity. For
122   example, dense bivalve populations sustain large ammonium (NH_4^+) fluxes to the bottom water either
123   via direct excretion or via the production of labile biodeposits stimulating microbial ammonification
124   and alleviating N limitation (Welsh et al. 2015; Smyth et al. 2018; Cardini et al. 2019). Deep
125   burrowing macrofauna, during ventilation, pump N- and O_2-rich bottom water downward (Nielsen et
126   al. 2004; Mermillod-Blondin and Rosenberg 2006; Renz and Foster 2013; Murphy and Reidenbach
127   2016). This stimulates microbial N-cycling pathways, including ammonification, nitrification and
128   denitrification (Tuominen et al. 1999; Bonaglia et al. 2013; Stief 2013; Bosch et al. 2015; Moraes et
129   al. 2018). Therefore, in macrofauna bioturbated sediments, the abundance and the activity of
130   microbial communities often exceed those of surrounding, non-bioturbated sediments (Gilbertson et
131   al. 2012; Laverock et al. 2014; Yazdani Foshtomi et al. 2018; Samuiloviene et al. 2019). The exterior
132   body of macrofauna or its digestive system offer additional habitats for microbial communities, which
133   are actively involved in different N-cycling pathways, such as nitrification, denitrification and
134   dissimilatory nitrate reduction to ammonium (DNRA) or dinitrogen (N_2) fixation (Ray et al. 2019;
135   Zilius et al. 2020; Marzocchi et al. 2021; Politi et al. 2021).

136   The present study shades light on how benthic biodiversity-ecosystem functioning affects N-
137 cycling in a shallow coastal system. The study was carried out in the Öre Estuary (northern Baltic
138 Sea), which is characterized by a low diversity macrofaunal community dominated by three taxa: the
139 surface deposit feeder amphipod *Monoporeia affinis* (Lindström), the surface deposit and suspension
140 feeding clam *Limnecola balthica* (L.) and the deep burrowing deposit feeding polychaetes
141 *Marenzelleria* spp. We hypothesized for the oligotrophic system under investigation tight interactions
142 among functionally distinct but complementary macrofaunal organisms. Complementary functions
143 include the link between benthic and pelagic compartments, by suspension feeding clams, the active
144 mixing and oxidation of surface sediments by shallow bioturbating amphipods, and the bioirrigation
145 of subsurface sediments with O_2-rich bottom water by deep burrowing polychaetes. Moreover, we
146 expected different microbes associated to the macrofauna, actively contributing to nutrient cycling
147 and reuse via various facilitation offered by their hosts (e.g. vertical migration across steep redox,
148 light or nutrient gradients, easy access to substrates due to advective rather than diffusive processes).
149 Consequently, we expected the main biogeochemical processes in sediment to be predominantly the
150 result of the collective effects of these different functional groups and their mutual interactions with
151 associated microbes. Therefore, the aim of this study was to disentangle such collective effects on N
152 transformations. We used a methodologically integrated approach, which included benthic
153 community (whole core) as well as holobiont (single individual) incubations, to disentangle and
154 reconstruct N-cycling in non-manipulated benthic community, highlighting hidden and interactive
155 effects among the abiotic environment, microbes and macrofauna.

156

2. Methods

158 2.1 Study site and sampling activities

159 The Öre Estuary is a boreal estuarine system (~71 km^2) located on the Swedish coast of the Quark
160 Strait, between the Bothnian Bay and Bothnian Sea (northern Baltic Sea) (Fig. 1). The estuary is
161 brackish (salinity < 6), and oligotrophic due to limited nutrient inputs from the watershed (Hellemann
162 et al. 2017; Voss et al. 2020), which mainly consists of coniferous forests and mires. This estuary is
163 stratified depending on spatiotemporal gradients of salinity, changing upon seasonal river discharge,
164 and summer temperature (Brydsten and Jansson 1989; Bartl et al. 2019). The estuarine sedimentary
165 environment varies from silt to fine sandy deposits (Hellemann et al. 2017).

166   Sediment and animals for experimental activities were collected on 29 and 31 July 2019 along a
167 grid of 9 sites within the dashed area comprised between monitoring stations NB3, N8 and NB7,
168 where water depths average 17 ± 3 m (Fig. 1). Sediment was collected on-board of R/V Botnica using
169 a box corer (20 × 20 cm). After each deployment of the box corer, two large cores (i.d. 8 cm, length
170 30 cm, surface area 50.2 cm^2) were subsampled for flux measurements and a small core (i.d. 4.2 cm,

171   length 25 cm, surface area 13.8 cm^2) was subsampled for sediment characterization. A total of 18

172   large cores and 9 small cores were collected. Nearly 200 L of bottom water (~ 20 m depth) was

173   collected in the proximity of station NB8 with a Niskin-Type water sampler (30 L) for sediment core

174   incubation and other experimental activities. In addition, macrofauna for holobiont incubations was

175   collected using a Van Veen grab, carefully sieving sediments. Macrofauna was transferred to 10 L

176   aquaria, containing continuously aerated bottom water and a nearly 2 cm thick layer of surface

177   sediment from the sampling area. In the laboratory, open sediment cores were placed into an

178   incubation tank, containing unfiltered aerated and well-stirred estuarine water in a temperature-

179   controlled room (12 °C). A stirring bar, driven by an external magnet at 40 rpm, was inserted in each

180   core approximately 9 cm above the sediment-water interface to maintain the water phase mixed

181   avoiding sediment resuspension. Sediment and macrofauna were maintained in the dark and pre-

182   incubated overnight. Afterwards, small sediment cores were sliced (top 0–2 cm sediment layer) for

183   the determination of bulk sediment density (dry weight per unit volume), porosity, grain size, and

184   elemental composition (organic carbon [C$_{org}$] and total nitrogen [TN]).

185

186   2.2 Whole core measurements

187   After overnight preincubation, a gas-tight lid was placed on the top of each core and a dark incubation

188   started. At the beginning of measurements, the water overlying sediments was 100% O$_2$ saturated.

189   The experiment lasted from 7 to 9 h in order to keep final O$_2$ concentration within 20–30% of the

190   initial value (Dalsgaard et al. 2000). At the beginning and end of the incubation, 20 mL water aliquots

191   were collected from each core, transferred into 12 mL exetainers (Labco Ltd) allowing twice

192   overflow, and fixed with 200 µL of 7 M ZnCl$_2$ for O$_2$:Ar measurements. In addition, aliquots of 30

193   mL were filtered (Frisenette GF/F filters) into 12 mL plastic test tubes (for inorganic N and silica

194   [DSi]) and in 10 mL glass tubes (for dissolved inorganic phosphorus [DIP]), and they were

195   immediately frozen at –20 ºC for later nutrient analysis (see section 2.4 for details).

196   After the flux measurements, cores were opened, and left submerged in the incubation tank for

197   13 h. Afterwards, nitrate (NO$_3^-$) reduction processes were measured following the revised isotope

198   pairing technique (r-IPT, Risgaard-Petersen et al. 2003). Briefly, all cores were spiked with ^{15}NO$_3^-$

199   tracer (20 mM Na^{15}NO$_3$, 98 atom % ^{15}N, Sigma Aldrich) to a final concentration of 10 µM (n = 9)

200   and 26 µM (n = 9). To calculate the isotopic enrichment, water samples for NO$_3^-$ analysis were

201   collected prior and after the tracer addition. The cores were then capped and incubated in the dark for

202   7 to 9 hours, limiting O$_2$ decrease to 20–30% as described for flux measurements (Dalsgaard et al.

203   2000). At the end of incubations, the water and the sediment phases (10–12.5 and 12.5–15 cm thick,

204   respectively) were gently mixed to a slurry. Thereafter, 20 mL aliquots of the slurry were transferred

205   into 12 mL exetainers (Labco Ltd) allowing twice overflow, and fixed with 200 µL of 7 M ZnCl$_2$ for

206   later $^{29}N_2$ and $^{30}N_2$ analyses. An additional 40 mL subsample was collected, transferred to 50 mL

207   falcon vials and treated with 2 g of KCl for the determination of the exchangeable NH_4^+ pool and the

208    $^{15}NH_4^+$ fraction (see section 2.4 for details). After the incubations the sediments from all cores were

209   carefully sieved (0.5 mm mesh size) to retrieve macrofauna for further taxonomic identification and

210   determination of abundance and biomass. Total denitrification and DNRA rates were divided into

211   rates of denitrification and ammonification of NO_3^- diffusing to anoxic sediments from the overlaying

212   water column (D_w and $DNRA_w$, respectively) and rates of denitrification and ammonification of NO_3^-

213   produced within sediments via nitrification (D_n and $DNRA_n$, respectively) (Bonaglia et al. 2014).

214

215   2.3 Holobiont incubations

216   Individual incubations were employed to assess N-cycling pathways associated with the animal's

217   holobionts. Incubations were carried out reproducing the experimental setup previously described in

218   Marzocchi et al. (2021) and Politi et al. (2021). Briefly, animals were incubated in small bottom-

219   capped Plexiglas cylindrical microcosms (total volume 227 ± 3 mL) partly filled with sterilized glass

220   beads (Ø 1–1.3 mm; 4 mL – for *M. affinis*, 5 mL – for *L. balthica*, and 16 mL – for *Marenzelleria*

221   spp. experiments), and with filtered and aerated *in situ* water, amended with different ^{15}N isotopes

222   (see sections 2.3.1 and 2.3.2 for details). Glass beads were added to create an artificial, 1–4 cm thick

223   sterilized substrate for the invertebrates. We noticed that burrowing organisms, when incubated in

224   water alone, tend to be stressed trying to dig and hide. Glass beads partially overcome this problem,

225   offer the possibility to invertebrates to burrow and feel more comfortable during the incubations and

226   to avoid overestimation of metabolic activities. The water was filtered (MCE filters, 142 mm

227   diameter, pore size 0.22 µM, MF-Millipore™) to remove phytoplankton, suspended particles and

228   microbes, so that metabolic rates measured in the incubation could be solely attributed to the animal's

229   microbiota growing inside (e.g. in the digestive system) or outside (e.g. the shell, cuticle or

230   exoskeleton) the macrofauna. All microcosms were equipped with a stirring magnet for continuous

231   water mixing (20 rpm) during incubation, and with gas tight lids on the top fitted with sampling ports

232   for water subsampling and replacement. Details on the incubations are reported in the following

233   sections.

234

235   2.3.1 Nitrate reduction

236   The r-IPT was used to assess NO_3^- reduction processes associated with animals, including

237   denitrification, DNRA and anammox (Thamdrup and Dalsgaard 2002; Risgaard-Petersen et al. 2003).

238   Three different macrofauna treatments, each with 5 replicates (containing 19–24 ind. of *M. affinis* or

239   2 ind. of *L. balthica* or 1–2 ind. of *Marenzelleria* spp.) and 1 control (only water), were applied. The

240   first treatment had low $^{15}NO_3^-$ addition to a final concentration of 8.6 µM, the second treatment had

241   high $^{15}NO_3^-$ addition to a final concentration of 25.3 µM, and the third treatment had simultaneous

242    $^{15}NH_4^+$ (15 mM $^{15}NH_4Cl$, 98 atom % ^{15}N, Sigma Aldrich) and $^{14}NO_3^-$ additions to final concentrations

243   of 32.0 and 25.9 µM, respectively. The different $^{15}NO_3^-$ concentrations of treatments 1 and 2 were

244   used to validate the IPT assumptions (Risgaard-Petersen et al. 2003). To calculate the degree of

245   isotopic enrichment, water samples for NH_4^+ and NO_3^- analysis were collected prior and after the

246   isotope addition. Microcosms were preincubated for 1–3 h to allow the tracer diffusion into the

247   animal's body before being capped. After this period, the microcosms were incubated at 12 °C and in

248   the dark for 20–39 h, depending on macrofauna species. The incubation time was set from pilot tests

249   on holobionts respiration rates and by real time monitoring of O_2 concentrations in the microcosms

250   with optodes (FireStingO2, PyroScience GmbH). The rationale was to avoid excess decrease of O_2

251   that may affect microbial activity (e.g. inhibit nitrification or stimulate denitrification), ultimately

252   leading to underestimated or overestimated *in situ* rates. During the incubations, water aliquots were

253   subsampled and replaced at three time points (+ time zero = four total incubation times) from each

254   replicate, transferred without headspace into 12 mL exetainers (Labco Ltd) allowing overflow. One

255   exetainer was poisoned with 200 µL of 7 M $ZnCl_2$ for labelled and unlabelled N_2 gas measurements

256   whereas a second exetainer was not poisoned for later measurement of labelled NH_4^+ production (see

257   section 2.4 for details).

258   Slopes of the linear regression of $^{29}N_2$ and $^{30}N_2$ concentrations versus time were used to calculate

259   rates of denitrification and anammox, using the equations from Thamdrup and Dalsgaard (2002). The

260   slope of the linear regression of $^{15}NH_4^+$ concentration versus time was used to calculate rates of

261   DNRA according to Bonaglia et al. (2016). The increase of the three ^{15}N species (i.e., $^{29}N_2$, $^{30}N_2$, and

262    $^{15}NH_4^+$) versus time was statistically tested via regression analysis using the whole dataset inclusive

263   of the four time points and only significant ($p < 0.05$) regressions were computed into NO_3^- reduction

264   rates. The NO_3^- reduction rates were then calculated as a function of biomass dry weight. Finally,

265   rates in the experimental chambers with animals were corrected with values detected in the controls.

266

267   2.3.2 Dinitrogen fixation

268   To determine rates of N_2 fixation, a stock solution of 0.22 µm twice-filtered and $^{30}N_2$-enriched water

269   was prepared using a modified version of the protocol described in Klawonn et al. (2015) as reported

270   in Marzocchi et al. (2021). Before starting the incubation, the stock solution was gently transferred

271   into five microcosms to minimize gas exchange with the atmosphere. After the macrofauna organisms

272   were added (2 ind. for each microcosm for *L. balthica* and *Marenzelleria* spp., and 3 ind. for each

273   microcosm for *M. affinis*), the cores were closed and incubated in the dark for 6.3 to 6.5 h. Three

274   additional microcosms were prepared and incubated as above but with unlabeled water to serve as a

275 control for isotopic contamination. At the end of the incubation, the macrofauna was collected,

276 weighted (wet weight), and stored at –20 °C for later ^{15}N incorporation analysis. Individuals of *L.*

277 *balthica* were dissected to remove the soft tissues from the shell, and to separate the muscular foot

278 from the pallial organs before being weighted in order to distinguish ^{15}N incorporation in the two

279 body compartments. In addition, 10 non-incubated specimens of each incubated macrofauna taxa

280 were weighted and stored as above for later determination of the natural abundance of N isotopes.

281 Prior to the isotopic analysis, animals' tissues were freeze-dried for 48 h, ground to fine powder and

282 weighed into tin capsules. Samples were analyzed for N elemental composition (%) and isotope ratios

283 (δ^{15}N). ^{15}N$_2$ incorporation rates were calculated as in Cardini et al. (2019), for the entire animal. ^{15}N$_2$

284 incorporation was considered significant for those samples that showed an atom% excess that was

285 more than 2-folds higher than the standard deviation of the atom% in the unlabelled samples.

286

287 2.3.3 Excretion and respiration

288 Macrofauna excretion and respiration were assessed to explain their contribution to net benthic fluxes.

289 Briefly, six 22-mL glass microcosms with *L. balthica* (2 ind. per vial), *M. affinis* (6 ind. per vial), and

290 *Marenzelleria* spp. (2 ind. per vial) with 0.22 μm twice-filtered water were set up and incubated in

291 the dark, under continuous monitoring of O$_2$ with optodes (FireStingO2, PyroScience GmbH). In

292 addition, two controls for each species incubation were added later to correct rates in vials with

293 animals. The incubation was carried out in the dark at 12 °C and lasted from 2.5 to 5.5 h depending

294 on macrofauna species. At the beginning and end of the incubation, a 5 mL aliquot was collected

295 form each vial and filtered (Frisenette GF/F filters) into plastic test tubes for later NH$_4^+$ analyses. At

296 the end of the experiment, animals were retrieved and weighed. Excretion and respiration rates were

297 then normalized to biomass dry weight.

298

299 2.4 Analytical methods

300 Dissolved nutrient concentrations (NH$_4^+$, NO$_2^-$, NO$_x^-$, DSi, and DIP) were measured with a 5-channel

301 continuous flow analyser (San^{++}, Skalar) using standard colorimetric methods (Grasshoff et al. 1983).

302 NO$_3^-$ concentration was calculated as the difference between NO$_x^-$ and NO$_2^-$. Dissolved O$_2$ was

303 quantified from O$_2$:Ar ratio measured by membrane inlet mass spectrometer (MIMS) at Ferrara

304 University (Bay Instruments; Kana et al. 1994) and corrected for Ar concentration and solubility

305 based on temperature and salinity (Colt 2012). ^{15}N-atom% in the dissolved N$_2$ pool in samples from

306 N$_2$ fixation experiment was also estimated using MIMS. Isotopic samples for ^{29}N$_2$ and ^{30}N$_2$

307 production were analysed by gas chromatography-isotopic ratio mass spectrometry (GC-IRMS,

308 Thermo Delta V Plus, Thermo Scientific) at the University of Southern Denmark following the

309   protocol described by De Brabandere et al. (2015). Samples for $^{15}NH_4^+$ production were analysed by

310   the same GC-IRMS after conversion of NH_4^+ to N_2 by the addition of alkaline hypobromite reagent

311   (Warembourg 1993).

312   The N content and its isotopic composition ($\delta^{15}N$) in animals were analysed by Isotope Ratio

313   Mass spectrometry (IRMS, Delta plus V, Thermo Scientific) coupled with an elemental analyzer

314   (Flash EA1112, Thermo Scientific) at Aarhus University (Denmark). Measured $\delta^{15}N$ values were

315   corrected using laboratory standards calibrated against international reference materials

316   (USGS40+41).

317   Sedimentary C_{org} and TN content were analyzed using an element analyzer (FlashEA 1112,

318   Thermo Electron Corporation) at the Center for Physical Sciences and Technology (Lithuania) after

319   carbonate removal from dried sediments with 1 M HCl. Median grain size was determined with laser

320   particle size analyzer (Analysette 22 MicroTec plus, Fritsch GmbH).

321

322   2.5 Statistical analysis

323   The linear regression was employed to explain variability in net benthic fluxes and NO_3^- reduction

324   processes using the dry biomass of benthic community (whole core incubations). The analysis of

325   variance (one-way ANOVA) was used to test the significance of differences in NO_3^- reduction rates

326   among species (holobiont incubations). The assumptions of normality and homogeneity of variance

327   were checked using Shapiro-Wilk and Cochran's tests, respectively. In the case of heteroscedasticity,

328   data were square root or log(x) transformed. If assumptions were not met after transformation, non-

329   parametric Mann-Whitney Rank Sum Test was used. For significant factors, post hoc pairwise

330   comparisons were performed using the Student-Newman-Keuls (SNK) test. In addition, the t-test was

331   used to validate tracer effect on denitrification rates (holobiont incubation). Analyses were performed

332   using SigmaPlot 14.0 software.

333   A distance-based linear model (distLM) was applied to explain the contribution of macrofauna

334   taxa (metabolism, bioturbation effect) to the variability of specific NO_3^- reduction process and

335   benthic fluxes. The biomass of dominant macrofauna taxa was used as a biological predictor. The

336   distLM was built on stepwise selection, employing 9999 permutations at a significance level of p <

337   0.05. The resemblance matrices were built on between-sample similarities of Euclidean distance

338   using normalized and logarithmically transformed fluxes and process rates obtained from 18

339   incubation cores (Clarke and Gorley 2006). Draftsman plots were used to examine distribution and

340   potential multi-collinearity ($|r| > 0.6$) among predictor variables to be included in the model. The

341   obtained results were visualized with distance-based redundancy analysis (db-RDA, Anderson et al.

342   2008), and vectors overlay for analysing predictor variables relationship with response vectors. The

343 analysis was performed using the PRIMER 6 statistical package with the PERMANOVA+ add-on

344 (Primer-E Ltd.; Clarke and Gorley 2006).

345

346 **3. Results**

347 3.1 Macrofauna abundance and biomass

348 In total, 10 species or higher order taxa with an average abundance of 63 ± 3 ind. $core^{-1}$ were

349 recovered after sieving sediments (Supplementary material, Table S1). The most abundant species *M.*

350 *affinis* (33 ± 3 ind. $core^{-1}$) was followed by oligochaetes (17 ± 2 ind. $core^{-1}$), *Marenzelleria* spp. (11

351 ± 2 ind. $core^{-1}$) and *L. balthica* (≤ 4 ind. $core^{-1}$) (Table 1). Other taxa (*Pygospio elegans*, *Saduria*

352 *entomon*, *Corophium volutator,* chironomids, and hydrobiids) were relatively rare (present in less

353 than 10% of cores) and contributed negligibly to the total density (<5%) and biomass (<1%) in the

354 cores.

355 The average biomass (91.1 ± 10.1 mg_{dw} $core^{-1}$) was typical for soft bottom coastal areas of the

356 central and northern Baltic with a clear dominance of the polychaete *Marenzelleria* spp. (39%), the

357 clam *L. balthica* (32%), and the amphipod *M. affinis* (26%) (Table 1).

358 The surface sediments at the studied area were mainly composed by fine deposits with low bulk

359 density, high porosity, and moderate C_{org} and TN content (Table 2). Overall, sediment characteristics

360 within the study area showed little variability.

361

362 3.2 Benthic fluxes and their relationship with macrofauna biomass

363 Measured total benthic O_2 uptake varied by a factor of nearly two, from -939.9 to -1626.9 µmol O_2

364 m^{-2} h^{-1} (Fig. 2a). The sediment was always a source of DIN (11.9–104.7 µmol N m^{-2} h^{-1}) to the

365 overlaying bottom water with equal contribution of NO_x^- and NH_4^+ (Fig. 2b). Net fluxes of NH_4^+

366 varied from 5.3 to 78.8 µmol N m^{-2} h^{-1}. The efflux of NO_3^- ranged from 2.1 to 45.9 µmol N m^{-2} h^{-1}

367 whereas the efflux of NO_2^- ranged between 0.6 and 20.3 µmol N m^{-2} h^{-1}. The mean net flux of DIP

368 was directed from the sediment to the near-bottom water, indicating sediment as a P source (Fig. 2c).

369 Similar to DIP, DSi was also released (85.3–362.0 µmol Si m^{-2} h^{-1}) to bottom water (Fig. 2c).

370 The variation coefficients of the measured solute fluxes were large (0.17–1.32), suggesting

371 pronounced small-scale variability of fluxes. Total macrofauna biomass explained 19–34% of the

372 variability in O_2, NH_4^+, and NO_2^- fluxes with marginal significance level, but was not related to the

373 transport of NO_3^-, DIP and DSi (Fig. 3).

374

375

376

377   3.3 Nitrate reduction in whole core incubations and its relationship with macrofauna biomass

378   Sedimentary NO_3^- reduction processes (denitrification and DNRA) were primarily (88–96%) fuelled

379   by NO_3^- produced within sediments via nitrification (Fig. 4a, b). The contribution of NO_3^- diffusion

380   from the overlaying bottom water (D_w and $DNRA_w$) was of minor importance. D_n rates differed by a

381   factor of two and ranged between 23.7 and 52.9 $\mu mol\ N\ m^{-2}\ h^{-1}$. D_w varied between 1.2 and 6.2 μmol

382     $N\ m^{-2}\ h^{-1}$. DNRA accounted for 18–23% of the total measured NO_3^- reduction, and was in the range

383   of 1.4–26.0 $\mu mol\ N\ m^{-2}\ h^{-1}$ (Fig. 4b). Both $DNRA_w$ (0.1–3.9 $\mu mol\ N\ m^{-2}\ h^{-1}$) and $DNRA_n$ (1.2–2.4

384     $\mu mol\ N\ m^{-2}\ h^{-1}$) were variable among the cores, without any significant correlation with macrofauna

385   biomass. Only the D_w was significantly related to the biomass of macrofaunal community (Fig. 5).

386   Anammox rates were negligible in the present study.

387

388   3.4 Partitioning of the macrofauna effects on N-cycling processes and fluxes

389   Our distLM model explained 29.1% (sum of all canonical eigenvalues) of the total variation in NO_3^-

390   reduction processes and fluxes using the biomass of the three dominant macrofauna taxa *L. balthica,*

391   *M. affinis* and *Marenzelleria* spp. The rest of macrofauna, mainly represented by oligochaetes, was

392   excluded from further model development due to its negligible contribution. Marginal test revealed

393   that *M. affinis* and *Marenzelleria* spp. were significant (F = 2.2, p = 0.035 and F = 2.1, p = 0.044,

394   respectively) in the distLM model, while *L. balthica* biomass was marginally significant (F = 2.0, p

395   = 0.055). Sequential tests showed that solely *M. affinis* had a significant effect (F = 2.2, p = 0.032)

396   on variation of process rates and fluxes, contributing to the 12% of the total variability. *Marenzelleria*

397   spp. (F = 0.8, p = 0.06) and *L. balthica* (F = 1.9, p = 0.08) explained numerically lower and marginally

398   significant part of the total variation (6% and 11%, respectively) when individually included into the

399   model. The main two axes, identified by the model, explained nearly 83% of the total variability.

400   The db-RDA depicted that net fluxes of DIP and NO_3^- reduction coupled to nitrification ($DNRA_n$

401   and D_n) were strongly associated to the biomass of *M. affinis* (Fig. 6). Nitrate reduction (D_w and

402     $DNRA_w$) fuelled by NO_3^- from the overlaying water column and DSi fluxes were positively and

403   strongly correlated to the biomass of *Marenzelleria* spp. The net O_2, NO_3^- and NH_4^+ fluxes were

404   associated with *L. balthica*.

405

406   3.5 Respiration and N-cycling associated with animal holobionts

407   Measured animal respiration was in the range of 9.5–52.3 $\mu mol\ O_2\ g_{dw}^{-1}\ h^{-1}$ with significantly higher

408   rates (SNK test, p < 0.05) observed for *M. affinis* as compared to the other two taxa (Fig. 7a). NH_4^+

409   production via animal excretion varied between 0.05 and 3.3 $\mu mol\ N\ g_{dw}^{-1}\ h^{-1}$. The results showed

410   marginally significant differences (SNK test, $p = 0.052$) in NH_4^+ excretion rates among macrofauna

411   taxa, peaking with *L. balthica*.

412   The highest denitrification rates (SNK test, $p < 0.05$) were measured in *M. affinis* followed by

413   *L. balthica* and *Marenzelleria* spp. (Fig. 7b). Mean denitrification rates were not significantly

414   different (t-test, $p > 0.05$) between low and high $^{15}NO_3^-$ levels in *M. affinis* and *Marenzelleria* spp.,

415   suggesting that the IPT assumptions were fulfilled. The same was not true for *L. balthica* incubations

416   (Mann-Whitney Rank Sum Test, $p = 0.016$). For the latter taxa, we remark methodological difficulties

417   when dealing with incubations of animals that due to the stress of manipulation or to the absence of

418   sediment keep the shells closed, which limits tracer diffusion into their body. Similar to

419   denitrification, significantly higher DNRA rates were observed in *M. affinis* (SNK test, $p < 0.05$),

420   where they accounted for ~7% of the total measured NO_3^- reduction. Additions of combined $^{15}NH_4^+$

421   and $^{14}NO_3^-$ revealed measurable $^{29}N_2$ production, suggesting the presence of putative anammox in *M.*

422   *affinis* and *L. balthica* holobionts. However, such process contributed by less than 0.5% to the total

423   N_2 production (data not shown). N_2 fixation was observed in *L. balthica* and *Marenzelleria* spp.

424   holobionts, with a tendency towards higher rates in the former taxa (Fig. 7b), but the difference in the

425   mean rates was not statistically significant (t-test, $p > 0.05$). Dissection of different clam body parts

426   for $\delta^{15}N$ analysis indicated that N_2 fixation was associated with the animal pallial organs and not with

427   the foot tissue, which showed no significant ^{15}N incorporation. Additionally, we found significant N_2

428   fixation only in 3 out of 10 individuals for both *L. balthica* and *Marenzelleria* spp. indicating a high

429   individual variability. N_2 fixation rates were below the detection limit of the method in *M. affinis*.

430

431   **4. DISCUSSION**

432   4.1. The effect of benthic community on biogeochemical processes

433   We studied benthic respiration, net N fluxes and N-related microbial processes in sediments colonized

434   by a relatively simple macrofaunal community, hosting three different functional groups. We aimed

435   at understanding how interactions among functionally distinct macrofauna affect specific-pathways

436   of the benthic N-cycling. While the effects of individual functional groups are quite well understood

437   (Mermillod-Blondin and Rosenberg 2006; Stief 2013, and references therein), relatively little is

438   known on their aggregated effect in a whole community context. The three taxa investigated

439   comprised 70% of the total macrofauna abundance and 98% of the total biomass in the low diversity

440   benthic community of the Öre Estuary, and explained nearly 30% of variation of the measured

441   biogeochemical processes. Other environmental factors driven by hydrological or watershed

442   attributes, such as sediment characteristics (e.g. redox state, electron acceptor availability) as well as

443   their spatial heterogeneity, are expected to account for the remaining variability (e.g. Gammal et al.

444   2018).

445   Single animal incubations allowed to quantify the direct contribution of macrofauna to O_2
446   respiration, which corresponded to nearly 22% of the total benthic O_2 uptake, within the range of 12–
447   25% reported for other marine and coastal systems (Piepenburg et al. 1995; Glud et al. 2003; Politi
448   et al. 2021). *Marenzelleria* spp. alone accounted for nearly half of macrofaunal community
449   respiration, indicating it as a keystone taxa in benthic metabolism. However, incubations of
450   macrofauna alone remain always challenging due to the stress of animals. This is particularly true for
451   burrowing worms. Reported rates and percentages should therefore be taken with caution. With this
452   respect, the results of the multivariate analysis applied to unmanipulated community in intact
453   sediments and associated benthic processes suggest that the net O_2 flux was primarily correlated with
454   higher density of clams. It appears that *L. balthica*, like other buried clams, may expel oxic water
455   through the pedal gape and thus maintain an oxic layer at the shell-sediment interface (Camillini et
456   al. 2019), which stimulates microbial and meiofaunal metabolism (Reise 1983; Karlson et al. 2005).
457   Although clams are semi-mobile subsurface dwelling organisms, and cannot produce comparable
458   effects on solute exchange as polychaetes or amphipods (e.g. Michaud et al. 2005), their biodeposition
459   of faeces may also significantly stimulate the activity of microbial community in surface sediments,
460   ultimately increasing the species role in benthic metabolism (Karlson et al. 2005).

461   It is difficult, however, to infer on the pathways that use O_2 in this benthic habitat, but oxidized
462   surface sediment and the absence of dissolved free sulphides in pore water in the upper 10 cm (see
463   also Lenstra et al. 2018) may indicate O_2 consumption via organic matter mineralisation, NH_4^+
464   oxidation to NO_3^- via nitrification or oxidation of metals (e.g. Mn^{2+} or Fe^{2+}). The vectors overlay in
465   db-RDA (O_2, NH_4^+ and NO_3^- fluxes) support the idea that O_2 is consumed for NH_4^+ production and
466   its subsequent oxidation. Considering NO_x^- efflux and NO_3^- reduction together, we can estimate how
467   much O_2 was consumed for NH_4^+ oxidation, and mineralization within sediment (Fig. 8). As 2 moles
468   of O_2 are used to oxidize 1 mole of NH_4^+ to NO_3^- then nitrification accounts for 11% of total O_2
469   uptake (70.2–206.3 μmol O_2 m^{-2} h^{-1}) in these sediments. Such O_2 demand for nitrification is the
470   highest in relative terms (as % of total O_2 consumption) among those reported in studies in the Baltic
471   Sea using the IPT (< 6%; Karlson et al. 2005; Bonaglia et al. 2014; Bartoli et al. 2021), indicating
472   favourable conditions for nitrifying bacteria. Besides the amount used to oxidize NH_4^+, a residual
473   67% of total O_2 uptake, corresponding to 949.0 ± 50.4 μmol O_2 m^{-2} h^{-1}, was likely used for organic
474   N ammonification. Assuming 1 molar ratio between CO_2 and O_2 as the respiratory quotient (Hargrave
475   and Phillips 1981) and measured C/N molar ratio of 10.5 in upper sediments, then theoretical
476   ammonification rates average 90.4 ± 1.4 μmol N m^{-2} h^{-1}. Alternatively, macrofaunal community
477   directly via excretion supplied 28.3 ± 4.1 μmol N m^{-2} h^{-1}, which accounts for ~24% of total NH_4^+
478   production (excretion + ammonification). Macrofauna excretion, on the other hand, was equivalent
479   to 90% of the measured net NH_4^+ efflux at the sediment-water interface (Fig. 8). Among the different

480　regressions between net fluxes and whole macrofaunal community biomass, those of net O_2 and NH_4^+

481　fluxes revealed a consistent trend. This was partly expected for the above mentioned reasons of direct

482　macrofauna contribution to O_2 consumption and NH_4^+ production. Thus, we may consider that most

483　of the NH_4^+ excreted by macrofauna was likely transferred to bottom waters, whereas another

484　fraction, primarily regenerated via organic matter ammonification, was oxidized, assimilated or

485　retained within sediments (Fig. 8). The results further show that clams alone contributed for up to

486　55% of measured excretion by the community. Our single macrofauna incubation suggests that

487　bivalves like *L. balthica* excreted higher amounts of NH_4^+ per unit biomass when compared to other

488　functional groups, as reported also in other studies (Vanni et al. 2017).

489　　　In the studied habitat, nearly 63% of all regenerated NH_4^+ was further oxidized to NO_x^- via

490　nitrification (Fig. 8). Without continuous NH_4^+ supply via ammonification, excretion and/or upward

491　transport from deeper layer such active nitrification would rapidly deplete the standing pool of NH_4^+

492　in the upper 2 cm sediment layer (473 µmol m^{-2}; Bartl et al. 2019). Multivariate analysis shows that

493　*M. affinis* primarily stimulated NO_3^- reduction pathways coupled to nitrification (D_n, $DNRA_n$),

494　whereas *Marenzelleria* spp., due to NO_3^- downward transport from bottom water, stimulated the

495　reduction of water column nitrate (D_w). The surface deposit dweller *M. affinis* actively mixes the

496　uppermost sediment layer, and thereby increases solute exchange and sediment oxygenation

497　(Viitasalo-Frösén et al. 2009; Bonaglia et al. 2019). This is also supported by our db-RDA results on

498　positive DIP relationship with *M. affinis*. In contrast, *Marenzelleria* spp*.,* capable for construction

499　and bioirrigation of relatively deep burrows, likely facilitated D_w and $DNRA_w$, in deeper layers.

500　Similar effects by amphipods and polychaetes on NO_3^- reduction pathways were previously observed

501　in experimental studies where individual functional groups were analyzed (Tuominen et al. 1999;

502　Karlson et al. 2005; Bonaglia et al. 2013). Although macrofauna functional groups can produce

503　different or contrasting effects on NO_3^- reduction pathways, these are largely regulated by NO_3^-

504　availability in bottom water (Karlson et al. 2005, 2007b; Bonaglia et al. 2013; Nogaro and Burgin

505　2014; Murphy et al. 2016).

506　　　In a recent work by Hellemann et al. (2017) it was questioned whether the oligotrophic Öre

507　Estuary is functioning as a filter for inorganic N. They suggest that due to limited water column

508　mixing and short water residence time, land generated NO_3^- is not readily available to denitrifiers in

509　sediment. The phytoplankton assimilation and later sedimentation to the bottom is a likely possible

510　link between surface and bottom layers (Bartl et al. 2019). Although particulate N associated to

511　sedimented detritus is recycled to NH_4^+ and subsequently oxidized to NO_3^-, only a fraction of N is

512　removed from the ecosystem through coupled nitrification-denitrification. Denitrification efficiency,

513　which is the ratio between N_2 production and the sum of N_2 and DIN ($NH_4^+ + NO_x^-$) effluxes (Eyre

514　and Ferguson 2009), was relatively low (40% on average), and suggested that ~60% of recycled

515   organic particulate N to DIN was released back to the bottom water where it could be assimilated or

516   nitrified (Bartl et al. 2019). Only a minor fraction of inorganic N was later removed through NO_3^-

517   diffusion into anoxic sediment layers (D_w and $DNRA_w$). Denitrification efficiency tended to decrease

518   when plotted as a function of total macrofauna biomass (data not shown), suggesting that excretion

519   and recycling had a relatively higher importance as compared to the stimulation of N losses. Overall,

520   the stoichiometry of regenerated benthic inorganic nutrient (N (flux+D_n+$DNRA_n$) : Si (flux) : P (flux)

521   = 28:52:1) suggested excess of N and Si, and P limitation. Such ecological nutrients stoichiometry is

522   likely favoured by the activity of functionally diverse macrofaunal community. Reworking and

523   bioirrigation activities by *M. affinis* and *Marenzelleria* spp. alter rates and pathways of organic matter

524   mineralization (Lehtonen and Andersin 1998; Karlson et al. 2007b; Quintana et al. 2018). This is

525   evident by the active ammonification within sediments (Fig. 8). However, *Marenzelleria* spp. effect

526   on mineralization varies among the co-occurring three sibling species, which have different

527   burrowing depth and bioirrigation activities (Renz and Foster 2013; Quintana et al. 2018). Future

528   studies are therefore required to elucidate the effect of three *Marenzelleria* species specifically on

529   benthic microbial N-cycling. The contribution of *L. balthica* to NH_4^+ mobilization is direct and less

530   mediated by the activity of microbes as the mollusc releases to the water column via excretion part

531   of the filtered/digested particulate N. Taken together all these community actions facilitate N

532   accumulation in bottom water. While reworking sediments, the two burrowers maintain sediments

533   oxidized, as suggested by limited reactive P release to the water column in other areas of the Baltic

534   (Karlson et al. 2007a; Norkko et al. 2011), despite active mineralization, and ultimately indicating

535   the regeneration of geochemical buffers by macrofauna (e.g. oxidized metals; Quintana et al. 2018).

536

537   4.2 Effects of macrofauna-microbes holobionts to soft-bottom habitat functioning

538   Macrofauna, besides bioturbating sediments and ventilating burrows also host complex microbiomes,

539   which consist of unique assemblages or overlap communities found in the surrounding environment,

540   that *contaminate* the host during feeding or burrowing activities (Poulsen et al. 2014; Ceullar-

541   Gempeler and Leibold 2018; Hochstein et al. 2019; Samuiloviene et al. 2019; Marzocchi et al. 2021).

542   Here, we show that microbes associated with three key Baltic macrofauna taxa were metabolically

543   diverse and capable of different N transformations such as denitrification, DNRA and/or N_2 fixation.

544   Scaling up these process rates with the average macrofauna biomass at the study area, we were able

545   to estimate the contribution of holobionts to multiple N-cycling pathways (Fig. 8). The holobionts of

546   whole benthic community, based on biomass estimations, together contributed 1% of denitrification

547   and 0.1% of DNRA measured in sediments, which was estimated to be 0.4 µmol N m^{-2} h^{-1}. The

548   holobiont of clams and polychaetes were also capable for N_2 fixation (0.03 and 0.01 µmol N m^{-2} h^{-1},

549   respectively) (Fig. 8). Although the holobiont contribution to the N-cycling pathways in sediment is

550   marginal in this study, this might be different in other seasons or habitats characterized by much

551   higher macrofauna densities or larger specimens. As the abundance of this soft bottom community

552   can be higher in the other Baltic Sea areas (Gogina and Zettler 2010), we may also expect there higher

553   holobionts contribution to the benthic N-cycling. However, it remains questionable to what extent

554   our upscaling reflects *in situ* rates of N transformations in holobionts as we incubated adult

555   macrofauna individuals while the community includes different generation specimens (adults and

556   juveniles). Our main assumption here is that the activity of invertebrate-associated microbes is

557   proportional to the invertebrate biomass and does not vary from juveniles to adults. Notably, the

558   holobionts of *M. affinis* due to their high denitrification rates and abundance can contribute up to ~8%

559   of NO_3^- reduction (3.7 µmol N m^{-2} h^{-1}) if abundance data are used for calculations. To better

560   understand the biomass- and abundance-specific effects on microbial processes in holobionts,

561   measurements of the appropriate metabolic pathways should be carried out across different host age

562   classes and biotic metrics in future studies.

563   Denitrification rates in macrofauna holobionts from the Öre Estuary were at least 66% higher

564   than those measured at similar temperatures in chironomid larvae (*C. plumosus*; Politi et al. 2021).

565   Added tracer concentrations markedly differed between these two experiments, with 2-fold higher

566   concentrations in *C. plumosus*, which indicates much higher metabolic activity under lower NO_3^-

567   concentration in *M. affinis* holobiont. The possible explanations for different rates might be attributed

568   to variable number of denitrifiers in hosts as well as their affinity for NO_3^- or quality of available

569   carbon. Since these hosts occupy different niches in sediments and microbial communities display

570   steep vertical zonation in sediments, different microorganisms with unique metabolic features

571   characterize holobionts. Moreover, our finding of high denitrification rates associated with *M. affinis*

572   was rather surprising given that transcription of denitrification marker genes, encoding NO_2^-

573   reduction and its derivatives, typically occurs under low O_2 conditions (Härtig and Zumft 1999),

574   similar to those in macrofaunal gut (Stief and Eller 2006; Bonaglia et al. 2017). We therefore expect

575   higher activity of denitrifiers in larger clam or polychaete gut. This allows to infer that animal body

576   weight (or size) does not necessarily constrains bacterial activity. NO_3^- was also reduced via DNRA

577   pathway, but this process was quantitatively less important. The re-occurrence of DNRA confirms

578   that NH_4^+ production, associated with macrofauna, is a complex process driven by both animal

579   excretion and the activity of associated DNRA bacteria (Zilius et al. 2020; Politi et al. 2021).

580   However, microbial NH_4^+ production in the studied macrofauna remains quantitatively smaller as

581   compared to excretion (Fig. 8).

582   Measured diazotrophic activity in macrofauna holobionts from the oligotrophic Öre Estuary was

583   in the range of that observed in other taxa from other eutrophic estuarine systems of the Baltic Sea

584   (21.9–517.1 nmol g_{DW}^{-2} d^{-1}; Marzocchi et al. 2021; Politi et al. 2021). In line with these studies, N_2

17

585 fixation resulted markedly higher in filter feeding macrofauna. However, such feeding mode does not
586 necessarily favour N₂ fixation, as for example *L. balthica* can shift between suspension and deposit
587 feeding (Riisgård and Kamermans 2001). Due to various feeding modes diazotrophic microorganisms
588 can inhabit different body parts including gills, foot, gut or body surface as has been seen from other
589 N-cycling pathways (Heisterkamp et al. 2013). Overall, our finding of diazotrophic activity in
590 holobionts at different coastal sites of the Baltic Sea suggests that this process is widespread across
591 diverse taxa of benthic macrofauna even when N concentrations are not limiting (Marzocchi et al.
592 2021; Politi et al. 2021) but also highlights a high individual variability. In the future, more studies
593 should address environmental or biological factors that regulate diazotrophic activity across different
594 functional groups of macrofauna.
595

596 **CONCLUSIVE REMARKS**

597 The oligotrophic Öre Estuary supports a simplified macrofaunal community that actively contributes
598 to benthic N-cycling. Direct contribution includes invertebrates metabolism and to a lesser extent
599 processes carried out by invertebrate-microbe associations. Indirect contribution includes sediments
600 burrowing, bioirrigation and oxidation, stimulating N mineralization processes. The macrofaunal
601 community promoted a moderate loss of nutrients from the benthic system and a limited release of
602 nutrients to the bottom water, suggesting an effective reuse of N, Si and P at the benthic level. The
603 ecological stoichiometry of regenerated nutrients indicated an excess of N and Si over P, likely due
604 to the 4–5 cm thick layer of oxidised and bioturbated sediment at the study area, retaining P and
605 buffering its release. Limited internal recycling of P contributes at maintaining oligotrophic
606 conditions in this area. Such view of the benthic system, in the perspective of the whole system
607 functioning, and of the stoichiometry of nutrient regeneration, can shed new light on macrofaunal
608 diversity and ecosystem functioning relationships along multiple environmental and human pressure
609 gradients. Results of this study suggest that all macrofauna functional groups interacted with
610 microbial communities as some rates of microbial N-transformations were measured in single
611 macrofauna incubations. The role of holobionts in the Öre Estuary was of minor importance as
612 compared to the activity of sediment-associated microbial communities, but this might be different
613 along seasons or habitats. Dramatic changes in macrofauna populations, as the decline of the native
614 amphipod *M. affinis* and the increase of non-native polychaetes of the genus *Marenzelleria*, have
615 already been observed in the studied area (Karlsson and Leonardsson 2003; Eriksson-Wiklund and
616 Andersson 2014). In a simplified community, the marked decrease of a single functional group, may
617 eventually alter biogeochemical *functions or services* (e.g. coupled ammonification-nitrification-
618 denitrification) in surface sediments.

ACKNOWLEDGEMENTS

FUNDING

CONFLICT OF INTEREST

The authors declare that they have no conflict of interest.

AVAILABILITY OF DATA AND MATERIAL

Data can be accessed upon request to the corresponding author.

AUTHOR CONTRIBUTIONS

M.Z., M.B., U.C. and S.B. conceived the ideas and designed methodology; M.Z., M.B., D.D., U.M. and U.C. carried out sampling and the incubation experiments; S.B., G.C. and U.M. carried out the mass spectrometry analyses and animal measurements; U.C., U.M. and S.B. led the data analysis; M.Z. and M.B. wrote the first draft of the manuscript. All authors contributed to the discussion and interpretation of data, and revised and approved the manuscript for submission.

REFERENCES

Anderson M, Gorley R, Clarke K (2008) PERMANOVA+ for PRIMER: guide to software and statistical methods. PRIMER-E, Plymouth, pp 214

650 Bartl I, Hellemann D, Rabouille Ch, Schulz K, Tallberg P, Hietanen S, Voss M (2019) Particulate organic
651   matter controls benthic microbial N retention and N removal in contrasting estuaries of the Baltic Sea.
652   Biogeosciences 16:3543-3564. https://doi.org/10.5194/bg-16-3543-2019

653 Bartoli M, Nizzoli D, Zilius M, Bresciani M, Pusceddu A, Bianchelli S, Sundbäck K, Razinkovas-Baziukas A
654   and Viaroli P (2021) Denitrification, nitrogen uptake, and organic matter quality undergo different
655   seasonality in sandy and muddy sediments of a turbid estuary. Front Microbiol 11:612700.
656   https://doi.org/10.3389/fmicb.2020.612700

657 Benelli S, Bartoli M, Zilius M, Vybernaite-Lubiene I, Ruginis T, Petkuviene J, Fano EA (2018)
658   Microphytobenthos and chironomid larvae attenuate nutrient recycling in shallow-water sediments. Freshw
659   Biol 63:187-201. https://doi.org/10.1111/fwb.13052

660 Bonaglia S, Bartoli M, Gunnarsson JS, Rahm L, Raymond C, Svensson O, Shakeri Yekta S, Brüchert V (2013)
661   Effect of reoxygenation and Marenzelleria spp. bioturbation on Baltic Sea sediment metabolism. Mar Ecol
662   Prog Ser 482:43-55. https://doi.org/10.3354/meps10232

663 Bonaglia S, Deutsch B, Bartoli M, Marchant HK, Bruchert V (2014) Seasonal oxygen, nitrogen and
664   phosphorus benthic cycling along an impacted Baltic Sea estuary: regulation and spatial patterns.
665   Biogeochemistry 119:139-160. https://doi.org/10.1007/s10533-014-9953-6

666 Bonaglia S, Klawonn I, De Brabandere L, Deutsch B, Thamdrup B, Brüchert V (2016) Denitrification and
667   DNRA at the Baltic Sea oxic–anoxic interface: Substrate spectrum and kinetics. Limnol Oceanogr
668   61(5):1900-1915. https://doi.org/10.1002/lno.10343

669 Bonaglia S, Brüchert V, Callac N, Vicenzi A, Fru EC, Nascimento FJA (2017) Methane fluxes from coastal
670   sediments are enhanced by macrofauna. Sci Rep 7:13145. https://doi.org/10.1038/s41598-017-13263-w

671 Bonaglia S, Marzocchi U, Ekeroth N, Brüchert V, Blomqvist S, Hall POJ (2019) Sulfide oxidation in deep
672   Baltic Sea sediments upon oxygenation and colonization by macrofauna. Mar Biol 166:149.
673   https://doi.org/10.1007/s00227-019-3597-y

674 Bosch JA, Cornwell JC, Kemp WM (2015) Short-term effects of nereid polychaete size and density on
675   sediment inorganic nitrogen cycling under varying oxygen conditions. Mar Ecol Progr Ser 524:155-169.
676   https://doi.org/10.3354/meps11185

677 Braeckman U, Provoost P, Gribsholt B, Van Gansbeke D, Middelburg JJ, Soetaert K, Vincx M, Vanaverbeke
678   J (2010) Role of macrofauna functional traits and density in biogeochemical fluxes and bioturbation. Mar
679   Ecol Progr Ser 399:173–186. https://doi.org/10.3354/meps08336

680 Brydsten L, Jansson M (1989) Studies of estuarine sediment dynamics using 137Cs from Tjernobyl accident
681   as tracer. Estuar Coast Shelf Sci 28:249–59.

682 Cardini U, Bartoli M, Lee R, Luecker S, Mooshammer M, Polzin J, Weber M, Petersen J (2019)
683   Chemosymbiotic bivalves contribute to the nitrogen budget of seagrass ecosystems. ISME J 13:3131-3134.
684   https://doi.org/10.1038/s41396-019-0486-9

685 Clare DS, Spencer M, Robinson LA, Frid CLJ (2016a) Species-specific effects on ecosystem functioning can
686   be   altered   by   interspecific   interactions.   PLoS   ONE   11(11):e01657.
687   https://doi.org/10.1371/journal.pone.0165739

688 Clare DS, Spencer M, Robinson LA, Frid CLJ (2016b) Species densities, biological interactions and benthic
689   ecosystem   functioning: an   in   situ   experiment.   Mar   Ecol   Prog   Ser   547:149-161.
690   https://doi.org/10.3354/meps11650

691 Clarke K, Gorley R (2006) PRIMER v6: User manual/tutorial. PRIMER-E, Plymouth, p 192

692 Colt J (2012) Dissolved gas concentration in water: Computation as functions of temperature, salinity and
693   pressure (2nd ed). Elsevier, London

694 Cuellar-Gempeler C, Leibold MA (2018) Multiple colonist pools shape fiddler crab-associated bacterial
695   communities. ISME J 12(3):825-837. https://doi.org/10.1038/s41396-017-0014-8

696 Dalsgaard T, Nielsen LP, Brotas V, Viaroli P, Underwood G, Nedwell D, Sundbäck K, Rysgaard S, Miles A,
697   Bartoli M, Dong L, Thornton DCO, Otossen LDM, Castaldelli G, Risgaard-Petersen N (2000) Protocol
698   handbook for NICE—nitrogen cycling in estuaries: a project under the EU research program: Marine
699   Science and Technology (MAST III). National Environmental Research Institute, Silkeborg

700 De Brabandere L, Bonaglia S, Kononets MY, Viktorsson L, Stigebrandt, A, Thamdrup B, Hall POJ (2015)
701   Oxygenation of an anoxic fjord basin strongly stimulates benthic denitrification and DNRA.
702   Biogeochemistry 126(1-2):131-152. https://doi.org/10.1007/s10533-015-0148-6

703 Dittami SM, Arboleda E, Auguet JC, Bigalke A, Briand E, Cárdenas P, Cardini U, Decelle J, Engelen AH,
704   Eveillard D, Gachon CMM, Griffiths SM, Harder T, Kayal E, Kazamia E, Lallier FH, Medina M, Marzinelli
705   EM, Morganti T, Núñez Pons L, Prado S, Pintado Valverde J, Saha M, Selosse M-A, Skillings D, Stock
706   W, Sunagawa S, Toulza E, Vorobev A, Leblanc C, Not F (2021) A community perspective on the concept
707   of marine holobionts: current status, challenges, and future directions. PeerJ 9:e10911.
708   https://doi.org/10.7287/peerj.preprints.27519v3 |

709 Eriksson Wiklund A-K, Andersson A (2014) Benthic competition and population dynamics of Monoporeia
710   affinis and Marenzelleria sp. in the northern Baltic Sea. Estuar Coast Shelf Sci 144:46-53.
711   https://doi.org/10.1016/j.ecss.2014.04.008

712 Eyre BD, Ferguson AJP (2009) Denitrification efficiency for defining critical loads of carbon in shallow
713   coastal ecosystems. In: Andersen JH, Conley DJ (eds). Eutrophication in Coastal Ecosystems: Towards
714   better understanding and management strategies Selected Papers from the Second International Symposium
715   on Research and Management of Eutrophication in Coastal Ecosystems, 20–23 June 2006, Nyborg,
716   Denmark. Springer Netherlands, Dordrecht, pp 137-146

717 Gamfeldt L, Lefcheck, JS, Byrnes, JEK, Cardinale, BJ, Duffy JE, Griffin JN (2014) Marine biodiversity and
718   ecosystem functioning: what's known and what's next? Oikos 124:252–265.
719   https://doi.org/10.1111/oik.01549

720 Gammal J, Järnström M, Bernard G, Norrko J, Norkko A (2018) Environmental context mediates biodiversity–
721   ecosystem functioning relationships in coastal soft-sediment habitats. Ecosystems 22:137-151.
722   https://doi.org/10.1007/s10021-018-0258-9

723 Gilbertson WW, Solan M, Prosser JI (2012) Differential effects of microorganism–invertebrate interactions
724   on benthic nitrogen cycling. FEMS Microbiol Ecol 82(1):11-22. https://doi.org/10.1111/j.1574-
725   6941.2012.01400.x

726 Glud RN, Gundersen JK, Røy H, Jørgensen BB (2003) Seasonal dynamics of benthic O_2 uptake in a semi-
727   enclosed bay: importance of diffusion and fauna activity. Limnol Oceanogr 48(3):1265-1276.

728 Gogina M, Nygård H, Blomqvist M, Daunys D, Josefson AB, Kotta J, Maximov A, Warzocha J, Yermakov
729   V. Gräwe U, Zettler ML (2016) The Baltic Sea scale inventory of benthic faunal communities. ICES J Mar
730   Sci 73(4):1196-1213. https://doi.org/10.1093/icesjms/fsv265

731 Gogina M, Zettler ML (2010) Diversity and distribution of benthic macrofauna in the Baltic Sea Data inventory
732   and its use for species distribution modelling and prediction. J Sea Res 64:313-32.
733   https://doi.org/10.1016/j.seares.2010.04.005

734 Grassoff M, Ehrhardt M, Kremling K (1983) Methods of Seawater Analysis, 2ed. Verlag Chemie, Weinheimm

735 Hargrave BT, Phillips GA (1981) Annual in situ carbon dioxide and oxygen flux across a subtidal marine
736   sediment, Estuar Costal Shelf Sci 12:725-737.

737 Härtig E, Zumft WG (1999) Kinetics of nirS expression (cytochrome cd1 nitrite reductase) in *Pseudomonas*
738 *stutzeri* during the transition from aerobic respiration to denitrification: evidence for a denitrification-
739 specific nitrate- and nitrite-responsive regulatory system. J Bacteriol Res 181(1):161-166.
740 https://doi.org/10.1128/JB.181.1.161-166.1999

741 Hedman EJ, Gunnarsson JS, Samuelsson G, Gilbert F (2011) Particle reworking and solute transport by the
742 sediment-living polychaetes *Marenzelleria neglecta* and *Hediste diversicolor*. J Exp Mar Biol Ecol
743 407:294-301. https://doi.org/10.1016/j.jembe.2011.06.026

744 Heisterkamp IM, Schramm A, Larsen LH, Svenningsen NB, Lavik G, de Beer D, Stief P (2013) Shell biofilm-
745 associated nitrous oxide production inmarine molluscs: processes, precursors andrelative importance.
746 Environ Microbiol 15(7):1943-1955. https://doi.org/10.1111/j.1462-2920.2012.02823.x

747 Hellemann D, Tallberg P, Bartl I, Voss M, Hietanen S (2017) Denitrification in an oligotrophic estuary: a
748 delayed sink for riverine nitrate. Mar Ecol Progr Ser 583:63-80. https://doi.org/10.3354/meps12359

749 Hochstein R, Zhang Q, Sadowsky JM, Forbes VE (2019) The deposit feeder Capitella teleta has a unique and
750 relatively complex microbiome likely supporting its ability to degrade pollutants. Sci Total Environ
751 670:547-554. https://doi.org/10.1016/j.scitotenv.2019.03.255

752 Kana TM, Darkangelo C, Hunt MD, Oldham JB, Bennett GE, Cornwell JC (1994) Membrane inlet mass
753 spectrometer for rapid high-precision determination of N_2, O_2, and Ar in environmental water samples.
754 Anal Chem 66(23):4166-4170. https://doi.org/10.1021/ac00095a009

755 Karlson K, Hulth S, Ringdahl K, Rosenberg R (2005) Experimental recolonisation of Baltic Sea reduced
756 sediments: survival of benthic macrofauna and effects on nutrient cycling. Mar Ecol Progr Ser 294:35-49.
757 https://doi.org/10.3354/meps294035

758 Karlsson A, Leonardsson K (2003) Mjukbottenfauna. In: Wiklund K (ed) Bottniska viken. Umeå marina
759 forskningcentrum, Umeå University, Umeå, pp 14-16.

760 Karlson K, Bonsdorff E, Rosenberg R (2007a) The impact of benthic macrofauna for nutrient fluxes from
761 Baltic Sea sediments. Ambio 36(2-3):161-167. https://www.jstor.org/stable/4315809

762 Karlson K, Hulth S, Rosenberg R (2007b) Density of *Monoporeia affinis* and biogeochemistry in Baltic Sea
763 sediments. J Exp Mar Biol Ecol 344(2):123-135. https://doi.org/10.1016/j.jembe.2006.11.016

764 Kauppi L, Bernard G, Bastrop R, et al. (2018) Increasing densities of an invasive polychaete enhance
765 bioturbation with variable effects on solute fluxes. Sci Rep 8:7619. https://doi.org/10.1038/s41598-018-
766 25989-2

767 Klawonn I, Lavik G, Böning P, Marchant H, Dekaezemacker J, Mohr W, Ploug H (2015) Simple approach for
768 the preparation of $^{15-15}N_2$-enriched water for nitrogen fixation assessments: evaluation, application and
769 recommendations. Front Microbiol 6:769. https://doi.org/10.3389/fmicb.2015.00769

770 König S, Gros O, Heiden SE, Hinzke T, Thürmer A, Poehlein A, Meyer S, Vatin M, Mbéguié-A-Mbéguié D,
771 Tocny J, Ponnudurai R, Daniel R, Becher D, Schweder T, Markert S (2016) Nitrogen fixation in a
772 chemoautotrophic lucinid symbiosis. Nat Microbiol 2(1): 16193.
773 https://doi.org/10.1038/nmicrobiol.2016.193

774 Kristensen E (2000) Organic matter diagenesis at the oxic/anoxic interface in coastal marine sediments, with
775 emphasis on the role of burrowing animals. Hydrobiologia 426:1–24.
776 https://doi.org/10.1023/A:1003980226194

777 Kristensen E (2001) Impact of polychaetes (*Nereis* spp. and *Arenicola marina*) on carbon biogeochemistry in
778 coastal marine sediments. Geochem Trans 2:92-103. https://doi.org/10.1186/1467-4866-2-92

779 Kristensen E, et al (2012) What is bioturbation? The need for a precise definition for fauna in aquatic sciences.
780 Mar Ecol Prog Ser 446:285-302. https://doi.org/10.3354/meps09506

781 Kristensen E, Delefosse M, Quintana CO, Flindt MR, Valdemarsen T (2014) Influence of benthic macrofauna
782   community shifts on ecosystem functioning in shallow estuaries. Front Mar Sci 1: 44.
783   https://doi.org/10.3389/fmars.2014.00041

784 Laverock B, Tait K, Gilbert JA, Osborn AM, Widdicombe S (2014) Impacts of bioturbation on temporal
785   variation in bacterial and archaeal nitrogen–cycling gene abundance in coastal sediments. Environ
786   Microbiol Rep 6:113-121. https://doi.org/10.1111/1758-2229.12115

787 Lehtonen KK, Andersin A-B (1998) Population dynamics, response to sedimentation and role in benthic
788   metabolism of the amphipod Monoporeia affinis in an open-sea area of the northern Baltic Sea. Mar Ecol
789   Prog Ser 168:71-85.

790 Lenstra WK, Egger M, van Helmond NAGM, Kritzberg E, Conley DJ, Slomp CP (2018) Large variations in
791   iron input to an oligotrophic Baltic Sea estuary: impact on sedimentary phosphorus burial. Biogeosciences
792   15:6979–6996. https://doi.org/10.5194/bg-15-6979-2018

793 Lohrer AM, Thrush SF, Gibbs MM (2004) Bioturbators enhance ecosystem function through complex
794   biogeochemical interactions. Nature 431:1092-1095. https://doi.org/10.1038/nature03042

795 Marzocchi U, Bonaglia S, Zaiko A, Quero GM, Vybernaite-Lubiene I, Politi T, Samuiloviene A, Zilius M,
796   Bartoli M, Cardini U (2021) Zebra mussel holobionts fix and recycle nitrogen in lagoon sediments. Front
797   Microbiol 11:610269. https://doi.org/10.3389/fmicb.2020.610269

798 Mermillod-Blondin F, Rosenberg R (2006) Ecosystem engineering: the impact of bioturbation on
799   biogeochemical processes in marine and freshwater benthic habitats. Aquat Sci 68:434-442.
800   https://doi.org/10.1007/s00027-006-0858-x

801 Moraes PC, Zilius M, Benelli S, Bartoli M (2018) Nitrification and denitrification in estuarine sediments with
802   tube-dwelling benthic animals. Hydrobiologia 819:217-230. https://doi.org/10.1007/s10750-018-3639-3

803 Murphy EAK, Reidenbach MA (2016) Oxygen transport in periodically ventilated polychaete burrows. Mar
804   Biol 163:208. https://doi.org/10.1007/s00227-016-2983-y

805 Nakamura Y, Kerciku F (2000) Effects of filter-feeding bivalves on the distribution of water quality and
806   nutrient cycling in a eutrophic coastal lagoon. J Mar Syst 26(2): 209-221. https://doi.org/10.1016/S0924-
807   7963(00)00055-5

808 Naldi M, Nizzoli D, Bartoli M, Viaroli P, Viaroli P (2020) Effect of filter-feeding mollusks on growth of green
809   macroalgae and nutrient cycling in a heavily exploited coastal lagoon Estuar Coast Shelf Sci 239: 106679.
810   https://doi.org/10.1016/j.ecss.2020.106679

811 Nielsen OI, Gribsholt B, Kristensen E, Revsbech NP (2004) Microscale distribution of oxygen and nitrate in
812   sediment inhabited by *Nereis diversicolor*: spatial patterns and estimated reaction rates. Aquat Microb Ecol
813   34:23-32. https://doi.org/10.3354/ame034023

814 Nogaro G, Burgin AJ (2014) Influence of bioturbation on denitrification and dissimilatory nitrate reduction to
815   ammonium   (DNRA)   in   freshwater   sediments.   Biogeochemistry   120:279-294
816   https://doi.org/10.1007/s10533-014-9995-9

817 Norkko J, Reed DC, Timmermann K, Norkko A, Gustafsson BG, Bonsdorff E, Slomp CP, Carstensen J,
818   Conley DJ (2011) A welcome can of worms? Hypoxia mitigation by an invasive species. Glob Chang Biol
819   8:422-434. https://doi.org/10.1111/j.1365-2486.2011.02513.x

820 Norkko J, Gammal J, Hewitt JE, et al (2015) Seafloor Ecosystem Function Relationships: In Situ Patterns of
821   Change   Across   Gradients   of   Increasing   Hypoxic   Stress.   Ecosystems   18:1424-1439.
822   https://doi.org/10.1007/s10021-015-9909-2

823 Pischedda L, Poggiale JC, Cuny P, Gilbert F (2008) imaging oxygen distribution in marine sediments. The
824   importance of bioturbation and sediment heterogeneity. Acta Biotheor 56:123-135.
825   https://doi.org/10.1007/s10441-008-9033-1

826 Quintana CO, Kristensen E, Valdemarsen T (2013) Impact of the invasive polychaete *Marenzelleria viridis* on
827   the biogeochemistry of sandy marine sediments. Biogeochemistry 115(1):95-109.
828   https://doi.org/10.1007/s10533-012-9820-2

829 Quintana CO, Raymond C, Nascimento FJA, Bonaglia A, Forster S, Gunnarsson JS, Kristensen E (2018)
830   Functional performance of three invasive marenzelleria species under contrasting ecological conditions
831   within the Baltic Sea. Estuar Coast 41:1766-1781. https://doi.org/10.1007/s12237-018-0376-9

832 Piepenburg D, Blackburn TH, von Dorrienl CF, Gutt J, Hall POJ, Hulth S, Kendall MA, Opalinski KW, Rachor
833   E, Schmid MK (1995) Partitioning of benthic community respiration in the Arctic (northwestern Barents
834   Sea). Mar Ecol Prog Ser 118:199-213. https://doi.org/10.3354/meps118199

835 Politi T, Zilius M, Castaldelli G, Bartoli M, Daunys D (2019) Estuarine macrofauna affects benthic
836   biogeochemistry in a hypertrophic lagoon. Water 11(6):1186. https://doi.org/10.3390/w11061186

837 Politi T, Barisevičiūte R, Bartoli M, Bonaglia S, Cardini C, Castaldelli G, et al. (2021) A bioturbator, a
838   holobiont and a vector: the multifaceted role of *Chironomus plumosus* in shaping N-cycling. Freshw Biol
839   66(6):1036-1048. https://doi.org/10.1111/fwb.13696

840 Poulsen M, Kofoed MV, Larsen LH, Schramm A, Stief P (2014) *Chironomus plumosus* larvae increase fluxes
841   of denitrification products and diversity of nitrate-reducing bacteria in freshwater sediment. Syst Appl
842   Microbiol 37:51-59. https://doi.org/10.1016/j.syapm.2013.07.006

843 Ray NE, Henning MC, Fulweiler RW (2019) Nitrogen and phosphorus cycling in the digestive system and
844   shell biofilm of the eastern oyster *Crassostrea virginica*. Mar Ecol Prog Ser 621:95-105.
845   https://doi.org/10.3354/meps13007

846 Reise K (1983) Biotic enrichment of intertidal sediments by experimental aggregates of the deposit-feeding
847   bivalve *Macoma balthica*. Mar Ecol Prog Ser 2:229-236.

848 Riisgård HU, Kamermans P (2001) Switching between deposit and suspension feeding in coastal zoobenthos.
849   In: Reise K (ed) Ecological Comparisons of Sedimentary Shores. Ecological Studies (Analysis and
850   Synthesis), vol 151. Springer, Berlin, Heidelberg, pp 73-101. https://doi.org/10.1007/978-3-642-56557-1_5

851 Risgaard-Petersen N, Nielsen LP, Rysgaard S, Dalsgaard T, Meyer RL (2003) Application of the isotope
852   pairing technique in sediments where anammox and denitrification coexist. Limnol Oceanogr-Meth 1:63-
853   73. https://doi.org/0.4319/lom.2004.2.315

854 Samuiloviene A, Bartoli M, Bonaglia S, Cardini U, Vybernaite-Lubiene I, Marzocchi U, Petkuviene J, Politi
855   T, Zaiko A, Zilius M (2019) The effect of chironomid larvae on nitrogen cycling and microbial communities
856   in soft sediments. Water 11:1931. https://doi.org/10.3390/w1109193

857 Smyth AR, Murphy AE, Anderson IC, Song B (2018). Differential effects of bivalves on sediment nitrogen
858   cycling in a shallow coastal bay. Estuaries Coast 41:1147–1163. https://doi.org/10.1007/s12237-017-0344-
859   9

860 Stief P, Eller G (2006) The gut microenvironment of sediment-dwelling *Chironomus plumosus* larvae as
861   characterised with O_2, pH, and redox microsensors. J Comp Physiol B 176:673-683.
862   https://doi.org/10.1007/s00360-006-0090-y

863 Stief P (2013) Stimulation of microbial nitrogen cycling in aquatic ecosystems by benthic macrofauna:
864   mechanisms and environmental implications. Biogeosciences 10:7829-7846. https://doi.org/10.5194/bg-
865   10-7829-2013

866 Thamdrup B, Dalsgaard T (2002) Production of N_2 through anaerobic ammonium oxidation coupled to nitrate
867   reduction in marine sediments. App Environ Microbiol 68(3):1312–1318. doi:10.1128/AEM.68.3.1312-
868   1318.2002

869 Thrush SF, Hewitt JE, Gibbs M, Lundquist C, Norkko A (2006) Functional role of large organisms in intertidal
870   communities: community effects and ecosystem function. Ecosystems 9:1029-1040.
871   https://doi.org/10.1007/s10021-005-0068-8

872 Tuominen L, Mäkelä K, Lehtonen KK, Haahti H, Hietanen S, Kuparinen J (1999) Nutrient fluxes, porewater
873   profiles and denitrification in sediment influenced by algal sedimentation and bioturbation by *Monoporeia*
874   *affinis*. Estuar Coast Shelf Sci 49(1):83-97. https://doi.org/10.1006/ecss.1999.0492

875 van der Heide T, Govers LL, de Fouw J, Olff H, van der Geest M, van Katwijk MM, Piersma T, van de Koppel
876   J, Silliman BR, Smolders AJP, van Gils JA (2012) A three-stage symbiosis forms the foundation of seagrass
877   ecosystems. Science 336(6087):1432-1434. https://doi.org/10.1126/science.1219973.

878 van Nugteren P, Moodley L, Brummer GJ, Heip CH, Herman PM, Middelburg JJ (2009) Seafloor ecosystem
879   functioning: the importance of organic matter priming. Mar Biol 156(11):2277-2287.
880   https://doi.org/10.1007/s00227-009-1255-5

881 Vanni MJ, McIntyre PB, Allen D, et al (2017) A global database of nitrogen and phosphorus excretion rates
882   of aquatic animals. Ecology 98:1475-1475. https://doi.org/10.1002/ecy.1792

883 Vasquez-Cardenas D, Quintana CO, Meysman FJR, Kristensen E, Boschker HTS (2016) Species-specific
884   effects of two bioturbating polychaetes on sediment chemoautotrophic bacteria. Mar Ecol Prog Ser 549:55-
885   68. https://doi.org/10.3354/meps11679

886 Viitasalo S, Laine A, Lehtiniemi M (2009) Habitat modification mediated by motile surface stirrers versus
887   semi-motile burrowers: Potential for a positive feedback mechanism in a eutrophied ecosystem. Mar Ecol
888   Progr Ser 376:21-32. https://doi.org/10.3354/meps07788.

889 Villnas A, Hewitt J, Snickars M, Westerbom M, Norkko A (2018) Template for using biological trait groupings
890   when exploring large-scale variation in seafloor multifunctionality. Ecol Appl 28(1):78-94.
891   https://doi.org/10.1002/eap.1630

892 Voss M, Asmala E, Bartl I, et al (2020) Origin and fate of dissolved organic matter in four shallow Baltic Sea
893   estuaries. Biogeochemistry. https://doi.org/10.1007/s10533-020-00703-5

894 Warembourg FR (1993) Nitrogen fixation in soil and plant systems. In: Knowles R, Blackburn TH (eds)
895   Nitrogen isotope techniques. Academic Press, San Diego, pp 127-156

896 Welsh DT, Nizzoli D, Fano EA, Viaroli P (2015) Direct contribution of clams (*Ruditapes philippinarum*) to
897   benthic fluxes, nitrification, denitrification and nitrous oxide emission in a farmed sediment. Estuar Coast
898   Shelf Sci 154:84-93. https://doi.org/10.1016/j.ecss.2014.12.021

899 Yazdani Foshtomi M, Leliaert F, Derycke S, Willems A, Vincx M, Vanaverbeke J (2018) The effect of bio-
900   irrigation by the polychaete *Lanice conchilega* on active denitrifiers: Distribution, diversity and
901   composition of nosZ gene. PLoS ONE 13(2): e0192391. https://doi.org/10.1371/journal.pone.0192391
902 Zilius M, Bonaglia S, Broman E, et al (2020) N_2 fixation dominates nitrogen cycling in a mangrove fiddler
903   crab holobiont. Sci Rep 10:13966. https://doi.org/10.1038/s41598-020-70834-0
904

TABLES

905

906

Table 1 Abundance and biomass of the main macrofauna taxa and community in incubated cores (n=18) from the Öre Estuary. Results are represented by mean and standard error, and min – max values in brackets

Taxonomic unit	Characteristics			
	Abundance (ind. core^{-1})		Biomass (mg$_{dw}$ core^{-1})	
	Average	Range	Average	Range
L. balthica	1.6 ± 0.4	(0–4)	38.3 ± 10.6	(0.0–160.5)
M. affinis	33.3 ± 2.7	(16–57)	17.2 ± 2.1	(0.4–31.4)
Marenzelleria spp.	9.4 ± 0.6	(5–14)	33.4 ± 6.6	(3.3–88.7)
Oligochaetes	16.8 ± 1.5	(9–32)	1.6 ± 0.3	(<0.1–4.0)
Others	1.9 ± 0.4	(0–6)	0.8 ± 0.2	(0.0–2.6)
Total	63.2 ± 3.4	(42–92)	91.1 ± 10.1	(10.1–185.4)

910

911

912

913

914

915

916

Table 2 Main sediment characteristics in the studied area from the Öre Estuary. Results are represented by mean and standard error (n=9), and min – max values

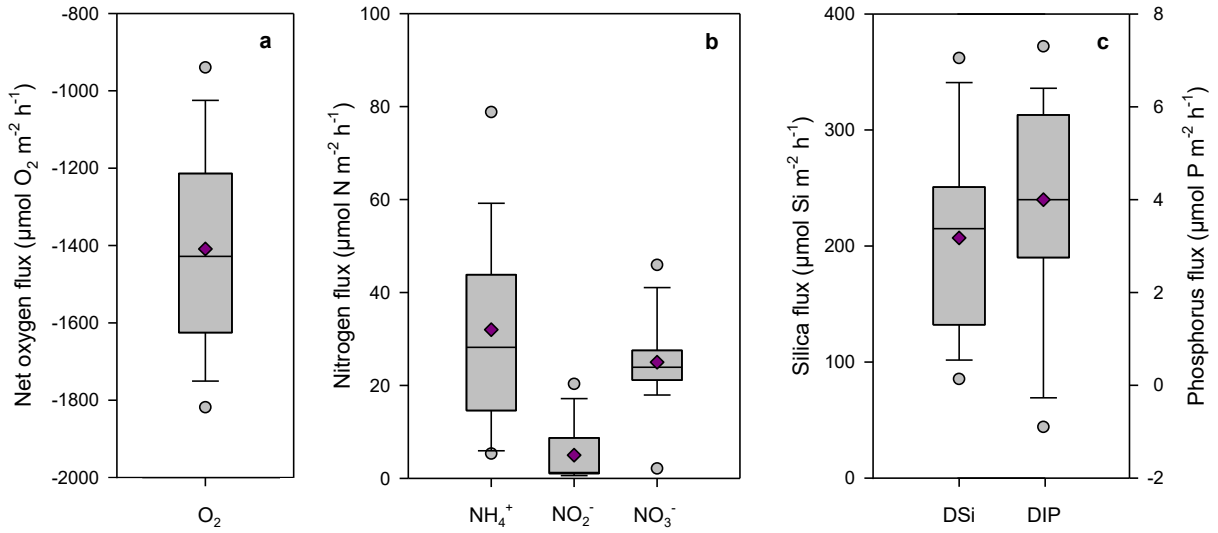| Characteristics	Average	Range
Density [g cm^{-3}]	1.11 ± 0.01	1.08–1.14
Porosity	0.89 ± 0.03	0.76–0.95
Median grain size [mm]	20.6 ± 1.1	16.7–23.3
C$_{org}$ [%]	3.9 ± 0.1	3.7–4.0
TN [%]	0.43 ± 0.01	0.42–0.45
C:N [mol:mol]	10.5 ± 0.1	10.2–10.5

919

FIGURES

921

922
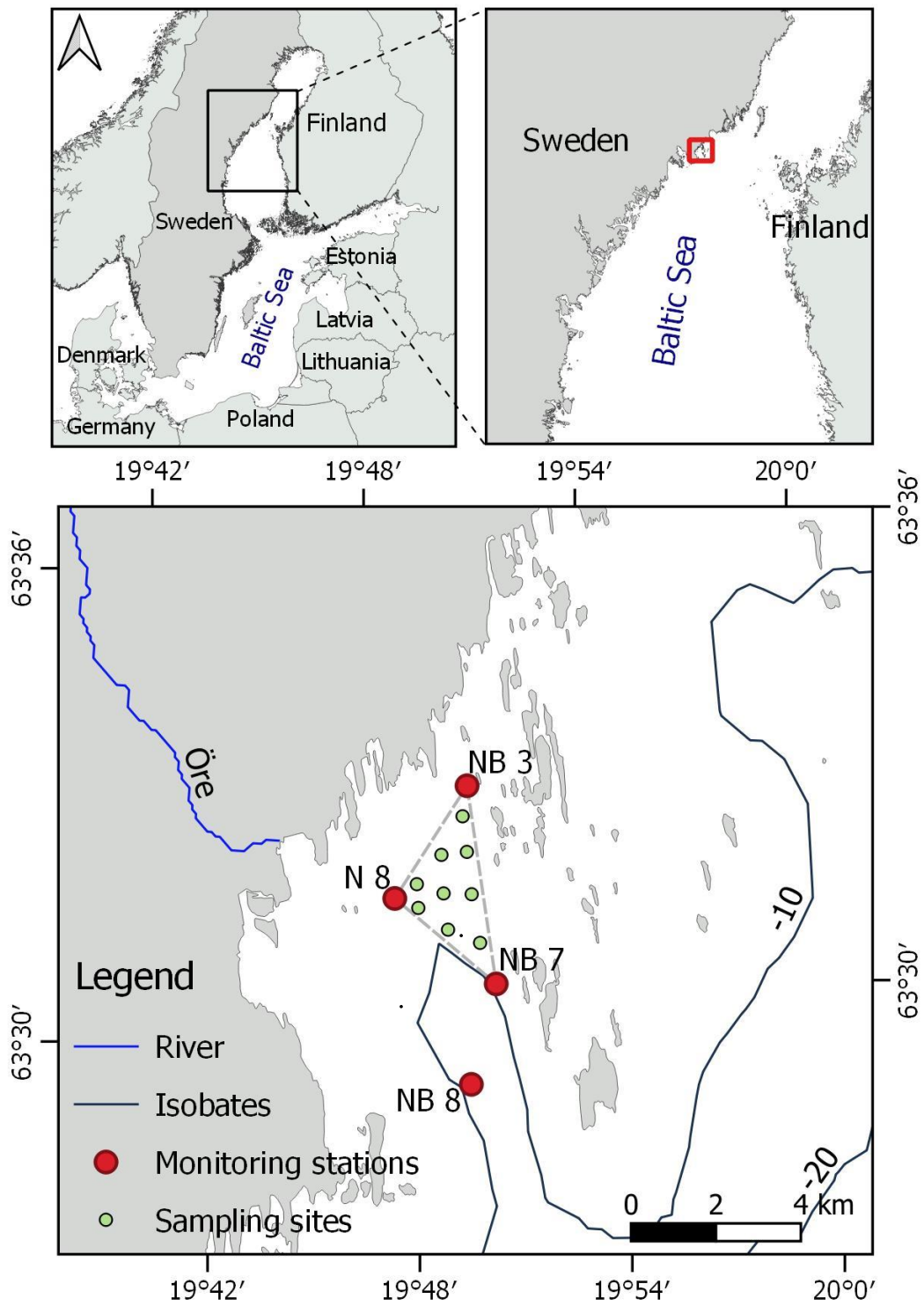
**Fig. 1** Map showing geographical location of Öre Estuary with the sampling sites

924

925

926

927

Fig. 2 Net fluxes of dissolved oxygen (a), inorganic nitrogen (b), and silica and phosphorus (c) at the sediment-water interface. Data range (whiskers), upper and lower quartiles (edges), the median (horizontal line), and the mean (diamonds), and outliers (circles) are represented for 18 replicates
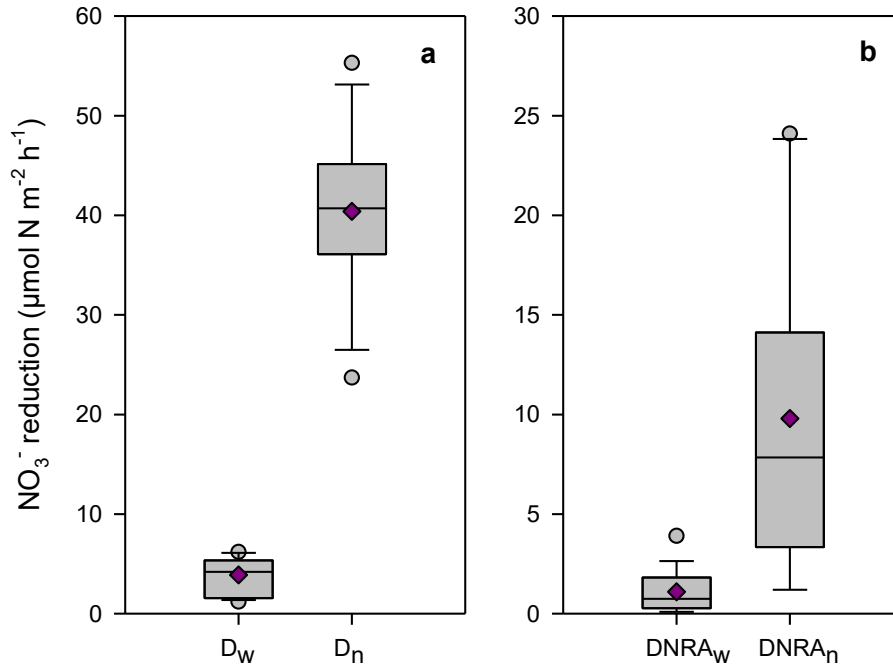
933

934

935
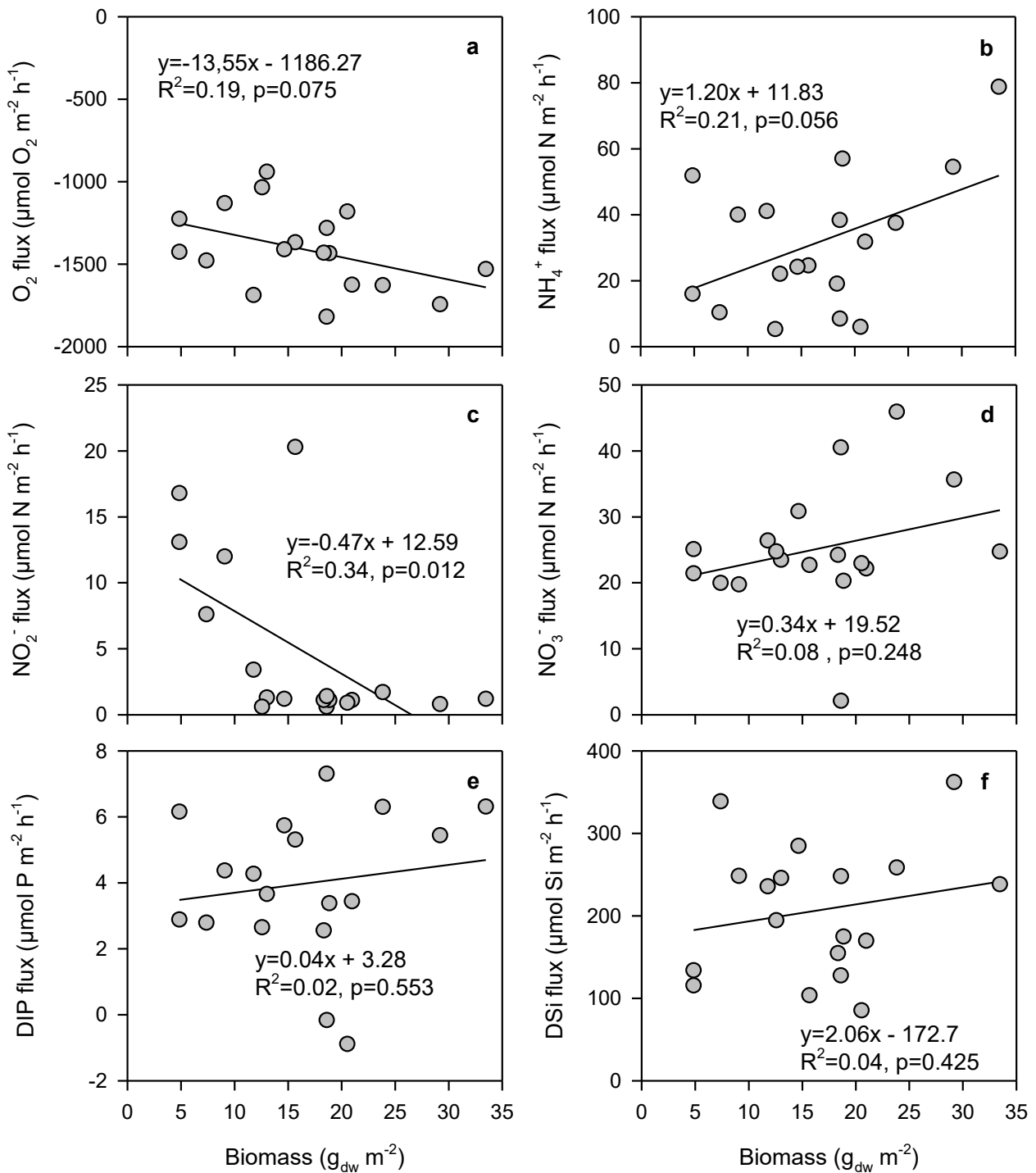
Fig. 3 Linear regressions between macrofauna biomass and net fluxes of dissolved oxygen (a) ammonium (b), nitrite (c), nitrate (d), inorganic phosphorus (e) and silica (f) measured in whole core incubations (n=18)

939

Fig. 4 Denitrification of water column NO_3^- (D_w) and coupled nitrification-denitrification (D_n; a) and dissimilative nitrate reduction to ammonium of water column NO_3^- ($DNRA_w$) and coupled nitrification-DNRA ($DNRA_n$; b) measured in whole core incubations. Data range (whiskers), upper and lower quartiles (edges), the median (horizontal line), and the mean (dark pink diamond), and outliers (grey circle) are represented for 18 replicates
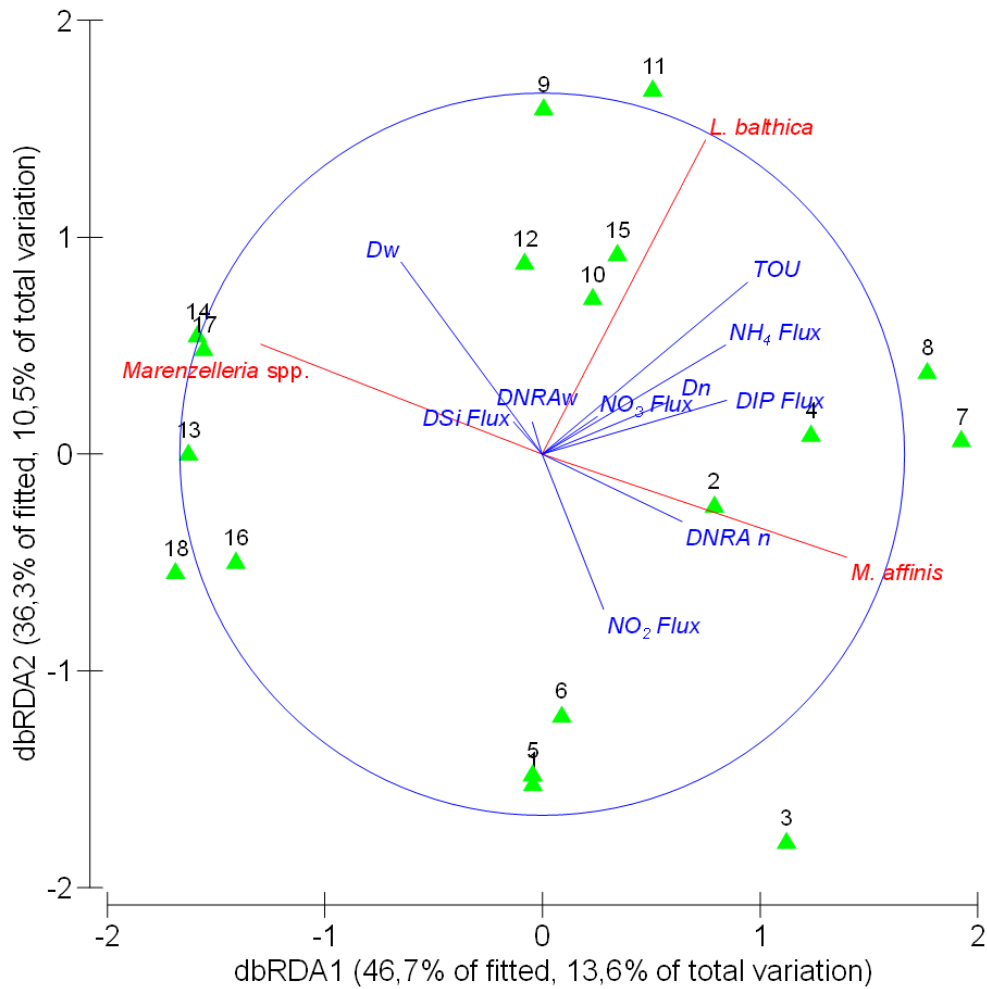
948

949

950

951

952
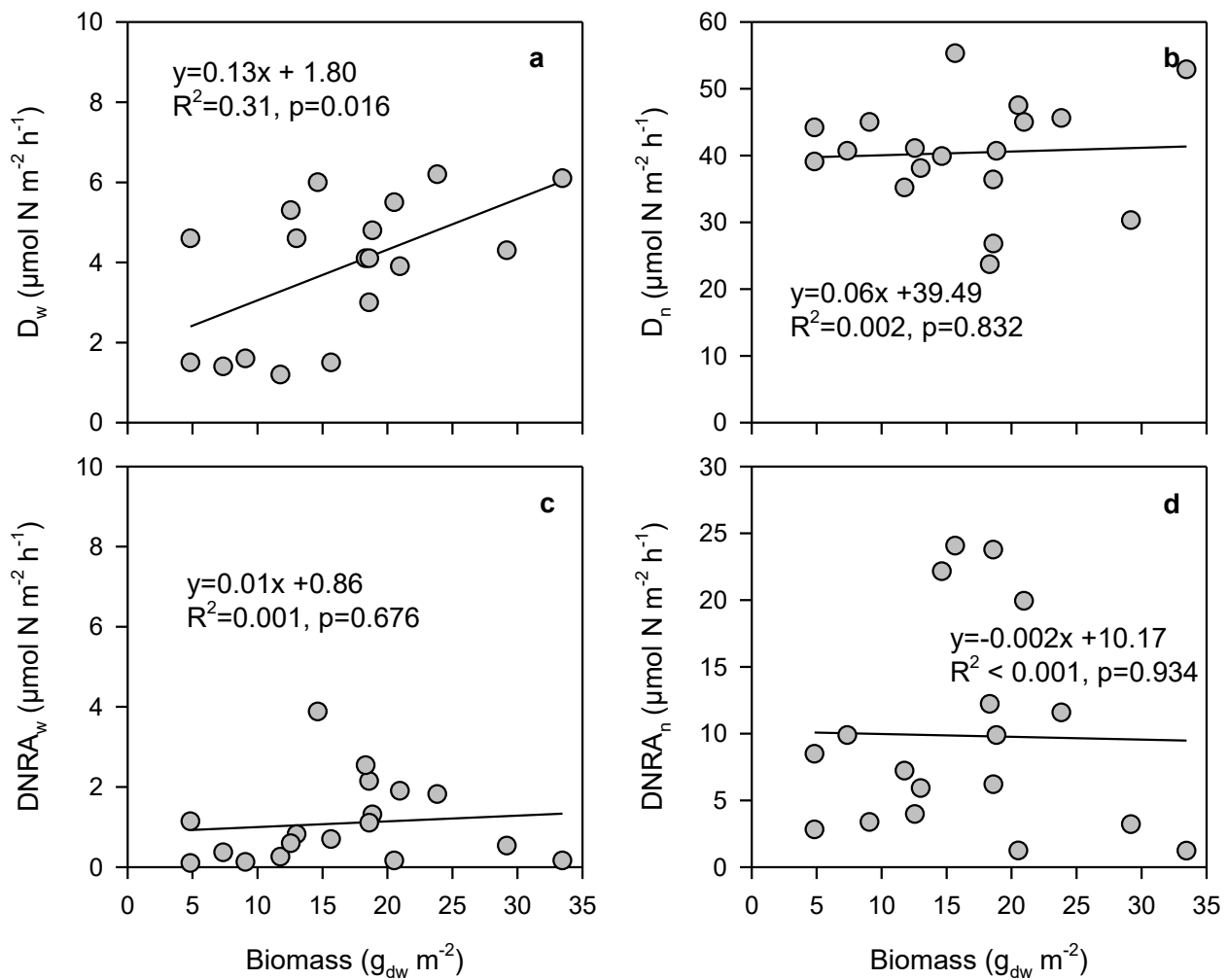
Fig. 5 Linear regressions between total macrofauna biomass and NO_3^- reduction processes: denitrification of water column NO_3^- (a), coupled nitrification-denitrification (b), and dissimilative nitrate reduction to ammonium (DNRA) of water column NO_3^- (c) and coupled nitrification-DNRA (d) measured in whole core incubations (n = 18)

958

959

960

961

962

963

Fig. 6 Distance based triplot of redundancy analysis (db-RDA) on net fluxes (O_2 - TOU, NH_4^+, NO_2^-, NO_3^-, DIP, and DSi) and processes (denitrification – D_w, D_n, and dissimilative nitrate reduction to ammonium – $DNRA_n$ and $DNRA_w$) in the Öre Estuary, using the biomass of the dominant benthic macrofauna (*L. balthica*, *M. affinis*, *Marenzelleria* spp.) as explanatory variable. Numbers indicate single cores collected in the sampling area. The projection of any sample onto vectors approximates the measured value in that sample

971

972

973

974
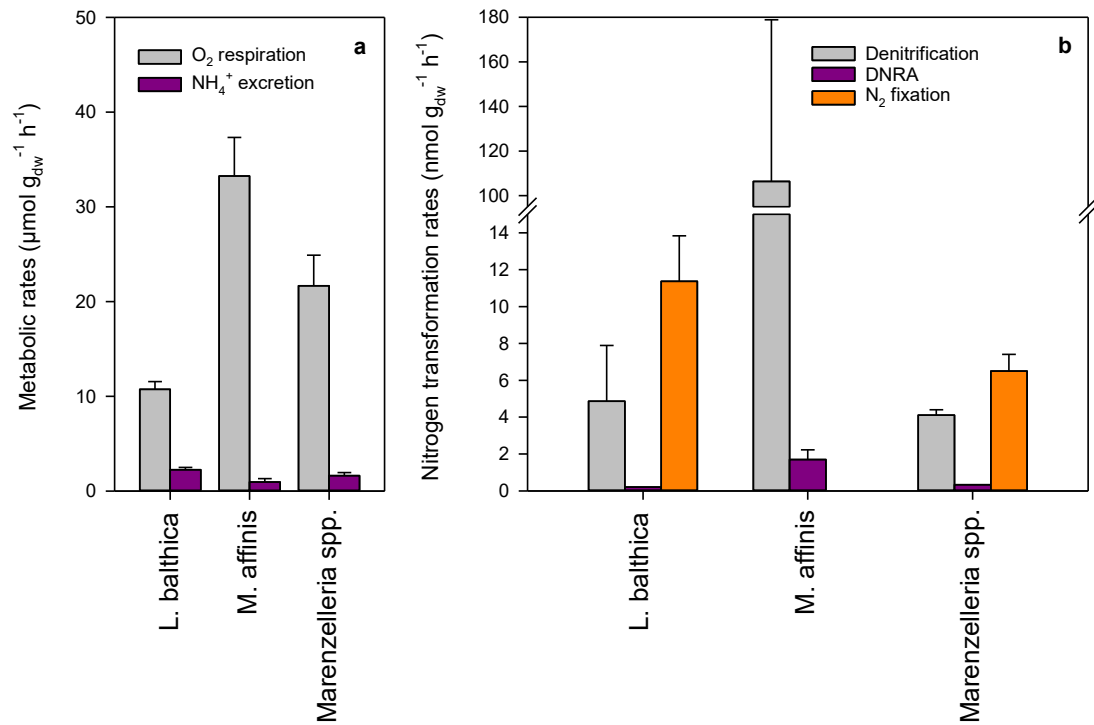
Fig. 7 The rates of macrofauna metabolism (respiration and excretion; a) and associated microbial nitrogen transformations (denitrification, dissimilative nitrate reduction to ammonium [DNRA] and N_2 fixation; b) are reported. N_2 fixation in *L. balthica* and *Marenzelleria* spp. was found in 3 out of 10 individuals. N_2 fixation in *L. balthica* was associated with the pallial organs. Bars report means and standard errors based on replicates
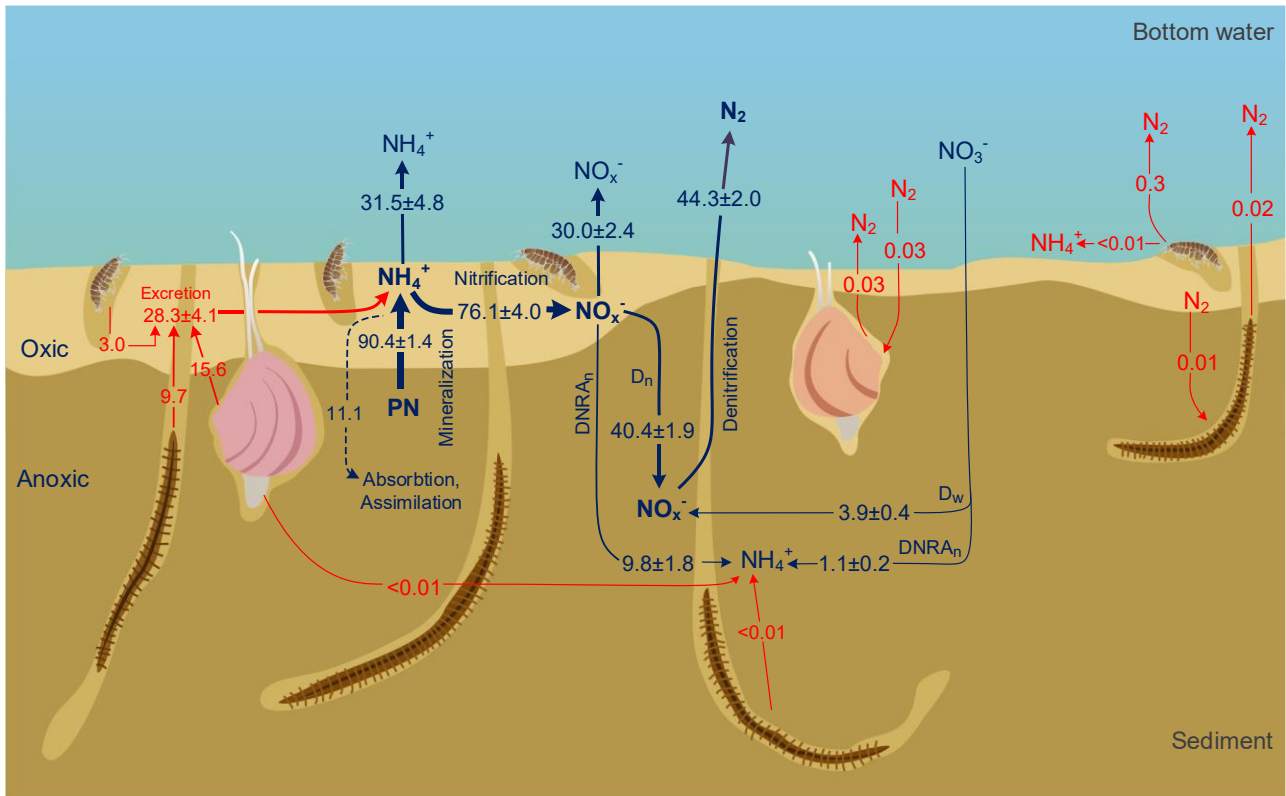
982

983

984

985

986

987

Fig. 8 Flowchart of N-cycling in the Öre estuarine sediments hosting the dominant macrofauna species *M. affinis*, *Marenzelleria* spp., and *L. balthica*. Nitrogen transformations were calculated combining measured fluxes and processes in benthic community (unmanipulated whole core incubations = sediment + macrofauna) and macrofauna alone (individual incubations). The animal excretion rates and holobionts-mediated N-cycling were calculated based on mean macrofauna biomass in the study area. Equations used to calculate fluxes and process rates are provided in the supplementary material (Table S2). Note that rates reported in the figure are expressed as µmol N m^{-2} h^{-1}. Results report means and standard errors based on experiment replicates (n=6 to 18, see the methods for details). Drawing by V. Gasiūnaitė